

Electronic Thesis and Dissertation Repository

9-4-2015 12:00 AM

Catalytic Conversion of Glycerol to Value-Added Chemical Products

Malaya Ranjan Nanda

Supervisor

Dr. Charles Xu

The University of Western Ontario

Graduate Program in Chemical and Biochemical Engineering

A thesis submitted in partial fulfillment of the requirements for the degree in Doctor of Philosophy

© Malaya Ranjan Nanda 2015

Follow this and additional works at: <https://ir.lib.uwo.ca/etd>

 Part of the [Catalysis and Reaction Engineering Commons](#), [Polymer Science Commons](#), and the [Thermodynamics Commons](#)

Recommended Citation

Nanda, Malaya Ranjan, "Catalytic Conversion of Glycerol to Value-Added Chemical Products" (2015). *Electronic Thesis and Dissertation Repository*. 3215.
<https://ir.lib.uwo.ca/etd/3215>

This Dissertation/Thesis is brought to you for free and open access by Scholarship@Western. It has been accepted for inclusion in Electronic Thesis and Dissertation Repository by an authorized administrator of Scholarship@Western. For more information, please contact wlsadmin@uwo.ca.

CATALYTIC CONVERSION OF GLYCEROL TO VALUE-ADDED CHEMICAL
PRODUCTS

(Thesis format: Integrated Article)

by

Malaya Ranjan Nanda

Graduate Program in Chemical and Biochemical Engineering

A thesis submitted in partial fulfillment
of the requirements for the degree of
Doctor of Philosophy

The School of Graduate and Postdoctoral Studies
The University of Western Ontario
London, Ontario, Canada

© Malaya Ranjan Nanda 2015

Abstract

Rapid expansion of the biodiesel industry has generated a huge amount of crude glycerol. This thesis aimed to explore utilization of glycerol for the production of solketal as an oxygenated fuel additive and 1, 2-propanediol as a polymer component via catalytic conversion.

The thesis work may be divided into two major parts. In the first part, the thermodynamics and kinetics of the glycerol ketalization for the synthesis of solketal were investigated in a batch reactor. From this information, a continuous-flow process was designed, developed and optimized using pure glycerol. Crude glycerol (13 wt% purity) was successfully upgraded into a purified crude glycerol product (> 96 wt% purity) and was used as feedstock in a modified reactor for the synthesis of solketal whose economic feasibility was demonstrated. In the second part, B₂O₃ promoted Cu/Al₂O₃ catalysts were used for selective hydrogenolysis of glycerol to 1, 2-propanediol in a flow reactor.

Surface properties, acidity, crystallinity, and reducibility of the catalysts were measured using N₂ adsorption, NH₃-temperature programmed desorption (TPD), X-ray diffraction (XRD), and H₂-temperature programmed reduction (TPR), respectively. The fuels/chemicals products obtained were analyzed by GC-MS/FID and Fourier-transformation infrared spectroscopy (FTIR).

The ketalization reaction equilibrium constants were determined experimentally in the temperature range of 293-323 K. The activation energy of the overall reaction was determined to be $55.6 \pm 3.1 \text{ kJ mol}^{-1}$. Langmuir-Hinshelwood equation was used to model the rate law. The activity of all catalysts tested in the flow reactor follows the order: Amberlyst wet \approx H-beta zeolite \approx Amberlyst dry > Zirconium sulfate > Montmorillonite > Polymax. At optimum conditions (25 °C, 500 psi, acetone-to-glycerol molar ratio of 4 and 2 h⁻¹ WHSV), the maximum solketal yield from pure glycerol was 94±2% over Amberlyst wet. Ketalization of purified crude glycerol over Amberlyst wet, led to 93± 3% glycerol conversion with 92 ±2% solketal yield at the optimum conditions. In the glycerol hydrogenolysis process with 10 wt% aqueous solution of glycerol as the feed, 5Cu-B/Al₂O₃

catalyst demonstrated a very high activity, yielding $98 \pm 1\%$ glycerol conversion and $98 \pm 1\%$ 1,2-propanediol selectivity at the optimum conditions ($250\text{ }^{\circ}\text{C}$, 6 MPa H_2 , and 0.1 h^{-1} WHSV).

Keywords

Glycerol, Crude glycerol, Purified crude glycerol, Catalyst, Amberlyst-36 wet, Solketal, 1,2-propanediol, Ketalization, Hydrogenolysis, Optimization, Thermodynamics, Kinetics, Flow reactor, Acidification, Regeneration, Copper catalyst, Deactivation.

Co-Authorship Statement

Chapter 2: General literature review

This chapter will be submitted as a review paper titled “Crude glycerol: A liability or an evolving opportunity” to *Biofuels, Bioproducts and Biorefining* for consideration of publication.

Authors: Nanda, M., Tymchyshyn, M., Yuan, Z., Qin, W., Xu, C.

Writing and literature data analysis were conducted by Malaya Nanda assisted by Matthew Tymchyshyn under the supervision of Dr. Zhongshun Yuan and Prof. Wensheng Qin. It was reviewed and revised by Prof. Charles (Chuanbao) Xu.

Chapter 3: Innovative and potential technologies towards the sustainable production of solketal as a fuel additive: A review.

This chapter will be submitted as a review paper to *Renewable and Sustainable Energy Review* for consideration of publication.

Authors: Nanda, M., Zhang, Y., Yuan, Z., Qin, W., Ghaziaskar, H., Xu, C.

Writing and literature data analysis were conducted by Malaya Nanda assisted by Dr. Yongsheng Zhang, and Dr. Zhongshun Yuan under the supervision of and Prof. Wensheng Qin and Prof. Hassan Ghaziaskar. It was reviewed and revised by Prof. Charles (Chuanbao) Xu.

Chapter 4: Recent advancements in catalytic conversion of glycerol into propylene glycol: A review

This chapter will be submitted as a review paper to *Industrial Crops and Products* for consideration of publication.

Authors: Nanda, M., Yuan, Z., Qin, W., Xu, C.

Writing and literature data analysis were conducted by Malaya Nanda assisted by Dr. Zhongshun Yuan under the supervision of and Prof. Wensheng Qin. It was reviewed and revised by Prof. Charles (Chuanbao) Xu.

Chapter 5: Thermodynamic and kinetic studies of a catalytic process to convert glycerol into solketal as an oxygenated fuel additive

This chapter is a published article: Nanda, M., Yuan, Z., Ghaziaskar, H.S., Qin, W., Poirier, M., Xu, C., Thermodynamics and kinetic studies of a catalytic process to convert glycerol into solketal as an oxygenated fuel additive, *Fuel*, 2014, 117, 470-477

The experimental work was conducted by Malaya Nanda under the supervision of Prof. Charles (Chuanbao) Xu and guidance of Dr. Zhongshun Yuan. Writing and data analysis were conducted by Malaya Nanda assisted by Wensheng Qin and Marc-Andre Poierer. It was reviewed and revised by Prof. Charles (Chuanbao) Xu, Dr. Zongshun Yuan and Prof. Hassan Ghaziaskar.

Chapter 6: A new continuous-flow process for catalytic conversion of glycerol to oxygenated fuel additive: catalyst screening

This chapter is a published article: Nanda, M., Yuan, Z., Qin, W., Ghaziaskar, H.S., Poirier, M., Xu, C., A new continuous-flow process for catalytic conversion of glycerol to oxygenated fuel additive: catalyst screening, *Applied Energy*, 2014, 123, 75-81

The experimental work was conducted by Malaya Nanda under the supervision of Prof. Charles (Chuanbao) Xu and guidance of Dr. Zhongshun Yuan. Writing and data analysis were conducted by Malaya Nanda assisted by Wensheng Qin and Marc-Andre Poierer. It was reviewed and revised by Prof. Charles (Chuanbao) Xu, Dr. Zongshun Yuan and Prof. Hassan Ghaziaskar.

Chapter 7: A Catalytic conversion of glycerol to oxygenated fuel additive in a continuous flow reactor: process optimization

This chapter is a published article: Nanda, M., Yuan, Z., Qin, W., Ghaziaskar, H.S., Poirier, M., Xu C., Catalytic conversion of glycerol to oxygenated fuel additive in a continuous flow reactor: process optimization, *Fuel*, 2014,128, 113-119

The experimental work was conducted by Malaya Nanda under the supervision of Prof. Charles (Chuanbao) Xu and guidance of Dr. Zhongshun Yuan. Writing and data analysis were conducted by Malaya Nanda assisted by Wensheng Qin and Marc-Andre Poierer. It was reviewed and revised by Prof. Charles (Chuanbao) Xu, Dr. Zongshun Yuan and Prof. Hassan Ghaziaskar.

Chapter 8: Purification of Crude Glycerol Using Acidification: Effects of Acid Types and Product Characterization

This chapter is a published article: Nanda, M., Yuan, Z., Qin, W., Poirier, M., Xu, C. Purification of Crude Glycerol Using Acidification: Effects of Acid Types and Product Characterization: *Austin J Chem Eng*, 2014, 1, 1-7.

The experimental work was conducted by Malaya Nanda under the supervision of Prof. Charles (Chuanbao) Xu and guidance of Dr. Zhongshun Yuan. Writing and data analysis were conducted by Malaya Nanda assisted by Wensheng Qin and Marc-Andre Poierer. It was reviewed and revised by Prof. Charles (Chuanbao) Xu, and Dr. Zongshun Yuan

Chapter 9: Catalytic conversion of purified crude glycerol in a continuous-flow process for the synthesis of oxygenated fuel additive

Authors: Nanda, M., Yuan, Z., Qin, W., Poirier, M., Xu, C.

This article has been submitted to *Biomass and Bioenergy* for consideration of publication.

The experimental work was conducted by Malaya Nanda, assisted by Dr. Zongshun Yuan under the supervision of Prof. Wensheng Qin. Writing and data analysis were conducted

by Malaya Nanda assisted by Marc-Andre Poierer. It was reviewed and revised by Prof. Charles (Chuanbao) Xu, and Dr. Zongshun Yuan

Chapter 10: B₂O₃ promoted Cu/Al₂O₃ catalysts for selective hydrogenolysis of glycerol and crude glycerol to produce 1,2-propanediol

This chapter will be submitted as a research article to *Green Chemistry* for consideration of publication.

Authors: Nanda, M., Yuan, Z., Qin, W., Xu, C.

The experimental work was conducted by Malaya Nanda and Dr. Zongshun Yuan under the supervision of Prof. Charles (Chuanbao) Xu. Writing and data analysis were conducted by Malaya Nanda assisted by Wensheng Qin. It was reviewed and revised by Prof. Charles (Chuanbao) Xu, and Dr. Zongshun Yuan

Chapter 11: Techno-economic analysis for production of an oxygenated fuel additive from crude glycerol in Canada

Authors: Nanda, M., Yuan, Z., Qin, W., Xu, C.

The experimental work, writing and data analysis was conducted by Malaya Nanda, assisted by Dr. Zongshun Yuan under the supervision of Prof. Wensheng Qin. It was reviewed and revised by Prof. Charles (Chuanbao) Xu.

Acknowledgments

I would like to express my sincere gratitude to my supervisor at University of Western Ontario, Prof. Chunbao (Charles) Xu and my co-supervisor at Lakehead University, Prof. Wensheng Qin for their invaluable support, advice, and help throughout my PhD study. I am extremely thankful to Dr. Zongshun Yuan, Prof. Hassan S. Ghaziaskar at Isfahan University of Technology of Iran and Dr. Marc-Andrea Poirier at Imperial Oil Ltd for their guidance and valuable suggestions at difficult times to finish this work. My appreciation extends to all the members of my advisory committee Professors Franco Beruti and Cedric Briens for their encouragement and suggestions.

I would also like to acknowledge Ms. Flora Cao for her help in different experiments and sample characterization at Institute for Chemicals and Fuels from Alternative Resources (ICFAR) and at University of Western Ontario (UWO) facilities. My special thanks to Dr. Katherine Albion for her help and assistance to set up the BioIndustrial Laboratory for some part of this research at Western-Sarnia-Lambton Research Park, Sarnia.

I would also like to thank Rob Taylor, Caitlin Marshall, Thomas Johnston, Tetyana Levchenko, Ehsan Ghiasi, Izad Behnia, Dr. Yongsheng Zhang, Dr. Shuna Cheng, Dr. Shanghuan Feng, Matthew Tymchyshyn, Dr. Hossein Kazemian, Jose Munoz and Professors Hugo de Lasa and Paul Charpentier for their help and support in different parts of the experiment and sample analysis.

I thank all my lab colleagues and friends for the inspiration and support given to me in different ways over the length of my research. This work couldn't have been completed without their support.

Finally, I gratefully acknowledge the financial assistance provided by Faculty of Engineering, the University of Western Ontario (for Teaching Assistantship, Graduate Research Assistantship), and the research grants awarded to Dr. Xu from Imperial Oil Ltd. (University Research Awards), NSERC (Discovery Grant) and MITACS (The Accelerate Internship Program).

Dedication

To The Divine Mother

Table of Contents

Abstract	ii
Co-Authorship Statement.....	iv
Acknowledgments.....	viii
Dedication	ix
Table of Contents	x
List of Tables	xviii
List of Figures.....	xxi
List of Schemes.....	xxvii
Abbreviations	xxix
Chapter 1	1
1 Introduction	1
1.1 Background.....	1
1.2 Sources of glycerol	2
1.3 Crude glycerol.....	4
1.4 Research objectives.....	5
1.5 Thesis structure	6
References	8
Chapter 2.....	12
2 General literature review.....	12
2.1 Catalytic processes for conversion of glycerol into various products	13
2.1.1 Esterification of glycerol.....	13
2.1.2 Carboxylation of glycerol	17
2.1.3 Dehydration of glycerol	19

2.1.4	Etherification of glycerol	21
2.1.5	Chlorination of glycerol.....	26
2.1.6	Oxidation of glycerol	27
2.1.7	Reforming glycerol to syngas	30
2.1.8	Acetalization of glycerol to acetals and ketals.....	31
2.1.9	Hydrogenolysis of glycerol.....	33
2.2	Conclusions and recommendations.....	38
	References	39
Chapter 3.....		50
3	Innovative and potential technologies towards the sustainable production of solketal as a fuel additive: A review	50
3.1	Introduction.....	51
3.2	Historical context	53
3.3	Synthesis of solketal from glycerol in batch reactors	54
3.4	Synthesis of solketal from glycerol in continuous-flow reactors.....	58
3.5	Influence of catalyst acidity	64
3.6	Performance of transition metal catalysts in glycerol ketalization	67
3.7	Reaction mechanism	67
3.8	Key operation issues of flow reactors and use of crude glycerol	70
3.9	Conclusions.....	73
	References	76
Chapter 4.....		83
4	Recent advancements in catalytic conversion of glycerol into propylene glycol: A review.....	83
4.1	Introduction.....	84

4.2	Historical context	87
4.3	Effects of catalyst preparation and activation methods	90
4.4	Development of the reaction processes.....	95
4.5	Development of effective catalysts.....	99
4.5.1	Noble metal based catalysts	99
4.5.2	3d transition metal-based catalysts	101
4.5.3	Mixed catalysts	104
4.6	Catalyst deactivation.....	104
4.7	Reaction mechanisms.....	105
4.8	Use of crude glycerol and bio-hydrogen as feedstock	108
4.9	Conclusions.....	109
	References	111
	Chapter 5.....	121
5	Thermodynamic and kinetics studies of a catalytic process to convert glycerol into solketal as an oxygenated fuel additive.....	121
5.1	Introduction.....	122
5.2	Experimental.....	124
5.2.1	Materials	124
5.2.2	Ketalization reaction of glycerol and acetone.....	125
5.2.3	Product analysis	126
5.3	Thermodynamic results.....	127
5.4	Kinetic results	130
5.4.1	Mass transfer resistance	132
5.4.2	Effects of catalyst loading.....	133
5.4.3	Effects of pressure.....	135

5.4.4	Effects of temperature.....	135
5.4.5	Effects of initial molar concentration of reactants	136
5.4.6	Moisture content	137
5.4.7	Kinetic model.....	138
5.5	Conclusions.....	142
	References	144
Chapter 6.....		147
6	A new continuous-flow process for the catalytic conversion of glycerol to oxygenated fuel additive: catalyst screening.....	147
6.1	Introduction.....	147
6.2	Materials and methods	150
6.2.1	Materials	150
6.2.2	Catalyst characterization.....	150
6.2.3	Synthesis of solketal in a continuous-flow reactor	150
6.2.4	Product analysis	152
6.3	Results and discussion	153
6.3.1	Fresh catalyst characterization.....	153
6.3.2	Product characterization.....	155
6.3.3	Catalyst activities	156
6.4	Conclusions.....	165
	References	166
Chapter 7.....		169
7	Catalytic conversion of glycerol to oxygenated fuel additive in a continuous flow reactor: process optimization	169
7.1	Introduction.....	170

7.2	Experimental	171
7.2.1	Materials	171
7.2.2	Experimental procedure	172
7.2.3	Product analysis	173
7.2.4	Experimental design.....	173
7.3	Result and discussion.....	175
7.3.1	Model fitting and statistical analysis.....	175
7.3.2	Response surface analysis.....	180
7.3.3	Optimization of reaction parameters.....	185
7.3.4	Effect of impurities on the solketal yield.....	185
7.3.5	Catalyst life-time tests.....	187
7.3.6	Economic (marginal benefit) analysis	188
7.4	Conclusions.....	189
	References	190
	Chapter 8.....	193
8	Purification of crude glycerol using acidification: effects of acid types and product characterization	193
8.1	Introduction.....	194
8.2	Materials and methods	197
8.2.1	Materials	197
8.2.2	Purification process.....	197
8.2.3	Characterization of crude and purified glycerol	197
8.3	Results and discussion	200
8.3.1	Crude glycerol analysis.....	200
8.3.2	Effects of acid type and pH value.....	202

8.3.3	Analysis of purified glycerol product	206
8.4	Conclusions.....	211
	References	213
Chapter 9	216
9	Catalytic conversion of purified crude glycerol in a continuous-flow process for the synthesis of oxygenated fuel additive	216
9.1	Introduction.....	217
9.2	Materials and methods	219
9.2.1	Materials	219
9.2.2	Analytical methods	220
9.2.3	Continuous reactor for the synthesis of solketal from purified crude glycerol	220
9.2.4	Product analysis	222
9.3	Results and discussion	223
9.4	Conclusions.....	229
	References	230
Chapter 10	233
10	B ₂ O ₃ promoted Cu/Al ₂ O ₃ catalysts for selective hydrogenolysis of glycerol and crude glycerol to 1,2-propanediol	233
10.1	Introduction.....	234
10.2	Experimental	237
10.2.1	Materials	237
10.2.2	Catalyst preparation	238
10.2.3	Catalyst characterization.....	238
10.2.4	Catalytic tests	239
10.2.5	Product analysis	240

10.3	Results and discussion	241
10.3.1	Catalyst characterization	241
10.3.2	Influence of process parameters.....	245
10.3.3	Effects of glycerol feedstock purity	250
10.3.4	Long term stability and catalyst deactivation	252
10.4	Conclusions.....	256
	References	256
Chapter 11		261
11	Techno-economic analysis for production of an oxygenated fuel additive from crude glycerol in Canada.....	261
11.1	Introduction.....	262
11.2	Solketal production processes.....	264
11.2.1	Plant capacity	264
11.2.2	Feedstock and materials	265
11.2.3	Pretreatment and production units	265
11.2.4	Byproducts	266
11.3	Results and discussion	266
11.3.1	Selection of operating conditions.....	266
11.3.2	Quality parameters	267
11.3.3	Economic assessment.....	268
11.4	Conclusions.....	272
	References	273
Chapter 12		276
12	Conclusions and future work	276
12.1	Conclusions.....	276

12.2 Future work.....	279
Appendices.....	281
Appendix A: Thermodynamic relations.....	281
Appendix B: Kinetic model.....	282
Appendix C: GC-MS/FID data for ketalization of glycerol to solketal.....	288
Appendix D: GC-MS/FID data for hydrogenation of glycerol to 1,2-PDO.....	292
Appendix E: Permission to Reuse Copyrighted Materials.....	298
Permission to Table 2.1 and Table 2.3.....	298
Permission to Scheme 2.13.....	299
Permission to Figure 3.1.....	300
Permission to Figure 3.2.....	301
Permission to Scheme 3.3.....	302
Permission to Figure 4.5.....	303
Permission to Figure 4.6.....	304
Permission to Figure 4.8.....	305
Permission to Chapter 5.....	306
Permission to Chapter 6.....	307
Permission to Chapter 7.....	308
Permission to Chapter 8.....	309
Curriculum Vitae.....	310

List of Tables

Table 1.1. Properties of Glycerol ²	1
Table 1.2 World scenario of crude glycerol (in billion liters)	4
Table 2.1 Performance of various heterogeneous catalysts in esterification of glycerol to mono-esters (adopted with permission ⁹).....	14
Table 2.2 Comparison of homogeneous and heterogeneous catalysts for glycerol etherification (modified from reference ⁴¹).....	22
Table 2.3 Selected results of catalytic oxidation of glycerol (adopted with permission) ⁹	29
Table 2.4 List of compounds that can be synthesized from glycerol (adopted and redrawn) ¹¹¹	36
Table 3.1 Performance of various catalysts for glycerol ketalization with different types of reactors.....	63
Table 3.2 Influence of catalyst acidity on solketal yield	66
Table 4.1 Effect of catalyst preparation methods on glycerol conversion and propylene glycol selectivity	93
Table 4.2 Effect of catalyst activation process on glycerol conversion and propylene glycol selectivity	94
Table 5.1 Characterization of the solid acid catalyst used.....	124
Table 5.2 Experimental data of equilibrium composition and equilibrium constants ^a ...	128
Table 5.3 Summary of the experiments at different conditions.....	132
Table 5.4 Kinetic modeling parameters k and K_w ^a	140

Table 6.1 Textural properties (measured by N ₂ isothermal adsorption) and acidity for the fresh catalysts used in this study	153
Table 6.2 Effect of acetone/glycerol molar ratio at fixed temperature (40 °C), pressure (600 psi) and WHSV (4 h ⁻¹).....	157
Table 6.3 Effect of weight hourly space velocity (WHSV, h ⁻¹) on solketal yield and glycerol conversion (Other reaction conditions: 40 °C, 600 psi and acetone equivalent of 2.0)	159
Table 6.4 Textural properties and acidity for the fresh and spent catalyst (after 24 h time-on-stream) of Amberlyst wet	162
Table 7.1 Catalyst characterization.....	172
Table 7.2 Actual and corresponding coded values of each parameter.....	175
Table 7.3 Experimental design matrix and measured response values.....	176
Table 7.4 ANOVA analysis for the reduced quadratic model of yield.....	177
Table 7.5 Predicted and experimental values of the response at the optimal conditions	185
Table 7.6 Economical analysis (marginal benefit) for production of 1 kg solketal.....	189
Table 8.1 Composition and physical properties of various glycerol samples.....	201
Table 8.2 Main compounds in crude glycerol detected by GC-MS analysis.....	202
Table 8.3 Performance of different acids in purification of crude glycerol.....	203
Table 8.4 Composition and physical properties of purified glycerol and commercial glycerol	207
Table 9.1 Composition of purified glycerol.....	220
Table 9.2 Characteristics of the fresh and spent catalysts	226

Table 10.1 Textural properties of the fresh/spent Cu/Al ₂ O ₃ catalysts loaded with various amounts of B ₂ O ₃ determined by N ₂ adsorption-desorption	241
Table 10.2 Effects of Cu loading on activity of Cu/Al ₂ O ₃ catalysts for glycerol hydrogenolysis	246
Table 10.3 Composition of different grades of glycerol.....	251
Table 11.1 Crude glycerol composition.....	263
Table 11.2 Quality analyses of the PCG and solketal product	268
Table 11.3 Pretreatment cost of crude glycerol	270
Table 11.4 Conversion cost of glycerol to solketal.....	271

List of Figures

Figure 1.1 Applications of glycerol in different fields ²	2
Figure 2.1 Structure of glycerol acetins	17
Figure 2.2. Hyper-branched polyglycerol	24
Figure 3.1 Membrane reactor for synthesis of solketal (adopted from reference, ⁴⁰ and used with copyright permission)	56
Figure 3.2 Continuous microwave reactor for synthesis of solketal (adopted and used with copyright permission) ⁵⁰	59
Figure 3.3 Schematic continuous glass flow reactor proposed by Monbaliu <i>et al.</i> ⁵² (with copyright permission from Elsevier)	61
Figure 3.4 Continuous-flow reactor developed in our laboratory for glycerol ketalization	62
Figure 3.5 The cyclic acetals from the reaction between glycerol and acetone: 5-hydroxy-2,2-dimethyl-1,3-dioxane (a) solketal i.e., 4-hydroxymethyl-2,2-dimethyl-1,3-dioxolane(b)	68
Figure 3.6 Deactivation of catalyst by impurities in the glycerol feed.	72
Figure 3.7 Flow reactor consisting of guard reactors allowing online removal of impurities in the glycerol feedstock and online regeneration of deactivated catalysts.....	73
Figure 4.1 Annual number of publications on the concept of glycerol hydrogenolysis (searched from database Scifinder as “glycerol” and “hydrogenolysis”)	85
Figure 4.2 Applications of propylene glycol in different fields ⁵ (Misc: Tobacco humectants, flavors and fragrances, and animal feed)	86
Figure 4.3 World scenario for the production of propylene glycol ⁶	86

Figure 4.4 Structure of dipropylene glycol and tripropylene glycol.....	88
Figure 4.5 Multiple slurry reactor used for the hydrogenolysis of glycerol ³⁵ (adopted with copyright permission)	96
Figure 4.6 Schematic diagram of the flow reactor set-up ⁴⁸ (adopted with copy right permission).....	98
Figure 4.7 Schematic diagram of the trickle-bed reactor developed by Xi and co-workers ⁵²	99
Figure 4.8 TEM micrographs of Ag/Al ₂ O ₃ catalyst: fresh (a), spent (b) and spent-washed-calcined (c) ⁸⁴ (adopted with copyright permission).....	105
Figure 5.1 Batch reactor.....	126
Figure 5.2 Plot of $\ln K_c$ vs. $1/T$	130
Figure 5.3 Effects of reactor stirring speed on the solketal yield (other reaction conditions: 323 K, acetone to glycerol molar ratio (A/G) of 2, catalyst loading (W_{cat}) of 1 wt% of glycerol)	133
Figure 5.4 Effects of the catalyst addition amount on the yield of solketal (other reaction conditions: 313 K and A/G = 2).....	134
Figure 5.5 Influence of temperature on the yield of solketal (other reaction conditions: A/G = 2 and W_{cat} = 1 wt% of glycerol)	136
Figure 5.6 Effects of initial acetone-to-glycerol (A/G) molar ratio on the yield of solketal (other reaction conditions: 298 K and W_{cat} = 1 wt% w.r.t. glycerol)	137
Figure 5.7 Effect of moisture content on the yield (other conditions: 298 K, W_{cat} = 1 wt% w.r.t. glycerol).....	138
Figure 5.8 Experimental data vs. theoretical curves based on the kinetics derived in this work (Other conditions: 313 K, W_{cat} = 1 wt% of glycerol).....	141

Figure 5.9 Plots of kinetic modeling parameters $\ln k$ or $\ln K_w$ vs. $1/T$	142
Figure 6.1 Schematic diagram of the continuous-flow reactor used for ketalization of glycerol	152
Figure 6.2 TGA profiles of fresh catalysts of Zirconium sulfate (a), Montmorillonite (b), Polymax (c), H-beta zeolite (d), Amberlyst dry (e) and Amberlyst wet (f).....	155
Figure 6.3 FTIR spectrum of a typical solketal product	156
Figure 6.4 Solketal yield vs. acidity (relative abundance of acidic sites) for catalysts of H-beta zeolite (6.2 eq/kg), Montmorillonite (4.6 eq/kg), Amberlyst dry (5.5 eq/kg) and Amberlyst wet (5.4 eq/kg). Experimental conditions: 40 °C, 600 psi and WHSV of 4 h ⁻¹ with different acetone equivalent ratios of 2.0 and 6.0.....	158
Figure 6.5 Variation of glycerol conversion (a) and solketal yield (b) with temperature for various catalysts (A: H-beta zeolite; B: Montmorillononite; C: Amberlyst dry; D: Amberlyst wet; E: Polymax; F: Zirconium sulfate). Other conditions were: P = 600 psi, molar ratio of acetone: glycerol: ethanol = 2:1:1, WHSV= 4 h ⁻¹)	161
Figure 6.6 Solketal yield vs. time-on-stream with catalysts of Amberlyst wet (a), H-beta zeolite (b), Amberlyst dry (c), Zirconium sulfate (d), Montmorillonite (e) and Polymax(f)	163
Figure 6.7 FTIR spectra of the fresh and spent Amberlyst wet (Experimental conditions: 40 °C, 600 psi and WHSV of 4 h ⁻¹ with acetone equivalent of 2)	164
Figure 7.1 The experimental results versus the model predicted results	179
Figure 7.2 The normal probability plot of the residuals	180
Figure 7.3 Matrix plot of X ₁ (temperature), X ₂ (acetone equivalent ratio) and X ₃ (WHSV)	181

Figure 7.4 Surface plots for effects of temperature and acetone equivalent ratio on solketal yield (a), effect of temperature and WHSV on solketal yield (b) and effect of acetone equivalent ratio and WHSV on solketal yield (c).....	183
Figure 7.5 Contour plots for effects of temperature and acetone equivalent ratio on solketal yield (a), effect of temperature and WHSV on solketal yield (b) and effect of acetone equivalent ratio and WHSV on solketal yield (c).....	184
Figure 7.6 Effects of impurities on the yield of solketal. (A: Ethanol as solvent; B: Methanol as solvent; C: 1 wt% NaCl in ethanol as impurity; D: 2 wt% water in ethanol as impurity; E: 1 wt% NaCl+ 2 wt% water in methanol as solvent).....	186
Figure 7.7 Solketal yield and glycerol conversion vs. time on stream up to 24 h from the operation under the optimum conditions with fresh and regenerated Amberlyst-36 catalyst	188
Figure 8.1 World's scenario of crude glycerol	195
Figure 8.2 Pictures of crude glycerol (A) and pure glycerol (B)	200
Figure 8.3 Photos showing the formation of three phases (A) and separation of purified glycerol phase from fatty acid layer (B)	204
Figure 8.4 Effects of pH levels on the weight percentages of various phases during acidification of crude glycerol using H ₃ PO ₄ acid	205
Figure 8.5 Composition of purified glycerol vs. pH (A: Glycerol B; MONG C: Water D: Ash).....	206
Figure 8.6 FTIR spectra of pure, purified and crude glycerol	208
Figure 8.7 UV-Vis spectra of pure, purified and crude glycerol	209
Figure 8.8 Purified glycerol before (A) and after (B) charcoal treatment	210
Figure 8.9 Spectra of ¹ H NMR (a) and ¹³ C NMR for the purified glycerol	211

Figure 9.1 Schematic diagram of the continuous flow reactor.	222
Figure 9.2 Solketal yield (%) vs. time-on-stream (h) in various operations: crude glycerol without guard reactor (CG-NGR), crude glycerol with the guard reactor (CG-GR), purified crude glycerol without guard reactor (PCG-NGR), and purified crude glycerol with the guard reactor after regeneration of the catalyst inside the guard reactor for 0 time (PCG-GR0), 1 time (PCG-GR1), 2 times (PCG-GR2) and 3 times (PCG-GR3).....	224
Figure 9.3 Fresh (A) and spent (B) catalysts	227
Figure 9.4 Particle size distributions of the fresh (A) and spent (B) catalysts.....	228
Figure 10.1 XRD patterns of the fresh Cu/Al ₂ O ₃ catalysts loaded with various amounts of B ₂ O ₃	242
Figure 10.2 H ₂ -TPR profiles of the fresh Cu/Al ₂ O ₃ catalysts loaded with various amounts of B ₂ O ₃	243
Figure 10.3 NH ₃ -TPD profiles of the fresh Cu/Al ₂ O ₃ catalysts loaded with various amounts of B ₂ O ₃	244
Figure 10.4 Effects of B loading (0-5 wt%) on 5Cu/Al ₂ O ₃ on activity of Cu/Al ₂ O ₃ catalysts for glycerol hydrogenolysis (Experimental conditions: 230 °C, 6 MPa H ₂ , 10 wt% aq. glycerol, WHSV 0.2 h ⁻¹).....	247
Figure 10.5 Effects of temperature on the activity of 5Cu-1B/Al ₂ O ₃ catalyst for glycerol hydrogenolysis (5 MPa H ₂ , 10 wt% aq. glycerol and WHSV 0.2 h ⁻¹).....	248
Figure 10.6. Effects of hydrogen pressure (2-8 MPa) on the performance of 5Cu-1B/Al ₂ O ₃ catalyst for glycerol hydrogenolysis (240 °C, 10 wt% aq. glycerol and WHSV 0.4 h ⁻¹).....	249
Figure 10.7 Effects of WHSV (0.05-0.8 h ⁻¹) on the performance of 5Cu-1B/Al ₂ O ₃ catalyst for glycerol hydrogenolysis (250 °C, 6 MPa H ₂ , 10 wt% aq. glycerol)	250

Figure 10.8. Influence of different grades of glycerol on glycerol conversion and product selectivities with 5Cu-1B/Al ₂ O ₃ catalyst (Reaction conditions: 250 °C, 10 wt% aq. glycerol feedstock, 6 MPa, WHSV 0.1 h ⁻¹).	252
Figure 10.9 Long term stability of 5Cu-1B/Al ₂ O ₃ catalyst in glycerol hydrogenolysis conducted at 250 °C, 6 MPa H ₂ flow and 0.1 h ⁻¹	253
Figure 10.10 TEM micrographs of fresh (a) spent catalyst (b) of 5Cu-1B/Al ₂ O ₃ after 70 h on stream.....	254
Figure 10.11 Thermogravimetric analysis of fresh and spent catalyst of 5Cu-1B/Al ₂ O ₃ after 70 h on stream.....	255
Figure 11.1 Process flow diagram for a large-scale solketal production process using crude glycerin.....	264

List of Schemes

Scheme 1.1 Scheme for production of glycerol.....	3
Scheme 2.1 Various glycerol conversion pathways	13
Scheme 2.2 Esterification of glycerol to mono, di and tri-esters.....	14
Scheme 2.3 Transesterification of glycerol to mono-ester	14
Scheme 2.4 Carboxylation of glycerol with carbon dioxide, dialkyl carbonate, and urea	18
Scheme 2.5 Synthesis of glycidol from glycerol carbonate.....	19
Scheme 2.6 Dehydration of glycerol to acrolein and acrylic acid	21
Scheme 2.7 Synthesis of glycerol ethers.....	22
Scheme 2.8 Synthesis of GTBE from glycerol.....	25
Scheme 2.9 Synthesis of glycerol telomers	26
Scheme 2.10 Chlorination of glycerol to epichlorohydrin.....	27
Scheme 2.11 Various oxidation products of glycerol.....	28
Scheme 2.12. Steam reforming of glycerol	30
Scheme 2.13 Acetalization of glycerol with different chemicals (adapted from reference with copyright permission from Elsevier) ⁶⁹	33
Scheme 2.14 Products of glycerol hydrogenolysis	35
Scheme 3.1 Glycerol as byproduct during biodiesel production	51
Scheme 3.2 Ketalization reaction between glycerol and acetone	53

Scheme 3.3 Schematic diagram of a multi-tray reaction distillation column for glycerol ketalization adopted from Clarkson <i>et al.</i> ⁵¹	61
Scheme 3.4 Mechanism proposed by Li <i>et al.</i> for the reaction of acetone and glycerol over Lewis acid catalyst (M is the metal atom) ^{64,68}	69
Scheme 3.5 Mechanism used by Nanda <i>et al.</i> for the reaction of acetone and glycerol over acid catalyst ⁵³	70
Scheme 4.1 Synthesis of propylene glycol from propylene glycol diacetate	87
Scheme 4.2 Different processes for the production of propylene oxide – precursor for propylene glycol: (A) Styrene monomer process; (B) Anthraquinone process; (C) tert-butyl alcohol process; (D) Cumene hydroperoxide process; (E) Chlorohydrin process ..	89
Scheme 4.3 Reaction pathway to the formation of propylene glycol from glycerol proposed by Montassier <i>et al.</i> ⁸⁶	107
Scheme 4.4 Reaction pathway to the formation of propylene glycol from glycerol proposed by Dasari <i>et al.</i> ^{23,54}	107
Scheme 4.5 Reaction pathway to the formation of propylene glycol from glycerol proposed by Chaminand <i>et al.</i> ⁵⁴	108
Scheme 5.1 Ketalization reaction between glycerol and acetone	123
Scheme 5.2 Mechanism of ketalization reaction of glycerol and acetone	131
Scheme 9.1 Reaction scheme of ketalization of glycerol with acetone.	217
Scheme 10.1 Hydrogenolysis of glycerol to different chemicals	236

Abbreviations

Abbreviation	Meaning
APR	Aqueous Phase Reforming
CTAB	Cetyl Trimethyl Ammonium Bromide
DHA	Dihydroxy Acetone
EG	Ethylene Glycol
FAME	Fatty Acid Methyl Ester
FFA	Free Fatty Acid
FTIR	Fourier Transform Infrared Spectroscopy
GC-MS/FID	Gas Chromatography -Mass Spectrometry/ Flame Ionization Detector
GTBE	Glycerol Tertiary Butyl Ether
ICP-AES	Inductive Coupled Plasma –Atomic Emission Spectroscopy
MTBE	Methyl Tertiary Butyl Ether
NMR	Nuclear Magnetic Resonance
PDO	Propanediol
PG	Propylene Glycol
SR	Steam Reforming
TEM	Transmission Electron Microscopy

TEOS	Tetra Ethyl Ortho Silicate
TGA	Thermogravimetric analysis
TPD	Temperature Programmed Desorption
TPR	Temperature Programmed Reduction
UV-Vis	Ultraviolet-Visible Spectroscopy
WHSV	Weight Hour Space Velocity
XRD	X-Ray Diffraction

Chapter 1

1 Introduction

1.1 Background

Glycerol (propane-1, 2, 3-triol) is a well-known chemical, discovered in 1779 by the Swedish chemist Carl Wilhelm Scheele during the alkali treatment of natural oils. However, the discovery of glycerol had no further impact up to 1866, until the production of dynamite by the Nobel brothers. At the end of the nineteenth century the rapid growth in the processing of natural oils and fats resulted in the production of large amount glycerol.¹

Glycerol is the simplest trihydric alcohol which is colorless, hygroscopic and sweet tasting in its pure form. Some of the properties of glycerol are given in Table 1.1.

Table 1.1. Properties of Glycerol²

Chemical formula	$C_3H_8O_3$
Molecular weight	92.09 g mol^{-1}
Density	1.261 g cm^{-3}
Boiling point (1 atm)	$290 \text{ }^\circ\text{C}$
Melting point	$18.17 \text{ }^\circ\text{C}$
Freezing point (66.7 % glycerol solution)	$-46.5 \text{ }^\circ\text{C}$
Viscosity (20 °C)	1499 centipoises
Specific heat (26 °C)	$0.579 \text{ cal/g/}^\circ\text{C}$
Flash point (99 % glycerol)	$177 \text{ }^\circ\text{C}$
Auto ignition point (on glass)	$429 \text{ }^\circ\text{C}$
Surface tension (20 °C)	63.4 dynes cm
Dissociation constant as weak acid	0.07×10^{-12}
Electrical conductivity (20 °C)	$0.1 \text{ } \mu\text{S}\cdot\text{cm}^{-1}$
Molar heat of solution	1381 Cal
Thermal conductivity (0 °C)	$0.000691 \text{ Cal/ sec/ cm/}^\circ\text{C}$

Heat of combustion	397.0 kcal/mol
--------------------	----------------

Pure glycerol has a wide range of applications primarily in pharmaceuticals, food and beverages and as a platform for different chemicals. The detailed applications of glycerol in different fields are given in Figure 1.1.

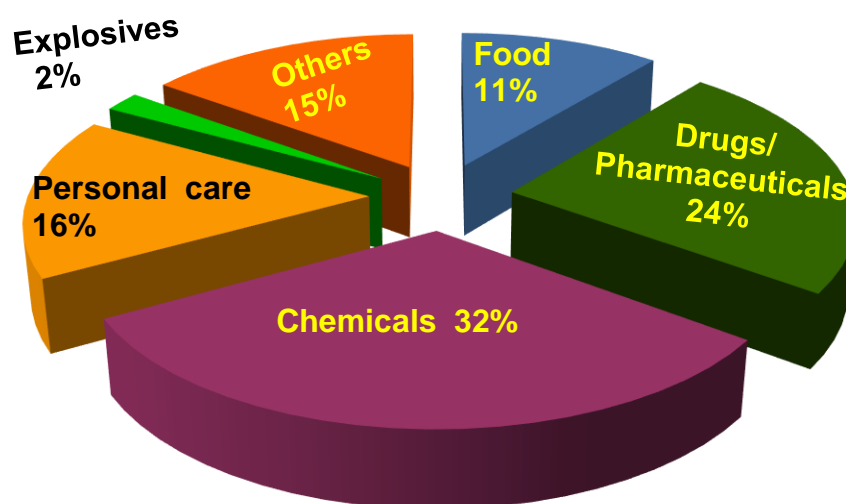


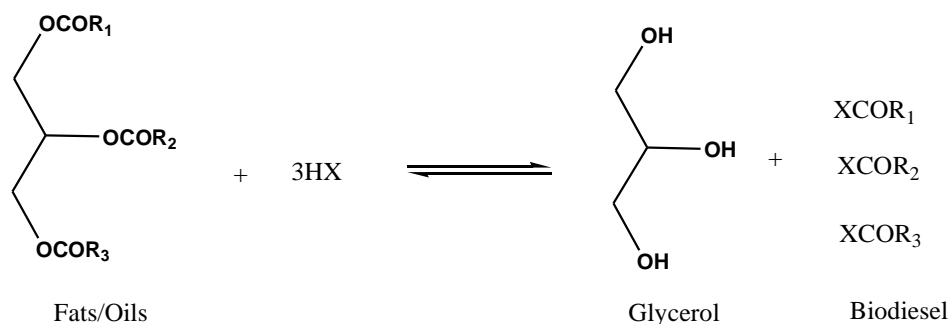
Figure 1.1 Applications of glycerol in different fields²

1.2 Sources of glycerol

Today glycerol is found in market in two forms, synthetic glycerol and natural glycerol. Synthetic glycerol is produced by the chemical conversion of propylene and constitutes around 10% of the total glycerol market. Natural glycerol is produced as a by-product in oleo-chemical industry mainly from biodiesel production. Biodiesel is a renewable fuel produced by the reaction between fats or oils with simple alcohols.³ The primary by-product of this process is crude glycerol. The only US supplier of synthetic glycerol, Dow

Chemical of Freeport Texas, closed its US plant in January 2006 due to the influx of this biodiesel derived crude glycerol.⁴

Nowadays the majority of the glycerol available on the market is from purification of crude glycerol. Crude glycerol is produced from fats and oils by three different processes: saponification, hydrolysis and transesterification, as shown in Scheme 1.1. Saponification of fats and oils with alkali yields glycerol and soap (X= ONa, OK in the Scheme 1.1).



Scheme 1.1 Scheme for production of glycerol

Hydrolysis yields glycerol and fatty acids (X= OH in Scheme 1.1), and transesterification yields glycerol and fatty acid methyl esters (FAME) known as biodiesel (X= OCH₃, OC₂H₅ in Scheme 1.1). Crude glycerol contains impurities due to the presence of un-reacted reactants (methanol or ethanol, and alkali), salts and soaps.⁵ These impurities need to be removed for high value applications of glycerol.

The environmental impacts of the fossil fuels are the main factors to draw the attention towards bio-fuels such as bio-ethanol and biodiesel.⁶ In 2005, the biodiesel production in Canada was 11 million US gallons.⁷ This value increased five-fold by 2010, when biodiesel production in Canada had grown to over 55 million US gallons.⁷ The biodiesel production in US is much higher than in Canada, and it is expected that above 10 billion US gallons of biodiesel per year will be produced by 2019.^{8,9}

1.3 Crude glycerol

The world-wide production of crude glycerol from the biodiesel industry is given in Table 1.2.⁹ As shown in the Table, the world wide generation of crude glycerol would reach 36 billion liters by 2018. As the biodiesel industry continues to grow, the increased amount of glycerol in the market is becoming a burden to producers who now have limited options for managing this co-product.^{10,11} The large scale producers are able to refine this co-product for the industrial applications, whereas small scale producers are unable to justify refining costs and instead pay a fee for glycerol removal.^{11,12}

Table 1.2 World scenario of crude glycerol (in billion liters)

Year	2003	2006	2009	2012	2015	2018
Canada	0.002	0.05	0.2	0.3	0.4	0.5
USA	0.03	0.8	1.6	3.6	3.9	4.0
World	-----	7.8	17.2	25.9	30.8	36

The current market value of pure glycerol is US \$0.30- 0.41 per pound and that of crude glycerol (having 80% pure glycerol) ranges from US \$0.04 – 0.09 per pound.^{10,13,14} After being implemented as automotive fuel, the production of biodiesel has been increased exponentially all over the world. Hence an increasingly large amount of glycerol is expected from the biodiesel industry. It is predicted that by 2020 the global production of glycerol will be 41.9 billion litres.⁹ This large amount of glycerol will significantly affect the glycerol price, once it enters into the market. Therefore value-added applications (e.g., in pharmaceuticals, chemicals, and materials, etc.) are essential for the sustainability of the biodiesel industry.

As discussed earlier, crude glycerol contains a large amount of impurities such as salts, soap and unused reactants. The primary components of crude glycerol include glycerol, methanol, salt, water and soap/ free fatty acids (FFAs). It has been reported that glycerol content in crude glycerol commonly ranges from 49% to 92%,^{15,16,17} methanol 0.01%-

38%,^{11,18} salt 1% - 12%,^{18,19} water 6%- 36%,^{17,20} and soap/ FFAs 1% -25% by weight.²¹ The presence of ash, heavy metals and lignin as impurities in smaller amount has also been reported. Due to the common practice of using alkaline catalysts in biodiesel process, a high pH (above 8) is characteristically observed for this by-product. Due to the above-mentioned contaminants, this renewable carbon source presents certain challenges for thermal and bioconversion processes such as plugging of reactors, deactivation of catalysts, and inhibition of bacterial activities.

1.4 Research objectives

From the above discussion it is concluded that a large amount of glycerol is entering into the market in near future and hence going to affect significantly the economy of biodiesel industry. In order to maintain the sustainability of the biodiesel industry the excess glycerol needs to be absorbed in high-value and high-volume applications. Fuel and polymer industries are among the fields where high-volume of glycerol can be used for value-added applications.²² Since glycerol cannot be used directly as fuel, its modification to different fuel additives such as triacetin, solketal, acetal and ethers is often considered.^{22,23,24} Among the fuel additives, solketal has demonstrated its potential as an efficient and eco-friendly fuel additive. Condensation of glycerol with acetone or formaldehyde has been reported.^{25,26} However, no proper kinetic and thermodynamic studies for the ketalization reaction of glycerol have been undertaken. Conventionally ketalization has been studied with batch reactors,²² and a semi-continuous reactor (continuous to acetone and water but batch to glycerol) for the synthesis of solketal.²⁵ Monbaliu *et al.* demonstrated a continuous process reactor for the synthesis of solketal, but a homogeneous acid catalyst (sulfuric acid) was used in the process, where the separation of catalyst and effluent disposal are the main challenges.²⁷ Furthermore the product needs to be neutralized. Therefore a continuous reactor technology which can address all these problems is essential for the ketalization of glycerol. Moreover, conversion of crude glycerol (a very cheap feedstock) to value-added chemicals has not been widely explored. As such, it is of great interest to study economically viable processes to utilize crude glycerol directly for chemical products.

The thermochemical conversion of glycerol to 1, 2-propanediol has been reported,^{28,29} most in batch type of reactors. Therefore in-expensive and continuous-flow processes are

required for the efficient conversion of glycerol to 1, 2-propanediol and other chemicals such as solketal.

The research work was to address the aforesaid shortcomings for the conversion of glycerol to different value-added products and to develop an inexpensive continuous-flow process for the conversion of glycerol to solketal - an oxygenated fuel additive, and 1, 2-propanediol –a polymer component. The detailed objectives of this thesis work were:

1. Thermodynamic and kinetic studies for the synthesis of solketal from glycerol using a batch reactor.
2. Development of an energy efficient and economically viable technology for continuous production of solketal from glycerol (both pure and crude glycerol) using a flow-type reactor with heterogeneous catalysts.
3. Investigation of the effect of process parameters and their optimization for the solketal production from glycerol
4. Continuous conversion of glycerol to 1, 2-propanediol using a flow reactor with heterogeneous catalysts.

1.5 Thesis structure

This thesis follows the “Integrated-Article Format” as outlined in the UWO Thesis Regulation. Chapter 1 gives a general introduction of the thesis work. The literature review is divided into three chapters; namely chapter 2, 3 and 4. Chapter 2 gives a general overview of the catalytic conversion of glycerol to various value-added chemicals. Chapter 3 and 4 outlines the recent advancements in the selective conversion of glycerol to solketal- an oxygenated fuel additive, and propylene glycol- a polymer component, respectively.

Chapter 5 describes the thermodynamic and kinetic studies of the ketalization reaction of glycerol and acetone over Amberlyst-35 in a batch reactor. The rate of the reaction is modeled according to Langmuir-Hinshelwood rate expression. The rate and equilibrium constants at different conditions are obtained and reported.

Chapter 6 reports the development of a continuous flow reactor for the synthesis of solketal using different heterogeneous catalysts. The effects of different process parameters on the glycerol conversion and product yield are investigated.

Chapter 7 describes the optimization of the flow process for ketalization of glycerol over Amberlyst-36 for the synthesis of solketal using surface response methodology (SRM). The comparison between the experimental and the model results is provided. The stability of the catalyst, influence of impurities on the product yield and feasibility of the process for commercialization are also discussed.

Chapter 8 presents an efficient method for purification of crude glycerol by acid treatment. Effects of different acids (hydrochloric acid, sulfuric acid, and phosphoric acid) on the crude glycerol purification efficiency are discussed. Also, a comparison between the properties of commercially available pure glycerol and the purified crude glycerol is provided.

Chapter 9 reports the development of a novel continuous-flow reactor consisting of 2 parallel guard reactors and a main pack-bed catalytic reactor for continuous ketalization of pure, crude and purified glycerol. The stability of the catalyst is investigated. The on-line regeneration and simultaneous ketalization is demonstrated in this novel flow reactor.

Chapter 10 investigates selective conversion of glycerol to propylene glycol (1, 2-propanediol, 1, 2-PDO) in a packed-bed flow reactor. Effects of process parameters on the conversion and product yield and selectivity are reported. Catalyst stability and causes of catalytic deactivation are discussed.

Chapter 11 reports a techno-economic study for a conceptually designed integrated process for the production of solketal using crude glycerol as the feedstock. Two integrated processing units of the process: pretreatment and production units are described in details with an economical feasibility analysis performed. The profit of the new process using crude glycerol is calculated and compared with that using commercially available pure glycerol as the feedstock.

Chapter 12 concludes the whole thesis and makes recommendations for future study in this area.

References

1. Glycerol | 56-81-5. Available at:
http://www.chemicalbook.com/ChemicalProductProperty_EN_CB5339206.htm.
Accessed January 31, 2015.

2. Pagliaro M, Ciriminna R, Kimura H, Rossi M, Della Pina C. From glycerol to value-added products. *Angewandte Chemie (International ed. in English)* 2007;46(24):4434-40. doi:10.1002/anie.200604694.
3. Lin L, Cunshan Z, Vittayapadung S, Xiangqian S, Mingdong D. Opportunities and challenges for biodiesel fuel. *Applied Energy* 2011;88(4):1020-1031. doi:10.1016/j.apenergy.2010.09.029.
4. Biodiesel Magazine- The latest news and data about biodiesel production. Available at: <http://www.biodieselmagazine.com/articles/1123/combating-the-glycerin-glut/>. Accessed January 30, 2015.
5. Behr A, Eilting J, Irawadi K, Leschinski J, Lindner F. Improved utilisation of renewable resources: New important derivatives of glycerol. *Green Chemistry* 2008;10(1):13. doi:10.1039/b710561d.
6. Subramaniam R, Dufreche S, Zappi M, Bajpai R. Microbial lipids from renewable resources: production and characterization. *Journal of Industrial Microbiology & Biotechnology* 2010;37(12):1271-87. doi:10.1007/s10295-010-0884-5.
7. Canadian Renewable Fuels Association. Available at: <http://greenfuels.org/>. Accessed January 30, 2015.
8. National Biodiesel Board - Jefferson City Missouri. Available at: <http://www.nbb.org/>. Accessed January 30, 2015.
9. Organization for Economic Co-operation and Development (OECD) and the Food and Agriculture Organization (FAO) of the United Nations, 2011-2020. Available at: <http://www.agri-outlook.org/48202074.pdf>. Accessed April 9, 2015.
10. Johnson DT, Taconi KA. The glycerin glut : Options for the value-added conversion of crude glycerol resulting from biodiesel production. *Environmental Progress* 2007;26(4):338-348. doi:10.1002/ep.10225
11. Thompson JC, He BB. Characterization of crude glycerol from biodiesel production from multiple feedstocks. *Applied Engineering in Agriculture* 2006;22(2):261-265. doi:10.1021/jf3008629.
12. Athalye SK, Garcia RA, Wen Z. Use of biodiesel-derived crude glycerol for producing eicosapentaenoic acid (EPA) by the fungus *Pythium irregulare*. *Journal of Agricultural and Food Chemistry* 2009;57(7):2739-44. doi:10.1021/jf803922w.
13. Yang S, Wang M, Liang Y, Sun J. Eco-friendly one-pot synthesis of acetals and ketals by heterogeneously catalyzed liquid-solid phase reaction. *Rare Metals* 2006;25(6):625-629. doi:10.1016/S1001-0521(07)60003-5.
14. B. Sims. Clearing the way for byproduct quality. 2011. <http://www.biodieselmagazine.com/articles/8137/clearing-the-way-forbyproduct->

quality|Reference|Scientific Research Publish. Available at:
<http://www.ljemail.org/reference/ReferencesPapers.aspx?ReferenceID=820106>.
Accessed December 3, 2014.

15. Rywińska A, Rymowicz W. High-yield production of citric acid by *Yarrowia lipolytica* on glycerol in repeated-batch bioreactors. *Journal of Industrial Microbiology & Biotechnology* 2010;37(5):431-5. doi:10.1007/s10295-009-0687-8.
16. Liu X, Jensen PR, Workman M. Bioconversion of crude glycerol feedstocks into ethanol by *Pachysolen tannophilus*. *Bioresource Technology* 2012;104:579-86. doi:10.1016/j.biortech.2011.10.065.
17. Liang Y, Cui Y, Trushenski J, Blackburn JW. Converting crude glycerol derived from yellow grease to lipids through yeast fermentation. *Bioresource Technology* 2010;101(19):7581-6. doi:10.1016/j.biortech.2010.04.061.
18. Saenge C, Cheirsilp B, Suksaroge TT, Bourtoom T. Potential use of oleaginous red yeast *Rhodotorula glutinis* for the bioconversion of crude glycerol from biodiesel plant to lipids and carotenoids. *Process Biochemistry* 2011;46(1):210-218. doi:10.1016/j.procbio.2010.08.009.
19. André A, Diamantopoulou P, Philippoussis A, Sarris D, Komaitis M, Papanikolaou S. Biotechnological conversions of bio-diesel derived waste glycerol into added-value compounds by higher fungi: production of biomass, single cell oil and oxalic acid. *Industrial Crops and Products* 2010;31(2):407-416. doi:10.1016/j.indcrop.2009.12.011.
20. Papanikolaou S, Aggelis G. Modelling aspects of the biotechnological valorization of raw glycerol: production of citric acid by *Yarrowia lipolytica* and 1,3-propanediol by *Clostridium butyricum*. *Journal of Chemical Technology & Biotechnology* 2003;78(5):542-547. doi:10.1002/jctb.831.
21. Chatzifragkou A, Makri A, Belka A, et al. Biotechnological conversions of biodiesel derived waste glycerol by yeast and fungal species. *Energy* 2011;36(2):1097-1108. doi:10.1016/j.energy.2010.11.040.
22. Deutsch J, Martin a, Lieske H. Investigations on heterogeneously catalysed condensations of glycerol to cyclic acetals. *Journal of Catalysis* 2007;245(2):428-435. doi:10.1016/j.jcat.2006.11.006.
23. Agirre I, Güemez MB, Ugarte a., et al. Glycerol acetals as diesel additives: Kinetic study of the reaction between glycerol and acetaldehyde. *Fuel Processing Technology* 2013;116:182-188. doi:10.1016/j.fuproc.2013.05.014.
24. Silva PHR, Gonçalves VLC, Mota CJ a. Glycerol acetals as anti-freezing additives for biodiesel. *Bioresource Technology* 2010;101(15):6225-9. doi:10.1016/j.biortech.2010.02.101.

25. Clarkson JS, Walker AJ, Wood MA. Continuous reactor technology for ketal formation : An improved synthesis of solketal. *Organic Process Research & Development* 2001;5(6):630-635. doi:10.1021/op000135p.
26. Agirre I, García I, Requies J, et al. Glycerol acetals, kinetic study of the reaction between glycerol and formaldehyde. *Biomass and Bioenergy* 2011;35(8):3636-3642. doi:10.1016/j.biombioe.2011.05.008.
27. Monbaliu J-CM, Winter M, Chevalier B, et al. Effective production of the biodiesel additive STBE by a continuous flow process. *Bioresource Technology* 2011;102(19):9304-7. doi:10.1016/j.biortech.2011.07.007.
28. Chaminand J, Djakovitch L auren., Gallezot P, Marion P, Pinel C, Rosier C. Glycerol hydrogenolysis on heterogeneous catalysts. *Green Chemistry* 2004;6(8):359. doi:10.1039/b407378a.
29. Gandarias I, Fernández SG, El Doukkali M, Requies J, Arias PL. Physicochemical Study of Glycerol Hydrogenolysis Over a Ni–Cu/Al₂O₃ Catalyst Using Formic Acid as the Hydrogen Source. *Topics in Catalysis* 2013;56(11):995-1007. doi:10.1007/s11244-013-0063-9.

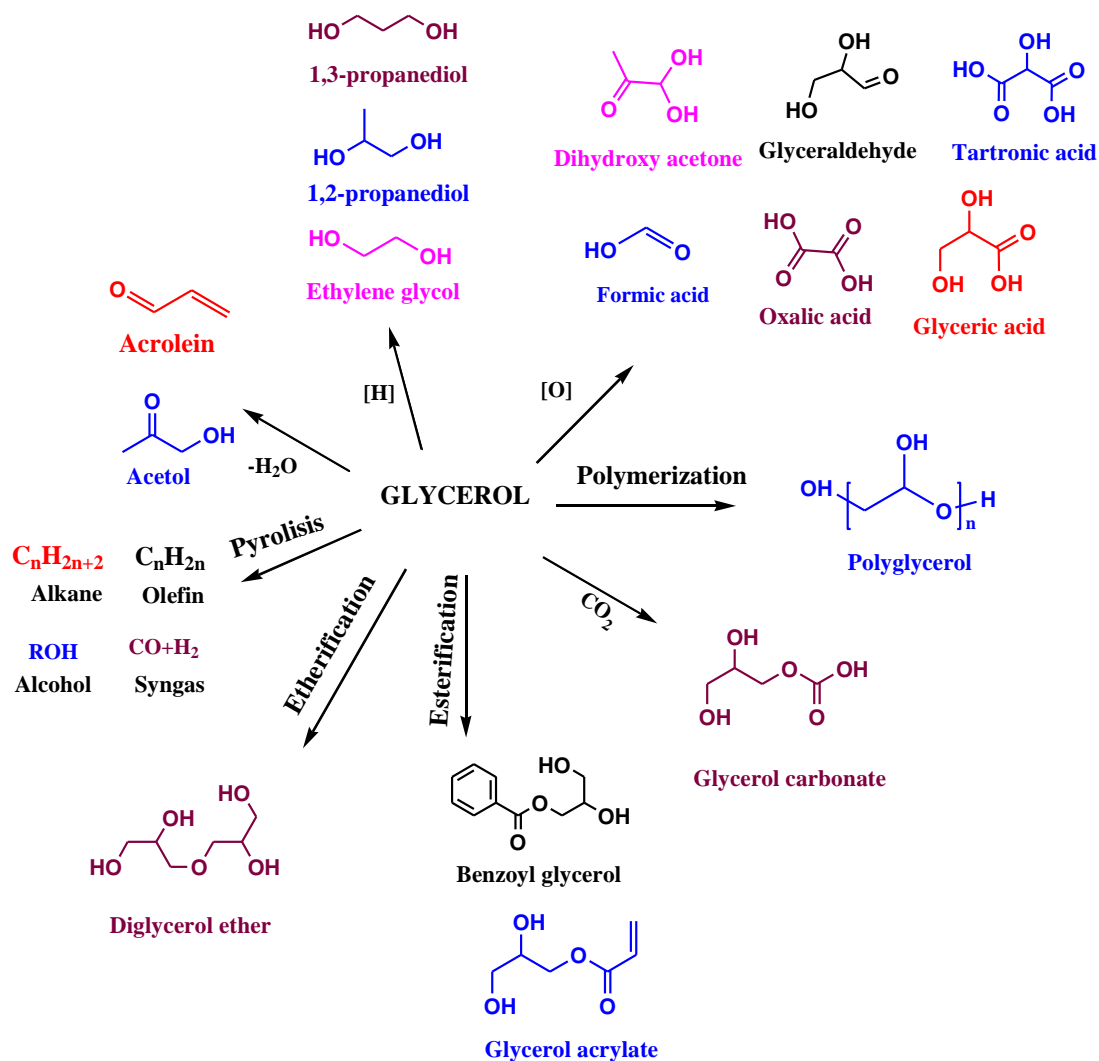
Chapter 2

2 General literature review

In recent years, the production of biodiesel has increased dramatically in different parts of the world, resulting in a large amount of glycerol as byproduct from the process.¹ It was predicted that the world wide generation of crude glycerol will reach 36 billion liters by 2018.² As the biodiesel industry continues to grow, the increased amount of glycerol in the market is becoming a burden to producers who now have limited options for managing this byproduct. Valorization of glycerol is thus needed to enhance the sustainability of the biodiesel industry.³

The glycerol obtained from biodiesel industry is commonly known as crude glycerol. It contains a number of impurities including water, methanol, inorganic salts, free fatty acids, un-reacted glycerides, methyl esters and other organic materials.^{4,5,6} The composition of crude glycerol depends on the nature of feedstock and the process used for production of biodiesel.⁷ As such, the crude glycerol without purification has very limited applications.

Glycerol, the simplest tri-hydroxy alcohol has many potential applications. The multifunctionality of glycerol makes it a suitable bio-renewable platform chemical. The different chemical reaction pathways of glycerol are given in Scheme 2.1. This chapter overviews the state-of-the-art of different catalytic processes for glycerol conversion, e.g., esterification, etherification, oxidation, dehydration, acetalization, hydrogenolysis, chlorination and catalytic reforming to value added chemicals.



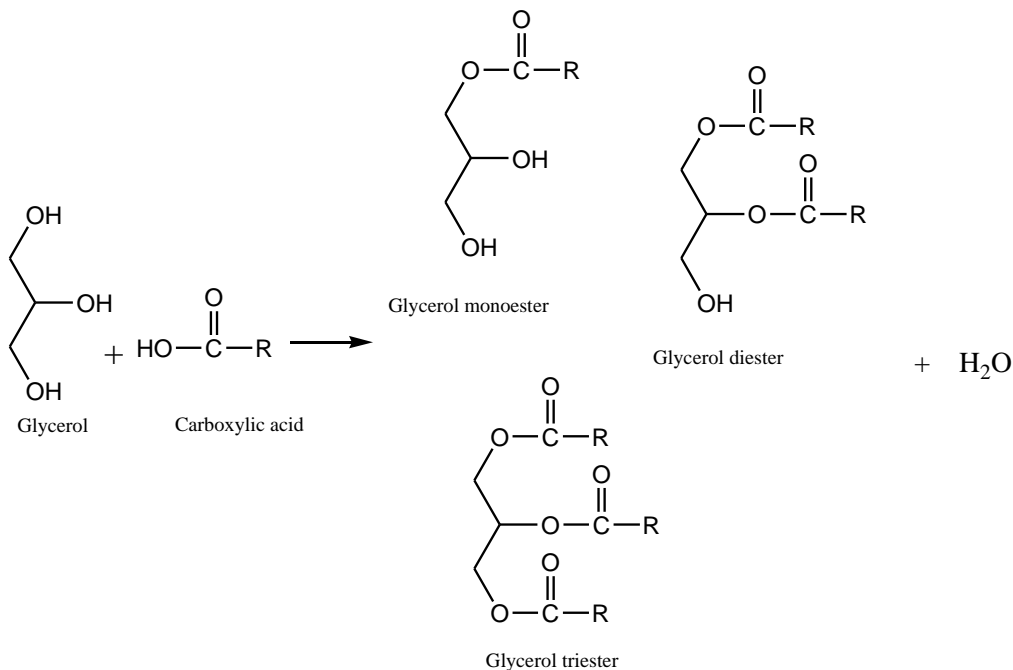
Scheme 2.1 Various glycerol conversion pathways

2.1 Catalytic processes for conversion of glycerol into various products

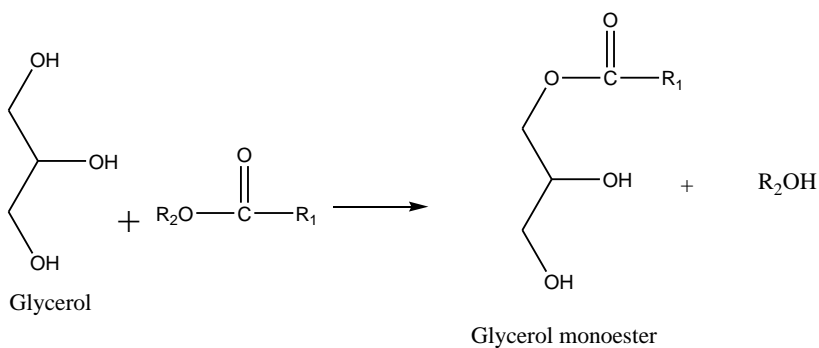
2.1.1 Esterification of glycerol

The esterification of glycerol with carboxylic acids yields glycerol mono, di and tri-esters. A schematic reaction of glycerol with carboxylic acid is shown in Scheme 2.2. The glycerol

mono-esters and their derivatives are widely used as emulsifier in food, pharmaceuticals and cosmetics industries.⁸ The mono-esters can be synthesized by the transesterification of glycerol as shown in Scheme 2.3



Scheme 2.2 Esterification of glycerol to mono, di and tri-esters



Scheme 2.3 Transesterification of glycerol to mono-ester

Table 2.1 Performance of various heterogeneous catalysts in esterification of glycerol to mono-esters (adopted with permission⁹)

Catalysts	Reactants	Molar ratio of reactants	Reaction conditions	%C	%S	Ref
ZnO	glycerol + methylstearate	1	493 K, 6 h	18	80	10

MgO	glycerol + methylstearate	1	493 K, 6 h	83	42	10
La ₂ O ₃	glycerol + methylstearate	1	493 K, 6 h	97	28	10
CeO ₂	glycerol + methylstearate	1	493 K, 6 h	4	100	10
ZnO	glycerol + stearic acid	1	160K, 16 h	63	83	11
ZnO	glycerol + lauric acid	1	433K, 16 h	56	73	11
ZnO	glycerol + oleic acid	1	433K, 16 h	45	91	11
MgAl-MCM-41	glycerol + lauric acid	3	493K, 20 h	80	70	12
ZnO	glycerol+ myristic acid	3	493K, 33 h	80	62	12
ZnO	glycerol+ stearic acid	3	493K, 44 h	80	50	12
Mg-Al hydrotalcite (calcined)	glycerol+ methyl stearate	6	473K, 8 h	95	67	13
Mg-Al hydrotalcite (calcined-rehydrated)	glycerol+ methyl stearate	6	473K, 8 h	98	80	13
KF/Al ₂ O ₃	glycerol+ methyl stearate	6	473	68	69	13
USY (Si/Al=14)	glycerol+ oleic acid	1	373K, 24 h	8	55	14
Beta (Si/Al=13)	glycerol+ oleic acid	1	373K, 24 h	9	64	14
Al-MCM-41 (Si/Al=15)	glycerol+ oleic acid	1	373K, 24 h	6	96	14
MCM-41 -F	glycerol+ oleic acid	1	373K, 24 h	11	68	14
MCM-41 -C	glycerol+ oleic acid	1	373K, 24 h	24	69	14
Phenyl-MCM-41	glycerol+ oleic acid	1	393K, 8 h	25	67	14
Methylsulfonic/phenylsulfonic-MCM-41	glycerol+ oleic acid	1	393K, 8 h	39	69	14

Barrault and co-workers reported a one pot process for transesterification of glycerol over a homogeneous catalyst (guanidine),¹⁵ in which the reaction was carried out at 110 °C for 3.5 h with the product selectivity of 64%, 32% and 4% for mono, di- and tri-esters, respectively. The authors observed a reduction in the selectivity of mono-esters from 64% to 47% by replacing the homogeneous catalyst with a heterogeneous catalyst; however a

reverse trend was observed for di and tri-esters. The authors attributed it to the steering effect caused by the hydrophobicity of the long alkyl chain. The use of basic catalysts such as MgO, CeO₂, La₂O₃, and ZnO, Mg-Al hydrotalcites, and MCM-41 has been reported for the transesterification of glycerol.¹⁶ The recent development in the synthesis of glycerol mono-esters over heterogeneous catalysts is summarized in Table 2.1. The use of organic solvents in the process was found to improve the product selectivity.¹¹ Transesterification in the absence of solvent has also been widely studied.¹⁰ Barrault *et al.* investigated the effect of solvent on esterification of glycerol and observed a very slow reaction rate in solvents that have low solubility for methyl esters, whereas a high reaction rate, similar to that of the reaction without solvent, was achieved in the solvents with high solubility for methyl esters.¹⁵

Perez-Pariente *et al.* investigated esterification of glycerol with oleic acid at an equimolar ratio using 5 wt% of functionalized mesoporous materials as catalyst at 100 °C.¹⁴ The effects of catalyst synthesis procedure, hydrophobicity and catalyst structure were also reported. Basic hydrotalcites have been used as catalysts for the conversion of glycerol to esters by Corma *et al.*¹³ The authors compared the effects of Lewis and Brønsted basic catalysts on the yield of mono-esters and found that under similar reaction conditions a Brønsted basic catalyst produced a higher yield (80%) than a Lewis basic catalyst (60%).

Moreover, the glycerol acetins; mono, di and tri-acetins (whose structure is illustrated in Figure 2.1) are important chemicals for textile industries. These can be synthesized by esterification of glycerol with acetic acid,¹⁷ where glycerol was first reacted partially with acetic acid and the reaction mixture reacted with acetic anhydride to form acetins.

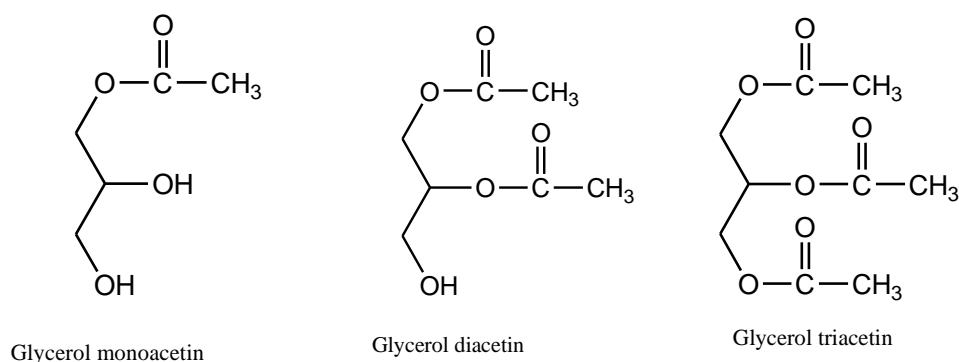
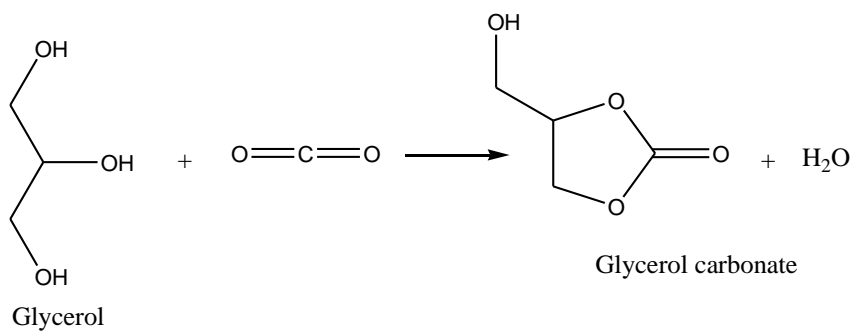
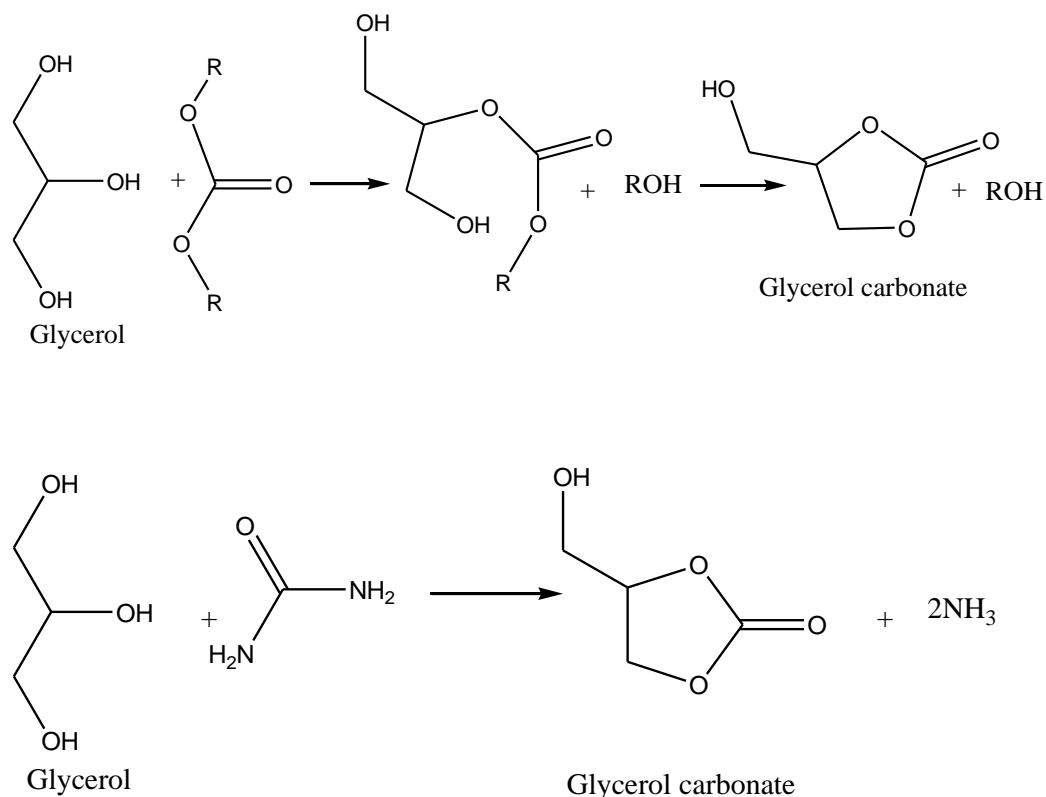


Figure 2.1 Structure of glycerol acetins

2.1.2 Carboxylation of glycerol

Glycerol carbonate (4-hydroxymethyl-1,3-dioxolan-2-one) is a relatively new material in chemical industry, mainly used as a solvent for different applications (e.g., varnishes, glues, cosmetics, pharmaceuticals, etc.), a monomer for the synthesis of polymers, an ideal component for gas separation membranes, and a lubricant for metallic surfaces, etc.⁹



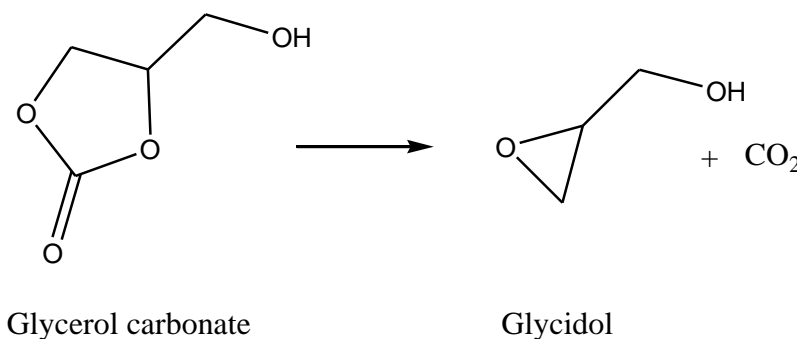


Scheme 2.4 Carboxylation of glycerol with carbon dioxide, dialkyl carbonate, and urea

Glycerol carbonate is usually prepared from ethylene oxide via a two-step process. In this method, the first step involves the formation of ethylene carbonate, which reacts subsequently with glycerol to form glycerol carbonate. However, glycerol carbonate can be synthesized in an economical way via a single-step process as shown in Scheme 2.4.^{18,19} Aresta *et al.* investigated the carboxylation of glycerol over di(*n*-butyl)tin dimethoxide, di(*n*-butyl)tin oxide and tin dimethoxide catalysts to synthesize glycerol carbonate in a single step. The authors reported a maximum glycerol conversion of 7% with di(*n*-butyl)tin dimethoxide among other catalysts under similar reaction conditions (453 K, 15 h, 5 MPa of CO₂, 0.003 moles of catalyst and 0.044 moles of glycerol).¹⁸ The use of supercritical

carbon dioxide for the reaction was investigated by Ballivet-Tkatchenko and co-workers using tin-based catalysts.²⁰ The synthesis of glycerol carbonate by reacting glycerol and urea over zinc sulfate has been reported by Yoo and Mouloungui,²¹ where a glycerol carbonate yield of 86% at 140 °C was reported.

Catalytic decomposition of glycerol carbonate yields glycidol, a monomer used for synthesis of a variety of polymers (Scheme 2.5). For instance, the decomposition over zeolite-A at 180 °C and 35 mbar produces a high yield of glycidol (86%) of 99% purity.²² Polymerization of glycidol produces polyglycerol that can be used for a variety of applications ranging from cosmetics to controlled drug release.²²



Scheme 2.5 Synthesis of glycidol from glycerol carbonate

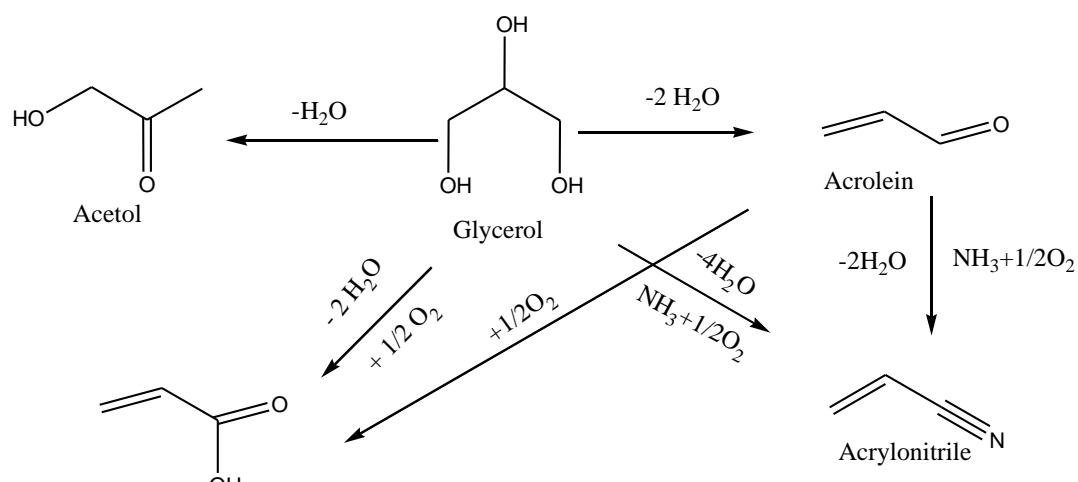
2.1.3 Dehydration of glycerol

The important dehydration products of glycerol are acrolein and acetol, while acrylic acid and acrylonitrile can also be produced by oxydehydration process of glycerol, as illustrated in Scheme 2.6. Acrolein is an important chemical mainly used for the production of acrylic acid esters, super-absorber polymers, and detergents, as well as a herbicide.²³ Dehydration of glycerol for acrolein is usually carried out either in liquid or vapor phase over acidic catalysts. The use of homogeneous catalyst (H_2SO_4) in the process with 74% acrolein yield has been reported.²⁴ Buhler *et.al.* reported 12% acrolein yield in a process using hot-

compressed water as solvent at its near supercritical condition (300 °C, 300 bar) without any catalyst.²⁵ Recently, the use of heterogeneous catalysts such as zeolites, Nafion, alumina, silicotungstic acids, or other acid salts (with a Hammett acidity function of less than 2) in the process have been reported with an excellent acrolein yield of more than 70% at temperatures in the range of 250-340 °C with complete glycerol conversion.²⁶

Acrylic acid is the oxydehydration product of glycerol used in adhesive, paint, plastic and rubber materials. The traditional process for the synthesis of acrylic acid is oxidation of acrolein,^{27,28} but the process has some serious environmental concerns.²⁹ In contrast, the oxydehydration process is considered a green process for the synthesis of acrylic acid in which glycerol is catalytically dehydrated in oxygen environment. A series of vanadium based catalysts have been reported for the oxydehydration of glycerol.^{27,28,30} More recently, oxydehydrations of glycerol over a tungsten-vanadium catalyst and molybdenum – vanadium based catalysts have demonstrated a yield of 25% and 28% of acrylic acid, respectively (Conditions: T= 573 K, GHSV= 2800 h⁻¹, Glycerol concentration= 40 wt%, Feed= N₂/O₂/H₂O/Glycerol in the ratio of 72/6/19/3, respectively).^{28,30} Chiericato *et al.* developed a W-V-Nb based catalyst and reported 34% yield of acrylic acid at similar conditions as listed above.³¹

Acrylonitrile is the monomer used for the synthesis of polyacrylonitrile and usually produced from petroleum resources (propylene). It can be synthesized from glycerol either in liquid or vapor phase.³² In this process glycerol first undergoes dehydration followed by ammoxidation of the dehydrated product.³³ Glycerol conversion of 83% with acrylonitrile selectivity of 58% has been reported in vapor phase over vanadium-antimony oxide based catalyst.³⁴

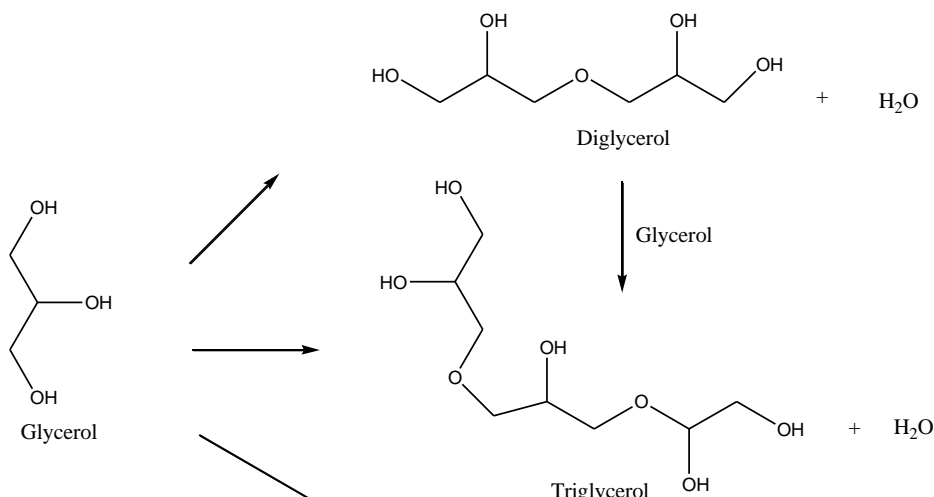


Scheme 2.6 Dehydration of glycerol to acrolein and acrylic acid

Acetol is an intermediate chemical compound for the production of propylene glycol. It can be produced by a reactive distillation, i.e., removal of a molecule of water from glycerol over a catalyst having low basic strength. Chiu *et al.* reported 32% yield of acetol with complete glycerol conversion at 493 K and ambient pressure in hydrogen atmosphere over Cu-based catalyst.³⁵ In another work, Vasconcelos and coworkers developed a CeO₂-ZrO₂ catalyst and demonstrated 94% glycerol conversion with 42% acetol selectivity.³⁶

2.1.4 Etherification of glycerol

Glycerol ethers such as diglycerol and triglycerols are formed by the linear combination of two and three glycerol molecules, respectively through their primary hydroxyl groups. The combination of more number of glycerol molecules by ether linkages (-O-) forms glycerol oligomers or polyglycerol as shown in Scheme 2.7.



Scheme 2.7 Synthesis of glycerol ethers

Glycerol ethers are one of the important chemical derivatives of glycerol used in various fields such as in cosmetics, food-additive, lubrication purposes, and fuel additives.³⁷ The synthesis of glycerol ethers have been reported by Cassel *et al.* and Ma'rquez Alvarez *et al.* using basic homogeneous catalysts.^{37,38} However, the use of heterogeneous catalysts is preferred since they can easily be separated from the products and give a high conversion of glycerol with high selectivity towards ethers.^{12,39,40} A comparison of typically used homogeneous and heterogeneous catalysts (acidic/basic) is given in Table 2.2.

Table 2.2 Comparison of homogeneous and heterogeneous catalysts for glycerol etherification (modified from reference⁴¹)

Catalyst	Type of catalyst	Conversion (%)	Selectivity (%)

			Digly -cerol	Trigl y- cerol	Tetrag l- lycerol	Higher oligomer s	
	Na ₂ CO ₃	Homogeneous	80 (8 h)	31	28	17	24
		s					
	Cs-MCM-41	Heterogeneous	95 (24 h)	59	30	11	<1
		us					
	Amberlyst- 16	Heterogeneous	35-40	85	15	<1	<1
		us					
	Amberlyst- 31	Heterogeneous	35-40	75	25	<1	<1
		us					

The above Table shows that under similar reaction conditions of temperature (533 K), pressure (ambient pressure) and amount of catalyst (2 wt% w.r.t.glycerol), the maximum glycerol conversion was 80% with the homogeneous catalyst, Na₂CO₃, and 95% with the heterogeneous catalyst, Cs-MCM-41. Moreover, contrary to the heterogeneous catalysts, a broader product distribution (from 31% of diglycerol to 24% of higher oligomers) was observed for homogeneous catalysts.

Sunder *et al.* reported the synthesis of hyper-branched polyglycerol ethers (Figure 2.2) from glycidol and trimethylolpropane.⁴² However, the hyper-branched polyglycerol is yet to be synthesized directly from glycerol.⁴³ Hyper-branched polyglycerol ethers can be used as a solvent to solubilise hydrophobic drugs.⁴⁴

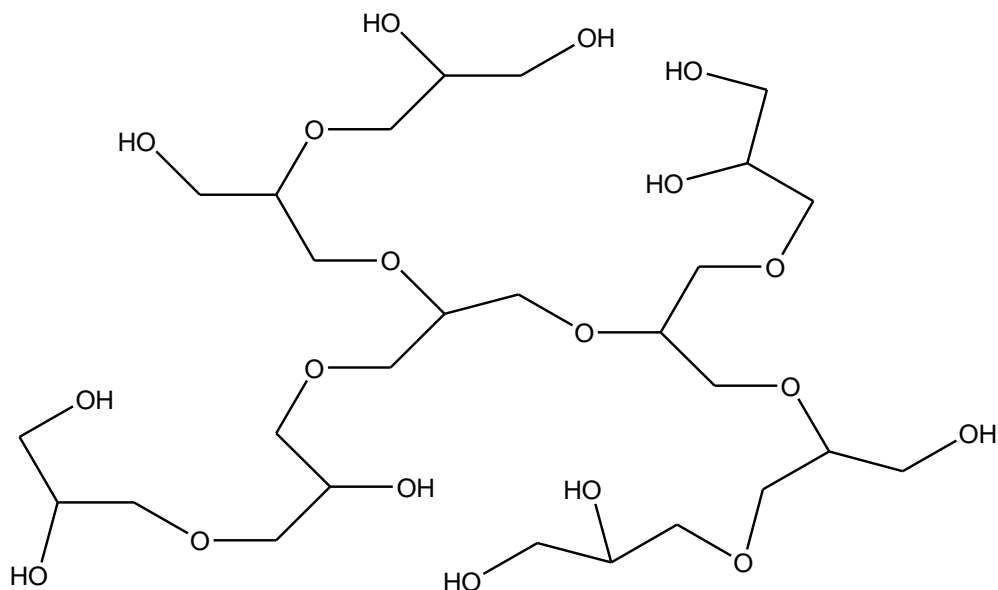
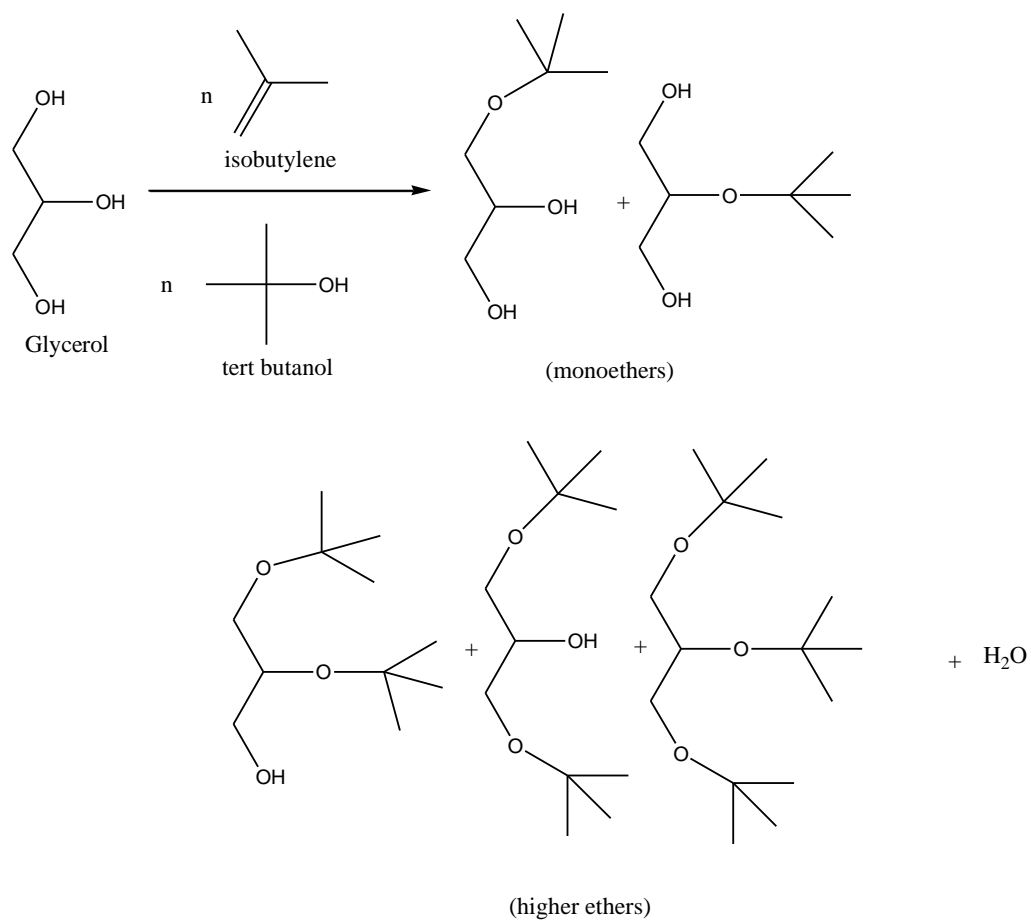


Figure 2.2. Hyper-branched polyglycerol

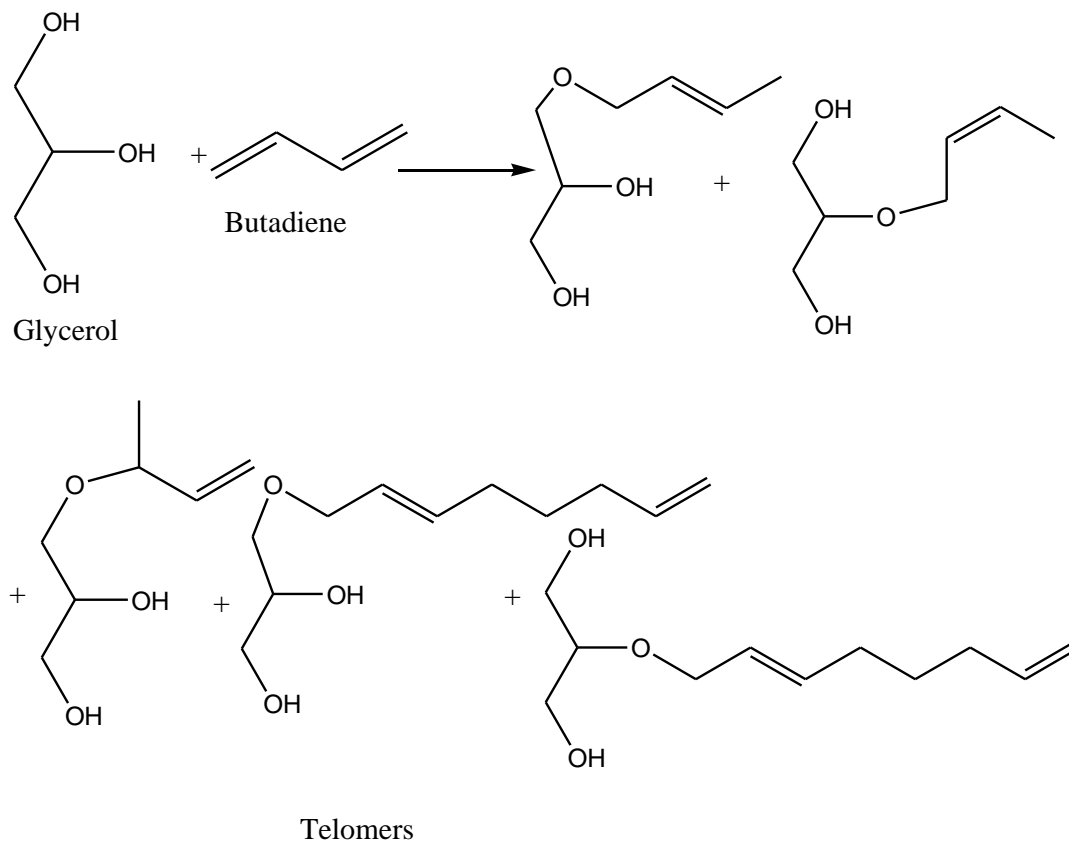
Moreover, glycerol alkyl ethers can be synthesized with the Williamson ether synthesis process by reacting sodium-glycerolate with an alkyl halide, or by the addition of a branched alkene to glycerol, or by condensation reaction between glycerol and aliphatic alcohol.⁴¹ Queste *et al.* produced glycerol monoethers as solvents or surfactants, by reacting 1, 2-isopropylidene glycerol (solketal) and different bromoalkanes in the presence of caustic potash.⁴⁵

It is well known that glycerol cannot be directly used as a fuel because of its very low heating value and its tendency to polymerize at elevated temperatures, which would thereby clog any engine. However, its etherification products such as glycerol tertiary butyl ether (GTBE) can be used as a valuable fuel additive. GTBE is synthesized by the reaction of glycerol with isobutylene or with tertiary butanol in the presence of an acid catalyst as shown in Scheme 2.8. The yield of GTBE could be maximized by carrying out the reaction in a two-phase reaction system: glycerol rich polar phase (with the acidic catalyst) and olefin-rich hydrocarbon phase from which the product ether can easily be separated out.²² GTBE (h-GTBE) has been considered to substitute methyl tertiary butyl ether (MTBE) as an octane –booster in gasoline.⁴⁶



Scheme 2.8 Synthesis of GTBE from glycerol

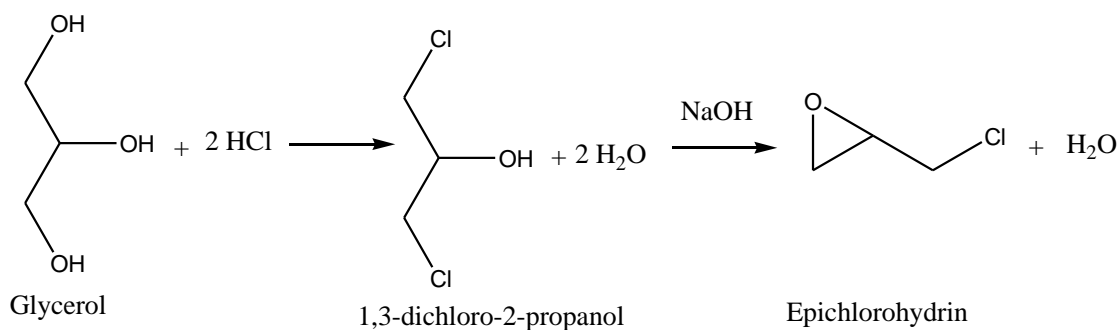
Glycerol reacts with butadiene in the presence of a transition metal catalyst such as palladium, nickel, etc. to produce alkenyl ethers known as telomers (Scheme 2.9) that can also be used as emulsifiers or surfactants.⁴⁷



Scheme 2.9 Synthesis of glycerol telomers

2.1.5 Chlorination of glycerol

Epoxides like epichlorohydrin can be synthesized from glycerol via a two-step reaction mechanism (Scheme 2.10). In the first step anhydrous hydrogen chloride reacts with glycerol to form 1, 3-dichloro-2-propanol at 110 °C. In the next step, 1, 3-dichloro-2-propanol reacts with sodium hydroxide to form epichlorohydrin. The process for synthesis of epichlorohydrin from glycerol is of more significance compared to the traditional propene-based process, owing to the use of renewable feedstock (glycerol) and less consumption of water in the conventional process.⁴⁸ Epichlorohydrin is widely used as a building block for epoxy resins and also a precursor for other polymers.



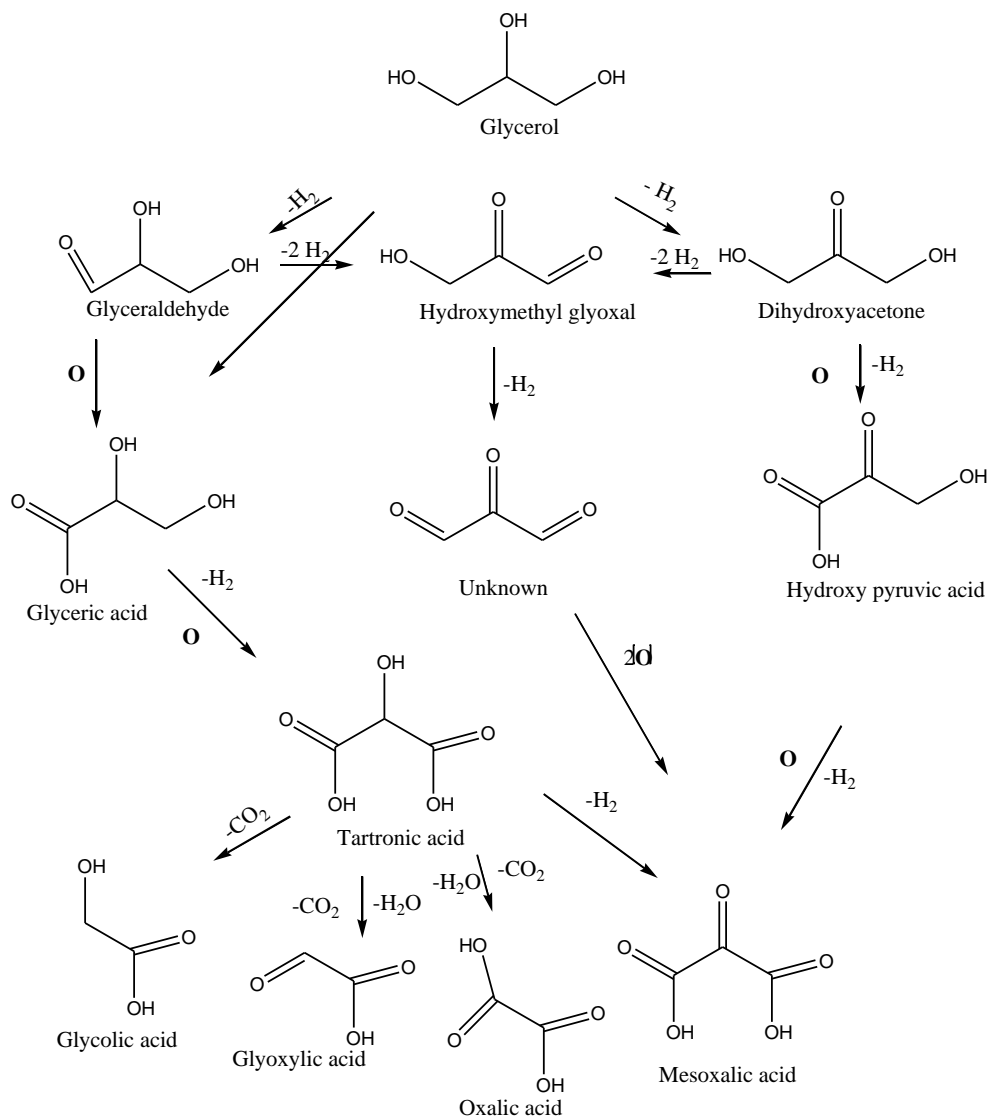
Scheme 2.10 Chlorination of glycerol to epichlorohydrin

2.1.6 Oxidation of glycerol

Glycerol can also directly be oxidized to a number of products (Scheme 2.11) using different oxidizing agents such as air, oxygen, and hydrogen peroxide. The products can be used as chemical intermediates or fine chemicals for the synthesis of polymers, biodegradable emulsifiers, cosmetics, pharmaceuticals and fabric softeners.⁹ Oxidation of one of the primary hydroxyl groups of glycerol in aqueous medium over a noble metal catalyst such as Au/C or Pt/C yields glyceraldehyde that can be further oxidized into glyceric acid. Glyceric acid yield over Au catalyst was reported to be 100% selective with 56% glycerol conversion at 60 °C, and 3 bar of oxygen after 3 h of reaction.^{49,50} Glyceraldehyde is often used as a standard to detect the optical activity of organic compounds (D and L- type).⁴¹

The selected results of catalytic oxidation of glycerol are comparatively summarized in Table 2.3. The oxidation of glycerol over Pd and Pt catalysts in alkaline medium gives glyceric acid as the main product with tartronic and oxalic acid as by-products. Further oxidation of glyceric acid yields hydroxyl pyruvic acid under same reaction conditions. Decarboxylation of tartronic acid generates glycolic acid, glyoxalic acid, oxalic acid and mesoxalic acid and some by-products such as formic acid and carbon dioxide.⁴⁸ Oxidation of both primary hydroxyl groups forms tartronic acid at a yield of 40% over Pt /CeO₂ at 323 K and a pH of 10-11.⁵¹ The major disadvantage of using noble metal catalyst for the

oxidation process that needs to be addressed is its tendency of deactivation (even at low partial pressure of oxygen).^{52,53}



Scheme 2.11 Various oxidation products of glycerol

Table 2.3 Selected results of catalytic oxidation of glycerol (adopted with permission)⁹

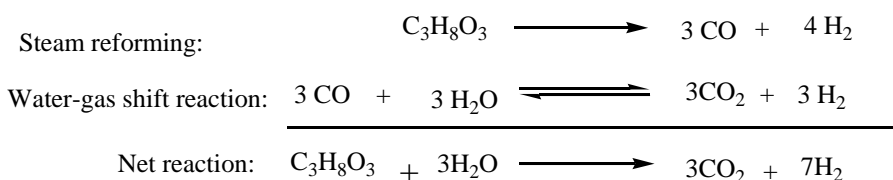
Catalysts	Oxidants	pH	Other reaction conditions	Conversion	Selectivity or yield	Ref
Pt/C	Air	2-4	10% gly, 323 K, 4 h	37%	4% (Y _{DHA})	54,55
Bi-Pt/C	Air	2-4	10% gly, 323 K, 4 h	30%	20% (Y _{DHA})	54,55
Pt-Bi/C	Air	N.A	50% gly, 323 K, O ₂ /gly(2mol)	80%	80% (S _{DHA})	54,55
Pd/C	Air	11	10% gly, 333 K, 5 h	100%	8% (S _{DHA}) 70% (S _{GLYAC})	56
Ti-Si	H ₂ O ₂	7	10 g gly, 353 K, 24 h	22%	37% (S _{GLYALD})	57
Au/C	O ₂	>7	0.3 M gly, 303 k, 20 h	100%	92% (S _{GLYAC})	58
Pt/C	Air	11	1 m GLY, 333 k, 21 h	60%	47.5% (S _{GLYAC})	59
Pd/graphite	O ₂	>7	0.3 M gly, 323 K, 1 h	90 %	62.4 % (S _{GLYAC})	60,61
Pd+Au/graphite	O ₂	>7	0.3 M gly, 323 K, 2 h	100%	39.1% (S _{GLYAC})	60,61
Pt/C	O ₂	>7	0.3 M gly, 323 K, 4 h	81.6%	50% (S _{GLYAC})	62
Au +Pt/C	O ₂	>7	0.3 M gly, 323 K, 4 h	69.3%	58.3 % (S _{GLYAC})	62
Au/C	O ₂	12	1.5 M gly, 333 K, 3 h	30%	75% (S _{GLYAC})	63
Au/C	O ₂	12	1.5 M gly, 333 K, 1.5 h	50%	26% (Y _{DHA}), 44% (Y _{HYPAC})	63
Au+Pt/C	O ₂	12	1.5 M gly, 333 K, 1.5 h	50%	36% (Y _{DHA}), 30% (Y _{HYPAC})	63

DHA: dihydroxyacetone; GLYAC: glyceric acid; HYPAC: hydroxypyruvic acid; GLYALD: glyceraldehyde

Selective oxidation of the secondary hydroxyl group of glycerol gives dihydroxy acetone (DHA, 1, 3-dihydroxypropan-2-one), which is used as the main composition in most of the skin care products and as a monomer for biopolymers.²² Conventionally, DHA is produced by microbial fermentation using *Gluconobactor oxydans*, however recently direct conversion of glycerol to DHA by electrocatalytic oxidation in the presence of organic nitroxyl radical TEMPO (2,2,6,6-tetramethylpiperidin-1-oxyl, as a catalyst or radicals maker) was achieved resulting in a high yield of DHA (25%) at 50 °C, greater than that of a biochemical process. The advantage of the TEMPO catalyzed process is that no chemical oxidant is used in the process and the TEMPO could be completely recovered at the end of the reaction.⁵⁵ Electrocatalytic oxidation of DHA can produce hydroxy pyruvic acid with high yield.

2.1.7 Reforming glycerol to syngas

Glycerol can be gasified to produce synthesis gas (syngas) by steam reforming (SR) or aqueous phase reforming (APR). Syngas can be used for the synthesis of methanol and F-T diesel fuels. Steam reforming is usually carried out at ambient pressure and high temperature (> 673 K) to yield syngas (Scheme 2.12.), where H₂ and CO are formed in the ratio of around 4:3. The water-gas shift reaction can be carried out to increase the hydrogen concentration in the syngas product. Noble metal catalysts, such as Pt, Ru, and Re supported on activated carbon, yttrium oxide or ceria washcoat, proved to be effective for this process.^{64,65,66} For instance, Hirai and co-workers reported a hydrogen yield of 82% at a temperature between 500-600 °C with a Ru catalyst.⁶⁴



Scheme 2.12. Steam reforming of glycerol

Recently, the use of Ni-based catalysts has received more interest because of their low cost and high thermal stability in the process. A Ni/CeO₂ catalyst demonstrated good selectivity towards hydrogen (75%) among other Ni-based catalysts at ≈ 900 K, ambient pressure, water to glycerol ratio of ≈ 5 with weight hourly space velocity (WHSV) of 1 h^{-1} .⁶⁷

In aqueous phase reforming (APR), the reaction is carried out in liquid phase under high pressure (25- 35 bar) and a low temperature (around 120 °C) to thermodynamically favor the equilibrium. The reactions are similar to those of the steam reforming process. Catalysts such as Pt, Pd or Ni-Sn have demonstrated high selectivity for hydrogen in the APR process.⁶⁸

2.1.8 Acetalization of glycerol to acetals and ketals

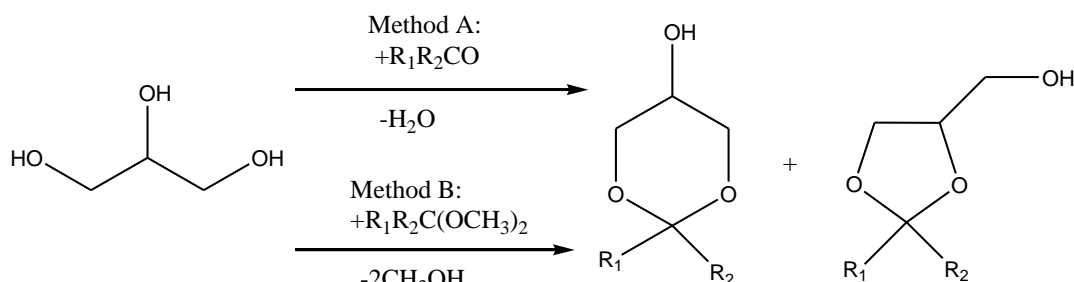
Acetals and ketals can be used as fuel additives. The high boiling point (290 °C under atmospheric pressure) and high polarity of glycerol make it unsuitable to be used as a direct fuel component. Acetalization- a process of condensation of glycerol with aldehydes or ketones to cyclic acetals or ketals, respectively, has been considered as an efficient approach for converting glycerol into a fuel component.^{69,70,71,72} Among the ketals, solketal or (2,2-dimethyl-1,3-dioxolan-4-yl) methanol is of particular interest, as it can potentially substitute metal-based fuel additives (such as iron, manganese, copper and barium) in biodiesel.^{73,74} The metal-based fuel additives have metal emission issues. Therefore, renewable and ash-free fuel additives such as solketal are promising candidates for biodiesel.⁷⁵ Not all acetals can be used as fuel additives. Only those acetals having a high flash point and meeting the diesel specifications can therefore be used as diesel additives. Generally acetals with a lower molecular weight are not suitable to be used as fuel additives, but they can be used as surfactants, flavors and disinfectants for the manufacture of cosmetics, fragrances, food and pharmaceuticals.^{71,75,76,77}

Traditionally acetals or ketals from glycerol are produced via homogeneous catalytic process using strong mineral acids such as sulfuric acid, hydrochloric acid, hydrofluoric acid, or p-toluene sulphonic acid.^{78,79} However, the homogeneous catalytic processes have some serious drawbacks related to corrosion and disposal of effluent. Also it is almost

impossible to recover the catalyst from the product effluent, which can be perfectly addressed by using heterogeneous catalysts.

Deutsch *et al.* studied the acetalization of glycerol using benzaldehyde, formaldehyde, acetone and their dimethyl acetals over various solid acids such as amberlyst-36, H-BEA, montmorillonite-K-10, nafion-H NR-50 and reported the formation of five membered and six membered acetal products (Scheme 2.13).⁶⁹ Vicente and co-workers investigated the acetalization of bio-glycerol with acetone over sulfonic mesostructured silica in a batch reactor and reported glycerol conversion of 90% at a high acetone-to-glycerol molar ratio (6) at 70 °C for 1 h.⁸⁰ Agirre *et al.* investigated the synthesis of glycerol acetals from glycerol and formaldehyde and studied the reaction kinetics.⁷³

Usually, acetalization was conducted in a batch process; however, Clarkson *et al.* developed a semi continuous process for the synthesis of solketal, where acetone was continuously fed to the reactor, but glycerol was fed in a batch mode.⁸¹ Monbaliu *et al.* reported a continuous process for the synthesis of solketal employing homogeneous acid catalyst i.e. sulfuric acid.⁸² Similarly, a continuous process was reported by Maksimov and co-worker, however no details of the reactor system were provided.^{83,84,85} Recently, a group of novel Zr, Ir and Hf based catalysts demonstrated high activity for this process.^{86,87,88}



Method A: Aldehyde or ketone R_1R_2CO

Benzaldehyde: $R_1 = C_6H_5$, $R_2 = H$

Formaldehyde: $R_1 = R_2 = H$

Acetone: $R_1 = R_2 = CH_3$

Method B: Dimethyl acetal $R_1R_2C(OCH_3)_2$

Benzaldehyde dimethyl acetal: $R_1 = C_6H_5$, $R_2 = H$

Formaldehyde dimethyl acetal: $R_1 = R_2 = H$

Acetone dimethyl acetal: $R_1 = R_2 = CH_3$

Scheme 2.13 Acetalization of glycerol with different chemicals (adapted from reference with copyright permission from Elsevier)⁶⁹

2.1.9 Hydrogenolysis of glycerol

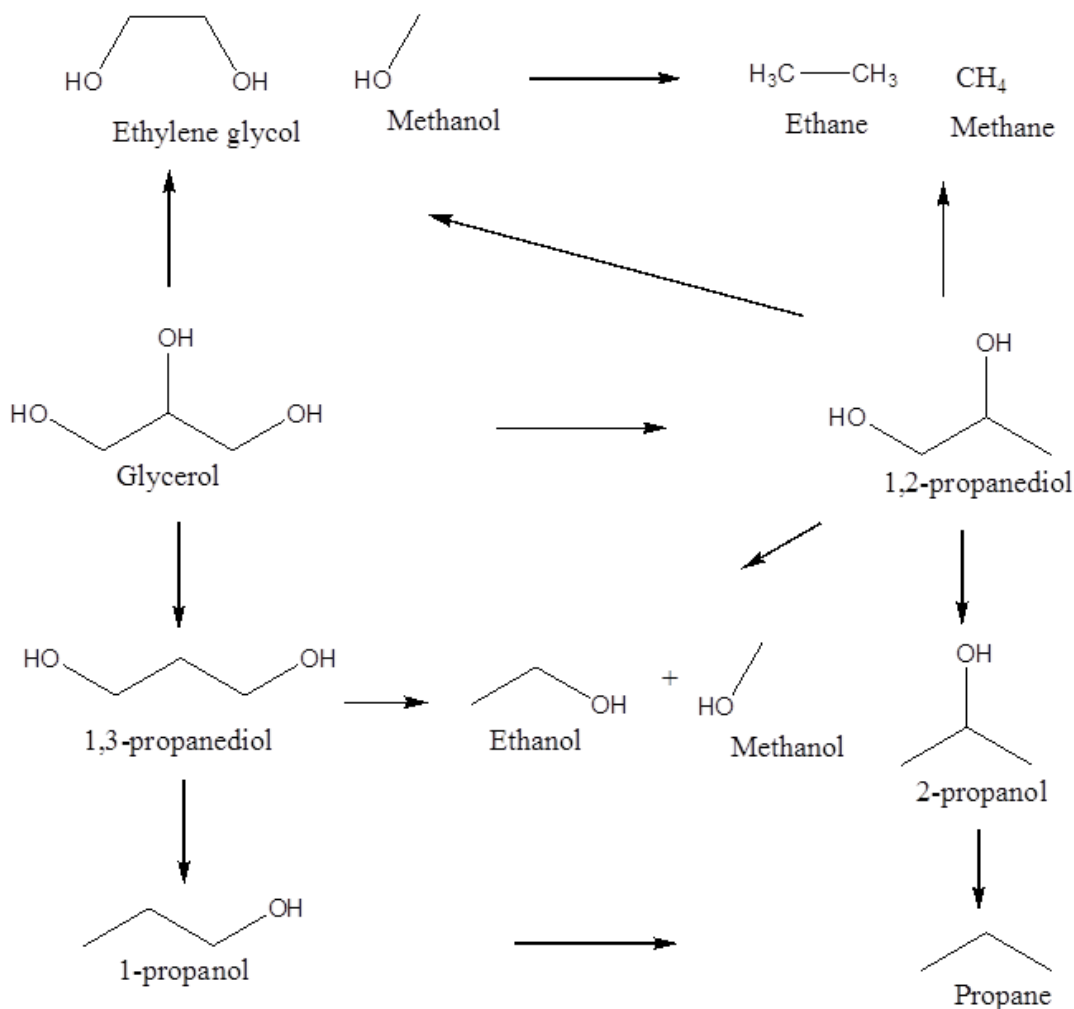
Hydrogenolysis of glycerol involves cleavage of C-C or C-O bonds of glycerol with simultaneous addition of hydrogen atom to the fragments, producing propylene glycol (1,2-propanediol, 1,2-PDO), 1,3-propanediol (1,3-PDO), ethylene glycol (EG), n-propanol (n-PrOH), 2-propanol (2-PrOH), ethanol, methanol, and some gaseous products such as propane, ethane and methane. Scheme 2.14 shows different products from hydrogenolysis of glycerol. All these hydrogenolysis products have different applications. 1,2-PDO is a non-toxic chemical, extensively used as a monomer for polyester resins, as an anti-freeze agent, and used in paints, liquid detergents, pharmaceuticals and food industries.^{89,90} 1,3-PDO can be used as a monomer to synthesize polymers such as polytrimethylene terephthalate (PTT) used in carpet and textile manufacturing.⁹¹ The other products such as n-propanol, 2-propanol, ethanol and methanol are also useful chemicals mainly used as

solvent and chemical intermediates for different compounds.⁹² Ethylene glycol is used as an antifreeze agent and a raw material for polyethylene terephthalate.⁴¹

Hydrogenolysis of glycerol was carried out in a batch reactor, using homogeneous catalysts (such as $\text{Rh}(\text{CO})_2(\text{acac})$) and tungstic acid at 473 K and 32 MPa (syngas).⁹³ The process produced 1,2-PDO and 1,3-PDO at a yield of 23% and 20%, respectively. The yield of n-propanol, 1,2-PDO and 1,3-PDO in the molar ratio of 47:22:31 has also been reported by Shell Oil using a homogeneous palladium complex in a water-sulfolane mixture.⁹⁴ The use of homogeneous catalysts and organic solvents in the process has some serious shortcomings such as the difficulty in recovery of catalyst and solvent from reaction mixtures. It is much more advantageous to operate the process using heterogeneous catalysts. Montassier and co-workers carried out the reaction at 30 MPa H_2 and 533 K over Raney Ni, Ru, Rh, and Ir catalysts, but the main product was methane, whereas propylene glycol was obtained as main product when Raney Cu was used as the catalyst.^{95,96} ZnO, carbon or alumina-supported Cu, Pd or Rh catalysts have been tested for hydrogenolysis of glycerol,⁹¹ where 100% selectivity towards 1,2-PDO was achieved with CuO/ZnO catalyst at 8 MPa and 453 K using aqueous glycerol as feedstock. Addition of tungstic acid (H_2WO_4) to Rh/C increased the selectivity towards 1,3-PDO during hydrogenolysis of glycerol in sulfolane solvent.⁹¹

Dasari *et al.* reported excellent performance of copper chromite as a catalyst for hydrogenolysis of concentrated glycerol, leading to 73% yield of 1,2-PDO at 473 K and 1.4 MPa H_2 .⁹⁷ In recent years, selective hydrogenolysis of glycerol to 1,2-PDO has been extensively studied in various aspects.^{97,98,99,100,101,102} Among many catalysts tested, Cu-based catalysts exhibited high catalytic activity and selectivity towards propylene glycol.^{103,104,105,106,107} For example boron (B) promoted Cu/ SiO_2 catalyst demonstrated a complete glycerol conversion with 100% selectivity towards 1,2-PDO.¹⁰⁸ The super performance of Cu-based catalysts is attributed to its low ability to cleave C-C bonds of glycerol molecule resulting in high selectivity towards 1,2-PDO. Despite several research reports, hydrogenolysis of glycerol to 1, 3-PDO is limited to laboratory scale tests with a relatively low yield and selectivity. Oh *et al.* reported the synthesis of 1, 3-PDO from glycerol over Pt-sulfated zirconia catalyst, and obtained glycerol conversion of 67% with

selectivity of 56% towards 1,3-PDO.¹⁰⁹ To improve the 1, 3-PDO yield, a new approach was investigated in which 1, 3-PDO was synthesized from glycerol using acetalization, tosylation and detosylation steps, achieving 72% yield of 1, 3-PDO.¹¹⁰

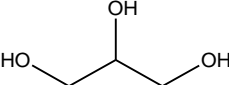
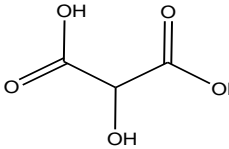
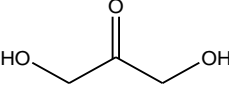
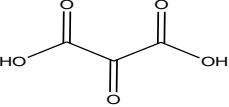
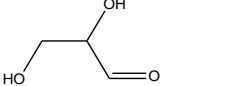
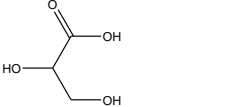


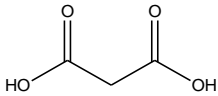
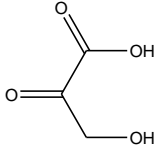
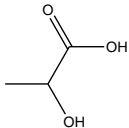
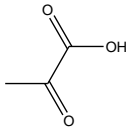
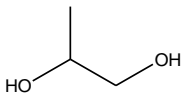
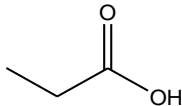
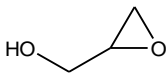
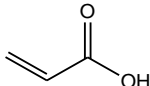
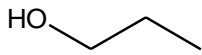
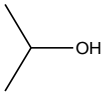
Scheme 2.14 Products of glycerol hydrogenolysis

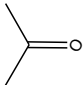
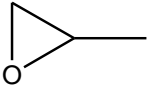
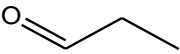
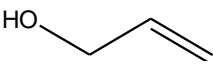
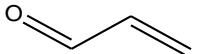
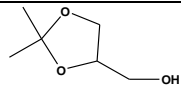
Compounds such as ethylene glycol, ethanol, methanol, n-propanol, 2-propanol and other gaseous products including methane, ethane and propane are also produced as by-products in the process due to excessive hydrogenolysis of glycerol.

Table 2.4 represents some of the compounds that can be derived from glycerol using either oxidation or reduction process. It is always advantageous to choose a product that has a large market and can absorb the extra glycerol and brings a higher price than glycerol. With a crude glycerol price of 4 cents/pound, it may not be difficult to achieve the later goal. However in many cases the crude glycerol must have to be upgraded to higher purity which brings the value to ~ 15 cents/pound (Please be noted that the price of commercial glycerol is ~40 cents/pound).¹¹¹

Table 2.4 List of compounds that can be synthesized from glycerol (adopted and redrawn)¹¹¹

Name	Chemical formula	Chemical structure	Price (\$/lbs)	US capacity (MMlbs)
Glycerol	$C_3H_8O_3$		0.04 - 0.45	8816,000
Tartronic acid	$C_3H_3O_5$		N/A	N/A
Dihydroxyacetone	$C_3H_6O_3$		2.00	N/A
Mesoxalic acid	$C_3H_2O_5$		a	N/A
Glyceraldehyde	$C_3H_5O_3$		N/A	N/A
Glyceric acid	$C_3H_6O_4$		b	N/A

Malonic acid	$C_3H_4O_4$		14.00	<1
Hydroxypyruvic acid	$C_3H_4O_4$		c	N/A
Lactic acid	$C_3H_6O_3$		0.7-0.85	<5
Pyruvic acid	$C_3H_4O_3$		N/A	N/A
Propylene glycol	$C_3H_8O_2$		0.81	1410
Propionic acid	$C_3H_6O_2$		0.46-0.62	440
Glycidol	$C_3H_6O_2$		>\$11,000	N/A
Acrylic acid	$C_3H_5O_2$		0.45 - 1.05	2880
Propanol	C_3H_8O		0.52	260
Isopropanol	C_3H_8O		0.28 - 0.49	1965

Acetone	C_3H_6O		0.13 – 0.42	3441
Propylene oxide	C_3H_6O		0.64 – 0.80	5190
Propionaldehyde	C_3H_6O		0.40	400
Allyl alcohol	C_3H_5O		1.00	60
Acrolein	C_3H_4O		0.64	>250
Solketal	$C_6H_{12}O_3$		N/A	N/A

MMlbs: Million metric pounds; ^a: Likely high- used in pharmaceuticals and preparation of anti-HIV drugs; ^b: Likely high- used for fine chemicals and pharmaceutical preparations; ^c: High- used for production of aminoacids

2.2 Conclusions and recommendations

The exponential increase in the biodiesel production in recent years has generated excess glycerol as a byproduct or waste stream from biodiesel plants. Economical use of glycerol is necessary to enhance the sustainability of the biodiesel industry. In this literature review, various pathways for the catalytic conversion of glycerol to different value added chemicals are discussed. Some key conclusions are listed below, and future directions of the catalytic conversion of glycerol are also suggested.

- 1) Esterification, etherification, dehydration, oxidation and acetalization of glycerol have opened up new opportunities for the synthesis of high value chemicals. Products such as glycerol mono-esters, glyceric acid, DHA, epichlorohydrin, glycidol and tartronic acid have proved their potential in different chemical industries. Fuel additives such as GTBE and solketal are potential substitutes for petroleum based additives (e.g., MTBE).

- 2) Catalytic synthesis of high-value chemicals such as lactic acid and acrylonitrile has been hardly investigated; hence intense research is still needed.
- 3) Selective hydrogenolysis of glycerol to 1, 2-PDO has attracted intensive research interest and achieved promising results. Nevertheless, synthesis of 1, 3-PDO at a high yield using inexpensive catalysts in aqueous media is yet to be realized. Thus, more research is needed.
- 4) The real challenge in valorization of crude glycerol containing impurities is associated with plugging of reactor and deactivation of catalysts over time.
- 5) Most of the catalytic processes developed so far are carried out in batch reactor which has inherent limitations such as process efficiency and scalability. Continuous-flow processes must be developed to enhance the production efficiency.
- 6) Catalyst deactivation over time is the main issue in most reported processes for glycerol conversion. Thus, intense research should be carried out to develop catalysts of high activity and superb stability.

References

1. Deng C, Duan X, Zhou J, Chen D, Zhou X, Yuan W. Size effects of Pt-Re bimetallic catalysts for glycerol hydrogenolysis. *Catalysis Today* 2014;234:208-214. doi:10.1016/j.cattod.2014.02.023.
2. Corma A, Iborra S, Velty A. Chemical routes for the transformation of biomass into chemicals. *Chemical reviews* 2007;107(6):2411-502. doi:10.1021/cr050989d.

3. Nakagawa Y, Tomishige K. Heterogeneous catalysis of the glycerol hydrogenolysis. *Catalysis Science & Technology* 2011;1(2):179. doi:10.1039/c0cy00054j.
4. Thompson JC, He BB. Characterization of crude glycerol from biodiesel production from multiple feedstocks. *Applied Engineering in Agriculture* 2006;22(2):261-265. doi:10.1021/jf3008629.
5. Liu X, Jensen PR, Workman M. Bioconversion of crude glycerol feedstocks into ethanol by *Pachysolen tannophilus*. *Bioresource Technology* 2012;104:579-86. doi:10.1016/j.biortech.2011.10.065.
6. Posada JA, Naranjo JM, López JA, Higuera JC, Cardona CA. Design and analysis of poly-3-hydroxybutyrate production processes from crude glycerol. *Process Biochemistry* 2011;46(1):310-317. doi:10.1016/j.procbio.2010.09.003.
7. Cheng L, Liu L, Ye XP. Acrolein production from crude glycerol in sub- and super-critical water. *Journal of the American Oil Chemists' Society* 2012;90(4):601-610. doi:10.1007/s11746-012-2189-5.
8. Baumann H, Bühler M, Fochem H, Hirsinger F, Zobelein H, Falbe J. Natural fats and oils—renewable raw materials for the chemical industry. *Angewandte Chemie International* 1988;27(1):41-62. doi:10.1002/anie.198800411.
9. Zhou C-HC, Beltramini JN, Fan Y-X, Lu GQM. Chemoselective catalytic conversion of glycerol as a biorenewable source to valuable commodity chemicals. *Chemical Society Reviews* 2008;37(3):527-49. doi:10.1039/b707343g.
10. Bancquart S, Vanhove C, Pouilloux Y, Barrault J. Glycerol transesterification with methyl stearate over solid basic catalysts. *Applied Catalysis A: General* 2001;218(1-2):1-11. doi:10.1016/S0926-860X(01)00579-8.
11. Pouilloux Y, Métayer S, Barrault J. Synthesis of glycerol mono-octadecanoate from octadecanoic acid and glycerol. Influence of solvent on the catalytic properties of basic oxides. *Comptes Rendus de l'Académie des Sciences - Series IIC - Chemistry* 2000;3(7):589-594. doi:10.1016/S1387-1609(00)01171-3.
12. Barrault J, Clacens J-M, Pouilloux Y. Selective oligomerization of glycerol over mesoporous catalysts. *Topics in Catalysis* 2004;27(1-4):137-142. doi:10.1023/B:TOCA.0000013548.16699.1c.
13. Corma A, Hamid S, Iborra S, Velty A. Lewis and Brønsted basic active sites on solid catalysts and their role in the synthesis of monoglycerides. *Journal of Catalysis* 2005;234(2):340-347. doi:10.1016/j.jcat.2005.06.023.
14. Pérez-Pariente J, Díaz I, Mohino F, Sastre E. Selective synthesis of fatty monoglycerides by using functionalised mesoporous catalysts. *Applied Catalysis A: General* 2003;254(2):173-188. doi:10.1016/S0926-860X(03)00481-2.

15. Barrault J, Pouilloux Y, Clacens J., Vanhove C, Bancquart S. Catalysis and fine chemistry. *Catalysis Today* 2002;75(1-4):177-181. doi:10.1016/S0920-5861(02)00062-7.
16. Corma A. Catalysts for the production of fine chemicals production of food emulsifiers, monoglycerides, by glycerolysis of fats with solid base catalysts. *Journal of Catalysis* 1998;173(2):315-321. doi:10.1006/jcat.1997.1930.
17. Bremus N, Dieckelmann G, Jeromin L, Rupilius W SH. Process for the continuous production of triacetin. 1983. Available at: <http://www.google.com/patents/US4381407>. Accessed May 13, 2015.
18. Aresta M, Dibenedetto A, Nocito F, Pastore C. A study on the carboxylation of glycerol to glycerol carbonate with carbon dioxide: The role of the catalyst, solvent and reaction conditions. *Journal of Molecular Catalysis A: Chemical* 2006;257(1-2):149-153. doi:10.1016/j.molcata.2006.05.021.
19. Yoo JW, Mouloungui Z. *Zeolites and Mesoporous Materials at the Dawn of the 21st Century, Proceedings of the 13th International Zeolite Conference*,. Elsevier; 2001. doi:10.1016/S0167-2991(01)81497-X.
20. Ballivet-Tkatchenko D, Chambrey S, Keiski R, *et al.* Direct synthesis of dimethyl carbonate with supercritical carbon dioxide: Characterization of a key organotin oxide intermediate. *Catalysis Today* 2006;115(1-4):80-87. doi:10.1016/j.cattod.2006.02.025.
21. Yoo J-W, Mouloungui Z. *Nanotechnology in Mesoporous Materials, Proceedings of the 3rd International Materials Symposium*. Elsevier; 2003. doi:10.1016/S0167-2991(03)80494-9.
22. Pagliaro M, Ciriminna R, Kimura H, Rossi M, Della Pina C. From glycerol to value-added products. *Angewandte Chemie (International ed. in English)* 2007;46(24):4434-40. doi:10.1002/anie.200604694.
23. Homer Adkins and W. H. Hartung, Hartung HA and WH. Acrolein. *Org. Synth.* 1941. Available at: <http://www.orgsyn.org/demo.aspx?prep=cv1p0015>. Accessed February 5, 2015.
24. Watanabe M, Iida T, Aizawa Y, Aida TM, Inomata H. Acrolein synthesis from glycerol in hot-compressed water. *Bioresource Technology* 2007;98(6):1285-90. doi:10.1016/j.biortech.2006.05.007.
25. Bühler W, Dinjus E, Ederer HJ, Kruse A, Mas C. Ionic reactions and pyrolysis of glycerol as competing reaction pathways in near- and supercritical water. *The Journal of Supercritical Fluids* 2002;22(1):37-53. doi:10.1016/S0896-8446(01)00105-X.

26. A process for the preparation of acrolein and the use thereof- German Patent. 1994. Available at: <http://www.google.com/patents/DE4238493C1?cl=en>. Accessed February 5, 2015.
27. Deleplanque J, Dubois J-L, Devaux J-F, Ueda W. Production of acrolein and acrylic acid through dehydration and oxydehydration of glycerol with mixed oxide catalysts. *Catalysis Today* 2010;157(1-4):351-358. doi:10.1016/j.cattod.2010.04.012.
28. Wang F, Dubois J-L, Ueda W. Catalytic dehydration of glycerol over vanadium phosphate oxides in the presence of molecular oxygen. *Journal of Catalysis* 2009;268(2):260-267. doi:10.1016/j.jcat.2009.09.024.
29. Witsuthammakul A, Sooknoi T. Direct conversion of glycerol to acrylic acid via integrated dehydration–oxidation bed system. *Applied Catalysis A: General* 2012;413-414:109-116. doi:10.1016/j.apcata.2011.10.045.
30. Wang F, Dubois J-L, Ueda W. Catalytic performance of vanadium pyrophosphate oxides (VPO) in the oxidative dehydration of glycerol. *Applied Catalysis A: General* 2010;376(1-2):25-32. doi:10.1016/j.apcata.2009.11.031.
31. Chiericato A, Basile F, Concepción P, *et al.* Glycerol oxidehydration into acrolein and acrylic acid over W–V–Nb–O bronzes with hexagonal structure. *Catalysis Today* 2012;197(1):58-65. doi:10.1016/j.cattod.2012.06.024.
32. Calvino-Casilda V, Guerrero-Pérez MO, Bañares MA. Efficient microwave-promoted acrylonitrile sustainable synthesis from glycerol. *Green Chemistry* 2009;11(7):939. doi:10.1039/b904689e.
33. Calvino-Casilda V, Guerrero-Pérez MO, Bañares MA. Microwave-activated direct synthesis of acrylonitrile from glycerol under mild conditions: Effect of niobium as dopant of the V-Sb oxide catalytic system. *Applied Catalysis B: Environmental* 2010;95(3-4):192-196. doi:10.1016/j.apcatb.2009.12.017.
34. Guerrero-Pérez MO, Bañares MA. New reaction: conversion of glycerol into acrylonitrile. *ChemSusChem* 2008;1(6):511-3. doi:10.1002/cssc.200800023.
35. Chiu C-W, Tekeei A, Sutterlin WR, Ronco JM, Suppes GJ. Low-pressure packed-bed gas phase conversion of glycerol to acetol. *AIChE Journal* 2008;54(9):2456-2463. doi:10.1002/aic.11567.
36. Vasconcelos SJS, Lima CL, Filho JM, *et al.* Activity of nanocasted oxides for gas-phase dehydration of glycerol. *Chemical Engineering Journal* 2011;168(2):656-664. doi:10.1016/j.cej.2011.01.053.
37. Cassel S, Debaig C, Benvegnu T, *et al.* Original synthesis of linear, branched and cyclic oligoglycerol standards. *European Journal of Organic Chemistry*

- 2001;2001(5):875-896. doi:10.1002/1099-0690(200103)2001:5<875::AID-EJOC875>3.0.CO;2-R.
38. Márquez-Alvarez C, Sastre E, Pérez-Pariente J. Solid catalysts for the synthesis of fatty esters of glycerol, polyglycerols and sorbitol from renewable resources. *Topics in Catalysis* 2004;27(1-4):105-117. doi:10.1023/B:TOCA.0000013545.81809.bd.
 39. Clacens J-M, Pouilloux Y, Barrault J. Selective etherification of glycerol to polyglycerols over impregnated basic MCM-41 type mesoporous catalysts. *Applied Catalysis A: General* 2002;227(1-2):181-190. doi:10.1016/S0926-860X(01)00920-6.
 40. Barrault J, Jerome F, Pouilloux Y. Polyglycerols and their esters as an additional use for glycerol. *Lipid Technology* 2005;17(6):131-135. Available at: <https://hal.archives-ouvertes.fr/hal-00289157/en/>. Accessed February 12, 2015.
 41. Behr A, Eilting J, Irawadi K, Leschinski J, Lindner F. Improved utilisation of renewable resources: New important derivatives of glycerol. *Green Chemistry* 2008;10(1):13. doi:10.1039/b710561d.
 42. Sunder A, Hanselmann R, Frey H, Mülhaupt R. Controlled synthesis of hyperbranched polyglycerols by ring-opening multibranching polymerization. *Macromolecules* 1999;32(13):4240-4246. doi:10.1021/ma990090w.
 43. Sunder A, Krämer M, Hanselmann R, Mülhaupt R, Frey H. Molecular nanocapsules based on amphiphilic hyperbranched polyglycerols. *Angewandte Chemie (International ed. in English)* 1999;38(23):3552-3555. Available at: <http://www.ncbi.nlm.nih.gov/pubmed/10602240>. Accessed February 12, 2015.
 44. Türk H, Shukla A, Alves Rodrigues PC, Rehage H, Haag R. Water-soluble dendritic core-shell-type architectures based on polyglycerol for solubilization of hydrophobic drugs. *Chemistry (Weinheim an der Bergstrasse, Germany)* 2007;13(15):4187-96. doi:10.1002/chem.200601337.
 45. Queste S, Bauduin P, Touraud D, Kunz W, Aubry J-M. Short chain glycerol 1-monoethers-a new class of green solvo-surfactants. *Green Chemistry* 2006;8(9):822. doi:10.1039/b603973a.
 46. Gottlieb K, Neitsch H, Wessendorf R. Glycerin - ein nachwachsender Rohstoff. *Chemie Ingenieur Technik* 1994;66(1):64-66. doi:10.1002/cite.330660108.
 47. Behr A, Urschey M. Highly selective biphasic telomerization of butadiene with glycols: scope and limitations. *Advanced Synthesis & Catalysis* 2003;345(11):1242-1246. doi:10.1002/adsc.200303087.

48. Zhou CH, Zhao H, Tong DS, Wu LM, Yu WH. Recent advances in catalytic conversion of glycerol. *Catalysis Reviews* 2013;55(4):369-453. doi:10.1080/01614940.2013.816610.
49. Carrettin S, McMorn P, Johnston P, *et al.* Oxidation of glycerol using supported gold catalysts. *Topics in Catalysis* 2004;27(1-4):131-136. doi:10.1023/B:TOCA.0000013547.35106.0d.
50. Demirel-Gülen S, Lucas M, Claus P. Liquid phase oxidation of glycerol over carbon supported gold catalysts. *Catalysis Today* 2005;102-103:166-172. doi:10.1016/j.cattod.2005.02.033.
51. Fordham P, Besson M, Gallezot P. Selective catalytic oxidation of glyceric acid to tartronic and hydroxypyruvic acids. *Applied Catalysis A: General* 1995;133(2):L179-L184. doi:10.1016/0926-860X(95)00254-5.
52. Besson M, Gallezot P. Selective oxidation of alcohols and aldehydes on metal catalysts. *Catalysis Today* 2000;57(1-2):127-141. doi:10.1016/S0920-5861(99)00315-6.
53. Biella S, Castiglioni G., Fumagalli C, Prati L, Rossi M. Application of gold catalysts to selective liquid phase oxidation. *Catalysis Today* 2002;72(1-2):43-49. doi:10.1016/S0920-5861(01)00476-X.
54. Kimura H, Tsuto K, Wakisaka T, Kazumi Y, Inaya Y. Selective oxidation of glycerol on a platinum-bismuth catalyst. *Applied Catalysis A: General* 1993;96(2):217-228. doi:10.1016/0926-860X(90)80011-3.
55. Kimura H. Selective oxidation of glycerol on a platinum-bismuth catalyst by using a fixed bed reactor. *Applied Catalysis A: General* 1993;105(2):147-158. doi:10.1016/0926-860X(93)80245-L.
56. Garcia R, Besson M, Gallezot P. Chemoselective catalytic oxidation of glycerol with air on platinum metals. *Applied Catalysis A: General* 1995;127(1-2):165-176. doi:10.1016/0926-860X(95)00048-8.
57. McMorn P, Roberts G, Hutchings GJ. Oxidation of glycerol with hydrogen peroxide using silicalite and aluminophosphate catalysts. *Catalysis Letters* 63(3-4):193-197. doi:10.1023/A:1019073122592.
58. Porta F, Prati L. Selective oxidation of glycerol to sodium glycerate with gold-on-carbon catalyst: an insight into reaction selectivity. *Journal of Catalysis* 2004;224(2):397-403. doi:10.1016/j.jcat.2004.03.009.
59. Carrettin S, McMorn P, Johnston P, Griffin K, Kiely CJ, Hutchings GJ. Oxidation of glycerol using supported Pt, Pd and Au catalysts. *Physical Chemistry Chemical Physics* 2003;5(6):1329-1336. doi:10.1039/b212047j.

60. Dimitratos N, Porta F, Prati L. Au, Pd (mono and bimetallic) catalysts supported on graphite using the immobilisation method. *Applied Catalysis A: General* 2005;291(1-2):210-214. doi:10.1016/j.apcata.2005.01.044.
61. Dimitratos N, Porta F, Prati L, Villa A. Synergetic effect of platinum or palladium on gold catalyst in the selective oxidation of D-sorbitol. *Catalysis Letters* 2005;99(3-4):181-185. doi:10.1007/s10562-005-2114-8.
62. Dimitratos N, Messi C, Porta F, Prati L, Villa A. Investigation on the behaviour of Pt(0)/carbon and Pt(0),Au(0)/carbon catalysts employed in the oxidation of glycerol with molecular oxygen in water. *Journal of Molecular Catalysis A: Chemical* 2006;256(1-2):21-28. doi:10.1016/j.molcata.2006.04.019.
63. Demirel S, Lehnert K, Lucas M, Claus P. Use of renewables for the production of chemicals: Glycerol oxidation over carbon supported gold catalysts. *Applied Catalysis B: Environmental* 2007;70(1-4):637-643. doi:10.1016/j.apcatb.2005.11.036.
64. Hirai T, Ikenaga N, Miyake T, Suzuki T. Production of hydrogen by steam reforming of glycerin on ruthenium catalyst. *Energy & Fuels* 2005;19(4):1761-1762. doi:10.1021/ef050121q.
65. Dauenhauer P, Salge J, Schmidt L. Renewable hydrogen by autothermal steam reforming of volatile carbohydrates. *Journal of Catalysis* 2006;244(2):238-247. doi:10.1016/j.jcat.2006.09.011.
66. Soares RR, Simonetti DA, Dumesic JA. Glycerol as a source for fuels and chemicals by low-temperature catalytic processing. *Angewandte Chemie (International ed. in English)* 2006;45(24):3982-5. doi:10.1002/anie.200600212.
67. Adhikari S, Fernando SD, To SDF, Bricka RM, Steele PH, Haryanto A. Conversion of glycerol to hydrogen via a steam reforming process over nickel catalysts. *Energy & Fuels* 2008;22(2):1220-1226. doi:10.1021/ef700520f.
68. Davda RR, Shabaker JW, Huber GW, Cortright RD, Dumesic JA. A review of catalytic issues and process conditions for renewable hydrogen and alkanes by aqueous-phase reforming of oxygenated hydrocarbons over supported metal catalysts. *Applied Catalysis B: Environmental* 2005;56(1-2):171-186. doi:10.1016/j.apcatb.2004.04.027.
69. Deutsch J, Martin A, Lieske H. Investigations on heterogeneously catalysed condensations of glycerol to cyclic acetals. *Journal of Catalysis* 2007;245(2):428-435. doi:10.1016/j.jcat.2006.11.006.
70. Agirre I, Güemez MB, Ugarte A., *et al.* Glycerol acetals as diesel additives: Kinetic study of the reaction between glycerol and acetaldehyde. *Fuel Processing Technology* 2013;116:182-188. doi:10.1016/j.fuproc.2013.05.014.

71. Silva PHR, Gonçalves VLC, Mota CJA. Glycerol acetals as anti-freezing additives for biodiesel. *Bioresource Technology* 2010;101(15):6225-9. doi:10.1016/j.biortech.2010.02.101.
72. Barros AO, Faísca AT, Lachter ER, Nascimento RS V, San Gil RAS. Acetalization of hexanal with 2-ethyl hexanol catalyzed by solid acids. *Journal of the Brazilian Chemical Society* 2011;22(2):359-363. doi:10.1590/S0103-50532011000200023.
73. Agirre I, García I, Requies J, *et al.* Glycerol acetals, kinetic study of the reaction between glycerol and formaldehyde. *Biomass and Bioenergy* 2011;35(8):3636-3642. doi:10.1016/j.biombioe.2011.05.008.
74. Burtscher H, Matter U, Skillas G. The effect of fuel additives on diesel engine particulate emissions. *Journal of Aerosol Science* 1999;30:S851-S852. doi:10.1016/S0021-8502(99)80436-4.
75. Capeletti MR, Balzano L, de la Puente G, Laborde M, Sedran U. Synthesis of acetal (1,1-diethoxyethane) from ethanol and acetaldehyde over acidic catalysts. *Applied Catalysis A: General* 2000;198(1-2):L1-L4. doi:10.1016/S0926-860X(99)00502-5.
76. Umbarkar SB, Kotbagi T V., Biradar A V., *et al.* Acetalization of glycerol using mesoporous MoO₃/SiO₂ solid acid catalyst. *Journal of Molecular Catalysis A: Chemical* 2009;310(1-2):150-158. doi:10.1016/j.molcata.2009.06.010.
77. Yang S, Wang M, Liang Y, Sun J. Eco-friendly one-pot synthesis of acetals and ketals by heterogeneously catalyzed liquid-solid phase reaction. *Rare Metals* 2006;25(6):625-629. doi:10.1016/S1001-0521(07)60003-5.
78. Frusteri F, Spadaro L, Beatrice C, Guido C. Oxygenated additives production for diesel engine emission improvement. *Chemical Engineering Journal* 2007;134(1-3):239-245. doi:10.1016/j.cej.2007.03.042.
79. Chopade SP, Sharma MM. Reaction of ethanol and formaldehyde: use of versatile cation-exchange resins as catalyst in batch reactors and reactive distillation columns. *Reactive and Functional Polymers* 1997;32(1):53-65. doi:10.1016/S1381-5148(96)00069-7.
80. Vicente G, Melero J a., Morales G, Paniagua M, Martín E. Acetalisation of bio-glycerol with acetone to produce solketal over sulfonic mesostructured silicas. *Green Chemistry* 2010;12(5):899. doi:10.1039/b923681c.
81. Clarkson JS, Walker AJ, Wood MA. Continuous Reactor Technology for Ketal Formation: An Improved Synthesis of Solketal. *Organic Process Research & Development* 2001;5(6):630-635. doi:10.1021/op000135p.

82. Monbaliu J-CM, Winter M, Chevalier B, *et al.* Effective production of the biodiesel additive STBE by a continuous flow process. *Bioresource Technology* 2011;102(19):9304-7. doi:10.1016/j.biortech.2011.07.007.
83. Maksimov AL, Nekhaev AI, Ramazanov DN, Arinicheva YA, Dzyubenko AA, Khadzhiev SN. Preparation of high-octane oxygenate fuel components from plant-derived polyols. *Petroleum Chemistry* 2011;51(1):61-69. doi:10.1134/S0965544111010117.
84. Nanda MR, Yuan Z, Qin W, Ghaziaskar HS, Poirier M-A, Xu C (Charles). A new continuous-flow process for catalytic conversion of glycerol to oxygenated fuel additive: Catalyst screening. *Applied Energy* 2014;123:75-81. doi:10.1016/j.apenergy.2014.02.055.
85. Nanda MR, Yuan Z, Qin W, Ghaziaskar HS, Poirier M-A, Xu CC. Thermodynamic and kinetic studies of a catalytic process to convert glycerol into solketal as an oxygenated fuel additive. *Fuel* 2014;117:470-477. doi:10.1016/j.fuel.2013.09.066.
86. Mota CJ a., da Silva CX a., Rosenbach, N, Costa J, da Silva F. Glycerin derivatives as fuel additives: The addition of glycerol/Acetone Ketal (solketal) in gasolines. *Energy & Fuels* 2010;24(4):2733-2736. doi:10.1021/ef9015735.
87. Crotti C, Farnetti E, Guidolin N. Alternative intermediates for glycerol valorization: iridium-catalyzed formation of acetals and ketals. *Green Chemistry* 2010;12(12):2225. doi:10.1039/c0gc00096e.
88. Li L, Korányi TI, Sels BF, Pescarmona PP. Highly-efficient conversion of glycerol to solketal over heterogeneous Lewis acid catalysts. *Green Chemistry* 2012;14(6):1611. doi:10.1039/c2gc16619d.
89. Anand KA, Anisia KS, Agarwal AK, Kumar A. Hydrogenolysis of glycerol with FeCo macrocyclic complex bonded to Raney Nickel support under mild reaction conditions. *The Canadian Journal of Chemical Engineering* 2010;n/a-n/a. doi:10.1002/cjce.20273.
90. Bienholz A, Schwab F, Claus P. Hydrogenolysis of glycerol over a highly active CuO/ZnO catalyst prepared by an oxalate gel method: influence of solvent and reaction temperature on catalyst deactivation. *Green Chemistry* 2010;12(2):290. doi:10.1039/b914523k.
91. Chaminand J, Djakovitch L auren., Gallezot P, Marion P, Pinel C, Rosier C. Glycerol hydrogenolysis on heterogeneous catalysts. *Green Chemistry* 2004;6(8):359. doi:10.1039/b407378a.
92. Organic Chemistry, 11th Edition - T. W. Graham Solomons, Craig B. Fryhle, Scott A. Snyder. Available at: <http://ca.wiley.com/WileyCDA/WileyTitle/productCd-EHEP002536.html>. Accessed December 3, 2014.

93. Catalyzing glycerol, carbon monoxide and hydrogen. 1987. Available at: <http://www.google.com/patents/US4642394>. Accessed December 26, 2014.
94. Hydrogenolysis of glycerol. 2000. Available at: <http://www.google.com/patents/US6080898>. Accessed December 26, 2014.
95. Montassier C, Ménézo JC, Hoang LC, Renaud C, Barbier J. Aqueous polyol conversions on ruthenium and on sulfur-modified ruthenium. *Journal of Molecular Catalysis* 1991;70(1):99-110. doi:10.1016/0304-5102(91)85008-P.
96. Montassier C, Dumas JM, Granger P, Barbier J. Deactivation of supported copper based catalysts during polyol conversion in aqueous phase. *Applied Catalysis A: General* 1995;121(2):231-244. doi:10.1016/0926-860X(94)00205-3.
97. Dasari M a., Kiatsimkul P-P, Sutterlin WR, Suppes GJ. Low-pressure hydrogenolysis of glycerol to propylene glycol. *Applied Catalysis A: General* 2005;281(1-2):225-231. doi:10.1016/j.apcata.2004.11.033.
98. Sharma R V., Kumar P, Dalai AK. Selective hydrogenolysis of glycerol to propylene glycol by using Cu:Zn:Cr:Zr mixed metal oxides catalyst. *Applied Catalysis A: General* 2014;477:147-156. doi:10.1016/j.apcata.2014.03.007.
99. Roy D, Subramaniam B, Chaudhari R V. Aqueous phase hydrogenolysis of glycerol to 1,2-propanediol without external hydrogen addition. *Catalysis Today* 2010;156(1-2):31-37. doi:10.1016/j.cattod.2010.01.007.
100. Ma L, He D. Influence of catalyst pretreatment on catalytic properties and performances of Ru–Re/SiO₂ in glycerol hydrogenolysis to propanediols. *Catalysis Today* 2010;149(1-2):148-156. doi:10.1016/j.cattod.2009.03.015.
101. Mane RB, Kondawar SE, Niphadkar PS, Joshi PN, Patil KR, Rode CV. Effect of preparation parameters of Cu catalysts on their physico-chemical properties and activities for glycerol hydrogenolysis. *Catalysis Today* 2012;198(1):321-329. doi:10.1016/j.cattod.2012.05.051.
102. Marinoiu A, Cobzaru C, Carcadea E, Capris C, Tanislav V, Raceanu M. Hydrogenolysis of glycerol to propylene glycol using heterogeneous catalysts in basic aqueous solutions. *Reaction Kinetics, Mechanisms and Catalysis* 2013;110(1):63-73. doi:10.1007/s11144-013-0596-8.
103. Bienholz A, Hofmann H, Claus P. Selective hydrogenolysis of glycerol over copper catalysts both in liquid and vapour phase: Correlation between the copper surface area and the catalyst's activity. *Applied Catalysis A: General* 2011;391(1-2):153-157. doi:10.1016/j.apcata.2010.08.047.
104. Auttanat T, Jongpatiwut S, Rirksomboon T. Dehydroxylation of glycerol to propylene glycol over Cu-ZnO / Al₂O₃ Catalyst : Effect of feed purity. *World Academy of Science, Engineering and Technology*, 2012, 6. 2012;6(4):400-403.

105. Miyazawa T, Koso S, Kunimori K, Tomishige K. Development of a Ru/C catalyst for glycerol hydrogenolysis in combination with an ion-exchange resin. *Applied Catalysis A: General* 2007;318(3):244-251. doi:10.1016/j.apcata.2006.11.006.
106. Vasiliadou ES, Eggenhuisen TM, Munnik P, de Jongh PE, de Jong KP, Lemonidou a. a. Synthesis and performance of highly dispersed Cu/SiO₂ catalysts for the hydrogenolysis of glycerol. *Applied Catalysis B: Environmental* 2014;145:108-119. doi:10.1016/j.apcatb.2012.12.044.
107. Vila F, López Granados M, Ojeda M, Fierro JLG, Mariscal R. Glycerol hydrogenolysis to 1,2-propanediol with Cu/ γ -Al₂O₃: Effect of the activation process. *Catalysis Today* 2012;187(1):122-128. doi:10.1016/j.cattod.2011.10.037.
108. Zhu S, Gao X, Zhu Y, Zhu Y, Zheng H, Li Y. Promoting effect of boron oxide on Cu/SiO₂ catalyst for glycerol hydrogenolysis to 1,2-propanediol. *Journal of Catalysis* 2013;303:70-79. doi:10.1016/j.jcat.2013.03.018.
109. Oh J, Dash S, Lee H. Selective conversion of glycerol to 1,3-propanediol using Pt-sulfated zirconia. *Green Chemistry* 2011;13(8):2004. doi:10.1039/c1gc15263g.
110. Wang K, Hawley MC, DeAthos SJ. Conversion of Glycerol to 1,3-Propanediol via Selective Dehydroxylation. *Industrial & Engineering Chemistry Research* 2003;42(13):2913-2923. doi:10.1021/ie020754h.
111. Taconi DTJ and Katherine A. The glycerin glut: Options for the value-added conversion of crude glycerol resulting from biodiesel production. *Environmental Progress* 2007;26(4):338-348. doi:10.1002/ep.

Chapter 3

3 Innovative and potential technologies towards the sustainable production of solketal as a fuel additive: A review

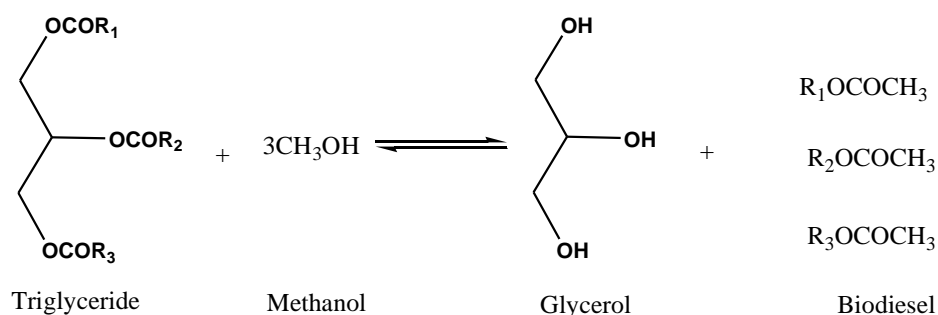
Abstract

The exponential growth of biodiesel industries all around the world has produced a large amount of glycerol as a byproduct, which must be valorized for the sustainability of the biodiesel industry. Ketalization of glycerol with acetone to synthesize solketal - a potential fuel additive is one of the most promising routes for valorization of glycerol. In this chapter, state-of-the-art of glycerol ketalization is reviewed, focusing on innovative and potential technologies towards sustainable production of solketal. The glycerol ketalization processes developed in both batch and continuous reactors and performances of some typical catalysts are compared. The mechanisms for the acid-catalyzed conversion of glycerol into solketal are presented. The main operation issues related to catalytic conversion of crude glycerol in a continuous-flow process and the direct use of crude glycerol are discussed.

Keywords: Glycerol; Ketalization; Solketal, Types of reactor; Catalyst; Crude glycerol

3.1 Introduction

The depletion of non-renewable fossil fuels and their environmental impacts are among the main factors that have drawn increasing attention towards biofuels, mainly bio-ethanol and biodiesel. Biodiesel is mainly produced by the transesterification of animal fats or vegetable oils (triglyceride) with a mono-alcohol (usually methanol) in presence of alkalis (mainly sodium or potassium hydroxide) as shown below (Scheme 3.1).^{1,2,3} This biodiesel can be used directly or after blending with fossil-based diesel fuel.



Scheme 3.1 Glycerol as byproduct during biodiesel production

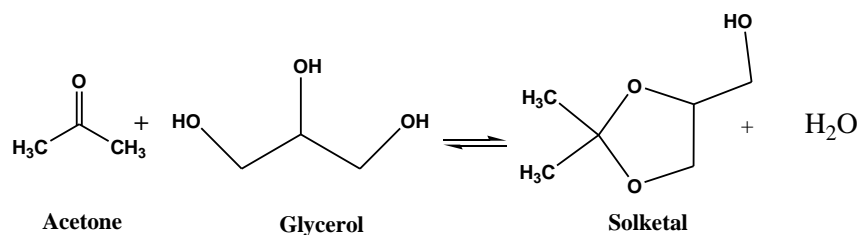
In the transesterification process, glycerol is formed as the principal byproduct. It is estimated that 10 wt% amount crude glycerol is generated for each amount of biodiesel produced.⁴ With the continued increase in the production of biodiesel, an excessive amount of glycerol is expected to accumulate. It is predicted that by 2020 the global production of glycerol will be 41.9 billion liters.⁵ The crude glycerol produced from biodiesel industry contains impurities such as water, inorganic salts (sodium or potassium salts), methanol, fatty acids, and esters etc.,^{6,7,8} hence it is commonly treated as the waste stream of biodiesel industry. It is economically viable for the large bio-diesel producers to refine this waste stream for the industrial applications, whereas for small bio-diesel producers, they are unable to leverage the treatment costs and instead they pay for glycerol removal. Due to the excessive amount generated, the current crude glycerol price is as low as 0.04-0.09

\$/lb.⁹ The predicted rapid growth of bio-diesel production will further lower the glycerol price once it enters into market.¹⁰ Therefore, new and economical ways of using glycerol must be developed to increase the value of crude glycerol to enhance the sustainability of biodiesel industries.

That being said, glycerol has diverse applications in different fields especially in the pharmaceuticals, food, cosmetics, and polymer industries.^{11,12,13} The versatility of glycerol is mainly due to its physical and chemical properties. The presence of three hydroxyl groups in glycerol makes it completely soluble in water and alcohols whereas insoluble in hydrocarbons. Furthermore, the inter and intra molecular hydrogen bonds due to the presence of hydroxyl groups lead to the high boiling point of glycerol (290 °C) at ambient pressure and high viscosity (1.412 Pa.s) at room temperature.¹⁴

On the other hand, catalytic and biological conversion of glycerol offer a tremendous potential to produce value-added chemicals such as propanediols, acrolein, dihydroxyacetone, glyceric acid, tartaric acid, epichlorohydrin, hydrogen, syngas, ethers, esters, etc.^{15,16,17,18,19,20} Hence glycerol can be considered as a platform chemical. A selection of these possibilities were reviewed recently.^{12,21,22} Production of cyclic acetals and ketals from glycerol with aldehydes and ketones, respectively, is believed to be one of the most promising glycerol applications as fuel/chemical intermediates.^{23,24,25,26}

The ketalization reaction between glycerol and acetone is given in Scheme 3.2, where solketal (2, 2-dimethyl-1, 3-dioxolane-4-methanol or 1,2-isopropylidenglycerol) is formed as the condensation product in the presence of an acid catalyst. Solketal can be used as a fuel additive to reduce the particulate emission and to improve the cold flow properties of liquid transportation fuels.²⁷ It helps to reduce the gum formation, improves the oxidation stability, and enhances the octane number when added to gasoline.²⁸ Maksimov *et al.* reported its use as a versatile solvent and a plasticizer in the polymer industry and a solubilizing and suspending agent in pharmaceutical preparations.²⁹



Scheme 3.2 Ketalization reaction between glycerol and acetone

This review chapter mainly over-views the state-of-the-art of the sustainable production of solketal by catalytic reaction of glycerol with acetone. Different types of processes and catalysts developed and their performances are compared. Fundamentals of reaction mechanisms for the acid-catalyzed conversion of glycerol into solketal are presented. The main operation issues related to catalytic conversion of crude glycerol in a continuous-flow process and the direct use of crude glycerol are discussed.

3.2 Historical context

It is well-known that ketals can be prepared by the reaction of an alcohol with a ketone in presence of an acid catalyst. Based on the public sources of literature, Fischer first prepared the solketal from acetone and glycerol in a batch reactor catalyzed by hydrogen chloride.³⁰ 25 years later Fischer and Pfahler reported ketalization of glycerol using hydrogen chloride and anhydrous sodium sulfate in a similar process.³¹ Later, in 1948, Renoll and Newmann published their work on the synthesis of solketal in a three neck flask with reflux equipped with a sealed mechanical stirrer.³² The authors chose petroleum ether as the reaction medium and p-toluenesulfonic acid (pTSA) monohydrate as the catalyst to achieve a high yield of solketal (87-90%). After the reaction, the products were separated by distillation under reduced pressure; however the reaction time was very long (21-36 h) in this process. These early studies on the synthesis of solketal remained without further advances until the end of the 20th century when massive amount of cheap glycerol was produced from biodiesel industry.

3.3 Synthesis of solketal from glycerol in batch reactors

A Spanish patent was filed in 1981-1982 aiming to utilize a large volume of glycerol.³³ The inventors studied the reaction of glycerol with acetone at the molar ratio of 1:1.1 to prepare solketal in a batch reactor. The experiments were conducted in the presence of an acid catalyst without a water entrainer. In their process water as the reaction by-product was removed under reduced pressure (10 torr) at the equilibrium point of the reaction. After distillation of solketal the yield never exceeded 80%, which is the major disadvantage of this process and a designed apparatus is required to work under reduced pressure. A very similar process was reported in the literature where the authors heated glycerol with an excess of acetone with pTSA as catalyst.³⁴ After neutralization and separation of the products, the yield of solketal was 56%. The low solketal yield is due to the presence of water in the reaction.

Mushrush *et al.*(1997) studied the conversion of glycerol to solketal in an organic solvent, toluene.³⁵ In their experiment, 4.5 moles (232g) of acetone was added to 1.1 moles (100g) of glycerol and 3.0 g of p-toluene sulfonic acid with 255g of 5 Å molecular sieves in a two neck round-bottomed flask of volume 2 L, equipped with a mechanical stirrer and a refluxing condenser. The stirred reaction mixture was heated under gentle reflux for 33 h using a heating mantle. The acidic reaction mixture was then neutralized with 3.0 g of sodium acetate and the molecular sieve catalyst was recovered by filtration. The products were distilled under vacuum (at 80-82 °C/10 mm of Hg) to give solketal at a yield of 88%.

Garcia *et al.* studied the reaction at an acetone-to-glycerol equivalent ratio of 3 over p-toluene sulfonic acid monohydrate.³⁶ The mixture was heated to reflux for 16 h. During the process wet acetone was distilled off and dry acetone was simultaneously introduced to the reactor to maintain the liquid concentration. The yield of solketal was about 90% and no further purification was required after solvent removal. Considering the fact that pTSA monohydrate is soluble in the reactants, the process can be classified as homogeneous catalysis, which causes a difficulty for catalyst recovery - typical drawback of reaction systems employing homogeneous catalysts. In fact, the use of homogeneous acid catalysts for chemical reaction processes has many serious shortcomings in addition to catalyst

recovery, such as corrosion of the reactor, and the environmental and economic concerns over the effluent disposal. Hence, it is of significance to explore heterogeneous acid catalysts for the glycerol ketalization process. Deutsch *et al.* reported the use of Amberlyst-36 (an arenesulfonic acid polymer) - a heterogeneous acid catalyst in a batch reactor with organic solvent (dichloromethane).²³ The authors reacted glycerol, acetone, dichloromethane in the presence of the solid catalyst in a 100 mL flask equipped with a refluxing condenser. A Dean-Stark trap was used to remove the formed water continuously. The maximum yield of solketal was 88% (related to glycerol) (reaction condition: 0.1 mol glycerol, 0.15 mol acetone, 17.5 mol dichloromethane, 0.5 g Amberlyst-36, 8 h reaction time at room temperature).

It is well known that the ketalization reaction has a very low equilibrium constant.³⁷ In this context, in order to reach high conversions of glycerol it is necessary to shift the equilibrium towards the formation of solketal. This could be achieved by either feeding excess amount of acetone or by removing the water generated during the reaction continuously. Removing water produced from solketal synthesis is an effective way to break the thermodynamic barriers. To remove the water from the reaction mixture, entrainers have been used in different processes.³⁸ Benzene is not a preferable entrainer for this process as acetone reactant is removed by distillation before benzene. Other entrainers for this process can be petroleum ethers and chloroform.³⁸ However, the efficiency of these entrainers is not great either because their boiling points are still higher than acetone. Acetone co-distillation creates the problem of low efficiency in azeotropic water removal. This phenomenon was evident from its very long reaction time when using petroleum ether as entrainer.¹⁶ The use of phosphorous pentoxide and sodium sulfate as catalysts as well as desiccants for the removal of water generated from the system has also been reported,³⁸ but high consumption of the catalysts in this case increased the operation costs. More recently, molecular sieves were used for this purpose.³⁹ All these processes are not economical on an industrial scale.

However, the above problems could be addressed more effectively by using excess acetone, which not only acts as a reactant but also acts as an entrainer for the removal of water from the system. The excess acetone could be distilled off and reused in the same or

other processes. Roldan *et al.* modified the batch reactor to a membrane batch reactor to remove the water from the reaction system.⁴⁰ The authors conducted the experiment by refluxing a mixture of glycerol, anhydrous acetone and heterogeneous acid catalyst, Montmorillonite K-10 (total weight 1 g) in a three-neck flask (250 mL) equipped with a reflux condenser, a septum cap and a zeolite membrane fixed in the central mouth in such a way that there is no contact between the liquid and the membrane (Figure 3.1). The membrane allowed the selected permeation of small sized water vapor instead of pervaporation. A maximum solketal yield of 82% was achieved by the authors using a very high acetone-to-glycerol molar equivalent ratio (20:1) for 2h of reaction. As expected, a negligible effect of the catalyst on the solketal yield was observed in this work.

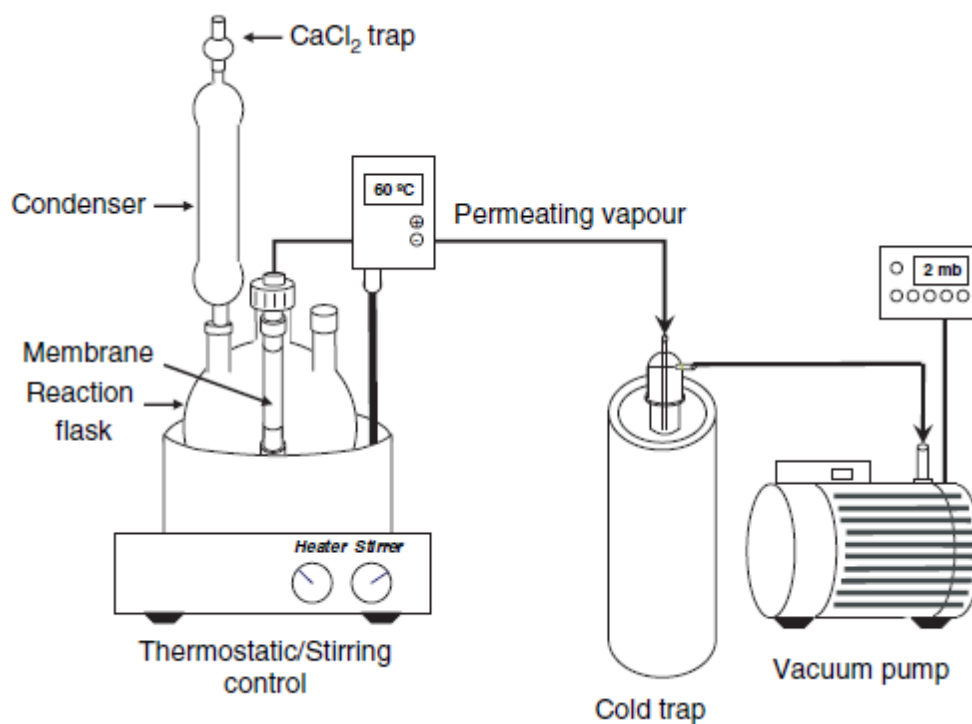


Figure 3.1 Membrane reactor for synthesis of solketal (adopted from reference,⁴⁰ and used with copyright permission)

Recently, Vicente *et al* attempted to remove water continuously from the reaction system by carrying out the reaction in a two-step batch mode operation.⁴¹ In the first step, the

reaction mixture (glycerol, acetone and a heterogeneous catalyst) was stirred under reflux at 70 °C in a 100 mL flask and in the second step, the water produced along with the excess amount of acetone was removed by vaporization under vacuum at 70 °C and fresh acetone was added to maintain the liquid level to start a new cycle. After three consecutive cycles (each cycle has two steps), a maximum solketal yield of 90% was achieved under the following reaction conditions; 70 °C, arenesulfonic acid-functionalized mesostructured silica (Ar-sBA-15) catalyst at a loading of 5 wt% of glycerol, and 30 min for each step.

To search for an effective heterogeneous catalyst for the glycerol ketalization process, Ferreira *et al.*, studied condensation of glycerol with acetone over a series of silica-induced heteropolyacid catalysts, i.e., tungsto-phosphoric acid (PW), tungsto-silicic acid (SiW), molybdo-phosphoric acid (PMo), and molybdo-silicic acid (SiMo) in a stirred batch reactor.⁴² The reported catalytic activities for the catalysts are in the order of: SiMo < PMo < SiWS < PWS, mainly owing to the increase in acidity.⁴² The authors reported glycerol conversion of more than 97% with a very high selectivity of 99% towards solketal at the reaction conditions: 70 °C, acetone-to-glycerol molar ratio of 12:1, catalyst (PW) loading of 0.2 g, and 2-3 h. The high yield of solketal in this work was attributed to the strong acidity of the catalyst that promoted the reaction kinetics and the high acetone-to-glycerol molar ratio (12:1). Good catalytic stability was also observed, as the catalyst lost its activity by ~15% after four consecutive batch runs using the same catalyst.

Glycerol is poorly miscible with acetone in normal conditions (25 °C and 1 atm) (only 5wt% of glycerol is soluble in acetone), which has become a major disadvantage for the synthesis of solketal. Royon *et al.* proposed to use the supercritical acetone with better solubility for glycerol to synthesize solketal without using any catalyst.⁴³ The authors carried out the experiments at 508 K and 48 bar in a batch reactor, where acetone was at its supercritical state. However, a maximum of 28% glycerol conversion with a selectivity of 80% towards solketal was observed after 4 h reaction at the acetone-to-glycerol mole ratio of >10. The low glycerol conversion and solketal yield might be due to the lack of active acid sites in acetone at supercritical condition. Hence, the result was not very encouraging. Since ketalization is an exothermic process,²⁴ temperature is another important factor that affects the equilibrium conversion. To seek highly active catalysts at

low temperature is another strategy to enhance the economy of the solketal production. Menezes *et al.* reported the highest ever yield of solketal obtained in a batch reactor operated at atmospheric pressure and room temperature,⁴⁴ where 10 mol% of stannous chloride (SnCl_2) (w.r.t. glycerol) was used as the catalyst and the acetone-to-glycerol mole ratio was 6 for 0.5- 2h reaction in the presence of methyl cyanide (CH_3CN) solvent.

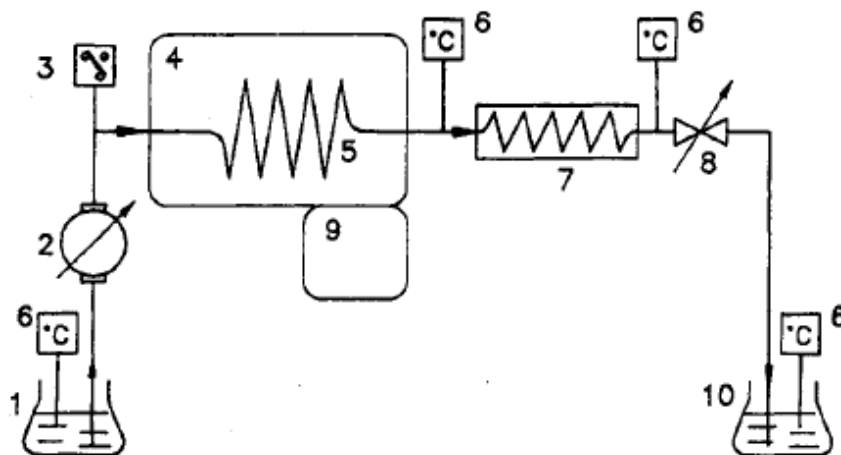
However, all the batch processes described above have common limitations in terms of the difficulty in scaling up for production of solketal on a large scale. Thus, the advances in glycerol ketalization with continuous-flow processes are discussed in the following section.

3.4 Synthesis of solketal from glycerol in continuous-flow reactors

As discussed earlier, the majority of the studies on synthesis of solketal were operated in batch reactors although using heterogeneous catalysts such as Zeolites,⁴⁰ Amberlysts,⁴¹ montmorillonite,⁴² silica induced heteropolyacids,⁴² nafion,²⁹ etc. However, a batch process has various limitations of which the main ones are a long time of reaction (usually exceeding 2 h) hence lower efficiency, and the difficulty in process scale-up.⁴⁵ Production of solketal in a continuous-flow reactor using heterogeneous catalysts is thus much more advantageous because the continuous-flow process enables better heat and mass transfer efficiency, and easy scaling-up of the process from laboratory to industrial scale as well as more environmental and economical benefits.^{46,47,48,49} The continuous operation of the process also offers constant quality of the end products.

The use of a continuous microwave reactor (CMR) for the synthesis of solketal was reported.⁵⁰ Some details of the continuous microwave reactor are given in Figure 3.2. In this CMR process, a solution of acetone, glycerol and pTSA as a homogeneous catalyst was mixed and pumped into the reaction coil (inside the microwave cavity) to react at a desired temperature. The authors reported a maximum 84% yield of solketal at acetone-to-glycerol mole ratio of 13.5:1, in the presence of pTSA under the reaction conditions of 132 °C, 1175 kPa, 1.2 minutes residence time and of 20 mL/min feeding rate. However, the

system was restricted only to homogeneous catalysts. Moreover, this technique would not be appropriate for conducting the reaction at a low temperature or for reactants that are not compatible with microwave energy.

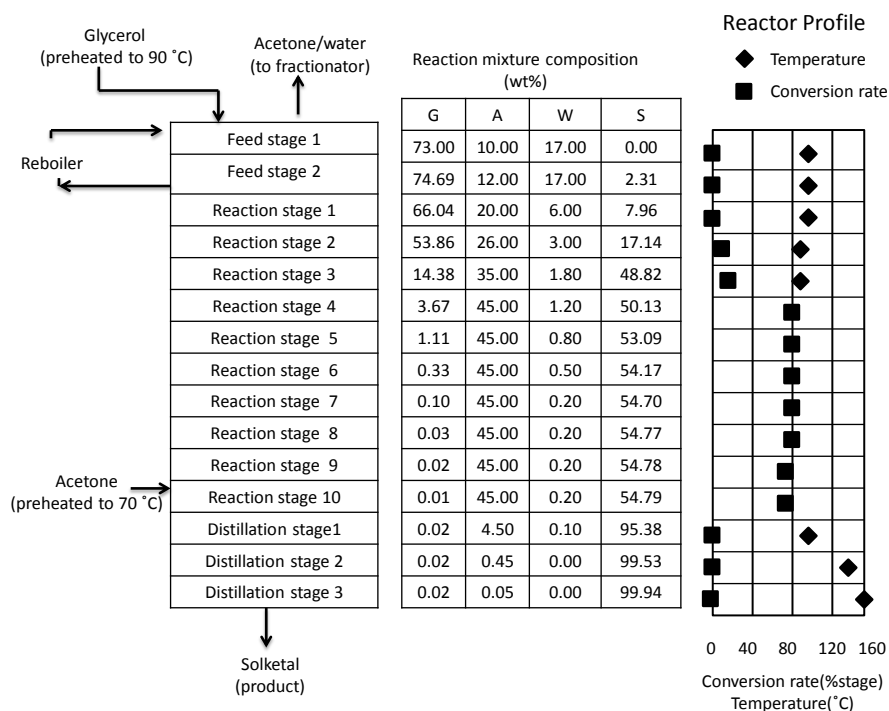


1: Reaction mixture; 2: Pump; 3: Pressure sensor; 4: Microwave cavity; 5: Reaction coil; 6: Temperature sensor; 7: Heat exchanger; 8: Pressure control valve; 9: Electronic key pad and display; 10: Product mixture

Figure 3.2 Continuous microwave reactor for synthesis of solketal (adopted and used with copyright permission)⁵⁰

Clarkson *et al.* used a multi-tray reactive distillation column with deep reaction stages containing catalyst (Amberlyst DPT-1) in suspension for the synthesis of solketal,⁵¹ as illustrated in Scheme 3.3. In their process, glycerol was preheated at 90 °C before feeding into the reaction column. An extra amount of acetone was added in the reaction stage to drive the reaction towards the production of solketal and the process has a long reaction time (more than 4 h). With this, the process is actually a semi-continuous process (continuous operation with respect to acetone, but batch mode for glycerol). The process

was found to be difficult to operate at a lower temperature due to the high viscosity of glycerol. A continuous glass flow reactor (Figure 3.3) made of several glass fluidic modules and connected in series has been reported by Monbaliu *et al.*⁵² In their work, the total volume of the reactor is 72 mL and the first two fluidic modules (FM01 and FM02) were used for feeding, preheating and premixing of the reactants. Glycerol (feed 1) was preheated (on FM01) and reacted with acetone in all other modules (FM03- FM09) for the solketal product. Acetone (feed 2) and sulfuric acid (feed 3) were premixed and preheated in the fluidic module FM02. The main challenges of this reactor system include: a high residence time of the reactants, unsuitable for using heterogeneous catalysts, difficulty in conducting the reaction at low temperature, and separation issues for the final product after neutralization, etc.



Scheme 3.3 Schematic diagram of a multi-tray reaction distillation column for glycerol ketalization adopted from Clarkson *et al.*⁵¹

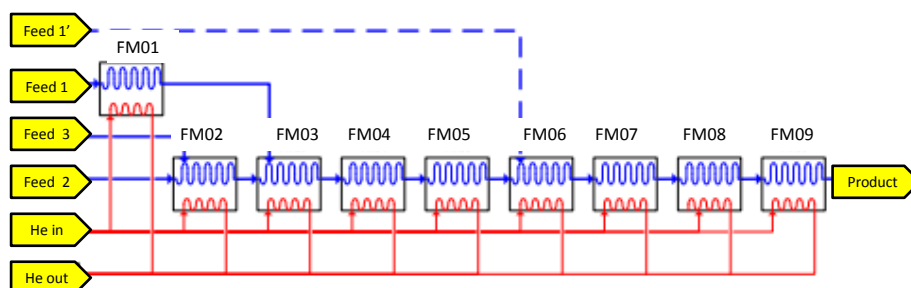


Figure 3.3 Schematic continuous glass flow reactor proposed by Monbaliu *et al.*⁵² (with copyright permission from Elsevier)

Maksimov *et al.* reported a continuous reactor for the preparation of high-octane oxygenate fuel components from plant-derived polyols, however no description of the reactor was given in the literature.²⁹ Recently, we have developed a continuous-flow reactor based on the concept of “Novel Process Windows” with respect to temperature, pressure and/or reactant concentration to enhance the intrinsic kinetics of the reaction for an optimum yield.^{53,54,55,56} The reactor is a continuous down-flow tubular reactor (Inconel 316 tubing, 9.55 mm OD, 6.34 mm ID and 600 mm length) heated with a tube furnace. A schematic diagram of the continuous-flow reactor system is shown in Figure 3.4. The feed, a homogeneous solution of reactants (acetone and glycerol) with the solvent (ethanol) mixed at a selected molar ratio, was pumped into the reactor using a HPLC pump at a specific flow rate. The reactor was maintained at a desired temperature and pressure. In each run, a pre-determined amount of catalyst was preloaded into the catalytic bed, where the catalyst particles were supported on a porous Inconel metal disc (pore size: 100 μm) and some

quartz wool. The amount of catalyst in each run was determined by the selected weight hourly space velocity (WHSV). This flow reactor can operate in a wide range of temperature and pressure using different heterogeneous catalysts. Amberlyst-36 wet was used to optimize the process, and the optimum process conditions are: 25 °C, 500 psi, acetone-to-glycerol molar ratio of 4, WHSV of 2 h⁻¹, under which a very high yield of solketal (94 ±2 wt%) was obtained.⁵⁷

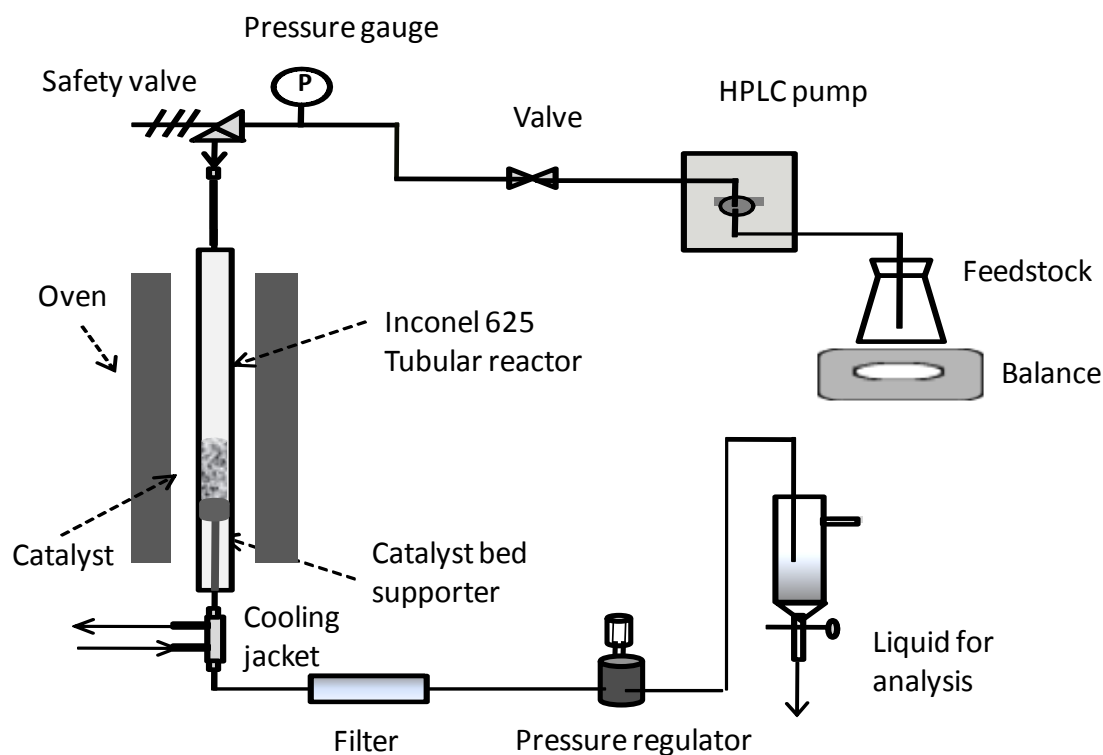


Figure 3.4 Continuous-flow reactor developed in our laboratory for glycerol ketalization

A summary of the performance of various catalysts for glycerol ketalization with different types of reactors is given in Table 3.1.

Table 3.1 Performance of various catalysts for glycerol ketalization with different types of reactors

T (°C)	P (psi)	A/G ratio ¹	Reaction time (h)	Catalyst	Reactor type	Solketal yield (%)	Ref.
Refluxed	N.A	4.09:1	33	TSOH	Batch	88	35
Refluxed	N.A	3:1	16	TSOH	Batch	90	36
38-40	N.A	1.5:1	8	Amberlyst-36	Batch	88	23
Refluxed	N.A	20:1	2	MMT K10	Batch	82	23
70	N.A	6:1	>2.5	Ar-SBA 15	Batch	90	41
70	N.A	12:1	2-3	SiTPacid	Batch	96	42
Ambient	N.A	6:1	0.5	SnCl ₂	Batch	97	44
132	170	13.5:1	0.02	TSOH	Flow	84	42
40	600	6:1	0.25	H-β zeolite	Flow	84	53
40	600	6:1	0.25	Amberlyst-36 wet	Flow	88	53
40	600	6:1	0.25	Amberlyst-35	Flow	86	53
40	600	6:1	0.25	ZrSO ₄	Flow	77	53
25	500	4:1	0.5	Amberlyst-36 wet	Flow	94±2	53

¹ Acetone-to-glycerol mole ratio

From the Table, it is clearly shown that a similar product yield was obtained with a continuous-flow reactor (77-96%) as that in a batch reactor (82-97%), but reaction time required is much shorter with a flow reactor (0.02-0.5 h) compared with a batch reactor (0.5-33 h). Therefore, development of continuous-flow processes is promising for production of solketal from glycerol on a large scale.

3.5 Influence of catalyst acidity

As discussed later, the ketalization reaction proceeds via an acid catalyzed mechanism, hence catalysts with stronger acidity (relatively more number of acid sites per unit mass) might lead to higher glycerol conversion. The influence of catalyst acidity on the solketal yield is shown in Table 3.2. It is clear that the catalyst acidity is a crucial parameter influencing the catalytic performance. Vicente *et al.* compared the performance of a series of catalysts with different acid strength (ranging from 0.12 to 4.8 meq/g, i.e., number of acid sites per unit mass) for ketalization of glycerol for solketal production:⁴¹ propylsulfonic acid-functionalized mesostructured silica (Pr-SBA-15), arenesulfonic acid-functionalized mesostructured silica (Ar-SBA-15), hydrophobised arenesulfonic acid-functionalized mesostructured silica (HAr-SBA-15), Amberlyst-15, silica bond-propylsulfonic acid, silica bond-tosic acid, and Nafion-SAC 13. They obtained a solketal yield of 74% for Nafion-SAC 13 catalyst (acidity 0.12 meq/g) and 85% for Amberlyst-15 (acidity 4.8 meq/gm). Thus, a catalyst with a stronger acidity would likely perform better in the ketalization of glycerol with acetone. On the other hand, the results as shown in the Table imply that surface area and the pore volume/size of a catalyst have negligible influence on the catalytic activity for the ketalization of glycerol. A recent study by our group also revealed the influence of the catalyst acidity on its activity for catalytic conversion of glycerol to solketal in a continuous flow reactor.⁵³ In our study, we observed that the activity of catalysts was in the order of Amberlyst wet \approx H-beta zeolite \approx Amberlyst dry > zirconium sulfate > montmorillonite > Polymax, which follows the same order of the catalytic acid strength (Table 3.2). Similar correlation between the catalyst acidity and the product yield was reported by Ferreira *et al.* in ketalization of glycerol by acetone.⁴²

Table 3.2 Influence of catalyst acidity on solketal yield

Active phase	Reaction conditions ¹ Temp(°C), A/G, T _r	Acidity (meq/g)	BET (m ² /g)	Pore size (nm)	Yield (%)	Ref.
H-β zeolite	40,6: 1, 0.25	5.7	480	2	84	53
Amberlyst-36 wet	40,6: 1, 0.25	5.6	33	24	88	53
Amberlyst-35	40,6: 1, 0.25	5.4	35	16.8	86	53
ZrSO ₄	40,6: 1, 0.25	---	--	--	77	53
Polymax	40,6: 1, 0.25	---	---	---	60	53
Montmorillonite K10	40,6: 1, 0.25	4.6	264	5.5	68	53
Amberlyst-36	38-40, 1.5: 1, 8	5.4	19	20	88	23
Pr-SBA-15	70, 6:1, 0.5	0.94	721	8	79	41
Ar-SBA-15	70, 6:1, 0.5	1.06	712	9	83	41
HAr-SBA-15	70, 6:1, 0.5	1.04	533	8	80	41
Amberlyst-15	70, 6:1, 0.5	4.8	53	30	85	41
Pr-SO ₃ H-SiO ₂	70, 6:1, 0.5	1.04	301	2-20	77	41
Tic acid-SiO ₂	70, 6:1, 0.5	0.78	279	2-20	73	41
Nafion SAC-13	70, 6:1, 0.5	0.12	>200	>10	74	41

¹A/G: acetone-to-glycerol molar ratio; T_r: reaction time (h)

3.6 Performance of transition metal catalysts in glycerol ketalization

Transition metal catalysts have demonstrated good catalytic performance in glycerol ketalization.⁵⁸ In fact, Iridium catalyzed ketalization reactions are promising and have been well studied among other transition metal catalysts.^{59,60,61,62,63} The most active catalyst for the ketalization reaction was $[\text{CpIrCl}_2]_2$ (Cp= pentamethylcyclopentadienyl),⁵⁸ with a glycerol conversion of 87% and 98% selectivity towards solketal in a batch reactor (Other experimental conditions were: 40 °C, $[\text{Ir}] = 3.0 \times 10^{-3} \text{ M}$, $[\text{glycerol}]/[\text{Ir}] = 500$, and 1h reaction time). Li's group specifically studied the performance of mesoporous substituted silicates,⁶⁴ in which the metal atoms were incorporated in the silicate framework. The authors reported that the Zr-TUD-1 and Hf-TUD-1 were prepared by a one-pot sol-gel procedure, where triethanolamine was used as chelating and template agent and zirconium propoxide and hafnium chloride as the metal precursors. Another catalyst Sn-MCM-41 was prepared by hydrothermal synthesis in a procedure similar to that of Li *et al.*,⁶⁴ using cetyltrimethylammonium bromide (CTAB) as the template in a gel formed from a solution of tetraethyl orthosilicate (TEOS), $\text{SnCl}_4 \cdot 5\text{H}_2\text{O}$ and tetraammonium silicate.⁶⁵ The conversion of glycerol reached around 64%, 65% and 62% for Zr-TUD-1, Hf-TUD-1 and Sn-MCM-1 catalysts, respectively, with almost 100% selectivity towards solketal in a batch reactor under the experimental conditions of: 80 °C, 6 h reaction time, and the acetone-to-glycerol molar ratio of 2:1.

3.7 Reaction mechanism

As discussed previously, the relative acidity of the catalysts has significant effects on the glycerol conversion and the solketal product yield. It is thus of significance to discuss the reaction mechanism for the glycerol ketalization reaction catalyzed by acid catalysts. The condensation reaction of glycerol with acetone leads to the formation of both five membered and six membered rings (ketals).⁶⁶ However the six membered ring ketal is less favorable because one of the methyl groups in the final product is in axial position of the chair conformation (Figure 3.5).^{29,67} So the resulting product has a ratio of 99:1 for five

membered ring (4-hydroxymethyl-2,2-dimethyl-1,3-dioxolane, or solketal) to six membered ring (5-hydroxy-2,2-dimethyl-1,3-dioxane). For the ketalization reaction catalyzed by Brønsted acids, the five membered ring solketal is dominantly formed through a mechanism involving a short-lived carbenium ion as an intermediate.^{64,68} According to this mechanism, the Lewis acid metal sites play a similar role in the MPV reduction (Meerwein-Ponndrof-Verley) or in Oppenauer oxidation reactions, by coordinating and activating the carbonyl group of the acetone. Then the carbon atom of the carbonyl group is attacked by the primary alcoholic group of glycerol accompanied by the formation of a bond between the carbonyl oxygen atom and the secondary carbon atom of glycerol followed by dehydration to form the five membered ring solketal. The detail mechanism is displayed in Scheme 3.4.

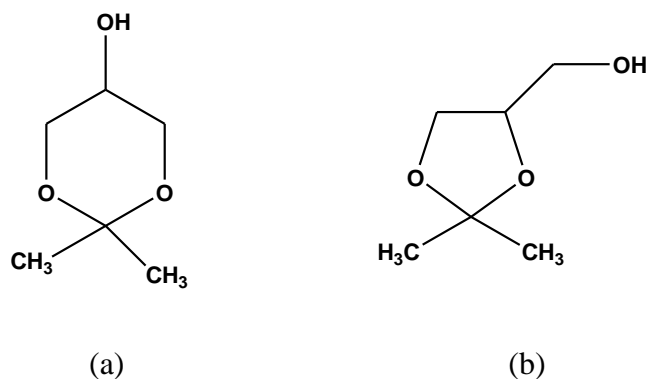
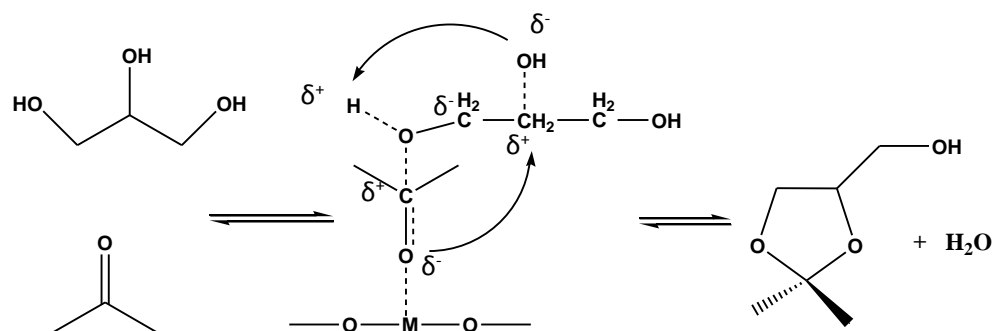
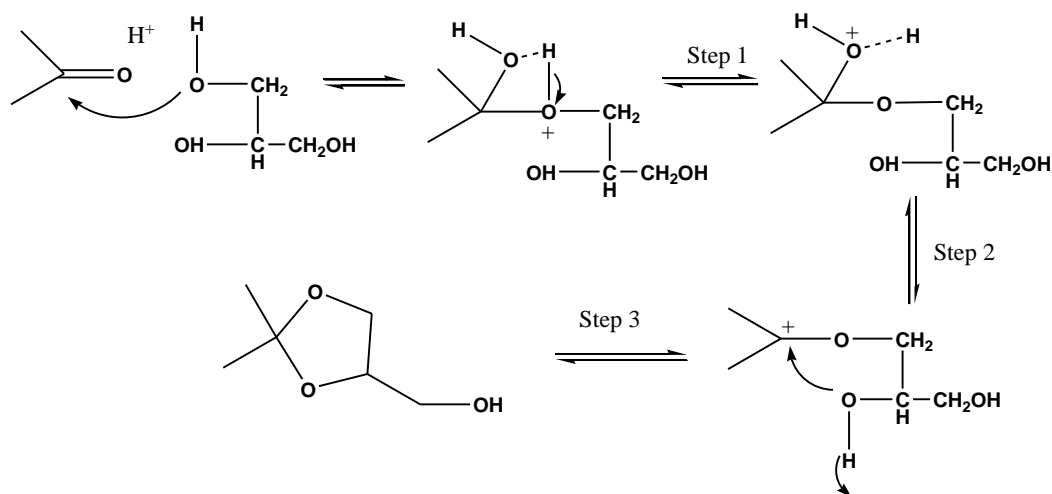


Figure 3.5 The cyclic acetals from the reaction between glycerol and acetone: 5-hydroxy-2,2-dimethyl-1,3-dioxane (a) solketal i.e., 4-hydroxymethyl-2,2-dimethyl-1,3-dioxolane(b)



Scheme 3.4 Mechanism proposed by Li *et al.* for the reaction of acetone and glycerol over Lewis acid catalyst (M is the metal atom)^{64,68}

We have also proposed a reaction framework (Scheme 3.5) for the ketalization reaction proceeding via acidic catalytic mechanism involving 3 steps. The first step involves the surface reaction between the adsorbed acetone and glycerol over the catalyst surface to form the hemi-acetal.³⁷ The next step is the removal of water leading to the formation of a carbocation on the carbonyl carbon atom. This step is known to be the rate-determining step of the reaction. The last step is the removal of the proton to form solketal.



Scheme 3.5 Mechanism used by Nanda *et al.* for the reaction of acetone and glycerol over acid catalyst⁵³

3.8 Key operation issues of flow reactors and use of crude glycerol

As discussed earlier, the ketalization reaction proceeds via an acid catalyzed mechanism, which means catalysts with stronger acidity might lead to higher glycerol conversion. However, catalysts with strong acidity would enhance fouling. Nevertheless, since the reaction is exothermic and carried out at a low temperature (usually below 80 °C), the deactivation of catalyst due to fouling can be avoided. We examined the catalytic deactivation process of different heterogeneous acid catalysts such as H-beta zeolite, Amberlyst-35 dry and Amberlyst-36 wet in a continuous-flow reactor and observed a slight reduction in the activities of these catalysts after 24 h on-stream as compared to that of the fresh catalyst.⁵³ To better understand these phenomena, we measured the textural properties and acidity as well FTIR spectra of the spent catalyst (Amberlyst-36 wet) after 24h on-stream and compared to the results of the fresh catalyst. The slight reduction in the activity of the spent catalyst was attributed to the loss of active acid sites during the reaction, not due to coking. In order to regain the initial activity of the catalyst, the spent catalyst was regenerated and the regenerated catalyst demonstrated almost the same activity (>93%

yield) as that of the fresh catalyst.⁶⁹ However, after a long time (days or months) operation of a continuous-flow reactor using heterogeneous catalysts, reactor clogging might occur, caused by fine particles of disintegrated catalysts.⁵³ This problem can be effectively alleviated by diluting the catalyst with glass beads /or by decreasing the catalytic bed height.

The price of glycerol depends on the technical grade. The refined pure glycerol is currently expensive, costing around US\$ 500-600 per ton.⁷⁰ Crude glycerol is available for only US\$ 40-90 per ton.⁹ Thus, use of crude glycerol for the production of value-added products is crucial for achieving a sustainable and economical production of solketal. However, as mentioned earlier, crude glycerol contains impurities including water, potassium or sodium salts, esters, fatty acids and alcohols. Therefore, the direct use of crude glycerol as feedstock may cause problems such as deactivation of catalyst (by poisoning the active sites by the impurities) or plugging of reactor (due to deposition of high boiling organic compounds or inorganic salts). To facilitate the use of crude glycerol, da Silva and Mota investigated the effect of impurities on the production of solketal in a batch reactor.⁷¹ They added impurities such as 10% water, 15% NaCl and 1% methanol (assuming that these are the common impurities present in crude glycerol) to pure glycerol and conducted the ketalization experiment in presence of heterogeneous catalysts such as Amberlyst-15 and H-beta zeolite. They observed significant reduction in glycerol conversion (from 95% to 47% for Amberlyst-15 and from 90% to 50% using H-beta zeolite) while switching the feed from pure glycerol to the impurities-added glycerol. A similar result has also been observed by our own research group in a continuous-flow reactor, as shown in the Figure 3.6.⁶⁹

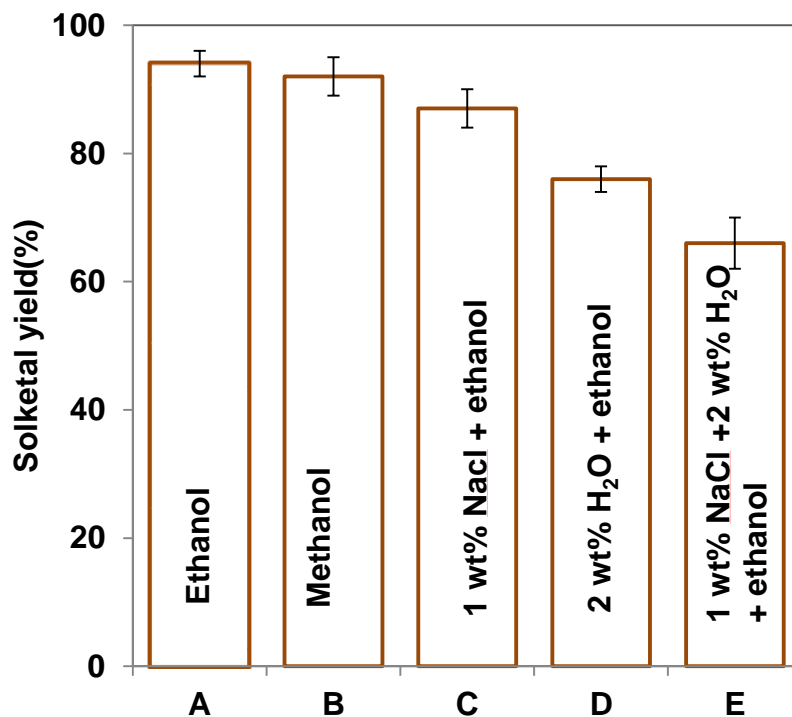


Figure 3.6 Deactivation of catalyst by impurities in the glycerol feed.

Our research group moved one step further and developed a modified continuous-flow reactor consisting of guard reactors allowing online removal of impurities in the glycerol feedstock and online regeneration of deactivated catalysts (Figure 3.7). Using crude glycerol and the modified continuous-flow reactor, a significant yield of solketal (~78%) was obtained after 1h on-stream. Moreover, we have carried out an on-line regeneration of the deactivated catalysts in the guard reactor and ketalization experiment simultaneously using purified crude glycerol ($\approx 96\%$ purity) as the feedstock and found that the catalyst (Amberlyst-36 wet) could be successfully regenerated for four consecutive cycles (96 h) with acceptable reduction in the solketal yield (from 92% to 81%).⁶⁹ For the regeneration of the catalyst (Amberlyst-36 wet) in the guard reactor, a 0.5 M sulfuric acid solution was used to flow through the guard reactor, followed by washing the regenerated catalysts with methanol solution and drying the bed with nitrogen for 5 h.

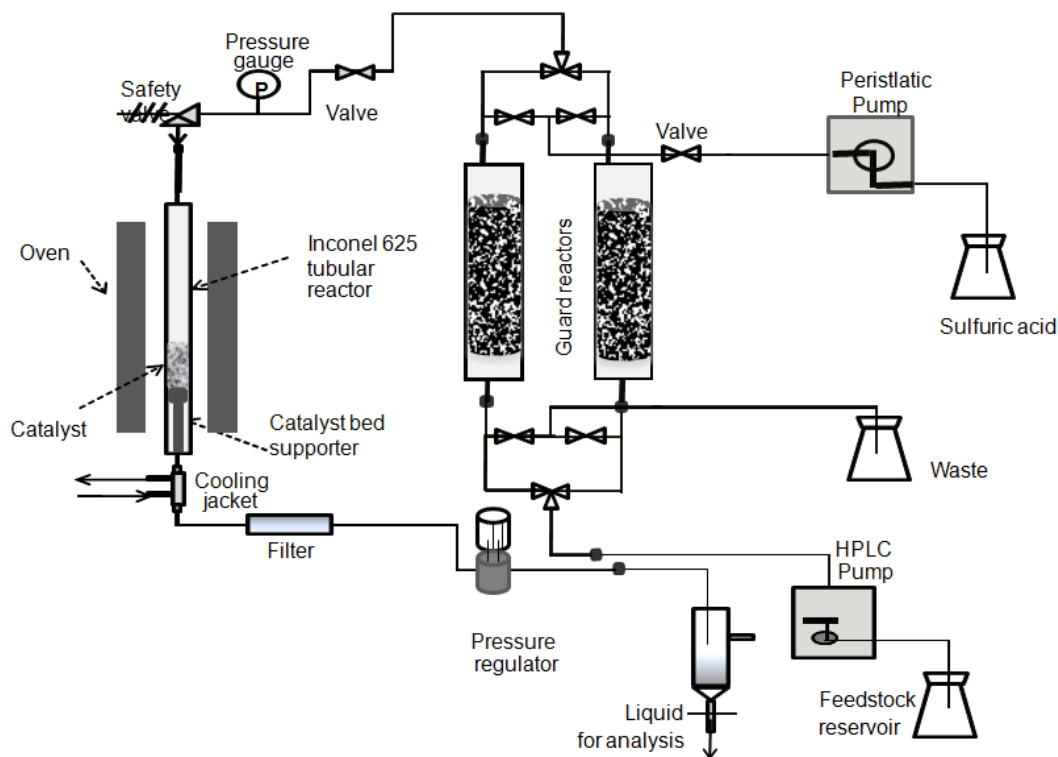


Figure 3.7 Flow reactor consisting of guard reactors allowing online removal of impurities in the glycerol feedstock and online regeneration of deactivated catalysts.

3.9 Conclusions

This review chapter over-views the state-of-the art of the sustainable production of solketal by catalytic reaction of glycerol with acetone. Different types of processes and catalysts developed and their performances are compared. Fundamentals of reaction mechanisms for the acid-catalyzed conversion of glycerol into solketal are presented. The main operation issues related to catalytic conversion of crude glycerol in a continuous-flow process and the direct use of crude glycerol are discussed. Some key conclusions are summarized below:

(1) Conversion of glycerol to solketal can proceed either using a homogeneous or heterogeneous catalyst; nevertheless the use of heterogeneous catalysts is preferred, as there are many shortcomings for using homogeneous catalysts, e.g., difficulty in catalyst recovery, corrosion to the reaction systems, and the environmental and economical concerns over the effluent disposal. Hence, it is of significance to explore heterogeneous acid catalysts for the glycerol ketalization process.

(2) The ketalization reaction has a very low equilibrium constant. In order to reach high conversions of glycerol it is necessary to shift the equilibrium towards the formation of solketal, by either feeding excess amount of acetone or by removing the water generated during the reaction continuously.

(3) All the batch processes have common limitation in terms of the difficulty in scaling up for production of solketal on a large scale. Compared with operation in a batch reactor, a continuous-flow process produces a similar product yield but requires much shorter reaction time. Therefore, development of continuous-flow processes is promising for production of solketal from glycerol on a large scale.

(4) The best yields of solketal were achieved by catalysts like Amberlyst-15, Amberlyst-35, Amberlyst-36, Ar-SBA-15, Zeolites, and SnCl_2 . The preferred reaction conditions are: catalysts with higher acidity, higher acetone to glycerol molar ratio, and lower temperature ($<70\text{ }^\circ\text{C}$). Using Amberlyst-36 wet catalyst, a very high yield of solketal ($94 \pm 2\text{ wt}\%$) was obtained at $25\text{ }^\circ\text{C}$, 500 psi, acetone-to-glycerol molar ratio of 4, WHSV of 2 h^{-1} .

(5) The ketalization reaction proceeds via acidic catalytic mechanism, hence catalysts with stronger acidity might lead to higher glycerol conversion.

(6) Heterogeneous catalysts for glycerol ketalization in a continuous-flow reactor can be deactivated, attributed to the loss of active acidic sites during the reaction, not due to coking. For a long time (days or months) operation, however, the reactor clogging might occur, caused by fine particles of disintegrated catalysts.

(7) Direct use of crude glycerol as feedstock may cause problems such as deactivation of catalyst (by poisoning the active sites by the impurities) or plugging of reactor (due to deposition of high boiling organic compounds or inorganic salts).

References

1. Subramaniam R, Dufreche S, Zappi M, Bajpai R. Microbial lipids from renewable resources: production and characterization. *Journal of Industrial Microbiology & Biotechnology* 2010;37(12):1271-87. doi:10.1007/s10295-010-0884-5.
2. Behr A, Eilting J, Irawadi K, Leschinski J, Lindner F. Improved utilisation of renewable resources: New important derivatives of glycerol. *Green Chemistry* 2008;10(1):13. doi:10.1039/b710561d.
3. Lin L, Cunshan Z, Vittayapadung S, Xiangqian S, Mingdong D. Opportunities and challenges for biodiesel fuel. *Applied Energy* 2011;88(4):1020-1031. doi:10.1016/j.apenergy.2010.09.029.
4. Johnson DT, Taconi KA. The glycerin glut : Options for the value-added conversion of crude glycerol resulting from biodiesel production. *Environmental Progress* 2009;26(4). doi:10.1002/ep.
5. Organization for Economic Co-operation and Development (OECD) and the Food and Agriculture Organization (FAO) of the United Nations, 2011-2020, available on <http://www.agri-outlook.org/48202074.pdf> (accessed April 9, 2015).
6. Thompson JC, He BB. Characterization of crude glycerol from biodiesel production from multiple feedstocks. *Applied Engineering in Agriculture* 2006;22:261-265.
7. Liu X, Jensen PR, Workman M. Bioconversion of crude glycerol feedstocks into ethanol by *Pachysolen tannophilus*. *Bioresource Technology* 2012;104:579-86. doi:10.1016/j.biortech.2011.10.065.
8. Liang Y, Cui Y, Trushenski J, Blackburn JW. Converting crude glycerol derived from yellow grease to lipids through yeast fermentation. *Bioresource Technology* 2010;101(19):7581-6. doi:10.1016/j.biortech.2010.04.061.
9. Biodiesel Magazine - The Latest News and Data About Biodiesel Production. Available at: <http://www.biodieselmagazine.com/articles/8137/clearing-the-way-for-byproduct-quality>. Accessed December 2, 2014.
10. Haas MJ, McAloon AJ, Yee WC, Foglia TA. A process model to estimate biodiesel production costs. *Bioresource Technology* 2006;97(4):671-8. doi:10.1016/j.biortech.2005.03.039.
11. Callam CS, Singer SJ, Lowary TL, Hadad CM. Computational analysis of the potential energy surfaces of glycerol in the gas and aqueous phases: effects of level of theory, basis set, and solvation on strongly intramolecularly hydrogen-bonded systems. *Journal of the American Chemical Society* 2001;123(47):11743-54.

12. Da Silva GP, de Lima CJB, Contiero J. Production and productivity of 1,3-propanediol from glycerol by *Klebsiella pneumoniae* GLC29. *Catalysis Today* 2014. doi:10.1016/j.cattod.2014.05.016.
13. Zhou C-HC, Beltramini JN, Fan Y-X, Lu GQM. Chemoselective catalytic conversion of glycerol as a biorenewable source to valuable commodity chemicals. *Chemical Society reviews* 2008;37(3):527-49. doi:10.1039/b707343g.
14. Pagliaro M, Ciriminna R, Kimura H, Rossi M, Della Pina C. From glycerol to value-added products. *Angewandte Chemie (International ed. in English)* 2007;46(24):4434-40. doi:10.1002/anie.200604694.
15. Zhu S, Gao X, Zhu Y, Zhu Y, Zheng H, Li Y. Promoting effect of boron oxide on Cu/SiO₂ catalyst for glycerol hydrogenolysis to 1,2-propanediol. *Journal of Catalysis* 2013;303:70-79. doi:10.1016/j.jcat.2013.03.018.
16. Chen L, Liang J, Lin H, Weng W, Wan H, Védrine JC. MCM41 and silica supported MoVTe mixed oxide catalysts for direct oxidation of propane to acrolein. *Applied Catalysis A: General* 2005;293:49-55. doi:10.1016/j.apcata.2005.06.029.
17. Hirai T, Ikenaga N, Miyake T, Suzuki T. Production of Hydrogen by Steam Reforming of Glycerin on Ruthenium Catalyst. *Energy & Fuels* 2005;19(4):1761-1762. doi:10.1021/ef050121q.
18. Cassel S, Debaig C, Benvegna T, *et al.* Original Synthesis of Linear, Branched and Cyclic Oligoglycerol Standards. *European Journal of Organic Chemistry* 2001;2001(5):875-896. doi:10.1002/1099-0690(200103)2001.
19. Kenar JA. Glycerol as a platform chemical: Sweet opportunities on the horizon? *Lipid Technology* 2007;19(11):249-253. doi:10.1002/lite.200700079.
20. Len C, Luque R. Continuous flow transformations of glycerol to valuable products: an overview. *Sustainable Chemical Processes* 2014;2(1):1. doi:10.1186/2043-7129-2-1.
21. Pagliaro M, Rossi M. *Future of Glycerol*. Cambridge: Royal Society of Chemistry; 2010. doi:10.1039/9781849731089.
22. Zheng Y, Chen X, Shen Y. Commodity chemicals derived from glycerol, an important biorefinery feedstock. *Chemical Reviews* 2008;108(12):5253-77. doi:10.1021/cr068216s.
23. Deutsch J, Martin a, Lieske H. Investigations on heterogeneously catalysed condensations of glycerol to cyclic acetals. *Journal of Catalysis* 2007;245(2):428-435. doi:10.1016/j.jcat.2006.11.006.

24. Agirre I, García I, Reques J, *et al.* Glycerol acetals, kinetic study of the reaction between glycerol and formaldehyde. *Biomass and Bioenergy* 2011;35(8):3636-3642. doi:10.1016/j.biombioe.2011.05.008.
25. M.T.M. Silva V, Rodrigues AE. Synthesis of diethylacetal: thermodynamic and kinetic studies. *Chemical Engineering Science* 2001;56(4):1255-1263. doi:10.1016/S0009-2509(00)00347-X.
26. Barros AO, Faísca AT, Lachter ER, Nascimento RS V, San Gil RAS. Acetalization of hexanal with 2-ethyl hexanol catalyzed by solid acids. *Journal of the Brazilian Chemical Society* 2011;22(2):359-363. doi:10.1590/S0103-50532011000200023.
27. Pariente S, Tanchoux N, Fajula F. Etherification of glycerol with ethanol over solid acid catalysts. *Green Chemistry* 2009;11(8):1256. doi:10.1039/b905405g.
28. Mota CJ a., da Silva CX a., Rosenbach, N, Costa J, da Silva F. Glycerin Derivatives as Fuel Additives: The Addition of Glycerol/Acetone Ketal (Solketal) in Gasolines. *Energy & Fuels* 2010;24(4):2733-2736. doi:10.1021/ef9015735.
29. Maksimov a. L, Nekhaev a. I, Ramazanov DN, Arinicheva Y a., Dzyubenko a. a., Khadzhiev SN. Preparation of high-octane oxygenate fuel components from plant-derived polyols. *Petroleum Chemistry* 2011;51(1):61-69. doi:10.1134/S0965544111010117.
30. Mićović VM, Stojiljković A. The condensations of polyhydric alcohols and monosaccharides with cyclopentanone and cyclohexanone. *Tetrahedron* 1958;4(1-2):186-196. doi:10.1016/0040-4020(58)88017-5.
31. O'Brien RD, Cheung L, Kimmel EC. Inhibition of the α -glycerophosphate shuttle in housefly flight muscle. *Journal of Insect Physiology* 1965;11(9):1241-1246. doi:10.1016/0022-1910(65)90116-2.
32. Cutter HB, Danielson CA, Golden HR. Polymethylene-bis-(p-aminophenyl Sulfones). *Journal of the American Chemical Society* 1945;67(7):1051-1053. doi:10.1021/ja01223a003.
33. Bernd Bruchmann, Karl Haberle, Helmut Gruner MH. Preparation of cyclic acetals and ketals, 1999, Patent US5917059.
34. Mushrush GW, Hardy D. Fuel system icing inhibitor and deicing composition, 1998, Patent US5705087 A.
35. Mushrush GW, Stalick WM, Beal EJ, Basu SC, Slone JE, Cummings J. The synthesis of acetals and ketals of the reduced sugar mannose as fuel system icing inhibitors. *Petroleum Science and Technology* 1997;15:237-244.

36. Garcı E, Laca M, Pe E, Garrido A. New Class of Acetal Derived from Glycerin as a Biodiesel Fuel Component. 2008;(15):4274-4280.
37. Nanda MR, Yuan Z, Qin W, Ghaziaskar HS, Poirier M-A, Xu CC. Thermodynamic and kinetic studies of a catalytic process to convert glycerol into solketal as an oxygenated fuel additive. *Fuel* 2014;117:470-477. doi:10.1016/j.fuel.2013.09.066.
38. Ag B. Cyclic acetal or ketal preparation from poly:ol and aldehyde or ketone, 1998, Patent DE19648960 A1.
39. He Dy, Li ZJ, Li ZJ, Liu YQ, Qiu Dx, Cai Ms. Studies on Carbohydrates X. A New Method for the Preparation of Isopropylidene Saccharides. *Synthetic Communications* 1992;22(18):2653-2658. doi:10.1080/00397919208021665.
40. Roldan L, Mallada R, Fraile JM, Mayoral JA, Menendez M. Glycerol upgrading by ketalization in a zeolite membrane. *Asia-Pacific Journal of Chemical Engineering* 2009; 4:279–284.
41. Vicente G, Melero J a., Morales G, Paniagua M, Martín E. Acetalisation of bio-glycerol with acetone to produce solketal over sulfonic mesostructured silicas. *Green Chemistry* 2010;12(5):899. doi:10.1039/b923681c.
42. Ferreira P, Fonseca IM, Ramos a. M, Vital J, Castanheiro JE. Valorisation of glycerol by condensation with acetone over silica-included heteropolyacids. *Applied Catalysis B: Environmental* 2010;98(1-2):94-99. doi:10.1016/j.apcatb.2010.05.018.
43. Royon D, Locatelli S, Gonzo EE. Ketalization of glycerol to solketal in supercritical acetone. *The Journal of Supercritical Fluids* 2011;58(1):88-92. doi:10.1016/j.supflu.2011.04.012.
44. Menezes FDL, Guimaraes MDO, da Silva MJ. Highly Selective SnCl₂ -Catalyzed Solketal Synthesis at Room Temperature. *Industrial & Engineering Chemistry Research* 2013;52(47):16709-16713. doi:10.1021/ie402240j.
45. Green D, Perry R. *Perry's Chemical Engineers' Handbook, Eighth Edition*. McGraw Hill Professional; 2007:2400.
46. Noël T, Buchwald SL. Cross-coupling in flow. *Chemical Society reviews* 2011;40(10):5010-29. doi:10.1039/c1cs15075h.
47. Hartman RL, McMullen JP, Jensen KF. Deciding whether to go with the flow: evaluating the merits of flow reactors for synthesis. *Angewandte Chemie (International ed. in English)* 2011;50(33):7502-19. doi:10.1002/anie.201004637.
48. Jähnisch K, Hessel V, Löwe H, Baerns M. *Chemistry in Microstructured Reactors.*; 2004:406-46. doi:10.1002/anie.200300577.

49. Chevalier B, Lavric ED, Cerato-Noyerie C, Horn CR, Woehl P. Microreactors for industrial multi-phase applications : Test reactions to develop innovative glass microstructure designs. *Chimica Oggi* 2008; 26: 38-42.
50. Cablewski T, Faux AF, Strauss CR. Development and Application of a Continuous Microwave Reactor for Organic Synthesis. *The Journal of Organic Chemistry* 1994;59(12):3408-3412. doi:10.1021/jo00091a033.
51. Clarkson JS, Walker AJ, Wood MA. Continuous Reactor Technology for Ketal Formation : An Improved Synthesis of Solketal. *Organic Process Research & Development* 2001; 5: 630-635.
52. Monbaliu J-CM, Winter M, Chevalier B, *et al.* Effective production of the biodiesel additive STBE by a continuous flow process. *Bioresource Technology* 2011;102(19):9304-7. doi:10.1016/j.biortech.2011.07.007.
53. Nanda MR, Yuan Z, Qin W, Ghaziaskar HS, Poirier M-A, Xu C (Charles). A new continuous-flow process for catalytic conversion of glycerol to oxygenated fuel additive: Catalyst screening. *Applied Energy* 2014;123:75-81. doi:10.1016/j.apenergy.2014.02.055.
54. Hessel V, Vural Gürsel I, Wang Q, Noël T, Lang J. Potential analysis of smart flow processing and micro process technology for fastening process development: use of chemistry and process design as intensification fields. *Chemical Engineering & Technology* 2012;35(7):1184-1204. doi:10.1002/ceat.201200038.
55. Razzaq T, Kappe CO. Continuous flow organic synthesis under high-temperature/pressure conditions. *Chemistry, an Asian journal* 2010;5(6):1274-89. doi:10.1002/asia.201000010.
56. Illg T, Löb P, Hessel V. Flow chemistry using milli- and microstructured reactors- from conventional to novel process windows. *Bioorganic & medicinal chemistry* 2010;18(11):3707-19. doi:10.1016/j.bmc.2010.03.073.
57. Nanda MR, Yuan Z, Qin W, Ghaziaskar HS, Poirier M-A, Xu C (Charles). Catalytic conversion of glycerol to oxygenated fuel additive in a continuous flow reactor: Process optimization. *Fuel* 2014;128:113-119. doi:10.1016/j.fuel.2014.02.068.
58. Crotti C, Farnetti E, Guidolin N. Alternative intermediates for glycerol valorization: iridium-catalyzed formation of acetals and ketals. *Green Chemistry* 2010;12(12):2225. doi:10.1039/c0gc00096e.
59. Sülü M, Venanzi LM. Acetalization and Transacetalization Reactions Catalyzed by Ruthenium, Rhodium, and Iridium Complexes with {2-{{Bis[3-(trifluoromethyl)phenyl]phosphino}methyl}-2-methylpropane- 1,3-diyl}bis[bis[3-(trifluoromethyl)phenyl]phosphine] (MeC[CH₂P(m-CF₃C₆H₄)₂]₃). *Helvetica*

Chimica Acta 2001;84(4):898-907. doi:10.1002/1522-2675(20010418)84:4<898::AID-HLCA898>3.0.CO;2-V.

60. Jiang Q, Rüegger H, Venanzi LM. Some new chain-like terdentate phosphines, their ruthenium(II) coordination chemistry and the activity of the cations [Ru(MeCN)₃(PhP{CH₂CH₂P(p-X-C₆H₄)₂)₂]₂⁺ (X=H, F, Me and OMe) as acetalization catalysts. *Inorganica Chimica Acta* 1999;290(1):64-79. doi:10.1016/S0020-1693(99)00117-6.
61. Barbaro P, Bianchini C, Oberhauser W, Togni A. Synthesis and characterization of chiral bis-ferrocenyl triphosphine Ni(II) and Rh(III) complexes and their use as catalyst precursors for acetalization reactions. *Journal of Molecular Catalysis A: Chemical* 1999;145(1-2):139-146. doi:10.1016/S1381-1169(99)00016-3.
62. Gorla F, Venanzi LM. Cationic Palladium(II), Platinum(II), and Rhodium(I) Complexes as Acetalisation Catalysts. *Helvetica Chimica Acta* 1990;73(3):690-697. doi:10.1002/hlca.19900730317.
63. Cataldo M, Nieddu E, Gavagnin R, Pinna F, Strukul G. Hydroxy complexes of palladium(II) and platinum(II) as catalysts for the acetalization of aldehydes and ketones. *Journal of Molecular Catalysis A: Chemical* 1999;142(3):305-316. doi:10.1016/S1381-1169(98)00299-4.
64. Li L, Korányi TI, Sels BF, Pescarmona PP. Highly-efficient conversion of glycerol to solketal over heterogeneous Lewis acid catalysts. *Green Chemistry* 2012;14(6):1611. doi:10.1039/c2gc16619d.
65. Corma A, Navarro MT, Nemeth L, Renz M. Sn-MCM-41 a heterogeneous selective catalyst for the Baeyer-Villiger oxidation with hydrogen peroxide. Electronic supplementary information (ESI) available: XRD pattern of as-prepared Sn-MCM-41. See <http://www.rsc.org/suppdata/cc/b1/b105927k/>. *Chemical Communications* 2001;(21):2190-2191. doi:10.1039/b105927k.
66. Vol'eva VB, Belostotskaya IS, Malkova AV., *et al.* New approach to the synthesis of 1,3-dioxolanes. *Russian Journal of Organic Chemistry* 2012;48(5):638-641. doi:10.1134/S1070428012050028.
67. Foster AB, Randall MH, Webber JM. 615. Aspects of stereochemistry. Part XX. Reaction of 3-O-methyl-D-glucitol with acetone and benzaldehyde. *Journal of the Chemical Society (Resumed)* 1965:3388. doi:10.1039/jr9650003388.
68. García H, García OI, Fraile JM. Solketal: Green and catalytic synthesis and its classification as a solvent : 2,2-dimethyl-4-hidroxymethyl-1,3-dioxolane, an interesting green solvent produced through heterogeneous catalysis. *Chimica oggi* 2008; 26: 10-12.

69. Nanda MR, Yuan Z, Qin W, Poirier M. Catalytic conversion of purified crude glycerol in a continuous-flow process for the synthesis of oxygenated fuel additive, *Biomass and Bioenergy*,2015, (submitted for publication).
70. Refined Glycerine 99.7% Indonesia Factory - Buy Refined Glycerine,Glycerine,Refined Glycerine 99.5% Product on Alibaba.com. Available at: http://www.alibaba.com/product-detail/refined-Glycerine-99-7-Indonesia-factory_543433395.html?s=p. Accessed December 8, 2014.
71. Da Silva CXA., Mota CJA. The influence of impurities on the acid-catalyzed reaction of glycerol with acetone. *Biomass and Bioenergy* 2011;35(8):3547-3551. doi:10.1016/j.biombioe.2011.05.004.

Chapter 4

4 Recent advancements in catalytic conversion of glycerol into propylene glycol: A review

Abstract

The recent boom in worldwide biodiesel production has created a large surplus of glycerol. As a result, the price of crude glycerol is a fraction of what it was 10 years ago. This in turn has renewed interest in the production of value-added products from this now-abundant and cheap feedstock. Selective hydrogenolysis of glycerol to propylene glycol (PG) is one of the most promising routes for glycerol valorization, since this compound is an important chemical intermediate in a number of applications. In this chapter, advancements in the conversion of glycerol into propylene glycol via selective hydrogenolysis are reviewed, which include advances in process development, effects of preparation and activation methods on catalytic activity and stability, and advances in catalysts, etc. The reaction mechanisms and challenges of utilizing crude glycerol for the hydrogenolysis reaction are also discussed.

Keywords: Glycerol; Propylene glycol; Hydrogenolysis; Process development; Catalyst; Mechanism; Crude glycerol

4.1 Introduction

Depletion in fossil fuel reserves and its increasing impact on the environment have intensified interest in the development of renewable fuels mainly bio-ethanol and bio-diesel.^{1,2} Currently, biodiesel is produced by the transesterification of triglycerides with simple alcohols such as methanol or ethanol catalyzed by alkaline or acidic catalysts. Glycerol is produced as a byproduct of this process, comprising ~10 wt% of the product stream. The increased production of biodiesel globally has resulted in a large surplus of glycerol that has caused the saturation of the glycerol market.³ Therefore, new economical ways of using glycerol for value-added products must be developed to strengthen the sustainable development of the biodiesel industry.

The presence of three hydroxyl groups in glycerol make it a versatile compound with a wide range of properties and it is used in a wide variety of applications, particularly in cosmetics, pharmaceuticals and food industries.⁴ Moreover, glycerol can be converted into different high-value chemicals via chemical and biochemical processes. In recent years only a few applications have been identified where glycerol could be utilized on a large scale. Hydrogenolysis of glycerol to propylene glycol (PG) is one of these applications which have attracted major attention both in research and industrial communities. This is quite evident from the increase in the number of papers relating to glycerol hydrogenolysis published in recent years (Figure 4.1).

Propylene glycol (PG) is a non-toxic chemical, produced by selective hydrogenolysis of glycerol. It is extensively used as a monomer for polyester resins, as an antifreeze agent, in liquid detergents, paints, cosmetics and food, etc. (Figure 4.2).⁵ World-wide production of propylene glycol is given in Figure 4.3. The current global production of propylene glycol is 2.18 million tons per year which is mainly produced from propylene oxide and sold at \$1.0-2.2 per kg.^{3,6} The world's PG market is growing at a rate of 4.5% per annum and is expected to reach 2.56 million tons by 2017.⁶ Dow Chemicals, Eastman Chemical, Lyondell Chemical, Global Bio-Chem Technology Group, Ineos Oxide, Archer Daniels Midland Co., SKC Chemicals Group, Arrow Chemical Group Corp., BASF AG, and Huntsman Corp are the major producers for PG.

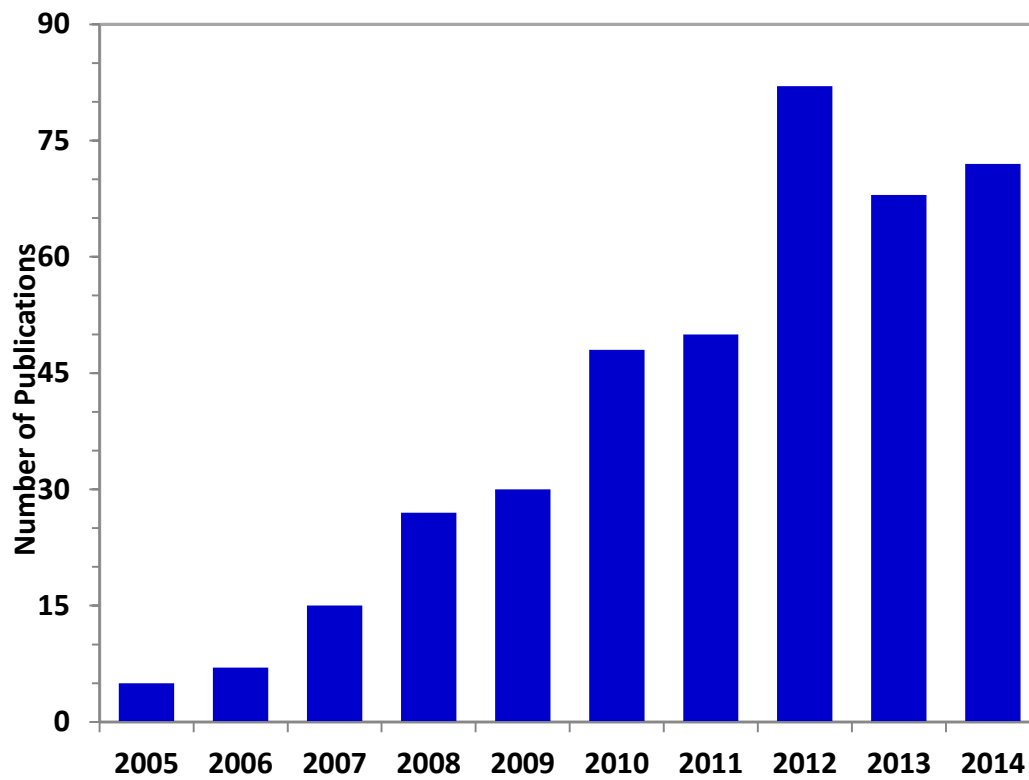


Figure 4.1 Annual number of publications on the concept of glycerol hydrogenolysis (searched from database Scifinder as “glycerol” and “hydrogenolysis”)

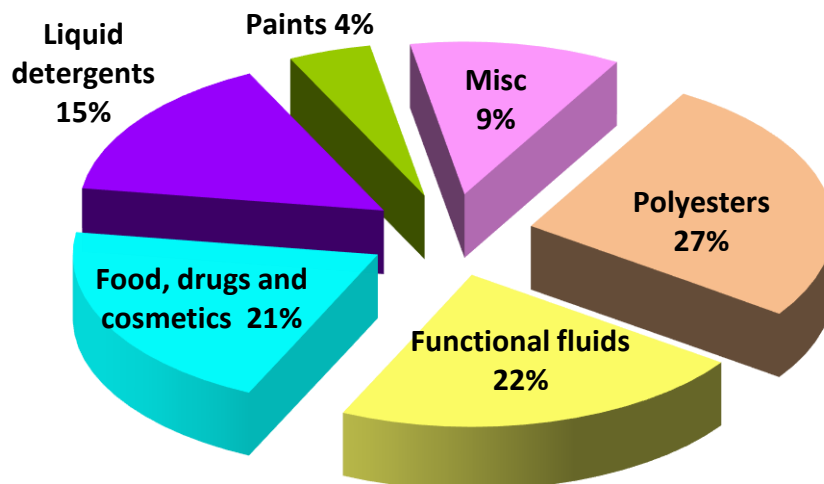


Figure 4.2 Applications of propylene glycol in different fields ⁵(Misc: Tobacco humectants, flavors and fragrances, and animal feed)

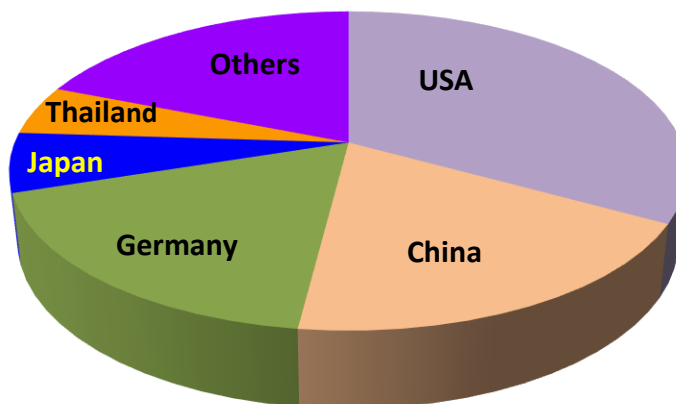


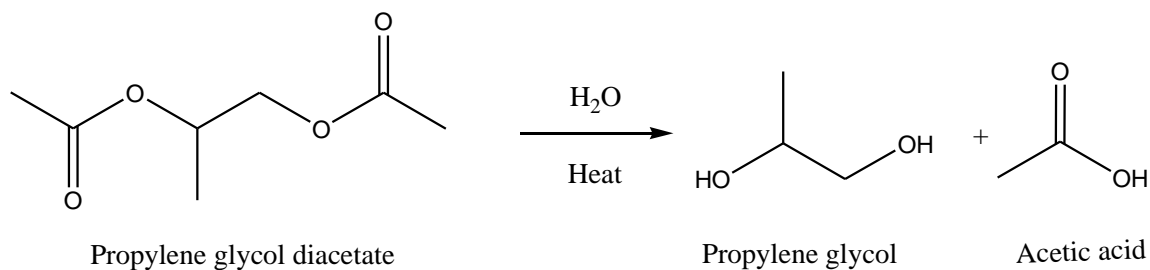
Figure 4.3 World scenario for the production of propylene glycol⁶

In this chapter, recent advancements in the production of propylene glycol are reviewed. The developments in reactor systems, the effects of catalyst preparation and activation methods on catalytic activity and stability, and the advances in catalysts are reported. The reaction mechanisms and the challenges of using crude glycerol as the feedstock for the glycerol hydrogenolysis reactions are discussed.

4.2 Historical context

Propylene glycol was first synthesized by Wurtz in 1859 by the hydrolysis of propylene glycol diacetate as given in Scheme 4.1.⁷ In the mid-1930s, DuPont produced propylene glycol as a by-product from the hydrogenation of coconut oil. However it was first commercialized by Carbide and Carbon Chemical Corporation in 1931 using the chlorohydrine route from propylene.⁷

The use of propylene glycol gained momentum during the World War II as it was used as a substitute for glycerol in pharmaceuticals, which led to opening of new production facilities by Dow Chemical in 1942 and Wyandotte Chemical Corp. in 1948.⁷



Scheme 4.1 Synthesis of propylene glycol from propylene glycol diacetate

Conventionally, propylene glycol is produced from propylene oxide derived from petroleum resources. Currently, five different technologies are used in the commercial production of propylene oxide; namely A) the styrene monomer process (LyondellBasel and Shell), B) the anthraquinone process (Dow Chemical and BASF), C) the tert-butyl

alcohol process (LyondellBasel and Huntsman Corp.), D) the cumene hydroperoxide process (Sumitomo Chemicals) and E) the chlorohydrine process (Dow Chemical).⁸ The reactions relating to these processes are shown in Scheme 4.2. The final product (propylene oxide) in all these processes is hydrolysed to form propylene glycol.

The conventional methods for the production of propylene glycol are normally non-catalytic processes at high temperature and pressure (a drawback). A large excess of water is used in the processes producing di- and tri-propylene glycol (Figure 4.4) as co-products.⁷

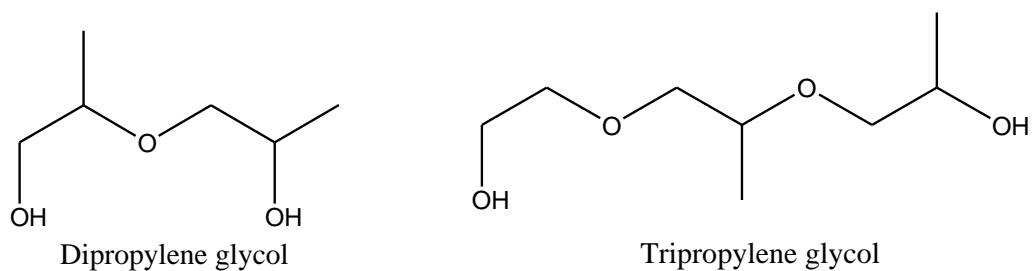
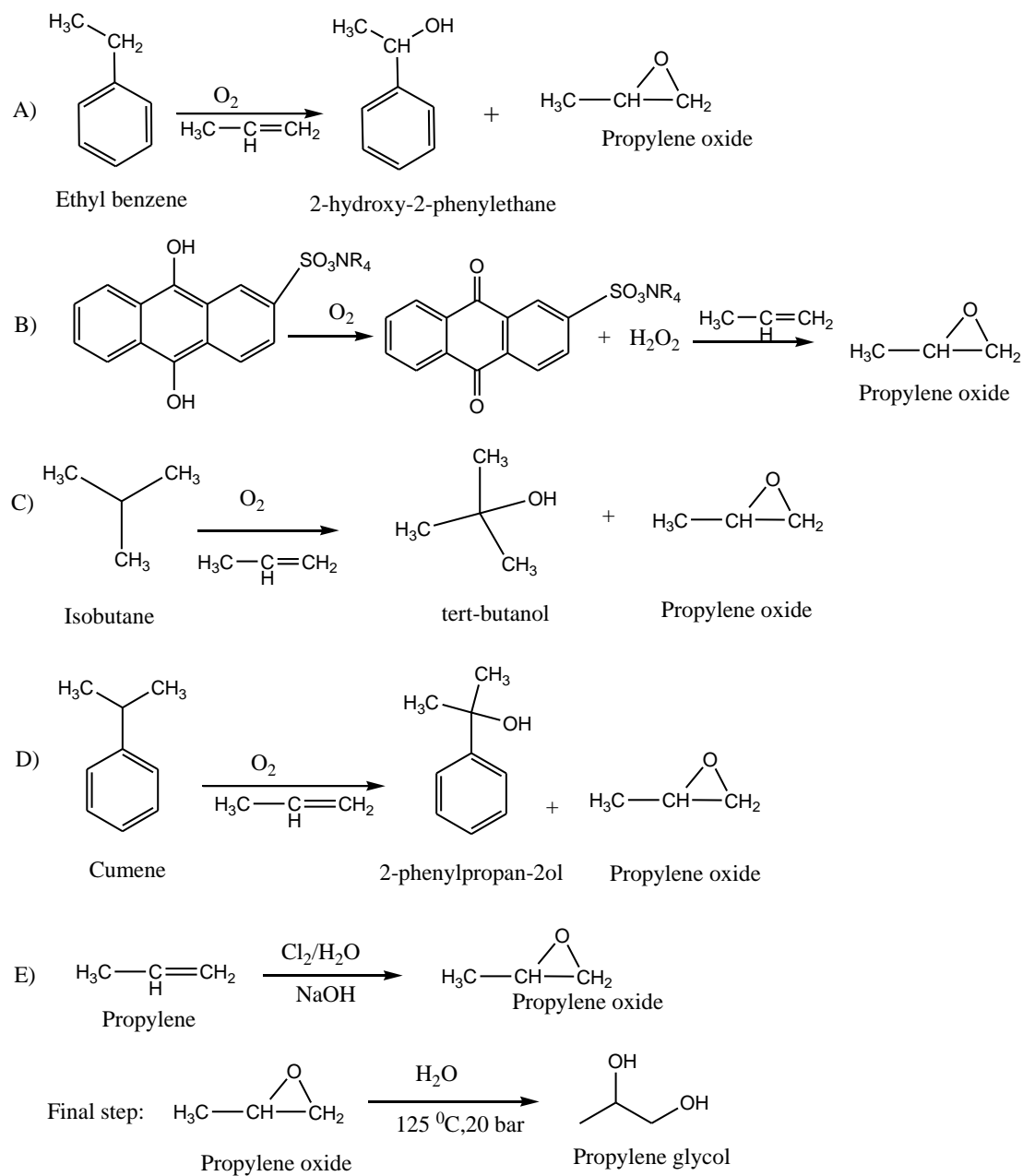


Figure 4.4 Structure of dipropylene glycol and tripropylene glycol



Scheme 4.2 Different processes for the production of propylene oxide – precursor for propylene glycol: (A) Styrene monomer process; (B) Anthraquinone process; (C) tert-butyl alcohol process; (D) Cumene hydroperoxide process; (E) Chlorohydrin process

Thus, as a greener process, hydrogenolysis of glycerol—as an abundant and inexpensive industrial byproduct or waste to propylene glycol (PG) is much more advantageous than the conventional processes described above.

4.3 Effects of catalyst preparation and activation methods

The methods of catalyst preparation for the hydrogenolysis of glycerol have significant effects on glycerol conversion and product selectivity. A wide variety of methods including impregnation (IM), adsorption, ion-exchange (IE), sol-gel (SG), (co)precipitation (CP), hydrothermal treatment (HT), solid fusion (SF), and carbon-microsphere-templating (CT) etc. have been reported in the preparation of highly dispersed catalysts.^{9,10,11,12,13} The effects of the different catalyst preparation methods on glycerol conversion and PG selectivity are given in Table 4.1. Huang *et al.* reported glycerol hydrogenolysis using a highly dispersed silica-supported copper catalyst (Cu/SiO₂) prepared by gel-precipitation and compared the activity of this catalyst to a reference Cu/SiO₂ catalyst prepared by impregnation.¹⁴ A very high selectivity (>98%) towards PG was observed with both catalysts, however, the catalyst prepared by gel-precipitation demonstrated much higher activity with better long term stability as compared to the catalyst prepared by impregnation. Bienholz *et al.* compared the activity of CuO/ZnO catalysts prepared by co-precipitation and oxalate-gel and found that the catalyst prepared by the oxalate-gel method exhibited higher glycerol conversion (46%) and space-time yield (9.8 g_{propylene glycol}/g_{Cu}/h) than the co-precipitation catalyst.¹⁵ In 2013, Li *et al.* investigated the performance of zinc incorporated copper catalysts over alumina support (Cu-ZnO/Al₂O₃) prepared by impregnation and co-precipitation.¹³ In their work, the Cu-ZnO/Al₂O₃-CP catalyst demonstrated higher glycerol conversion (86%) and PG selectivity (85%) than the Cu-ZnO/Al₂O₃-IM (conversion: 64% and selectivity: 68%). Similar observations have been reported by Kim *et al.* using a Cu/Cr₂O₃ catalyst,¹⁶ Yuan *et al.* using CuO/MgO catalyst,¹⁷ and Balraju *et al.* using Ru/TiO₂ catalyst.¹⁸ Almost in each case, the catalysts prepared by co-precipitation method demonstrated better performance than that prepared by impregnation method. These authors attributed the high performance of the co-precipitation catalysts to their greater surface area and higher dispersion of the Cu metal. In contrast to these results, Panyad *et al.* compared the activity of Cu-ZnO/Al₂O₃ catalysts prepared by impregnation, co-precipitation and sol-gel method and found the order of catalytic activity and stability (after 12 h) to be: impregnation > co-precipitation > sol-

gel.¹⁰ In this case, the greater activity and stability of the impregnated catalysts was ascribed to decreased levels of coke deposition.

Hydrogenolysis of glycerol over Ni/ZnO catalysts prepared by impregnation, co-precipitation, hydrothermal treatment, and carbon microsphere hard-template methods was investigated by Hu *et al.*¹¹ The authors carried out the reaction in a flow reactor by reacting 10 wt% glycerol aqueous solution at 508 K under 3.1 MPa of H₂ over a catalyst loading of 0.5 g. The process was an integration of reforming and hydrogenolysis reaction. The activity of the catalysts, at all WHSV tested, was found to increase as follows: impregnation < co-precipitation < hydrothermal treatment < carbon microsphere hard-template, which is attributed to the large surface area and high Ni dispersion of the catalyst. In 2012, Mane *et al.* also published their work on the effect of preparation methods on the activity of the catalysts meant for the hydrogenolysis of glycerol.⁹ They prepared Cu/Al₂O₃ catalysts using the co-precipitation and solid state fusion methods. The best results were obtained at 493 K, 5.2 MPa of H₂ using a 20 wt% aqueous glycerol solution and 0.01 g/mL of catalyst. Under these conditions, glycerol conversion and PG selectivity for Cu/Al₂O₃-CP were 58% and 88%, respectively, whereas the conversion and selectivity for Cu/Al₂O₃-SF catalyst were 5% and 74%, respectively. One of the main issues in this work was the large particle size (and correspondingly smaller surface area) of the catalyst prepared by solid state fusion.

Yu and co-workers investigated the role of activation processes on the performance of Ni/AC (activated carbon) catalysts.¹⁹ They prepared Ni/AC catalyst by incipient wetness impregnation. Samples of the as-prepared catalyst (Ni/AC) were subjected to carbothermal and hydrogen reduction in a tubular furnace with 90 min ramp and 180 min hold at 723 K under flow N₂ and H₂, respectively. The samples were designated Ni/AC-C and Ni/AC-H, respectively as shown in Table 4.2. Samples of Ni/AC-C and Ni/AC-H were treated with KBH₄ in 0.2 M NaOH. These catalysts were designated Ni/AC-CB and Ni/AC-HB, respectively. The Ni/AC-CB was found to be the most active in the hydrogenolysis of glycerol. The authors attributed the high activity of the Ni/AC-CB catalyst to the synergistic effects of hydrogen centre and acidity generated from the processes.

The research group of Vila also published a paper on glycerol hydrogenolysis with Cu/ γ -Al₂O₃, where the effects of activation processes including calcination, reduction and re-oxidation were investigated.²⁰ In this work, the Cu-Al₂O₃ catalyst was prepared by the impregnation method. The catalyst was then dried at 393 K for 12 h. Three samples of this material were taken and pretreated as follows (i) calcination at 673 K under 20 vol% O₂ in Ar at a flow of 100 mL/min with a heating rate of 10 K/min for 0.5 or 2 h (ii) reduction in 5 vol% H₂/Ar flow at 573 K for 1 h (iii) re-oxidation in N₂O/N₂ flow at 353 K for 0.25 h. The glycerol conversion rate was found to be higher for the catalysts that were calcined for a longer time. Irrespective of the calcination time, the selectivity of the reduced catalyst was significantly higher than those measured with the calcined and reoxidized catalysts. However, significant differences in PG selectivity were observed for the reduced catalysts, indicating that other factors may also be relevant. Moreover, Vasiliadou *et al.* studied the effect of activation processes on the activity of glycerol hydrogenolysis catalysts.²¹ They observed that the conversion of glycerol using Cu/SiO₂ catalysts that were calcined in flowing air or NO was higher (~50% conversion) compared to catalysts calcined under stagnant air. For the SBA and SBA900C-supported catalysts, the different calcination atmosphere (air or NO flow) also influenced catalytic activity. The effect of calcination atmosphere was more pronounced with in SBA900C-supported catalysts. The samples calcined in NO resulted in higher glycerol conversion compared with those calcined in air. They observed that the air-calcined catalysts presented almost empty pores with large copper particles on the exterior of the support, which could have affected the performance of the catalysts.

In brief summary, the glycerol conversion and PG selectivity is usually lower for the catalysts prepared by the impregnation method. The catalysts activated by calcination and reduction using flow air and H₂, respectively, performed better than those activated using stagnant air and H₂.

Table 4.1 Effect of catalyst preparation methods on glycerol conversion and propylene glycol selectivity

Catalyst	Method	Surface area (m ² /g)	Reaction conditions	%Conv (glycerol)	%Sel (PG)	Ref
Cu/SiO ₂	IM	38.6 (Cu)	80% aq glycerol 80 g, 9 MPa, 4 g cat, 12 h , 433 K	2	99	14
Cu/SiO ₂	PG	198.9		19	98	14
CuO/ZnO	OG	30.1 (Cu)	140 mL pure glycerol, 3 g cat, 5 MPa H ₂ , 473 K	46	90	15
CuO/ZnO	CP	16.7		17	87	15
Cu/Cr ₂ O ₃	IM	-	50 g glycerol, 1 g cat, 8 MPa, 493 K	32	41	16
Cu/Cr ₂ O ₃	pre	--		80	85	16
CuO/MgO	CP	----	75 wt% aq glycerol 8.0 mL, 1.0 g cat, 3.0 MPa H ₂ , 453 K, 20 h	72	98	17
CuO/MgO	IM	----		30	93	17
Ru/TiO ₂	IM	2.4	20 wt% aq glycerol, 6 MPa H ₂ , 8 h, 453 K, catalyst loading 6wt% of solution	31	59	18
Ru/TiO ₂	CP	7.2		44	58	18
Cu-ZnO/Al ₂ O ₃	IM	---	80 wt% aq glycerol, 523K, 3.2 MPa H ₂ , 2.8 h ⁻¹ , H ₂ :Gly= 4:1	100 (12h)	90 (15h)	10
Cu-ZnO/Al ₂ O ₃	CP	---		100 (6h)	90 (5h)	10
Cu-ZnO/Al ₂ O ₃	SG	---		100 (2h)	90 (2h)	10
Ni/ZnO	IM		10 wt% aq glycerol, W _{cat} =0.5 g, 508K, 3.1 MPa H ₂ ,	45	44	11
Ni/ZnO	CP			80	46	11
Ni/ZnO	HT			84	50	11
Ni/ZnO	CT			88	55	11
Cu-Al ₂ O ₃	CP		20 wt% aq glycerol, 0.01 g/mL cat, 493K, 5.2 MPa H ₂ , 5 h, 100 ml batch reactor	58	88	9
Cu-Al ₂ O ₃	Solid fusion			5	74	9
Cu-ZnO/Al ₂ O ₃	IM		80 wt% aq glycerol, 523K, 0.05h ⁻¹ , H ₂ :gly= 150:1, after 10 h on-stream	64	68	13
Cu-ZnO/Al ₂ O ₃	CP			86	85	13

Table 4.2 Effect of catalyst activation process on glycerol conversion and propylene glycol selectivity

Catalyst	Activation process	Reaction conditions	%Conv (glycerol)	%Sel (PG)	Ref
Cu-SG	Air (stag)	40 vol% alcoholic solution glycerol, 8 MPa H ₂ , 513K, Catalyst/Glycerol ratio 0.006 (w/w), 5 h reaction time	33	94	21
Cu-SG	NO		51	95	21
Cu-SG	Air		52	97	21
Cu-SBA	NO		49	96	21
Cu-SBA	Air		52	96	21
Cu-SBA 900C	NO		37	96	21
Cu-SBA900C	Air (flow)		20	92	21
Cu-Al ₂ O ₃	C	50 g of 80% aq glycerol sol, 0.8 g catalyst, 2.4 MPa H ₂ , 493 K, 8h reaction.	13	38	20
Cu-Al ₂ O ₃	C-r		14	75	20
Cu-Al ₂ O ₃	C-r-o		19	35	20
Cu-Al ₂ O ₃	C2		19	25	20
Cu-Al ₂ O ₃	C2-r		23	37	20
Cu-Al ₂ O ₃	C2-r-o		30	34	20
Ni/AC	C	150g 25wt.% aq glycerol, 0.695 g Ni in the cat, 5 MPa H ₂ , 473 K, 6 h	7	18	19
Ni/AC	H		6	32	19
Ni/AC	CB		43	76	19
Ni/AC	HB		11	64	19

4.4 Development of the reaction processes

Traditionally, homogeneous catalysts have been used for the hydrogenolysis of glycerol to propylene glycol. Tessie patented a method for the catalytic production of propylene glycol from glycerol in aqueous solution using a homogeneous catalyst composed of a mixture of Rhodium complex and tungstic acid at reaction conditions of 31.7 MPa H₂ and 473 K.^{22,23} During the reaction, PG (1,2-PDO) and 1,3-propanediol (1,3-PDO) were produced with yields of 23% and 20%, respectively.²⁴ The use of homogeneous ruthenium iodocarbonyl complex catalyst species [Ru(CO)₃I₃]⁻ has been reported for the hydrogenolysis reaction of polyols.²⁵ A process using a palladium-based homogeneous catalyst in a water-sulfolane mixture was developed by Shell Oil in which the yields of n-propanol, PG and 1,3-PDO, after a 10 h reaction period, were found to be in the weight ratio of 47:22:31.^{24,26}

The hydrogenolysis of glycerol via homogeneous catalytic processes however, has some apparent shortcomings including corrosion, separation/recovery of the catalyst from the product stream and the use of expensive/toxic solvents in the reaction, which raises environmental and economic concerns for these processes. Therefore, heterogeneous catalysts were sought to address these problems. The use of heterogeneous catalysts such as Ni, Ru, Rh, Cu, Re, Pd, etc. over different support materials is to be reviewed in the next sections.

Synthesis of PG from glycerol in a batch reactor using either homogeneous or heterogeneous catalysts has been extensively studied.^{27,28,29,30,31} However, these processes have some major disadvantages including long reaction times, high labor cost per unit of production, difficulty in scale up and commercialization, long down times for reactor cleaning, etc.^{32,33} To overcome some of these issues and to enhance the PG production, Torres *et al.*, studied the hydrogenolysis of glycerol in a batch-slurry reactor using a bimetallic Ru-Re catalyst over carbon support.³⁴ The reactor system was made up of a parallel array of six autoclave reactors that could be operated simultaneously at different temperatures and pressures using computer control. These authors reported a maximum glycerol conversion of 58% with a PG selectivity of 37% at 493 K and 6.9 MPa H₂. A similar multiple slurry reactor was used by Roy *et al.* for aqueous phase hydrogenolysis of

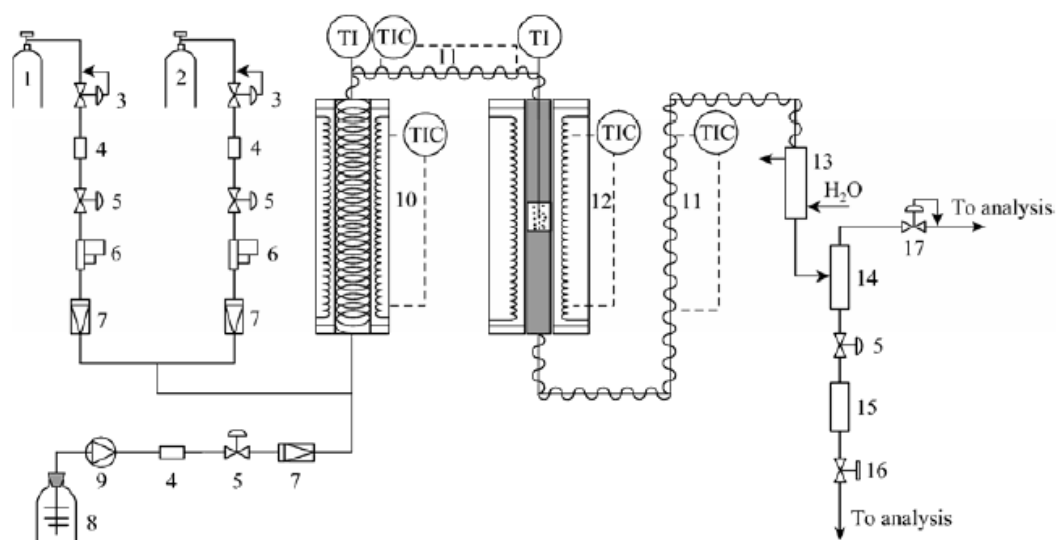
glycerol, as shown in Figure 4.5.³⁵ In their study, an admixture of 1 wt%:1 wt% of 5wt% Ru/Al₂O₃ and 5 wt% Pt/Al₂O₃ was used to obtain glycerol conversion of 50% with PG selectivity of 47% after 6 h at 493 K and 41 bar without external hydrogen (or using internally generated hydrogen from glycerol steam reforming) and a glycerol loading of 3 g. In 2012, Checa *et al.* investigated the hydrogenolysis of glycerol in a slurry phase reactor using Pt, Pd, Rh, and Au supported on ZnO in the absence of external hydrogen too.³⁶ They observed that the activity of the catalysts for glycerol conversion under similar reaction conditions followed the sequence of Pt > Rh > Pd > Au. Though hydrogenolysis of glycerol using slurry reactor moved the process one step closer towards commercialization, it has some concerns including difficulty in process design, generation of fine particles during the process (having the potential to plug-up the reactor), difficulty in sampling and higher catalyst consumption (hence poorer economics), etc.³⁷



Figure 4.5 Multiple slurry reactor used for the hydrogenolysis of glycerol³⁵ (adopted with copyright permission)

In order to make glycerol hydrogenolysis processes more efficient and economical, a variety of efforts have been made in developing flow reactors.^{38,39,40,41,42,43} It is obvious that the production of PG in a continuous-flow reactor using heterogeneous catalysts is

advantageous as the process has advantages of both high heat and mass transfer efficiency, ease of scale-up from laboratory to industrial scale, and high surface to volume ratios.⁴⁴ Moreover, the concept of “Novel Process Windows” with respect to temperature, pressure and reactant concentration can be exploited and the intrinsic kinetics of the reaction can be enhanced in flow processes to improve the yield of the desired products.^{45,46,47} Zhou *et al.* used a flow reactor to study the kinetics of the hydrogenolysis conversion of glycerol over ZnO-Al₂O₃ catalyst.⁴⁸ A similar type of reactor was used for the vapour phase hydrogenolysis of glycerol.^{12,49} The details of this reactor are given in Figure 4.6. In this set up, an aqueous or vaporized glycerol solution (80 wt%) was first passed through a pre-heated zone to reduce the viscosity of the solution before feeding it into the reactor. Hao and co-workers developed a flow reactor for the hydrogenolysis reaction in presence of Cu-H₄SiW₁₂O₄₀/Al₂O₃ without the use of a pre-heater, but using a 10 wt% glycerol aqueous solution for the reaction.⁵⁰ Very good results were achieved in this reactor system, with 90% PG selectivity at 90% glycerol conversion. Similar fixed-bed reactors have been reported in literature.^{10,11,13,51}



1: Nitrogen; 2: Hydrogen; 3: Pressure regulator; 4: Filter; 5: Ball valve; 6: Mass flow controller; 7: Check valve; 8: Liquid feed; 9: Metering pump; 10: Pre-heater; 11: Heater

and thermal insulator; 12: Reactor; 13: Condenser; 14: Gas-liquid separator; 15: Sampling pipe; 16: Needle valve; 17: Back-pressure regulator

Figure 4.6 Schematic diagram of the flow reactor set-up⁴⁸ (adopted with copy right permission)

Xi and co-workers developed a kinetic and mass transfer model for glycerol hydrogenolysis over carbon-supported metals (2.5 wt% Co, 0.5 wt% Pd, and 2.4 wt% Re) using a trickle-bed reactor with a volume of 40 cm³.⁵² The schematic of the reactor is illustrated in Figure 4.7. In this reactor, the catalyst was sandwiched between a layer of 2 mm diameter glass beads at the bottom of the bed and 2 mm diameter stainless steel beads at the top of the bed to facilitate liquid distribution and preheating prior to reaction. The authors showed that the model predictions agreed well with experimental data and accurately predicted the trends in reactor performance indicating the possible commercialization of this reaction system.

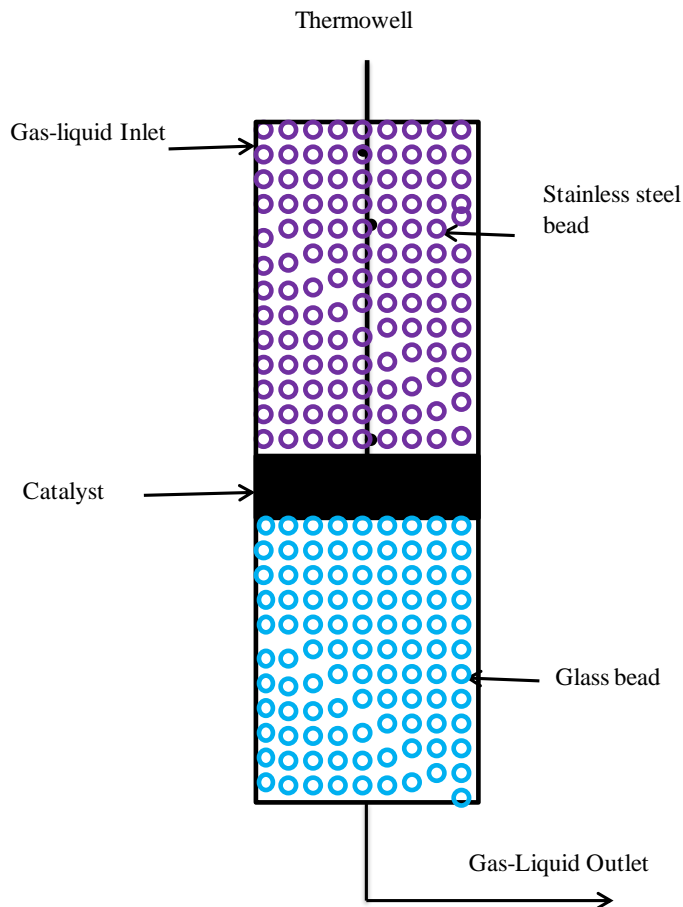


Figure 4.7 Schematic diagram of the trickle-bed reactor developed by Xi and co-workers⁵²

4.5 Development of effective catalysts

This section is divided into three parts based on the nature of the catalyst used: noble metal-based catalysts; transition metal-based catalysts and mixed catalysts.

4.5.1 Noble metal based catalysts

Noble metals are well known for their ability to adsorb hydrogen and facilitate hydrogenation reactions. To exploit this behavior, Montassier *et al.* used Rh and Ru (also sulfur modified Ru) catalysts for hydrogenolysis of glycerol and found that at 483 K Ru/C

mainly gives ethylene glycol (EG selectivity: 50%), ethane (25%) and PG (12%).⁵³ Interestingly, sulfur poisoning of the Ru surface increased the selectivity of PG to 79%. Chaminand *et al.* provided an insight into the hydrogenolysis of glycerol with Rh and Pd catalysts by using different solvents (water, sulfolane and dioxane).⁵⁴ Miyazawa and co-workers investigated the use of Ru, Rh, Pd and Pt over carbon support and observed that Ru/C has the highest activity in terms of glycerol conversion and product selectivity.⁵⁵

The activity of different noble metal catalysts such as Ru/C, Pd/C, Ru/Al₂O₃, and Pt/C etc. was also studied by Dasari *et al.*²³ At 473 K, Pd/C showed the least activity with glycerol conversion of 5% and PG yield of 3.6%. In another study, Pt/C demonstrated greater PG selectivity than Ru/C.⁵⁶ Furicado's research group studied the activity of Rh, Ru, Pt and Pd supported on C, SiO₂ or Al₂O₃ in the hydrogenolysis of glycerol at a low temperature (393 K).⁵⁷ The Pd and Pt catalysts, regardless of support, exhibited extremely low activity (<1% conversion). For Ru catalysts, activated C was found to be a better support (3.5% conversion) than either SiO₂ (0.2% conversion) or Al₂O₃ (0.3% conversion). Among all the catalysts, Rh/SiO₂ exhibited the highest glycerol conversion of 7.2% at this low reaction temperature.

It was observed that the use of noble metals without an acidic or basic additive have low selectivity to PG.⁵⁸ The use of Ru/C along with Amberlyst-70 was reported by Miyazawa *et al.*,⁵⁹ where the presence of the acidic co-catalyst was found to increase the reaction rate as well as PG selectivity. Balaraju *et al.* investigated the hydrogenolysis of glycerol in the presence of Ru/C with different inorganic solid acids including niobia- and zirconia-supported tungstophosphoric acid at 453 K, and observed glycerol conversion of 63% with PG selectivity of 67% with the co-presence of niobia acid.⁶⁰ Hydrogenolysis of aqueous glycerol using a ruthenium-incorporated acidic hetero-polysalt (Cs_{2.5}H_{0.5}PW₁₂O₄₀) catalyst was reported and a high PG selectivity of 96% was obtained at 423 K. However the glycerol conversion in the process was low (21%).⁶¹

The activity of Ru over different support materials (SiO₂, γ -Al₂O₃, NaY zeolite, C, and TiO₂) was investigated by Feng *et al.* who found Ru/TiO₂ to be the most active catalyst but, at the same time, the least selective for PG.⁶² Hydrogenolysis of glycerol over Ru/TiO₂

in the presence of different bases including LiOH, NaOH, KOH, Li₂CO₃, Na₂CO₃, and K₂CO₃ at 443 K has been reported in literature.⁶³ The addition of LiOH and NaOH enhanced glycerol conversion as well as PG selectivity. The highest glycerol conversion (90%) and PG selectivity (87%) was obtained using Ru/TiO₂ with LiOH. Maris and Davis compared the activity of Ru/C and Pt/C with the activity of a base-incorporated catalyst, and noticed that the presence of 0.8 M NaOH or CaO enhanced the rate of glycerol hydrogenolysis over the control catalyst (Ru/C or Pt/C). Yuan and co-workers investigated the hydrogenolysis of 20 wt% glycerol aqueous solution over different solid base supported Pt catalysts. They noticed that Pt/MgO and Pt/hydrotalcite catalyst exhibit higher glycerol conversion (50% and 92%) and PG selectivity (82% and 93%) than Pt/C catalyst incorporated with NaOH (7% conversion and 82% selectivity).¹⁷

Shinmi *et al.* modified Rh/SiO₂ catalyst with Re, Mo, and W as a promoter and observed a significant improvement in catalytic activity for hydrogenolysis of glycerol at a Re/Rh ratio of 0.5.⁶⁴ The Rh-ReO_x/SiO₂ (Re/Rh= 0.5) catalyst exhibited a higher glycerol conversion (80%) than the Rh/SiO₂ catalyst. The authors also noted that metal-oxide modified noble metal catalysts appear to be suitable for the selective synthesis of 1, 3-PDO. The improvement in the activity of the Rh-ReO_x/SiO₂ catalyst was attributed to the presence of low-valent ReO_x clusters covering the surface of the Rh particles, which enhanced the C-O hydrogenolysis activity of Rh metal and suppressed C-C hydrogenolysis activity.

4.5.2 3d transition metal-based catalysts

The cheap availability of transition metal-based catalysts is one of the main reasons to gain more interest over the noble metal catalysts in a wide variety of processes including the hydrogenolysis process. Montassier *et al.* reported hydrogenolysis of glycerol with glycerol conversion of 85% and PG yield of 66% at 513 K and 30 bar of hydrogen.⁶⁵ Chimanand *et al.* achieved 100% selectivity to PG over CuO/ZnO at 453 K and 80 bar of hydrogen, but the activity of the catalyst was so low that it took 90 h to reach 20% glycerol conversion.⁵⁴ A similar result of high selectivity (>93%) of PG but low glycerol conversion

(12%) using Raney Ni was reported by Perosa and Tundo.⁶⁶ Wang and Liu showed that smaller Cu particles are very active for the synthesis of PG.⁶⁷

In order to reduce the process and capital costs, Dasari *et al.* investigated the hydrogenolysis of a 80% glycerol solution in a batch reactor at lower temperatures and pressures and reported glycerol conversion of 65.3% with PG selectivity of 90% after 24 h at 473 K, and 300 psi using a copper-chromite catalyst.²³

Recently, copper catalysts have attracted much attention for the conversion of glycerol to PG because of their intrinsic ability to selectively cleave the C-O bonds in glycerol rather than the C-C bonds. To increase the activity of Cu metal, Cu-based catalysts such as Cu-Cr,^{16,42,68,69} Cu-Al,²⁰ Cu-Mg^{17,70} have been developed to promote the hydrogenolysis reaction. Bienholz *et al.* prepared a highly dispersed silica-supported copper catalyst (Cu/SiO₂) using an ion-exchange method and achieved 100% glycerol conversion with 87% PG selectivity at optimum conditions of 5 mL/h of 40 wt% aqueous glycerol solution, 528 K, and 300 mL/min of H₂ at 1.5 MPa.¹²

Zhu and co-workers studied the promoting effect of boron oxide on Cu/SiO₂ catalyst for hydrogenolysis of glycerol. They observed that the Cu/SiO₂ catalyst exhibited glycerol conversion of 62% with PG selectivity of 90% at the reaction conditions of 473 K, 5 MPa, 10 wt% glycerol aqueous solution, H₂/glycerol of 123:1 (mol/mol) and WHSV of 0.075 h⁻¹. The incorporation of 3 wt% boron to the above catalyst improved glycerol conversion to 100% with PG selectivity of 98% under same reaction conditions.⁷¹ The effect of precipitation agents (NaOH, Na₂CO₃, NH₄OH, and NH₄HCO₃) and rare earth additives (La, Ce, Y, Pr and Sm) on the catalytic performance of Cu/SiO₂ catalyst was investigated by Huang *et al.*⁷² The authors observed that the incorporation of precipitation agents and/or rare earth additives had a detrimental effect on glycerol conversion due to decrease in BET surface area, increase in Cu particle size and difficulties in CuO reduction. However, the additives maintained the propylene glycol selectivity, thermal stability and long-term stability of the Cu-SiO₂ catalyst.

Marnoiu *et al.* studied the synthesis of PG from glycerol in a batch reactor using a Ni/SiO₂-Al₂O₃ and observed a high selectivity to PG (98%) at 30% glycerol conversion under

moderate conditions: 473 K, 20 bar of H₂, 5 wt% loading of catalyst and reaction time of 8 h.⁷³ Searching for reusable and green catalysts for the hydrogenolysis reaction, Guo and co-workers used a CoAl alloy as a catalyst and observed 100% glycerol conversion with 70% selectivity to PG in a batch reactor at 433 K, 4 MPa H₂, 1 g catalyst in 30 mL of 10% aqueous glycerol solution.⁷⁴

Ni/SiO₂ is well known for its mild activity in hydrogenolysis reactions.⁷⁵ Huang *et al.* incorporated phosphorus (P) to Ni/SiO₂ in an attempt to improve its catalytic activity in hydrogenolysis of glycerol. They noted a significant improvement in the glycerol conversion (95% vs. 73%) and PG selectivity (86% vs. 50%) by P-loading. The authors ascribed the improvement in the catalytic activity to the electronic effect in which electrons transferred from Ni to P resulting in a lower electron density in the Ni comprising the Ni₂P phase as compared to metallic Ni. Also, P increases the Ni-Ni distance. These factors reduce the activity of Ni₂P/SiO₂ for the cleavage of C-C bonds.

The effects of different kinds of zeolite (γ -Al₂O₃, HY, 13X, HZSM-5, H β) as support materials on the performance of Cu for hydrogenolysis of glycerol were studied by Guo *et al.*⁷⁶ The order of activity followed the sequence Cu/Al₂O₃ > Cu-H β > Cu-HY > Cu-HZSM \approx Cu-13X. Alumina is a well-known support for dehydration reactions; it is obvious that alumina could possess an appropriate acidity to catalyze the dehydration of glycerol to form acetol. Similar results were reported by Sato *et al.*⁷⁷ The failure of other acidic supports was attributed to the formation of acrolein instead of acetol. Zhao's group also studied the effects of different support materials (NaMOR zeolite, NaZSM-5 zeolite, NaA zeolite, NaX zeolite SiO₂ and γ -Al₂O₃) on the performance of metallic Ni catalyst.⁷⁸ In a batch reactor at 473 K, 6 MPa of H₂, 16 g of 25 wt.% glycerol aqueous solution, 2.0 g catalyst and 10 h reaction, glycerol conversion followed the order Ni/Al₂O₃ (97%, 40% selectivity towards PG) > Ni/NaX (95%, and 72% selectivity towards PG) > Ni/SiO₂ (57%) > Ni/NaZSM-5 (48%) > Ni/NaMOR(14%) > Ni/NaA(10%). The high conversion and selectivity of Ni/NaX catalyst was attributed to its acidity and the ability of NaX to adsorb glycerol molecules and increase their concentration on the surface of the catalyst.

4.5.3 Mixed catalysts

More recently, the selective hydrogenolysis of glycerol has been studied using mixed metal oxide catalysts including oxides of Cu, Zn, Cr and Zr. These mixed metal catalysts have attracted much interest because it is possible to obtain desired the catalytic performance by varying the proportions of the different metals in the catalyst, to achieve glycerol conversion of 100% with PG selectivity of 97% in a batch reactor at reaction conditions of 513 K, 4 MPa H₂, 100 g of 80% glycerol solution, with 3.0 g of catalyst for 10 h.⁷⁹ Wu *et al.* investigated hydrogenolysis of glycerol over carbon nanotube-supported Cu-Ru catalyst at 473 K and observed glycerol conversion of 100% with PG selectivity of 87%.⁸⁰ The high activity of the catalyst was ascribed to the high dispersion of Ru clusters on the external surface of the Cu particles. These Ru clusters generated active hydrogen sites that were transferred to the Cu surface via hydrogen spill-over enhancing the hydrogenolysis reactions. Similar hydrogen spill-over phenomena with glycerol conversion more than 88% and 100% PG selectivity was reported by Xia *et al.* and Kim *et al.* using Pd_xCu_{0.4}Mg_{5.6-x}Al₂(OH)₁₆CO₃) and Pd-CuCr₂O₄ catalysts, respectively.^{81,82} Recently, Liu's group studied the glycerol hydrogenolysis over Ru-Cu catalyst supported on different acidic supports including SiO₂, Al₂O₃, NaY zeolite, TiO₂, ZrO₂ and HY zeolite.⁸³ The best activity was observed for Ru-Cu/ZrO₂ with 100% glycerol conversion and 84% PG selectivity. The high activity of this catalyst was attributed to the synergistic effect of Ru in the catalyst related to hydrogen spill-over as discussed above.

4.6 Catalyst deactivation

As discussed previously, there are a number of very effective catalysts discovered for the hydrogenolysis of glycerol. However, these catalysts tend to be unstable under the reaction conditions and exhibit decreased activity over time. The deactivation of the catalysts could be due to poisoning, coking, sintering, or leaching of the metal(s).

Bienholz and co-workers studied the deactivation of CuO/ZnO catalyst in glycerol hydrogenation processes.¹⁵ Fresh catalyst exhibited glycerol conversion of 46% with PG selectivity of 90%, however, when the catalyst was used in a subsequent run under the

same conditions only 10% glycerol conversion was observed (but high PG selectivity was maintained). The authors attributed the reduction in catalyst activity to increased CuO and ZnO particle size due to sintering during the reaction and/or the presence of water in the reaction medium leading to a decrease in the active surface area of the catalyst. Similar observations were reported by Panyad *et al.* for Cu-ZnO/Al₂O₃ catalyst, where the authors observed that the deactivation of the catalyst was mainly due to coking and sintering.¹⁰

The deactivation of Ag/Al₂O₃ in the hydrogenolysis process of glycerol was studied by Zhou *et al.*⁸⁴ A tremendous increase in the Ag particle size was observed by TEM (Figure 4.8) of the spent catalyst (10 nm in fresh catalyst vs. 30 nm in the spent catalyst). Glycerol conversion using the spent catalyst dropped drastically from 46% with the fresh catalyst to 21%. The authors regenerated the catalyst by washing with deionized water followed by calcination. There was negligible difference in glycerol conversion using the regenerated catalyst vs. the fresh catalyst, implying that the main causes of catalyst deactivation in the process were sintering and coking.

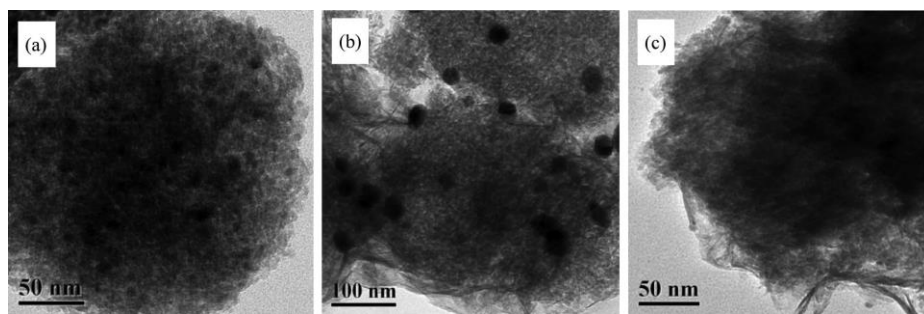


Figure 4.8 TEM micrographs of Ag/Al₂O₃ catalyst: fresh (a), spent (b) and spent-washed-calcined (c)⁸⁴ (adopted with copyright permission)

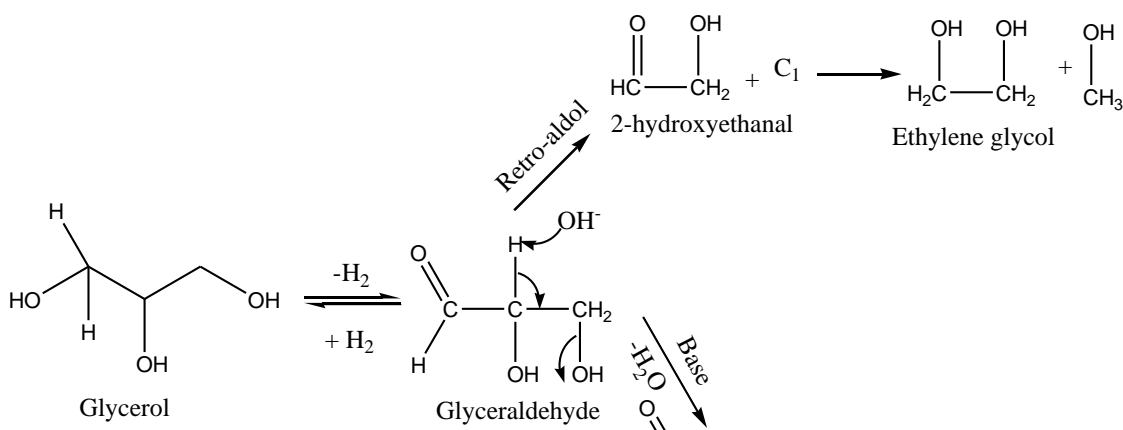
4.7 Reaction mechanisms

It is certainly of great significance to understand the reaction mechanisms of a reaction, which requires the identification of intermediate steps and an explanation of formation of

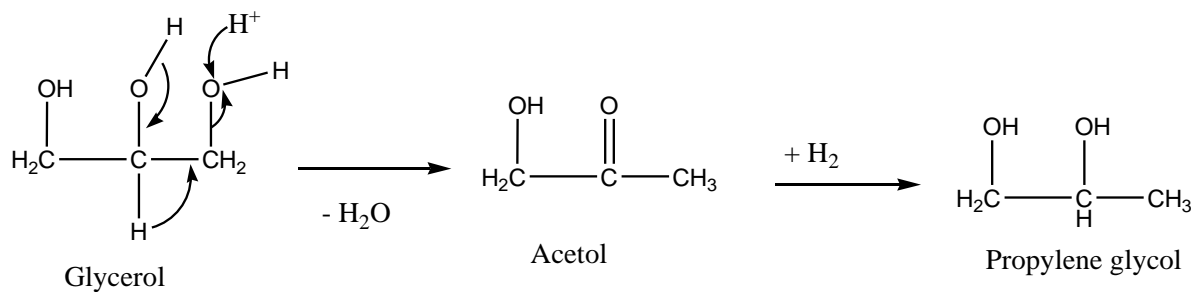
any byproducts. In the late 1980s, Montassier *et al.* published a number of papers on the conversion of glycerol.^{53,65,85} They proposed a dehydrogenation-dehydration-hydrogenation mechanism for the synthesis of propylene glycol from glycerol (Scheme 4.3). In their mechanism, the first step was controversial as the dehydrogenation of glycerol at a high pressure is thermodynamically unfavorable.⁸⁶ That is, there is a high possibility of re-hydrogenation of the glyceraldehydes to glycerol under these conditions. To avoid this re-hydrogenation and to shift the equilibrium towards PG, the rate of glyceraldehyde dehydration should be faster than the rate of glycerol dehydrogenation. Other byproducts from C-C cleavage such as ethylene glycol and methanol were also reported mainly due to retro-aldol reactions promoted in the alkaline medium.⁵⁶

Dasari *et al.* subsequently proposed a more formal reaction framework (Scheme 4.4).^{23,54} The first step, glycerol dehydration, leads to the formation of an intermediate enol, which is in tautomeric equilibrium with the hydroxyl acetone (acetol). The second step is the hydrogenation step where the acetol is hydrogenated to propylene glycol. This mechanism was supported by several other studies.^{14,59,79}

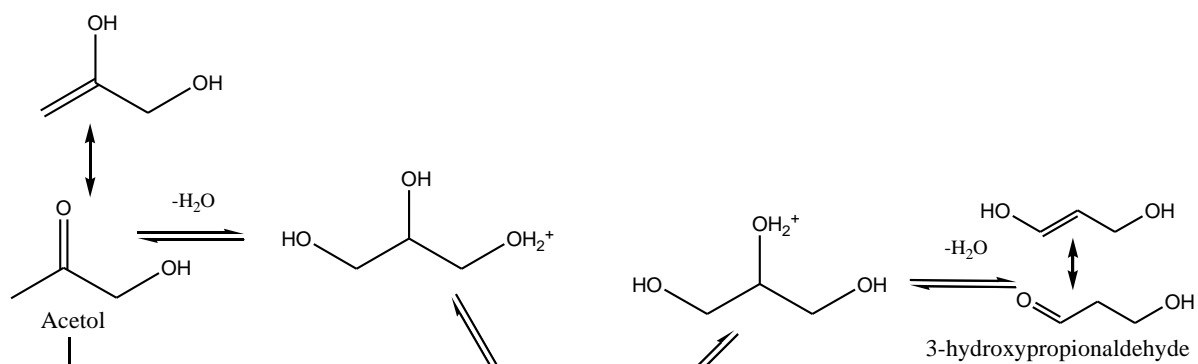
The same basic mechanism was proposed by Chaminand *et al.* who added two more pathways for the hydrogenolysis of glycerol to propylene glycol, i.e., direct hydrogenation and chelation (Scheme 4.5).⁵⁴ This scheme is interesting for a first approach, but an even deeper analysis is needed to explain the formation of the observed intermediates and byproducts. Similar direct hydrogenation and chelation mechanisms have been proposed by Shinmi *et al.* and Amada *et al.*, respectively.^{64,87}



Scheme 4.3 Reaction pathway to the formation of propylene glycol from glycerol proposed by Montassier *et al.*⁸⁶



Scheme 4.4 Reaction pathway to the formation of propylene glycol from glycerol proposed by Dasari *et al.*^{23,54}



Scheme 4.5 Reaction pathway to the formation of propylene glycol from glycerol proposed by Chaminand *et al.*⁵⁴

4.8 Use of crude glycerol and bio-hydrogen as feedstock

The use of crude glycerol as a feedstock for the synthesis of propylene glycol is an important concept for the economical production of propylene glycol and sustainability of biodiesel industry. However, as mentioned earlier, crude glycerol contains various impurities derived from the biodiesel production processes, including water, sodium or potassium hydroxides, esters, fatty acids, and alcohols. When crude glycerol is used as a feedstock for the conversion reaction, the impurities would cause operating problems by either deactivating the catalyst or plugging the reactors. Hosgun and co-workers used crude glycerol as feedstock for the synthesis of propylene glycol over Raney Ni catalyst in a batch reactor and compared the results with that of pure glycerol.⁸⁸ The authors reported almost equal glycerol conversion (~77%), and propylene glycol selectivity (~25%) under similar reaction conditions (20 wt% aq. glycerol, 503 K and 4 MPa H₂) for both type of feedstock (pure glycerol and crude glycerol). The authors attributed the unexpected

positive performance of crude glycerol to the presence of alkali impurities that acted as co-catalysts to enhance the conversion and product selectivity.

In another study by Sharma *et al.*, a Cu:Zn:Cr:Zr based catalyst was used for selective hydrogenolysis of glycerol to propylene glycol again in a batch reactor.⁷⁹ It was observed that incorporation of zinc and zirconium in the Cu:Cr catalyst matrix improved glycerol conversion and propylene glycol selectivity, due to increases in acidity and Cu dispersion in the catalyst matrix. The liquid phase reaction was carried out with 80 wt% of glycerol solution at 513 K, with 4 MPa of hydrogen pressure and 3 wt% catalyst loading. The selected catalyst Cu:Zn:Cr:Zr with the elemental molar ratio of 3:2:1:3 gave 100% of glycerol conversion and 97% of propylene glycol selectivity when using pure glycerol as the feedstock. Whereas when a simulated crude glycerol with 80% purity (remaining 20% contains mono, di and tri fatty acid ester) was used, the yield of propylene glycol decreased to 90% under the same conditions as described above, suggesting slight deactivation of the catalyst. However, real crude glycerol normally contains various impurities derived from the biodiesel production processes, which may seriously deactivate the catalysts for hydrogenolysis of glycerol, and cause reactor plugging when the reaction is operated in a flow reactor. There is not much research carried so far on hydrogenolysis of real crude glycerol in a flow reactor, so more work is needed in this regard.

4.9 Conclusions

The recent boom in biodiesel production has resulted in the generation of large volumes of glycerol as a byproduct (or waste stream). Therefore, the use of this waste stream from the biodiesel industry as a renewable feedstock to produce high-value chemicals such as propylene glycol, as reviewed in this chapter, is of great significance for better economics and sustainability of the biodiesel industry. This review has outlined the advancements in catalytic conversion of glycerol into propylene glycol. Some key conclusions are summarized below.

- (1) Hydrogenolysis of glycerol to propylene glycol has been widely conducted in batch reactors, various types of flow reactors including slurry phase and trickle bed reactors as well as continuous-flow tubular reactor. The use of continuous-flow

reactors with water as a green solvent demonstrates a great potential for commercialization of the process.

- (2) The use of heterogeneous catalysts is economical (easy recovery) and environmentally benign, thus more preferable than using homogeneous catalysts.
- (3) The methods of catalyst preparation were found to have significant effects on the activity and stability of the catalyst. Catalysts prepared by co-precipitation have larger active surface areas as compared to catalyst prepared by impregnation, leading to higher glycerol conversion and propylene glycol selectivity. Catalyst activation steps such as calcination, reduction, and re-oxidation, as well as the duration and treatment environment have also been shown to affect the formation of active hydrogen sites on the catalyst surface.
- (4) Different types of catalysts including noble metal-based catalysts, transition metal-based catalysts, and mixed metal oxide-catalysts have demonstrated high activity and selectivity in hydrogenolysis of glycerol to propylene glycol. Very high propylene glycol yields have been achieved using transition metal-based catalysts, particularly Cu-based catalysts over silica or alumina supports, with yields in the range of 80-100%. Nevertheless, the main problem in the process is the rapid deactivation of these catalysts due to coke deposition and sintering.
- (5) The use of crude glycerol as a feedstock for the synthesis of propylene glycol is an important concept for the economical production of propylene glycol and sustainability of biodiesel industry. However, real crude glycerol normally contains various impurities derived from the biodiesel production processes, including water, sodium or potassium hydroxides, esters, fatty acids, and alcohols, which may seriously deactivate the catalysts for hydrogenolysis of glycerol, and cause reactor plugging when the reaction is operated in a flow reactor. There is not much research carried so far on hydrogenolysis of real crude glycerol in a flow reactor, so more work is needed in this regard.

References

1. Behr A, Eilting J, Irawadi K, Leschinski J, Lindner F. Improved utilisation of renewable resources: New important derivatives of glycerol. *Green Chemistry* 2008;10(1):13. doi:10.1039/b710561d.
2. Corma A, Iborra S, Velty A. Chemical routes for the transformation of biomass into chemicals. *Chemical Reviews* 2007;107(6):2411-502. doi:10.1021/cr050989d.

3. Johnson DT, Taconi KA. The glycerin glut: Options for the value-added conversion of crude glycerol resulting from biodiesel production. *Environmental Progress* 2007;26(4):338-348. doi:10.1002/ep.10225.
4. Katryniok B, Paul S, Bellière-Baca V, Rey P, Dumeignil F. Glycerol dehydration to acrolein in the context of new uses of glycerol. *Green Chemistry* 2010;12(12):2079. doi:10.1039/c0gc00307g.
5. Chemical prices and chemical industry trends from ICIS pricing. Available at: <http://www.icispricing.com/>. Accessed January 23, 2015.
6. World propylene glycol market to reach supply-demand balance in 2015 | Merchant Research & Consulting, Ltd. Available at: <http://mcgroup.co.uk/news/20140418/propylene-glycol-market-reach-supplydemand-balance-2015.html>. Accessed January 20, 2015.
7. Glycols-Propylene glycols. Available at: http://msdssearch.dow.com/PublishedLiteratureDOWCOM/dh_006e/0901b8038006e13c.pdf?filepath=propyleneglycol/pdfs/noreg/117-01785.pdf&fromPage=GetDoc. Accessed December 13, 2014.
8. Marinas A, Bruijninx P, Ftouni J, Urbano FJ, Pinel C. Sustainability metrics for a fossil- and renewable-based route for 1,2-propanediol production: A comparison. *Catalysis Today* 2015;239:31-37. doi:10.1016/j.cattod.2014.02.048.
9. Mane RB, Kondawar SE, Niphadkar PS, Joshi PN, Patil KR, Rode CV. Effect of preparation parameters of Cu catalysts on their physico-chemical properties and activities for glycerol hydrogenolysis. *Catalysis Today* 2012;198(1):321-329. doi:10.1016/j.cattod.2012.05.051.
10. Panyad S, Jongpatiwut S, Sreethawong T, Rirksomboon T, Osuwan S. Catalytic dehydroxylation of glycerol to propylene glycol over Cu–ZnO/Al₂O₃ catalysts: Effects of catalyst preparation and deactivation. *Catalysis Today* 2011;174(1):59-64. doi:10.1016/j.cattod.2011.03.029.
11. Hu J, Liu X, Wang B, Pei Y, Qiao M, Fan K. Reforming and hydrogenolysis of glycerol over Ni/ZnO catalysts prepared by different methods. *Chinese Journal of Catalysis* 2012;33(7-8):1266-1275. doi:10.1016/S1872-2067(11)60405-1.
12. Bienholz A, Hofmann H, Claus P. Selective hydrogenolysis of glycerol over copper catalysts both in liquid and vapour phase: Correlation between the copper surface area and the catalyst's activity. *Applied Catalysis A: General* 2011;391(1-2):153-157. doi:10.1016/j.apcata.2010.08.047.
13. Li T, Fu C, Qi J, Pan J, Chen S, Lin J. Effect of zinc incorporation manner on a Cu–ZnO/Al₂O₃ glycerol hydrogenation catalyst. *Reaction Kinetics, Mechanisms and Catalysis* 2013;109(1):117-131. doi:10.1007/s11144-012-0538-x.

14. Huang Z, Cui F, Kang H, Chen J, Zhang X, Xia C. Highly dispersed silica-supported copper nanoparticles prepared by precipitation–gel method: A simple but efficient and stable catalyst for glycerol hydrogenolysis. *Chemistry of Materials* 2008;20(15):5090-5099. doi:10.1021/cm8006233.
15. Bienholz A, Schwab F, Claus P. Hydrogenolysis of glycerol over a highly active CuO/ZnO catalyst prepared by an oxalate gel method: influence of solvent and reaction temperature on catalyst deactivation. *Green Chemistry* 2010;12(2):290. doi:10.1039/b914523k.
16. Effect of preparation method on structure and catalytic activity of Cr-promoted Cu catalyst in glycerol hydrogenolysis. Available at: http://download.springer.com.proxy1.lib.uwo.ca/static/pdf/400/art%3A10.1007%2Fs11814-010-0070-5.pdf?auth66=1418684396_d9eacf7d769ba5fd8d3a386294c7fd27&ext=.pdf. Accessed December 15, 2014.
17. Yuan Z, Wang J, Wang L, et al. Biodiesel derived glycerol hydrogenolysis to 1,2-propanediol on Cu/MgO catalysts. *Bioresource Technology* 2010;101(18):7099-103. doi:10.1016/j.biortech.2010.04.016.
18. Balaraju M, Rekha V, Devi BLAP, Prasad RBN, Prasad PSS, Lingaiah N. Surface and structural properties of titania-supported Ru catalysts for hydrogenolysis of glycerol. *Applied Catalysis A: General* 2010;384(1-2):107-114. doi:10.1016/j.apcata.2010.06.013.
19. Yu W, Xu J, Ma H, et al. A remarkable enhancement of catalytic activity for KBH₄ treating the carbothermal reduced Ni/AC catalyst in glycerol hydrogenolysis. *Catalysis Communications* 2010;11(5):493-497. doi:10.1016/j.catcom.2009.12.009.
20. Vila F, López Granados M, Ojeda M, Fierro JLG, Mariscal R. Glycerol hydrogenolysis to 1,2-propanediol with Cu/ γ -Al₂O₃: Effect of the activation process. *Catalysis Today* 2012;187(1):122-128. doi:10.1016/j.cattod.2011.10.037.
21. Vasiliadou ES, Eggenhuisen TM, Munnik P, de Jongh PE, de Jong KP, Lemonidou a. a. Synthesis and performance of highly dispersed Cu/SiO₂ catalysts for the hydrogenolysis of glycerol. *Applied Catalysis B: Environmental* 2014;145:108-119. doi:10.1016/j.apcatb.2012.12.044.
22. Catalyzing glycerol, carbon monoxide and hydrogen. 1987. Available at: <http://www.google.com/patents/US4642394>. Accessed December 26, 2014.
23. Dasari M a., Kiatsimkul P-P, Sutterlin WR, Suppes GJ. Low-pressure hydrogenolysis of glycerol to propylene glycol. *Applied Catalysis A: General* 2005;281(1-2):225-231. doi:10.1016/j.apcata.2004.11.033.

24. Zhou C-HC, Beltramini JN, Fan Y-X, Lu GQM. Chemoselective catalytic conversion of glycerol as a biorenewable source to valuable commodity chemicals. *Chemical Society Reviews* 2008;37(3):527-49. doi:10.1039/b707343g.
25. Braca G, Raspolli Galletti AM, Sbrana G. Anionic ruthenium iodorcarbonyl complexes as selective dehydroxylation catalysts in aqueous solution. *Journal of Organometallic Chemistry* 1991;417(1-2):41-49. doi:10.1016/0022-328X(91)80159-H.
26. Drent E. Hydrogenolysis of glycerol. 2000. Available at: <http://www.google.com/patents/US6080898>. Accessed May 14, 2015.
27. Rodrigues R, Isoda N, Gonçalves M, Figueiredo FCA, Mandelli D, Carvalho WA. Effect of niobia and alumina as support for Pt catalysts in the hydrogenolysis of glycerol. *Chemical Engineering Journal* 2012;198-199:457-467. doi:10.1016/j.cej.2012.06.002.
28. Sánchez T, Salagre P, Cesteros Y, Bueno-López A. Use of delaminated hectorites as supports of copper catalysts for the hydrogenolysis of glycerol to 1,2-propanediol. *Chemical Engineering Journal* 2012;179:302-311. doi:10.1016/j.cej.2011.11.011.
29. Yuan Z, Wang L, Wang J, et al. Hydrogenolysis of glycerol over homogeneously dispersed copper on solid base catalysts. *Applied Catalysis B: Environmental* 2011;101(3-4):431-440. doi:10.1016/j.apcatb.2010.10.013.
30. Vasiliadou ES, Lemonidou AA. Parameters affecting the formation of 1,2-propanediol from glycerol over Ru/SiO₂ catalyst. *Organic Process Research & Development* 2011;15(4):925-931. doi:10.1021/op2000173.
31. Mane RB, Hengne AM, Ghalwadkar A a., et al. Cu:Al nano catalyst for selective hydrogenolysis of glycerol to 1,2-propanediol. *Catalysis Letters* 2010;135(1-2):141-147. doi:10.1007/s10562-010-0276-5.
32. Marinoiu A, Ionita G, Gáspár C-L, Cobzaru C, Oprea S. Glycerol hydrogenolysis to propylene glycol. *Reaction Kinetics and Catalysis Letters* 2009;97(2):315-320. doi:10.1007/s11144-009-0032-2.
33. Feng J, Fu H, Wang J, Li R, Chen H, Li X. Hydrogenolysis of glycerol to glycols over ruthenium catalysts: Effect of support and catalyst reduction temperature. *Catalysis Communications* 2008;9(6):1458-1464. doi:10.1016/j.catcom.2007.12.011.
34. Torres A, Roy D, Subramaniam B, Chaudhari R V. Kinetic modeling of aqueous-phase glycerol hydrogenolysis in a batch slurry reactor. *Industrial & Engineering Chemistry Research* 2010;49(21):10826-10835. doi:10.1021/ie100553b.

35. Roy D, Subramaniam B, Chaudhari R V. Aqueous phase hydrogenolysis of glycerol to 1,2-propanediol without external hydrogen addition. *Catalysis Today* 2010;156(1-2):31-37. doi:10.1016/j.cattod.2010.01.007.
36. Checa M, Auneau F, Hidalgo-Carrillo J, et al. Catalytic transformation of glycerol on several metal systems supported on ZnO. *Catalysis Today* 2012;196(1):91-100. doi:10.1016/j.cattod.2012.02.036.
37. Auneau F, Michel C, Delbecq F, Pinel C, Sautet P. Unravelling the mechanism of glycerol hydrogenolysis over rhodium catalyst through combined experimental-theoretical investigations. *Chemistry (Weinheim an der Bergstrasse, Germany)* 2011;17(50):14288-99. doi:10.1002/chem.201101318.
38. Dulescu C, Bolocan I. The glycerol hydrogenolysis on new supported catalysts. *Revista De Chimie* 2012;(3):305-309. Available at: http://www.revistadechimie.ro/pdf/DULESCU_C_3_12.pdf. Accessed December 15, 2014.
39. Liao X, Li K, Xiang X, et al. Mediator role of K, Cu and Mo over Ru/SiO₂ catalysts for glycerol hydrogenolysis. *Journal of Industrial and Engineering Chemistry* 2012;18(2):818-821. doi:10.1016/j.jiec.2011.10.004.
40. Feng Y, Yin H, Wang A, Shen L, Yu L, Jiang T. Gas phase hydrogenolysis of glycerol catalyzed by Cu/ZnO/MO_x (MO_x=Al₂O₃, TiO₂, and ZrO₂) catalysts. *Chemical Engineering Journal* 2011;168(1):403-412. doi:10.1016/j.cej.2011.01.049.
41. Mane RB, Ghalwadkar AA, Hengne AM, Suryawanshi YR, Rode CV. Role of promoters in copper chromite catalysts for hydrogenolysis of glycerol. *Catalysis Today* 2011;164(1):447-450. doi:10.1016/j.cattod.2010.10.032.
42. Rode C V., Ghalwadkar AA, Mane RB, Hengne AM, Jadkar ST, Biradar NS. Selective hydrogenolysis of glycerol to 1,2-propanediol: Comparison of batch and continuous process operations. *Organic Process Research & Development* 2010;14(6):1385-1392. doi:10.1021/op1001897.
43. Wawrzetz A, Peng B, Hrabar A, Jentys A, Lemonidou AA, Lercher JA. Towards understanding the bifunctional hydrodeoxygenation and aqueous phase reforming of glycerol. *Journal of Catalysis* 2010;269(2):411-420. doi:10.1016/j.jcat.2009.11.027.
44. Nanda MR, Yuan Z, Qin W, Ghaziaskar HS, Poirier M-A, Xu C (Charles). A new continuous-flow process for catalytic conversion of glycerol to oxygenated fuel additive: Catalyst screening. *Applied Energy* 2014;123:75-81. doi:10.1016/j.apenergy.2014.02.055.
45. Hessel V, Vural Gürsel I, Wang Q, Noël T, Lang J. Potential analysis of smart flow processing and micro process technology for fastening process development:

- Use of chemistry and process design as intensification fields. *Chemical Engineering & Technology* 2012;35(7):1184-1204. doi:10.1002/ceat.201200038.
46. Razzaq T, Kappe CO. Continuous flow organic synthesis under high-temperature/pressure conditions. *Chemistry, an Asian journal* 2010;5(6):1274-89. doi:10.1002/asia.201000010.
 47. Illg T, Löb P, Hessel V. Flow chemistry using milli- and microstructured reactors-from conventional to novel process windows. *Bioorganic & Medicinal Chemistry* 2010;18(11):3707-19. doi:10.1016/j.bmc.2010.03.073.
 48. Zhou Z, Li X, Zeng T, Hong W, Cheng Z, Yuan W. Kinetics of hydrogenolysis of glycerol to propylene glycol over Cu-ZnO-Al₂O₃ catalysts. *Chinese Journal of Chemical Engineering* 2010;18(3):384-390. doi:10.1016/S1004-9541(10)60235-2.
 49. Vanama PK, Kumar A, Gijnjupalli SR, Komandur VRC. Vapor-phase hydrogenolysis of glycerol over nanostructured Ru/MCM-41 catalysts. *Catalysis Today* 2014. doi:10.1016/j.cattod.2014.03.036.
 50. Hao S-L, Peng W-C, Zhao N, Xiao F-K, Wei W, Sun Y-H. Hydrogenolysis of glycerol to 1,2-propanediol catalyzed by Cu-H₄SiW₁₂O₄₀/Al₂O₃ in liquid phase. *Journal of Chemical Technology & Biotechnology* 2010;(May):n/a-n/a. doi:10.1002/jctb.2456.
 51. Yadav GD, Chandan PA, Tekale DP. Hydrogenolysis of glycerol to 1,2-propanediol over nano-fibrous Ag-OMS-2 catalysts. *Industrial & Engineering Chemistry Research* 2012;51(4):1549-1562. doi:10.1021/ie200446y.
 52. Xi Y, Holladay JE, Frye JG, Oberg AA, Jackson JE, Miller DJ. A kinetic and mass transfer model for glycerol hydrogenolysis in a trickle-bed reactor. 2010. Available at: <http://pubs.acs.org.proxy1.lib.uwo.ca/doi/abs/10.1021/op900336a>. Accessed December 15, 2014.
 53. Montassier C, Ménézo JC, Hoang LC, Renaud C, Barbier J. Aqueous polyol conversions on ruthenium and on sulfur-modified ruthenium. *Journal of Molecular Catalysis* 1991;70(1):99-110. doi:10.1016/0304-5102(91)85008-P.
 54. Chaminand J, Djakovitch L auren., Gallezot P, Marion P, Pinel C, Rosier C. Glycerol hydrogenolysis on heterogeneous catalysts. *Green Chemistry* 2004;6(8):359. doi:10.1039/b407378a.
 55. Miyazawa T, Kusunoki Y, Kunimori K, Tomishige K. Glycerol conversion in the aqueous solution under hydrogen over Ru/C + an ion-exchange resin and its reaction mechanism. *Journal of Catalysis* 2006;240(2):213-221. doi:10.1016/j.jcat.2006.03.023.

56. Maris E, Davis R. Hydrogenolysis of glycerol over carbon-supported Ru and Pt catalysts. *Journal of Catalysis* 2007;249(2):328-337. doi:10.1016/j.jcat.2007.05.008.
57. Furikado I, Miyazawa T, Koso S, Shima A, Kunimori K, Tomishige K. Catalytic performance of Rh/SiO₂ in glycerol reaction under hydrogen. *Green Chemistry* 2007;9(6):582. doi:10.1039/b614253b.
58. Nakagawa Y, Tomishige K. Heterogeneous catalysis of the glycerol hydrogenolysis. *Catalysis Science & Technology* 2011;1(2):179. doi:10.1039/c0cy00054j.
59. Miyazawa T, Koso S, Kunimori K, Tomishige K. Development of a Ru/C catalyst for glycerol hydrogenolysis in combination with an ion-exchange resin. *Applied Catalysis A: General* 2007;318(3):244-251. doi:10.1016/j.apcata.2006.11.006.
60. Balaraju M, Rekha V, Prasad PSS, Devi BLAP, Prasad RBN, Lingaiah N. Influence of solid acids as co-catalysts on glycerol hydrogenolysis to propylene glycol over Ru/C catalysts. *Applied Catalysis A: General* 2009;354(1-2):82-87. doi:10.1016/j.apcata.2008.11.010.
61. Alhanash A, Kozhevnikova EF, Kozhevnikov I V. Hydrogenolysis of glycerol to propanediol over Ru: Polyoxometalate bifunctional catalyst. *Catalysis Letters* 2007;120(3-4):307-311. doi:10.1007/s10562-007-9286-3.
62. Feng J, Xiong W, Xu B, Jiang W, Wang J, Chen H. Basic oxide-supported Ru catalysts for liquid phase glycerol hydrogenolysis in an additive-free system. *Catalysis Communications* 2014;46:98-102. doi:10.1016/j.catcom.2013.11.031.
63. Feng J, Wang J, Zhou Y, Fu H, Chen H, Li X. Effect of base additives on the selective hydrogenolysis of glycerol over Ru/TiO₂ catalyst. *Chemistry Letters* 2007;36(10):1274-1275. doi:10.1246/cl.2007.1274.
64. Shinmi Y, Koso S, Kubota T, Nakagawa Y, Tomishige K. Modification of Rh/SiO₂ catalyst for the hydrogenolysis of glycerol in water. *Applied Catalysis B: Environmental* 2010;94(3-4):318-326. doi:10.1016/j.apcatb.2009.11.021.
65. Montassier C, Dumas JM, Granger P, Barbier J. Deactivation of supported copper based catalysts during polyol conversion in aqueous phase. *Applied Catalysis A: General* 1995;121(2):231-244. doi:10.1016/0926-860X(94)00205-3.
66. Perosa A, Tundo P. Selective Hydrogenolysis of Glycerol with Raney Nickel †. *Industrial & Engineering Chemistry Research* 2005;44(23):8535-8537. doi:10.1021/ie0489251.
67. Wang S, Liu H. Selective hydrogenolysis of glycerol to propylene glycol on Cu–ZnO catalysts. *Catalysis Letters* 2007;117(1-2):62-67. doi:10.1007/s10562-007-9106-9.

68. Xiao Z, Li C, Xiu J, Wang X, Williams CT, Liang C. Insights into the reaction pathways of glycerol hydrogenolysis over Cu–Cr catalysts. *Journal of Molecular Catalysis A: Chemical* 2012;365:24-31. doi:10.1016/j.molcata.2012.08.004.
69. Xiao Z, Wang X, Xiu J, Wang Y, Williams CT, Liang C. Synergetic effect between Cu⁰ and Cu⁺ in the Cu-Cr catalysts for hydrogenolysis of glycerol. *Catalysis Today* 2014;234:200-207. doi:10.1016/j.cattod.2014.02.025.
70. Niu L, Wei R, Yang H, Li X, Jiang F, Xiao G. Hydrogenolysis of glycerol to propanediols over Cu-MgO/USY catalyst. *Chinese Journal of Catalysis* 2013;34(12):2230-2235. doi:10.1016/S1872-2067(12)60695-0.
71. Zhu S, Gao X, Zhu Y, Zhu Y, Zheng H, Li Y. Promoting effect of boron oxide on Cu/SiO₂ catalyst for glycerol hydrogenolysis to 1,2-propanediol. *Journal of Catalysis* 2013;303:70-79. doi:10.1016/j.jcat.2013.03.018.
72. Huang Z, Liu H, Cui F, Zuo J, Chen J, Xia C. Effects of the precipitation agents and rare earth additives on the structure and catalytic performance in glycerol hydrogenolysis of Cu/SiO₂ catalysts prepared by precipitation-gel method. *Catalysis Today* 2014;234:223-232. doi:10.1016/j.cattod.2014.02.037.
73. Marinoiu A, Cobzaru C, Carcadea E, Capris C, Tanislav V, Raceanu M. Hydrogenolysis of glycerol to propylene glycol using heterogeneous catalysts in basic aqueous solutions. *Reaction Kinetics, Mechanisms and Catalysis* 2013;110(1):63-73. doi:10.1007/s11144-013-0596-8.
74. Guo X, Yin A, Guo X, Guo X, Dai W, Fan K. Robust CoAl alloy: Highly active, reusable and green catalyst in the hydrogenolysis of glycerol. *Chinese Journal of Chemistry* 2011;29(8):1563-15662. doi:10.1002/cjoc.201180281.
75. Huang J, Chen J. Comparison of Ni₂P/SiO₂ and Ni/SiO₂ for hydrogenolysis of glycerol: A consideration of factors influencing catalyst activity and product selectivity. *Chinese Journal of Catalysis* 2012;33(4-6):790-796. doi:10.1016/S1872-2067(11)60375-6.
76. Guo L, Zhou J, Mao J, Guo X, Zhang S. Supported Cu catalysts for the selective hydrogenolysis of glycerol to propanediols. *Applied Catalysis A: General* 2009;367(1-2):93-98. doi:10.1016/j.apcata.2009.07.040.
77. Sato S, Akiyama M, Takahashi R, Hara T, Inui K, Yokota M. Vapor-phase reaction of polyols over copper catalysts. *Applied Catalysis A: General* 2008;347(2):186-191. doi:10.1016/j.apcata.2008.06.013.
78. Zhao J, Yu W, Chen C, Miao H, Ma H, Xu J. Ni/NaX: A bifunctional efficient catalyst for selective hydrogenolysis of glycerol. *Catalysis Letters* 2009;134(1-2):184-189. doi:10.1007/s10562-009-0208-4.

79. Sharma R V., Kumar P, Dalai AK. Selective hydrogenolysis of glycerol to propylene glycol by using Cu:Zn:Cr:Zr mixed metal oxides catalyst. *Applied Catalysis A: General* 2014;477:147-156. doi:10.1016/j.apcata.2014.03.007.
80. Wu Z, Mao Y, Wang X, Zhang M. Preparation of a Cu–Ru/carbon nanotube catalyst for hydrogenolysis of glycerol to 1,2-propanediol via hydrogen spillover. *Green Chemistry* 2011;13(5):1311. doi:10.1039/c0gc00809e.
81. Xia S, Yuan Z, Wang L, Chen P, Hou Z. Hydrogenolysis of glycerol on bimetallic Pd-Cu/solid-base catalysts prepared via layered double hydroxides precursors. *Applied Catalysis A: General* 2011;403(1-2):173-182. doi:10.1016/j.apcata.2011.06.026.
82. Kim ND, Park JR, Park DS, Kwak BK, Yi J. Promoter effect of Pd in CuCr2O4 catalysts on the hydrogenolysis of glycerol to 1,2-propanediol. *Green Chemistry* 2012;14(9):2638. doi:10.1039/c2gc00009a.
83. Liu H, Liang S, Jiang T, Han B, Zhou Y. Hydrogenolysis of glycerol to 1,2-propanediol over Ru–Cu bimetals supported on different supports. *CLEAN - Soil, Air, Water* 2012;40(3):318-324. doi:10.1002/clen.201000227.
84. Zhou J, Zhang J, Guo X, Mao J, Zhang S. Ag/Al2O3 for glycerol hydrogenolysis to 1,2-propanediol: activity, selectivity and deactivation. *Green Chemistry* 2012;14(1):156. doi:10.1039/c1gc15918f.
85. Montassier C, Ménézo JC, Moukolo J, et al. Polyol conversions into furanic derivatives on bimetallic catalysts: Cu□Ru, Cu□Pt and Ru□Cu. *Journal of Molecular Catalysis* 1991;70(1):65-84. doi:10.1016/0304-5102(91)85006-N.
86. Martin A, Armbruster U, Gandarias I, Arias PL. Glycerol hydrogenolysis into propanediols using in situ generated hydrogen - A critical review. *European Journal of Lipid Science and Technology* 2013;115(1):9-27. doi:10.1002/ejlt.201200207.
87. Amada Y, Shinmi Y, Koso S, Kubota T, Nakagawa Y, Tomishige K. Reaction mechanism of the glycerol hydrogenolysis to 1,3-propanediol over Ir–ReOx/SiO2 catalyst. *Applied Catalysis B: Environmental* 2011;105(1-2):117-127. doi:10.1016/j.apcatb.2011.04.001.
88. Hoşgün HL, Yıldız M, Gerçel HF. Hydrogenolysis of aqueous glycerol over raney nickel catalyst: Comparison of pure and biodiesel by-product. *Industrial & Engineering Chemistry Research* 2012;51(10):3863-3869. doi:10.1021/ie201781q.

Chapter 5

5 Thermodynamic and kinetics studies of a catalytic process to convert glycerol into solketal as an oxygenated fuel additive

Abstract

Glycerol is a byproduct of biodiesel industry and can be converted into high value-added compounds. The heterogeneous ketalization of glycerol with acetone was conducted over a solid acid catalyst; Amberlyst-35 in a batch reactor. The thermodynamics and kinetics of the ketalization reaction for the synthesis of solketal were investigated. The reaction equilibrium constants were determined experimentally in the temperature range of 293-323 K, with which the following standard molar properties (at 298 K) were obtained: $\Delta H^\circ = -30.1 \pm 1.6 \text{ kJ mol}^{-1}$, $\Delta G^\circ = -2.1 \pm 0.1 \text{ kJ mol}^{-1}$, $\Delta S^\circ = -0.1 \pm 0.01 \text{ kJ mol}^{-1}\text{K}^{-1}$. Effects of various experimental conditions (stirring speed, catalyst addition amount, pressure, temperature, moisture content and the feed composition) on the reaction kinetics (glycerol conversion and solketal yield vs. time) were also investigated in this work. A two-parameter kinetic law based on a Langmuir-Hinshelwood rate expression was used. The activation energy of the overall ketalization reaction was determined to be $55.6 \pm 3.1 \text{ kJ mol}^{-1}$. The obtained solketal could be synthesized from renewable resources like bioglycerol and biomass derived acetone, seem to be a good candidate for different applications such as fuel additive and in pharmaceutical industries. The work is an important step for further development of a technology for the continuous synthesis and separation of solketal from glycerol and acetone.

Keywords: Adsorption; Batch reactor; Glycerol; Ion exchange resin; Kinetics; Solketal

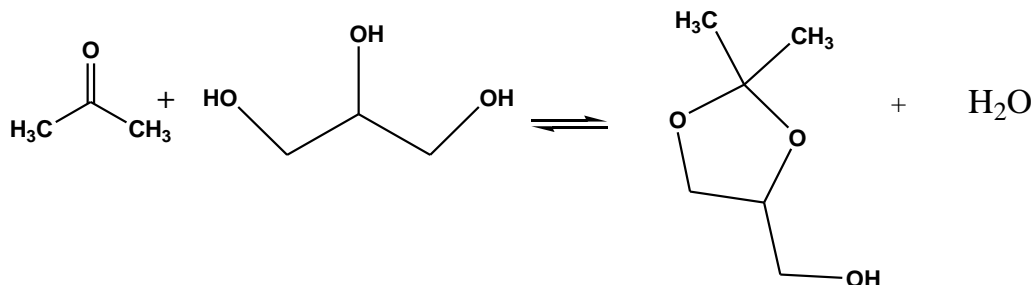
5.1 Introduction

Glycerol (propane-1, 2, 3- triol) is the simplest trihydric alcohol, commercially known as glycerin. It is well known for its versatile applications in diverse fields such as the food, pharmaceutical, polymer and fuel industries.¹

Glycerol is produced in large amounts as a byproduct or waste stream from biodiesel production via transesterification reactions. The biodiesel production generates approximately 10% of glycerol by volume.² Due to the increased concerns over the environment and energy security associated with petroleum-based transportation fuels, the interest in producing bio-fuels (bio-ethanol and biodiesel) has been intensified worldwide in last decade. The production of biodiesel has increased exponentially all over the world. Hence a large amount of glycerol is expected to be generated from the biodiesel industry. It was predicted that by 2020 the global production of glycerol will be 41.9 billion litres.³ The large scale producers are able to refine this waste stream for the industrial applications whereas small scale producers are unable to justify refining costs and instead pay a fee for glycerol removal. The current crude glycerol price is as low as 4-10 cents/lb.⁴ The predicted generation of large amounts of glycerol will further lower the glycerol price once it enters the market. Therefore proper utilization of glycerol is required in different value-added applications for the sustainability of the biodiesel industry.

The presence of three hydroxyl groups in glycerol makes it unsuitable to be used as a direct fuel component due to its low heating value. Various processes have been investigated for conversion of glycerol into fuel components. Condensation of glycerol with aldehydes and ketones to cyclic acetals and ketals, respectively, is often considered one of the most promising glycerol applications for fuels/chemical intermediates.^{5,6,7,8} The ketalization reaction between glycerol and acetone is given in Scheme 5.1, where solketal (2, 2-dimethyl-1, 3-dioxolane-4-methanol) is formed as the condensation product in the presence of an acid catalyst. Solketal can be used as a fuel additive to reduce the particulate emission and to improve the cold flow properties of liquid transportation fuels.⁹ It helps reduce the gum formation, improves the oxidation stability, and enhances the octane number when added to gasoline.¹⁰ Maksimov *et al.* reported its use as a versatile solvent and a plasticizer

in the polymer industry and a solubilizing and suspending agent in pharmaceutical preparations.¹¹



Scheme 5.1 Ketalization reaction between glycerol and acetone

Traditionally, the ketalization of glycerol is carried out via a homogeneous catalytic process using mineral acids like H_2SO_4 , HCl , HF , or *p*-toluenesulphonic acid, etc.^{12,13} These processes have serious shortcomings such as corrosion and catalyst separation from the product stream, hence raising environmental and economic concerns for the effluent disposal. Most of these problems could be addressed by using heterogeneous catalysts. Studies of ketalization of glycerol using solid acid catalysts like Amberlyst-15,¹⁴ Amberlyst-36,⁵ Montmorillonite K-10,¹⁵ H-beta zeolite,^{11,14} silica supported heteropoly acids,¹⁶ and mesoporous silicates containing arylsulfonate groups were reported.¹⁷ Among these catalysts, Amberlyst has demonstrated its potential for the synthesis of solketal. Deutsch *et al.* investigated the reactivity of different heterogeneous catalysts for the formation of cyclic ketals by the condensation of glycerol with aldehydes.⁵ A high yield of solketal (more than 90% with high selectivity) was reported at a high molar ratio (approx. 6:1) of acetone to glycerol in a batch reactor.¹⁷ However, so far kinetics and thermodynamics of the ketalization reaction of glycerol with acetone over solid acid catalysts have not been reported.

It is of no question that to understand thermodynamics and kinetics of the ketalization reaction is important for further development of the glycerol ketalization technology. Thus, the main objective of this work is to thoroughly investigate the thermodynamics and kinetics of the ketalization reaction of glycerol and acetone in a batch reactor over solid

acid catalyst of Amberlyst-35. The results of this research would help to suggest a reaction mechanism and a rate equation with experimentally measured kinetic parameters. Furthermore, it will be advantageous for the development of a continuous process for the industrial production of solketal from glycerol.

5.2 Experimental

5.2.1 Materials

Glycerol and acetone (both >99 wt% purity) were procured from Sigma Aldrich and used as received, and commercial grade ethanol was supplied from Commercial Alcohols Inc. Solketal [(S-) (+) – 1, 2- Isopropylidenglycerol, 99 wt%] was also obtained from Sigma Aldrich as a calibration standard for GC analysis. The solid acid catalyst: Amberlyst-35 dry was obtained from Rohm and Hass Co. (USA) and used as received. The characteristics of the catalyst are given in Table 5.1.

Table 5.1 Characterization of the solid acid catalyst used

Catalyst properties	
Acidity ^a (eq/kg)	5
Particle size (μm)	490
Average pore diameter ^b (nm)	30
Max. operating temp ^c (°C)	150
Pore volume ^b (mL/g)	0.35
BET surface area ^b (m ² /g)	50

^a Determined by ammonia TPD; ^b Measured by N₂ isothermal adsorption at 77 K;

^c Obtained from the catalyst supplier.

5.2.2 Ketalization reaction of glycerol and acetone

The glycerol ketalization reactions were carried out in a 100 mL three-neck glass reactor in a water bath equipped with a magnetic stirrer and a condenser (Figure 5.1) in order to condense and reflux all the vapours and keep the reaction volume almost constant. The reaction temperature was precisely controlled for an accuracy of ± 0.03 K with an external thermostat containing an external thermocouple placed inside the reacting mixture. In a typical run, the composition of reaction mixture was 22.83 g of acetone, 18.11 g of glycerol, 9.06 g of ethanol, 0.1811 g of catalyst and the total volume of the mixture was 55 mL. At the beginning of the experiment, known amounts of glycerol, ethanol and acetone were charged into the reactor. Amberlyst-35 catalyst was placed in a basket at the top of the condenser and added to the reactor only after the stabilization of temperature of the system (time zero). The use of ethanol as solvent was mainly to improve the solubility of glycerol in acetone and the homogeneity of the solution was observed by the formation of a single phase (naked eye observation), but also checked by GC-FID. The reaction of acetone with ethanol to form hemiketal/ketal under this experimental conditions is highly unfavourable,^{18,19} and the yields of other undesired products were very small ($< 2\%$).¹¹ The total mass of the reaction substrate (M) was maintained to be 50 g, unless otherwise specified. A small amount of samples were withdrawn at regular intervals of time for analysis by GC-FID. The reaction was kept at the specific temperature until the equilibrium state was achieved (when the reactants/products concentrations did not vary with time) which was verified by quantitative GC-FID in a regular interval of time.



Figure 5.1 Batch reactor

5.2.3 Product analysis

The main components in the product mixture were first identified with a gas chromatograph, equipped with a mass selective detector [Varian 1200 Quadrupole GC/MS (EI), Varian CP-3800 GC equipped with VF-5 MS column (5% phenyl/95% dimethylpolysiloxane, 30 m \times 0.25 mm \times 0.25 μ m)], using helium as the carrier gas at a flow rate of 5×10^{-7} m³/s. The oven temperature was maintained at 120 °C for 2 min and then increased to 280 °C at a ramp rate of 40 °C/min. Injector and detector block temperature were maintained at 300 °C. The components were identified using the NIST 98 MS library with the 2002 update. The concentration of the glycerol and solketal in the products was analyzed with a GC-FID (Shimadzu -2010) under the similar conditions as used for the GC-MS measurement after careful calibration with glycerol and solketal of varying concentrations and dimethyl sulfoxide (DMSO) as an internal standard at a fixed concentration. Appendix C provides a typical GC-MS spectrum and the calibration tables and curves for GC-FID.

The solketal yield and glycerol conversion were calculated using the following equations:

$$Yield (mol\%) = \frac{\text{Moles of solketal formed}}{\text{Initial moles of glycerol}} \times 100\% \quad (1)$$

$$Conversion (mol\%) = \frac{\text{Reduction in moles of glycerol in the reaction}}{\text{Initial moles of glycerol}} \times 100\% \quad (2)$$

In all runs throughout the experiment, the product selectivity, i.e., ratio of solketal yield to glycerol conversion, was close to 100%.

5.3 Thermodynamic results

Thermodynamic studies of the glycerol ketalization reaction were carried out in a 100 mL batch reactor at a relatively low temperature range of 293- 323 K, as the reaction is exothermic so thermodynamically unfavorable at higher temperatures.²⁰ In this series of experiments, a high initial molar ratio of acetone to glycerol (6:1) was used, and the catalyst loading in the batch reactor was fixed at 5 wt% of the mass of glycerol. To ensure equilibrium of the reaction, all the experiments were carried out for sufficiently long time while monitoring the glycerol conversion and solketal yield vs. time till no change in the measured results were observed (indicator of the reaction equilibrium). The equilibrium compositions at various experimental conditions are listed in Table 5.2.

Table 5.2 Experimental data of equilibrium composition and equilibrium constants^a

Temp (K)	I_A	I_G	F_A	F_G	F_S	F_W	K_C	X_E
298	0.6817	0.1145	0.5747	0.0075	0.1070	0.1070	2.6562	0.9345
303	0.694	0.1132	0.5907	0.0099	0.1033	0.1033	1.8247	0.9125
313	0.6823	0.1153	0.5807	0.0137	0.1016	0.1016	1.2975	0.8812
323	0.6827	0.1137	0.5854	0.0164	0.0973	0.0973	0.9861	0.8558

^a I_A = Initial mole of acetone; I_G = Initial mole of glycerol; F_A = Final mole of acetone; F_G = Final mole of glycerol; F_S = Final mole of solketal; F_W = Final mole of water; K_C = Equilibrium constant; X_E = Equilibrium conversion.

The equilibrium constant (K_C) for the liquid phase reaction was calculated using the following equation and the results are presented in Table 5.2

$$K_C = \frac{[S][W]}{[A][G]} \quad (3)$$

Where [S], [W], [A], and [G] are the molar concentration of solketal, water, acetone, and glycerol, respectively. As shown by the data from Table 5.2, with an increase in the reaction temperature, the equilibrium constant K_C decreases gradually, indicating the exothermicity of the reaction. To achieve a higher equilibrium conversion of glycerol, a lower temperature is preferred. However, as expected the lower the reaction temperature the longer the time required to reach the equilibrium state.

The thermodynamic properties such as entropy and enthalpy can be predicted by plotting the experimental values of $\ln K_C$ vs. $1/T$ (K^{-1}) (van't Hoff equation). In a narrow temperature range in the vicinity of room temperature, the plot of $\ln K_C$ vs. $1/T$ would follow a linear correlation as displayed in Figure 5.2:

$$\ln K_C = \frac{\Delta S^0}{R} - \frac{\Delta H^0}{R} \frac{1}{T} \quad (4)$$

where ΔS° is the standard entropy at 298 K ($\text{kJ mol}^{-1} \text{K}^{-1}$), ΔH° is the standard enthalpy at 298 K (kJ mol^{-1}), R is the universal gas constant ($\text{J mol}^{-1} \text{K}^{-1}$) and T is the reaction temperature (K). The linear fitting of experimental data (in Figure 5.2) according to above equation gives:

$$\ln K_c = (3615.4/T) - 11.31 \quad (5)$$

By solving equations (4) and (5), we get $\Delta H^\circ = -30.1 \pm 1.6 \text{ kJ mol}^{-1}$ and $\Delta S^\circ = -0.1 \pm 0.01 \text{ kJ mol}^{-1} \text{K}^{-1}$ from the slope and the intercept, respectively. The standard state Gibbs free energy change (ΔG°) can be related to the standard state enthalpy and entropy changes for the system as:

$$\Delta G^\circ = \Delta H^\circ - T\Delta S^\circ \quad (6)$$

With the above, ΔG° is found to be $-2.1 \pm 0.1 \text{ kJ mol}^{-1}$, suggesting the reaction can take place at standard state (room temperature). The ΔG° value obtained is similar to the result reported in the literature for the synthesis of acetal from butanol and acetaldehyde.²¹

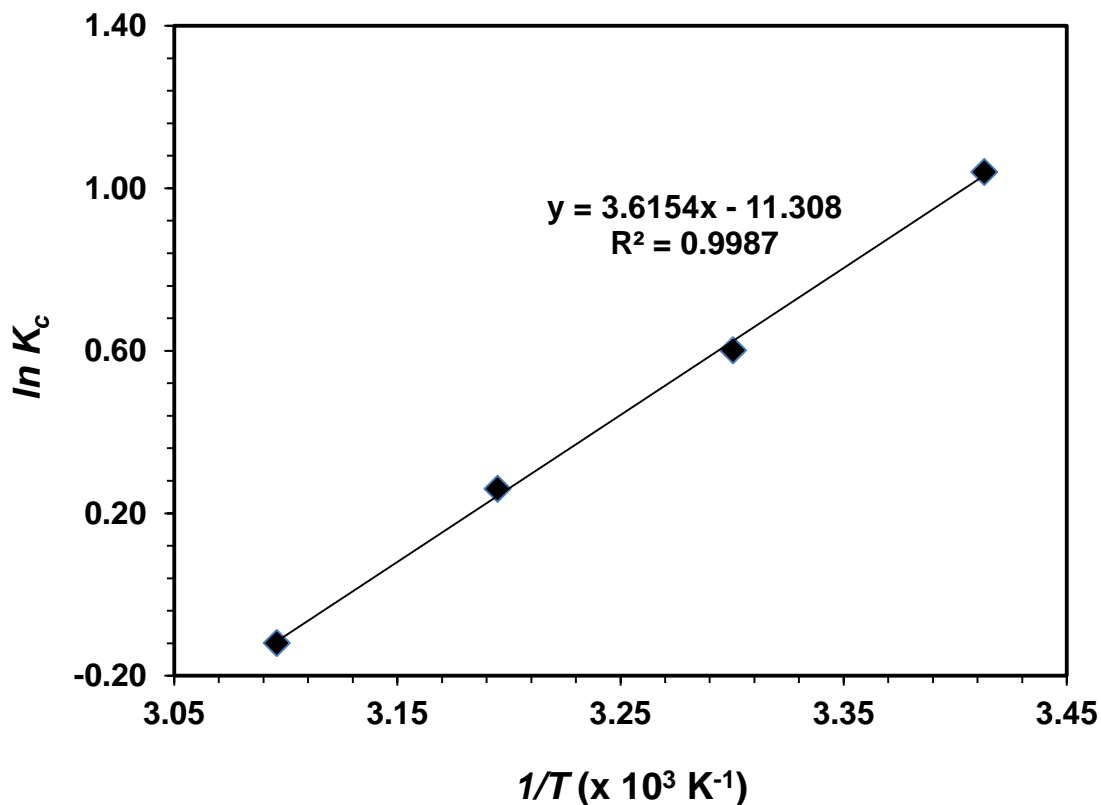
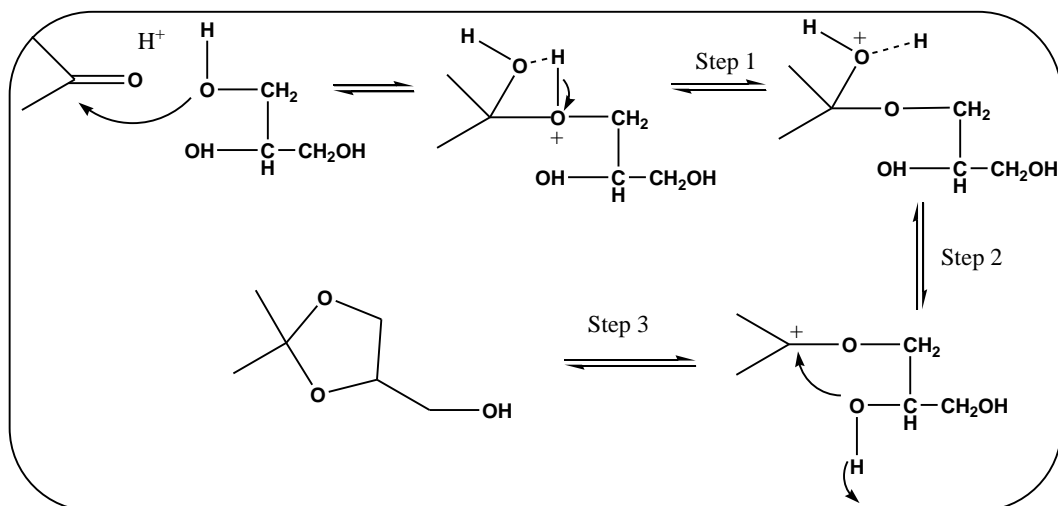


Figure 5.2 Plot of $\ln K_c$ vs. $1/T$

5.4 Kinetic results

Referring to the mechanism proposed for the synthesis of acetal in the presence of a homogeneous catalyst,²² and the mechanism proposed by Maksimov *et al.* for the synthesis of ketals from plant-derived diols,¹¹ we proposed a similar mechanism for ketalization of glycerol over a heterogeneous catalyst as illustrated in Scheme 5.2. The most important steps in the mechanism are:

- (1) Reaction between the adsorbed acetone and glycerol to give the hemi-acetal (Step 1);
- (2) Reaction to form water (Step 2-considered to be the rate limiting step);
- (3) Reaction to form solketal (Step 3).



Scheme 5.2 Mechanism of ketalization reaction of glycerol and acetone

In this study, we investigated various experimental conditions (stirring speed, catalyst addition amount, pressure, temperature, moisture content and the reactor feed composition) on the reaction kinetics (glycerol conversion and solketal yield vs. time). The results of this study are summarized in Table 5.3 and presented as follows.

Table 5.3 Summary of the experiments at different conditions

Entry number	Catalyst loading (wt% of glycerol)	Stirring speed (rpm)	Temperature (K)	Acetone: glycerol: ethanol (mole)	Solketal yield (%)
1	1	400	323	2:1:1	60
2	1	1100	323	2:1:1	60
3	1	700	298	2:1:1	72
4	1	700	303	2:1:1	70
5	1	700	308	2:1:1	67
6	1	700	313	2:1:1	64
7	1	700	323	2:1:1	60
8	2	700	313	2:1:1	64
9	1	700	298	1.48 :1:1	68
10	1	700	298	2.46 :1:1	74
11	1	700	298	2.04 : 1:1	72
12 ^a	1	700	298	2:1:1	68
13 ^b	1	400	298	2:1:1	72
14 ^c	1	400	298	2:1:1	72

^a with 3.15 wt% moisture; ^b and ^c are conducted in a pressure reactor at 1 and 54 atm, respectively with a stirring speed of 400 rpm

5.4.1 Mass transfer resistance

To investigate the effects of mass transfer on the reaction kinetics, a wide range of agitation (stirring) speeds (from 400 rpm to 1150 rpm) were tested in the experiments. The solketal yields vs. time under two different stirring speeds (400 and 1100 rpm) are illustrated in Table 5.3(entry 1 and 2) and Figure 5.3. Clearly, at the same conditions (323 K, acetone to glycerol molar ratio (A/G) of 2, and catalyst loading (W_{cat}) of 1 wt% of glycerol) both tests under 400 and 1100 rpm led to the same equilibrium yield of solketal (60%) as well as the initial formation rate of solketal (determined from the slope of the trend-line of the solketal yield vs. time at the beginning of the experiment). Thus, no effect of the agitation speed on

the reaction rate was observable at >400 rpm. Hence, all further experiments were carried out at 700 rpm to eliminate the external mass transfer resistance. The catalyst used in this study was a macroscopic ion exchange resin (Table 5.1). In a macroscopic resin, the reactants are able to diffuse into the pores without any resistance. Hence no internal mass transfer resistance was expected.^{23,24}

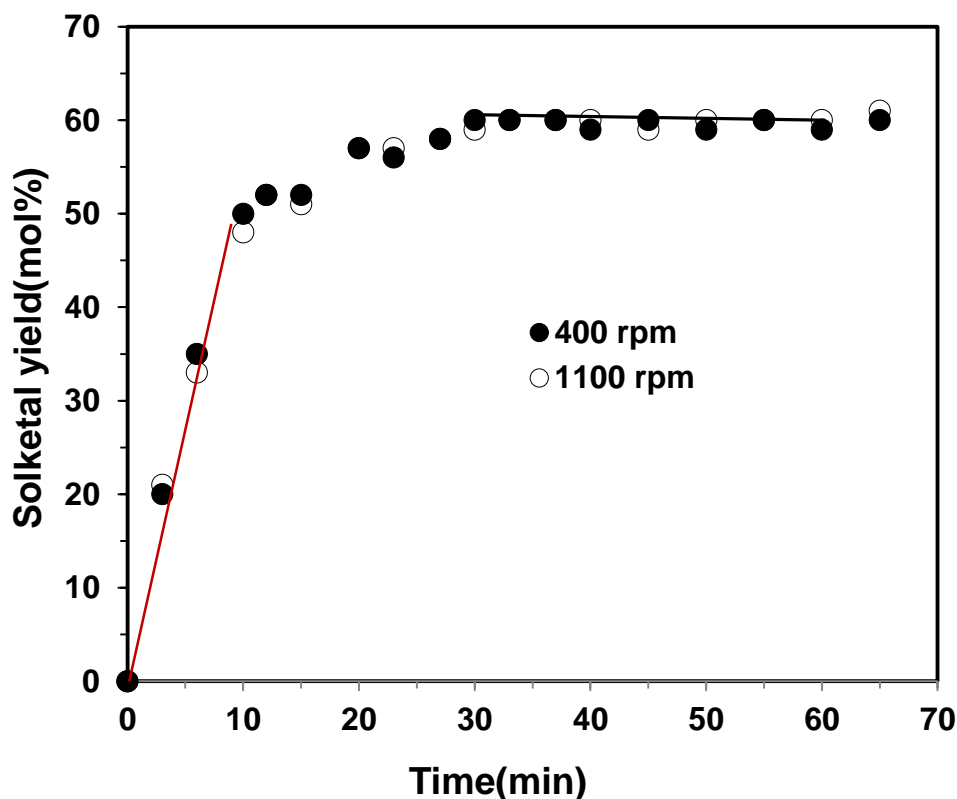


Figure 5.3 Effects of reactor stirring speed on the solketal yield (other reaction conditions: 323 K, acetone to glycerol molar ratio (A/G) of 2, catalyst loading (W_{cat}) of 1 wt% of glycerol)

5.4.2 Effects of catalyst loading

The effects of the catalyst load on the reaction kinetics were investigated under the conditions of 313 K and A/G = 2 with catalyst loads (i.e., W_{cat} = 1 wt% and 2 wt% in relation

to glycerol). The results are given in Table 5.3 (entry 6 and 8) and Figure 5.4, from which essentially the increase in the catalyst load from 1 wt% to 2 wt% does not change the final (equilibrium) yield of solketal (64%) as expected by thermodynamics. Under the same experimental conditions, a two fold increase in the mass of catalyst approximately doubled the initial reaction rate for solketal formation, suggesting that the reaction rate can be promoted by increasing the catalyst amount or number of the active sites in the reactor system, as similarly observed in the literature for the synthesis of acetal from butanol and acetaldehyde.²⁵

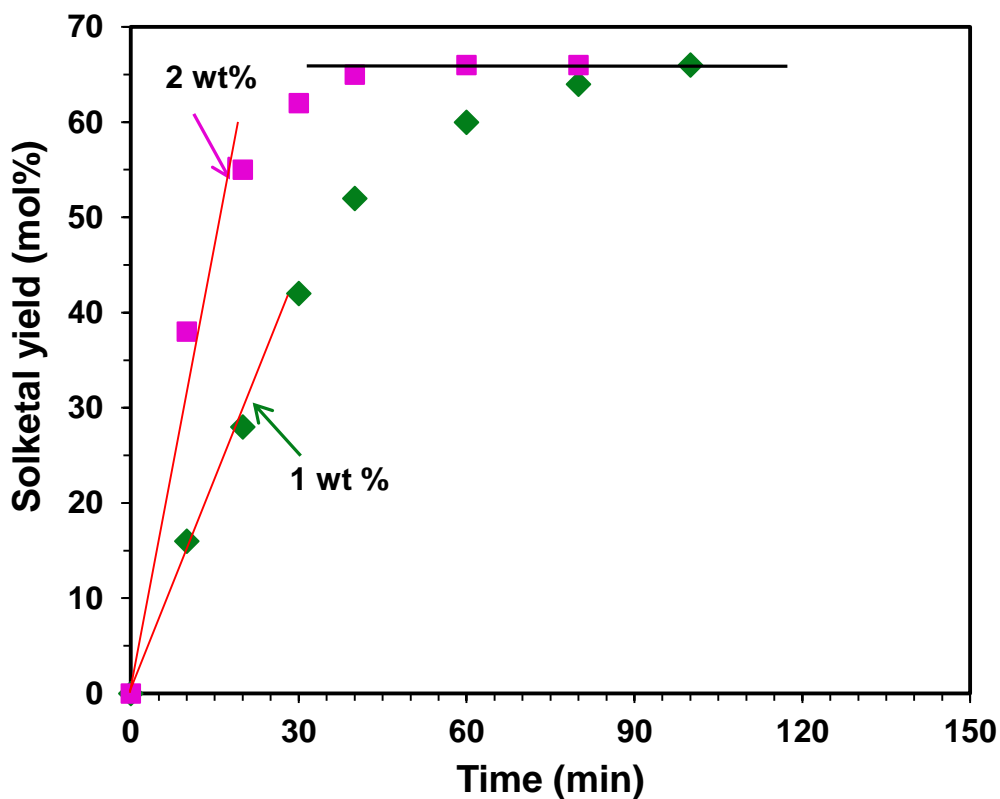


Figure 5.4 Effects of the catalyst addition amount on the yield of solketal (other reaction conditions: 313 K and A/G = 2)

5.4.3 Effects of pressure

The effects of pressure (1- 54 atm) on the reaction was tested, and it was found that pressure showed a negligible effect on either the equilibrium product yields or the reaction rate, which is expected for liquid phase reactions (Table 5.3: entry 13 and 14). In the present study, the reactor pressure for all reported results was fixed at 1 atm, where the maximum number of molecules in gas phase was found to be very small (2.1%) at the maximum operating temperature and the maximum acetone equivalent.

5.4.4 Effects of temperature

Effects of temperature on ketalization of glycerol were studied at various temperatures ranging from 298 to 323 K under the conditions of $A/G = 2$ and $W_{\text{cat}} = 1$ wt% of glycerol, as shown in Table 5.3 (entry 3-7) and Figure 5.5. A higher temperature led to a lower equilibrium product yield, typical of exothermic reactions, as evidenced previously by the thermodynamics results. It is also clear that the initial rate of the ketalization reaction increases with increasing the reaction temperature as expected.

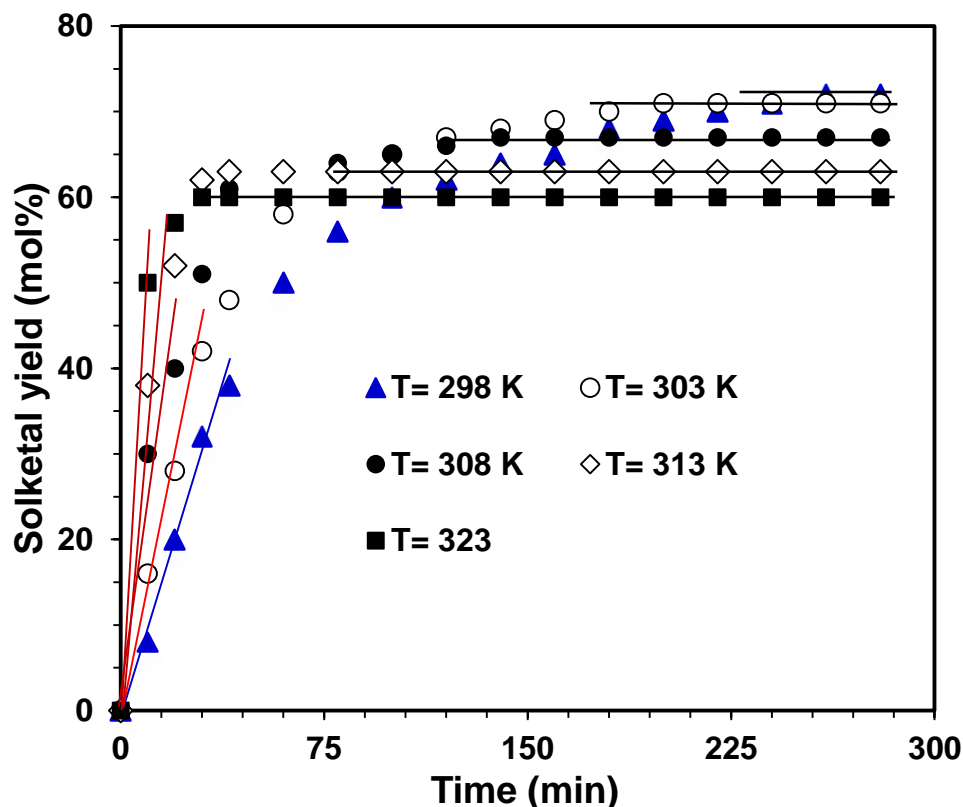


Figure 5.5 Influence of temperature on the yield of solketal (other reaction conditions: $A/G = 2$ and $W_{\text{cat}} = 1$ wt% of glycerol)

5.4.5 Effects of initial molar concentration of reactants

According to both reaction thermodynamics and kinetics, the initial molar concentration of a reactant would influence the equilibrium conversion and the reaction rate. In this work, we conducted the reaction at 298 K with a catalyst load of 1 wt% w.r.t. glycerol while varying the initial acetone-to-glycerol molar ratio from $A/G = 1.48$ to 2.46. The results are presented in Table 5.3 (entry 9-11) and Figure 5.6. As clearly shown in the Figure, the reaction thermodynamics and kinetics are strongly affected by A/G molar ratio: a higher A/G ratio led to a higher reaction rate and larger equilibrium yield of solketal. These results are actually expected, and similar observations were reported by Agirre *et al.*⁶ We have also examined the effect of initial ethanol concentration on the ketalization reaction at various ethanol-glycerol molar ratios, but the effect was found to be negligible due to the

minimal reaction between acetone and ethanol under the present reaction conditions (reaction time, temp, amount of catalyst used, amount of glycerol and acetone used).

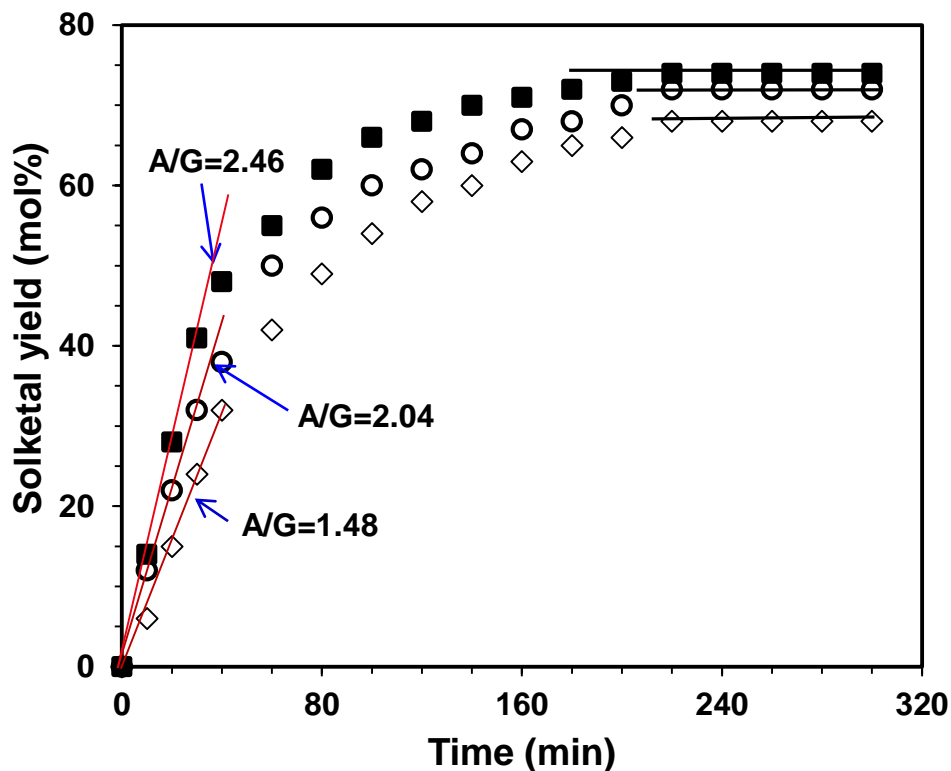


Figure 5.6 Effects of initial acetone-to-glycerol (A/G) molar ratio on the yield of solketal (other reaction conditions: 298 K and $W_{\text{cat}} = 1$ wt% **w.r.t.** glycerol)

5.4.6 Moisture content

The role of water in the reaction was investigated (Table 5.3: entry 3 and 12, Figure 5.7) by using 3.15 wt% water in the solution for the ketalization and the yield of solketal (66%) was compared to that of without moisture experiment (72%) under similar reaction conditions (Temperature: 298 K, acetone to glycerol molar ratio (A/G) of 2, catalyst loading (W_{cat}) of 1 wt% of glycerol). The lower yield of solketal in the latter case may be

attributed to the adsorption of water on the catalyst surface which inhibits the forward reaction to form solketal.²⁶

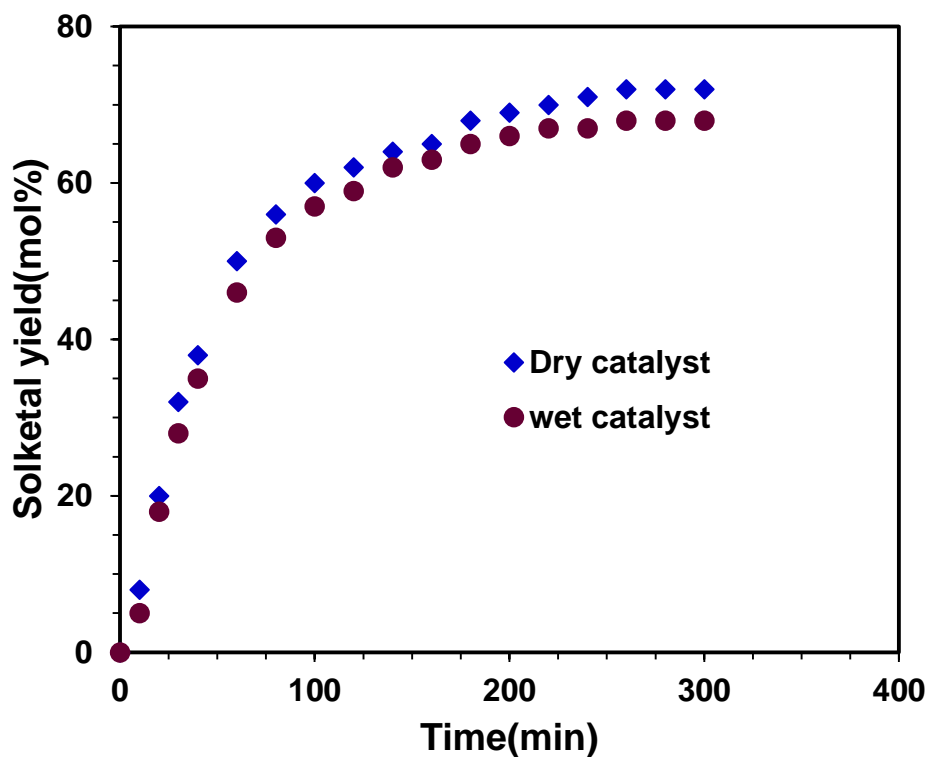


Figure 5.7 Effect of moisture content on the yield (other conditions: 298 K, $W_{\text{cat}} = 1$ wt% w.r.t. glycerol)

5.4.7 Kinetic model

The general reaction rate expression for the ketalization of glycerol with acetone could be expressed in the form of Langmuir- Hinshelwood model with surface reaction as the rate determining step.^{27,28,29} The key reaction steps of this model are given as follows:

- a) The surface reaction between the adsorbed species of glycerol (GF) and acetone (AF) to give adsorbed hemiacetal (HF)



where F is the vacant site on the catalyst.

- b) Surface reaction for formation of adsorbed water (WF)



where IF represents for the reactive intermediate formed.

- c) Formation of adsorbed solketal (SF)



As agreed upon in the literature, the surface reaction for the formation of adsorbed water (WF) is commonly considered as the rate determining step.^{30,31,32} Thus the rate of the reaction (r) can be given as:^{25,33}

$$R = k \frac{C_G C_A - \frac{C_S C_W}{K_c C_G}}{\left[1 + K_{F,G} C_G + K_{F,A} C_A + K_{F,S} C_S + K_{F,W} C_W + K_{I_1} C_G C_A + K_{I_2} \frac{C_S}{C_G} \right]^2} \quad (10)$$

Where R is the rate of the reaction, k is the kinetic constant based on the kinetic model and K_F are the adsorption constant for different components. A detailed derivation of the rate equation is given in the *Appendix B*. In order to reduce the number of optimization parameters, only compounds that have stronger adsorption were taken into consideration in the model. Water has the strongest adsorption on the catalyst resin surface.²⁵ Thus, for simplicity adsorption of the other compounds was neglected in this work. The simplified rate expression used to describe the experimental data is given as:^{25,31,32}

$$r = k \frac{[G][A] - [S][W]/K_c [G]}{\left\{ 1 + K_w [W] \right\}^2} \quad (12)$$

where $K_w (=K_{F,W})$ is the equilibrium constant for water adsorption on the catalyst surface. According to the above kinetic model two parameters (kinetic constant; k and water adsorption constant; (K_w)) are to be estimated at each temperature.

The mass balance in the batch reactor for solketal in the liquid phase at constant temperature can be given as:⁷

$$\frac{dn_c}{dt} = W_{cat} r \quad (13)$$

where n_c is the number of moles of solketal, t is the time, W_{cat} is the mass of catalyst and r is the reaction rate with respect to the catalyst mass.

The above equation can be modified using the initial moles ($n_{l,0}$), stoichiometric coefficient of limiting reactant (ν_l) and conversion (X) as:²⁵

$$\frac{n_{l,0}}{W_{cat} |\nu_l|} \frac{dX}{dt} = r\{[G],[A],[S],[W]\} \quad (14)$$

The theoretical rate of the reaction (equation 14) was fitted to the experimentally measured rates at different temperature and is given in Figure 5.8. The values of k and K_w at different temperatures were calculated using a non-linear regression method and are given in Table 5.4

Table 5.4 Kinetic modeling parameters k and K_w ^a

Temperature (K)	k (Lmoles ⁻¹ min ⁻¹)	K_w
298	0.112	2.650
303	0.158	1.498
308	0.239	1.090
313	0.329	0.726
323	0.630	0.335

^a k = kinetic constant; K_w = equilibrium constant for water adsorption on the catalyst surface

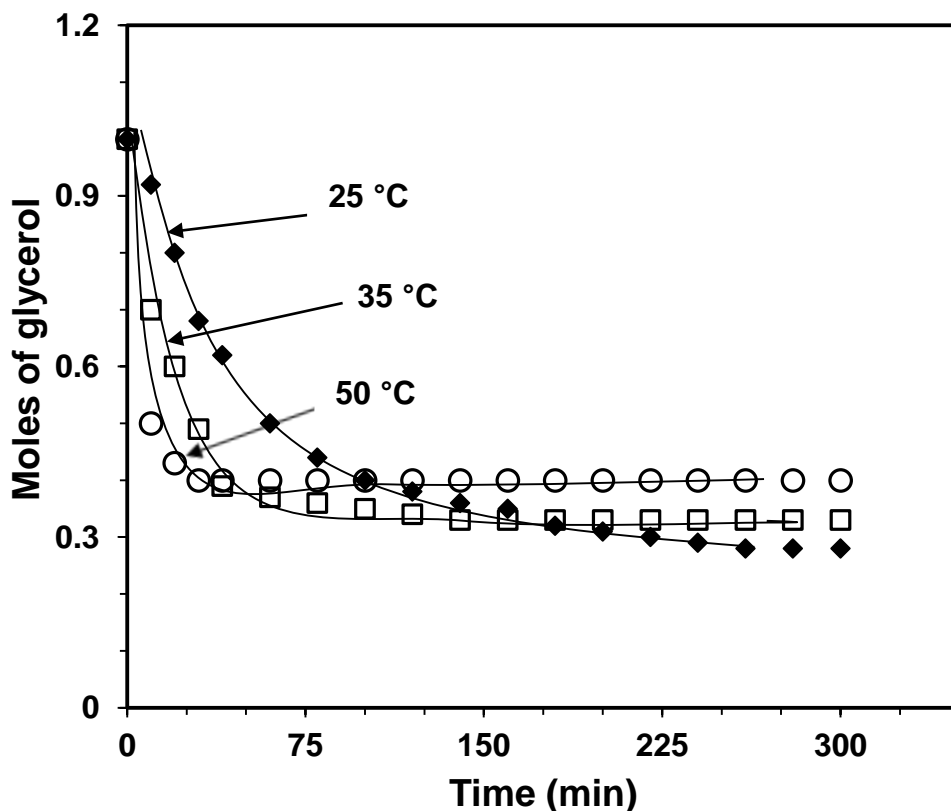


Figure 5.8 Experimental data vs. theoretical curves based on the kinetics derived in this work (Other conditions: 313 K, $W_{\text{cat}} = 1$ wt% of glycerol)

The temperature dependence of k and K_w can be given by the Arrhenius equations:

$$k = k_r \exp\left(-\frac{E_a}{RT}\right) \quad (15)$$

$$K_w = K_a \exp\left(-\frac{\Delta H_a}{RT}\right) \quad (16)$$

where k_r and K_a are the Arrhenius constants for equations (16) and (17), respectively. E_a and ΔH_a are the activation energy of the overall reaction and enthalpy of the water adsorption reaction, respectively. The predicted values of k and K_w are presented as a function of temperature in plots of $\ln k$ or $\ln K_w$ vs. $1/T$ in Figure 5.9. From the plots, the

values of E_a and ΔH_a were determined to be 55.6 ± 3.1 and -64.7 ± 4.3 kJ mol⁻¹, respectively.

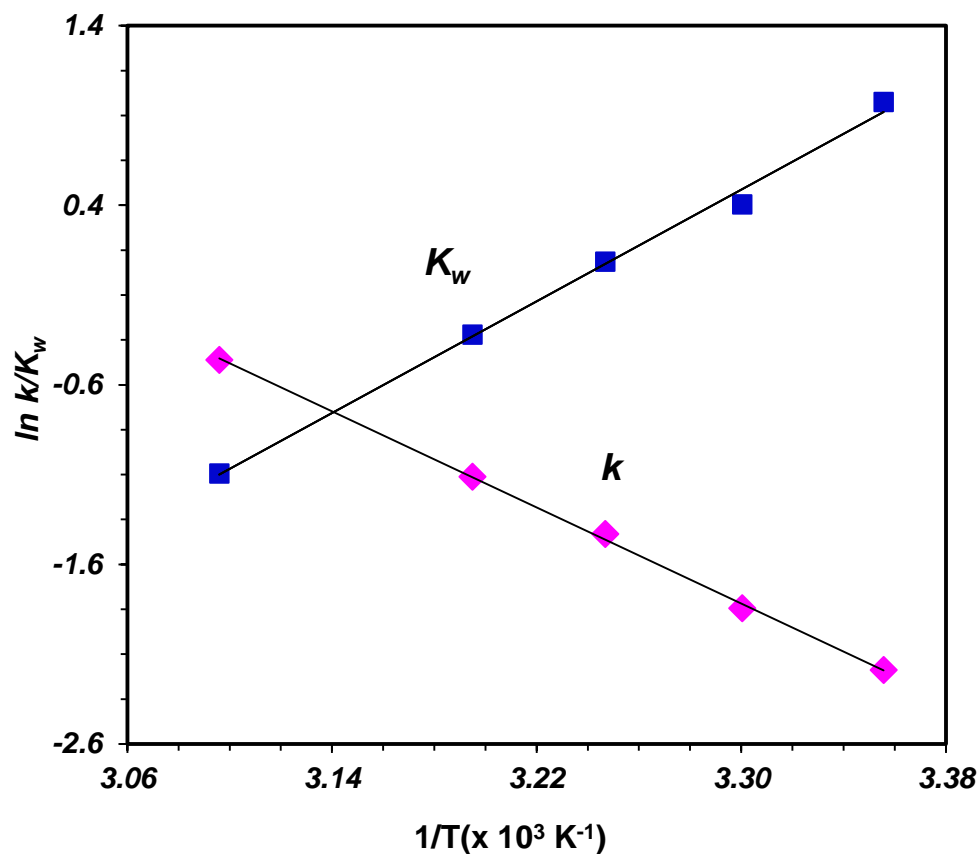


Figure 5.9 Plots of kinetic modeling parameters $\ln k$ or $\ln K_w$ vs. $1/T$

5.5 Conclusions

Thermodynamic and kinetic studies for the synthesis of solketal in the liquid phase were carried out in a well-controlled batch reactor in the presence of an acid catalyst (Amberlyst-35). The thermodynamic equilibrium constant K_c at various temperatures ranging from 293 to 323 K was determined. The reaction is exothermic and the standard enthalpy, entropy and Gibbs free energies at 298 K were found to be -30.1 ± 1.6 kJ mol⁻¹, -0.1 ± 0.01 kJ mol⁻¹

$^1 \text{ K}^{-1}$ and $-2.1 \pm 0.1 \text{ kJ mol}^{-1}$, respectively. The kinetic studies of the same reaction demonstrated that the rate of the reaction increased with increasing temperature, the catalyst addition amount and acetone-to-glycerol (A/G) molar ratio. In this batch study of the liquid phase reaction, pressure showed negligible influence on the reaction thermodynamics and kinetics as expected, and no effect of the agitation speed on the reaction rate was observable at $>400 \text{ rpm}$. Langmuir- Hinshelwood model demonstrated to be useful for describing the kinetic mechanism of the ketalization reaction of glycerol with acetone. Based on the Langmuir- Hinshelwood model, the values of the activation energy (E_a) of the overall reaction was determined to be $55.6 \pm 3.1 \text{ kJ mol}^{-1}$.

The future study of this project includes the development of a continuous reactor for the synthesis of solketal from both pure and crude glycerol using the thermodynamic and kinetic concepts where the recycle (recovery and reuse) of un-reacted reagents could be considered as an added advantage to the system.

References

1. Johnson DT, Taconi KA. The Glycerin Glut : Options for the Value-Added Conversion of Crude Glycerol Resulting from Biodiesel Production. 2009;26(4). doi:10.1002/ep.
2. Karinen RS, Krause a. OI. New biocomponents from glycerol. *Applied Catalysis A: General* 2006;306:128-133. doi:10.1016/j.apcata.2006.03.047.
3. Organization for Economic Co-operation and Development (OECD) and the Food and Agriculture Organization (FAO) of the United Nations, 2011-2020. Available at: <http://www.agri-outlook.org/48202074.pdf>. Accessed April 9, 2015.
4. B. Sims, "Clearing the Way for Byproduct Quality," 2011. <http://www.biodieselmagazine.com/articles/8137/clearing-the-way-forbyproduct-quality>|Reference|Scientific Research Publish. Available at: <http://www.ljemail.org/reference/ReferencesPapers.aspx?ReferenceID=820106>. Accessed December 3, 2014.
5. Deutsch J, Martin a, Lieske H. Investigations on heterogeneously catalysed condensations of glycerol to cyclic acetals. *Journal of Catalysis* 2007;245(2):428-435. doi:10.1016/j.jcat.2006.11.006.
6. Agirre I, García I, Requies J, *et al.* Glycerol acetals, kinetic study of the reaction between glycerol and formaldehyde. *Biomass and Bioenergy* 2011;35(8):3636-3642. doi:10.1016/j.biombioe.2011.05.008.
7. M.T.M. Silva V, Rodrigues AE. Synthesis of diethylacetal: thermodynamic and kinetic studies. *Chemical Engineering Science* 2001;56(4):1255-1263. doi:10.1016/S0009-2509(00)00347-X.
8. Barros AO, Faísca AT, Lachter ER, Nascimento RS V, Gil Rass. Acetalization of hexanal with 2-ethyl hexanol th catalyzed by solid acids, *Journal of Brazilian Chemical Society*. 2011;22(2):359-363.
9. Faria RP V., Pereira CSM, Silva VMTM, Loureiro JM, Rodrigues AE. Glycerol Valorization as Biofuel: Thermodynamic and Kinetic Study of the Acetalization of Glycerol with Acetaldehyde. *Industrial & Engineering Chemistry Research* 2013;52(4):1538-1547. doi:10.1021/ie302935w.
10. Mota CJA, Silva CX, Ribeiro PHS, Gonçalves VLC. Glycerine derivatives as fuel additives: The addition of glycerol/acetone ketal (solketal) in gasolines. *Energy Fuels* 2010;24(4):2733-2736.
11. Maksimov a. L, Nekhaev a. I, Ramazanov DN, Arinicheva Y a., Dzyubenko a. a., Khadzhiev SN. Preparation of high-octane oxygenate fuel components from plant-derived polyols. *Petroleum Chemistry* 2011;51(1):61-69. doi:10.1134/S0965544111010117.

12. Cablewski T, Faux AF, Strauss CR. Development and Application of a Continuous Microwave Reactor for Organic Synthesis. *The Journal of Organic Chemistry* 1994;59(12):3408-3412. doi:10.1021/jo00091a033.
13. Krief A, Provins L, Froidbise A. Diastereoselective synthesis of dimethyl cyclopropane-1,1-dicarboxylates from a γ -alkoxy-alkylidene malonate and sulfur and phosphorus ylides. *Tetrahedron Letters* 1998;39(11):1437-1440. doi:10.1016/S0040-4039(97)10822-X.
14. Silva PHR, Gonçalves VLC, Mota CJ a. Glycerol acetals as anti-freezing additives for biodiesel. *Bioresource Technology* 2010;101(15):6225-9. doi:10.1016/j.biortech.2010.02.101.
15. Roldan L, Mallada R, Fraile JM, Mayoral JA, Menendez M. Glycerol upgrading by ketalization in a zeolite membrane. *Asia-Pacific Journal of Chemical Engineering* 2009; 4:279–284.
16. Ferreira P, Fonseca IM, Ramos a. M, Vital J, Castanheiro JE. Valorisation of glycerol by condensation with acetone over silica-included heteropolyacids. *Applied Catalysis B: Environmental* 2010;98(1-2):94-99. doi:10.1016/j.apcatb.2010.05.018.
17. Vicente G, Melero J a., Morales G, Paniagua M, Martín E. Acetalisation of bio-glycerol with acetone to produce solketal over sulfonic mesostructured silicas. *Green Chemistry* 2010;12(5):899. doi:10.1039/b923681c.
18. Organic Chemistry (7th Edition). Available at: <http://www.amazon.com/Organic-Chemistry-7th-Edition-Wade/dp/032159231X>. Accessed December 3, 2014.
19. Da Silva CX a., Mota CJ a. The influence of impurities on the acid-catalyzed reaction of glycerol with acetone. *Biomass and Bioenergy* 2011;35(8):3547-3551. doi:10.1016/j.biombioe.2011.05.004.
20. García H, García OI, Fraile JM. Solketal: Green and catalytic synthesis and its classification as a solvent : 2,2-dimethyl-4-hidroxymethyl-1,3-dioxolane, an interesting green solvent produced through heterogeneous catalysis. *Chimica oggi* 26(3):10-12.
21. Grac NS, Pais S, Silva VMTM, Rodrigues E. Oxygenated Biofuels from Butanol for Diesel Blends : Synthesis of the Acetal 1, 1-Dibutoxyethane Catalyzed by Amberlyst-15 Ion-Exchange. *Resin.Industrial & Engineering Chemistry Research* 2010;49(15):6763-6771.
22. Organic Chemistry, 11th Edition - T. W. Graham Solomons, Craig B. Fryhle, Scott A. Snyder. Available at: <http://ca.wiley.com/WileyCDA/WileyTitle/productCd-EHEP002536.html>. Accessed December 3, 2014.

23. Yadav G., Thathagar M. Esterification of maleic acid with ethanol over cation-exchange resin catalysts. *Reactive and Functional Polymers* 2002;52(2):99-110. doi:10.1016/S1381-5148(02)00086-X.
24. Bart HJ, Kaltenbrunner W, Landschutzer H. Kinetics of esterification of acetic acid with propyl alcohol by heterogeneous catalysis. *International Journal of Chemical Kinetics* 1996;28(9):649-656. doi:10.1002/kin.2.
25. Zhou L, Nguyen TH, Adesina AA. The acetylation of glycerol over amberlyst-15: Kinetic and product distribution. *Fuel Process Technology* 2012; 104 (1): 310-8.
26. Rat M, Zahedi-Niaki MH, Kaliaguine S, Do TO. Sulfonic acid functionalized periodic mesoporous organosilicas as acetalization catalysts. *Microporous and Mesoporous Materials* 2008;112(1-3):26-31. doi:10.1016/j.micromeso.2007.09.010.
27. Izci A, Bodur F. Liquid-phase esterification of acetic acid with isobutanol catalyzed by ion-exchange resins. *Reactive and Functional Polymers* 2007;67(12):1458-1464. doi:10.1016/j.reactfunctpolym.2007.07.019.
28. Kaufhold M, Ei-Chawi MT. Process for preparing acetaldehyde diethyl acetal. *U.S. Patent* 1996; 5, 527,969.
29. Deutsch J, Prescott H, Muller D, Kemnitz E, Lieske H. Acylation of naphthalenes and anthracene on sulfated zirconia. *Journal of Catalysis* 2005;231(2):269-278. doi:10.1016/j.jcat.2005.01.024.
30. Organic Chemistry, . Available at: <http://www.amazon.com/Organic-Chemistry-Edition-Robert-Morrison/dp/0136436692>. Accessed December 3, 2014.
31. Report of Analysis.Methes Biodiesel. 2012.
32. Rabindran Jermy B, Pandurangan A. Al-MCM-41 as an efficient heterogeneous catalyst in the acetalization of cyclohexanone with methanol, ethylene glycol and pentaerythritol. *Journal of Molecular Catalysis A: Chemical* 2006;256(1-2):184-192. doi:10.1016/j.molcata.2006.04.045.
33. Xiao Y, Gao L, Xiao G, Lv J. Kinetics of the Transesterification Reaction Catalyzed by Solid Base in a Fixed-Bed Reactor. *Energy & Fuels* 2010;24(11):5829-5833. doi:10.1021/ef100966t.

Chapter 6

6 A new continuous-flow process for the catalytic conversion of glycerol to oxygenated fuel additive: catalyst screening

Abstract

A new continuous-flow reactor was designed for the conversion of glycerol to solketal; an oxygenated fuel additive, through ketalization with acetone. Six heterogeneous catalysts were investigated with respect to their catalytic activity and stability in a flow reactor. The acidity of the catalysts positively influences the catalyst's activity. Among all the solid acid catalysts tested, the maximum solketal yield from experiments at 40 °C, 600 psi and WHSV of 4 h⁻¹ reached 73% and 88% at an acetone /glycerol molar ratio of 2.0 and 6.0, respectively, with Amberlyst wet. Based on the solketal yield and glycerol conversion results, the activity of all catalysts tested follows the sequence: Amberlyst wet \approx H-beta zeolite \approx Amberlyst dry > Zirconium sulfate > Montmorillonite > Polymax. An increase in acetone /glycerol molar ratio or a decrease in WHSV enhanced the glycerol conversion as expected. This process offers an attractive route for converting glycerol, the main by-product of biodiesel, to solketal-a value-added green product with potential industrial applications as a valuable fuel additive or combustion promoter for gasoline engines.

Keywords: Catalytic conversion; Catalyst screening; Flow reactor; Glycerol; Solketal

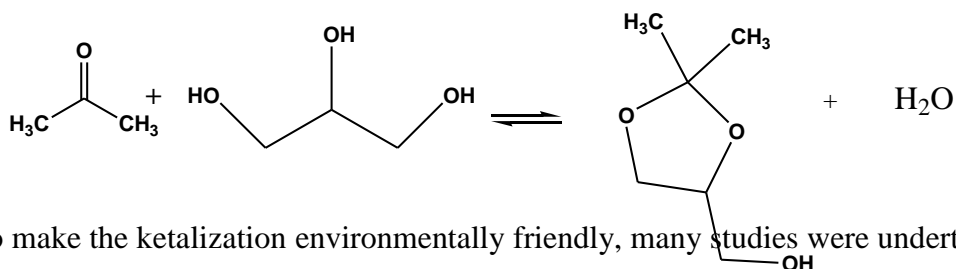
6.1 Introduction

The booming biodiesel industry all over the world has led to the generation of a large amount of glycerol as a byproduct. It was predicted that by 2020 the global production of

glycerol will be 41.9 billion liters annually.¹ In order to avoid the saturation of global glycerol market, it is urgent to develop value-added products to consume the excessive glycerol for the sustainability of biodiesel industry. In this regard, the fuel industry seems to be a suitable market where a high volume of glycerol could be absorbed for value added applications.

The direct use of glycerol as fuel is however not encouraged due to its low calorific value, high boiling point and high polarity. Nevertheless, its conversion into ketals and ethers has demonstrated potential for their use as oxygenated fuel additives.^{2,3,4} Ketals and ethers can be utilized as oxygenated fuel additives or combustion promoters as the addition of ketals and ethers in gasoline engines improves the octane number, cold flow and ignition properties of the fuel with reduced particulate emission, and gum formation.^{5,6,7} The aquatox fish test requested by the authors' group on the toxicity of the solketal showed that solketal (with a LC₅₀ for fish to be as high as 3162 ppm) has demonstrated much less environmental toxicity than the common fuel additive Methyl tert-butyl ether (MTBE) with a LC₅₀ <<1000 ppm.

Conventionally, ketalization reaction of glycerol with acetone, whose reaction scheme is shown below, has been performed in homogeneous liquid phase in batch reactors. The reaction is catalyzed by strong Brønsted acids such as; sulfuric acid, hydrochloric acid, phosphoric acid or p-toluene sulfonic acid etc., where corrosion of reactors, product separation and effluent disposal are the main challenges with respect to operating costs and environmental burdens.^{8,9,10}



In order to make the ketalization environmentally friendly, many studies were undertaken mostly in batch reactors using heterogeneous catalysts such as zeolites,¹¹ amberlysts,¹² montmorillonite,⁵ silica supported heteropolyacids,¹³ nafion,² and bio-based reagents, etc.. Our previous study reported the thermodynamics and kinetics of the ketalization reaction

using a heterogeneous catalyst- Amberlyst-35 in a batch reactor.¹⁴ However, the synthesis of solketal in a batch reactor using either homogeneous or heterogeneous catalysts requires long reaction time (usually exceeding 2 h total reaction time). Although, mechanical stirrers are commonly used in batch reactors in order to improve mass transfer within the reactor, the yield was strongly dependent on the stirring intensity and efficiency.¹⁵ In addition, a batch process has some major limitations for scale-up. Clarkson *et al.* developed a technology for the synthesis of solketal in a semi-batch reactor where acetone was fed continuously but glycerol was fed batch-wisely.¹⁶ The high viscosity of glycerol at low temperatures was found to be the main obstacle in making the process continuous. In another attempt, Monbaliu *et al.* used a glass reactor for the continuous synthesis of solketal in the presence of a homogeneous catalyst (i.e., sulfuric acid).¹⁷ However, the process is not economical and environmentally friendly due to the aforementioned corrosion and waste disposal problems associated with the use of sulfuric acid. Inspired by the stated landmark papers,^{16,17} we took an attempt to engineer a continuous flow reactor for the production of solketal using heterogeneous catalysts, which, to the best of our knowledge, is the first work of this kind reported. It is obvious that the production of solketal in a continuous-flow reactor using heterogeneous catalysts is preferable because the process has advantages of high heat and mass transfer efficiency, ease of scale-up from laboratory to industrial scale, and high surface to volume ratios.^{18,19,20} To boost the reaction in a flow reactor, the concept of “Novel Process Windows” with respect to temperature, pressure and/or reactant concentration could be exploited and the intrinsic kinetics of the reaction could be determined.^{21,22,23} In the present study an attempt was made to use a continuous flow reactor to achieve ketalization of glycerol in a much shorter residence time as compared to that of a batch reactor.

Ketalization of glycerol strongly depends on the experimental conditions used; therefore, it is not easy to make a comparison among the performances of different heterogeneous catalysts reported in the literature. In the present study the main objectives were to 1) construct a continuous-flow reactor for the conversion of glycerol to solketal; 2) compare the activities of different solid acid catalysts used in the process under the same experimental conditions for catalyst screening; and (3) investigate the effect of their intrinsic properties on the activity in a continuous-flow reactor system.

6.2 Materials and methods

6.2.1 Materials

Glycerol and acetone (both >99 wt% purity) were purchased from Sigma Aldrich and used as received. Reagent grade anhydrous ethanol was supplied from Commercial Alcohols Inc. Solketal (1, 2- isopropylidene glycerol, 99 wt%), for GC calibration was also obtained from Sigma Aldrich. The catalysts of Amberlyst-35 dry and Amberlyst-36 wet were obtained from Rohm and Hass Co. (USA), and used as received. H-beta zeolite (CP 814 C) in the acid form was procured from Zeolyst International (USA) and was calcined at 500 °C for 6 h before use. Montmorillonite (K-10) was obtained from Sigma-Aldrich and was dried at 120 °C for 3 h before use. Zirconium sulfate was prepared according to literature from zirconium sulfate hydrate purchased from Sigma-Aldrich.²⁴ Polymax (845) was provided by Süd Chemie group and was dried at 120 °C for 2 h prior to use.

6.2.2 Catalyst characterization

The surface area, total pore volume and average pore diameter of the selected catalysts were determined by nitrogen isothermal (at -196 °C) adsorption with a Micromeritics ASAP 2010 BET apparatus. The catalysts; H-beta zeolite, and Montmorillonite were degassed at 120 °C and amberlyst was dried at 90 °C overnight under vacuum prior to the surface area measurements. The acidity (the number of acid sites per unit mass) of the catalysts was measured by an ammonia temperature programmed desorption (NH₃-TPD) test using a Micromeritics AutoChem II analyzer. Thermal stability of the catalysts was evaluated using thermogravimetric analyser (TA Q500) at a heating rate of 10 °C/min in N₂ flow of 30 ml/min. Fourier Transform Infrared Spectroscopy (FTIR) (Thermo scientific-Nicolet 6700) was used to identify the functional groups present in the catalysts.

6.2.3 Synthesis of solketal in a continuous-flow reactor

The synthesis of solketal was carried out in a bench scale continuous down-flow tubular reactor (Inconel 316 tubing, 9.55 mm OD, 6.34 mm ID and 600 mm length) heated with an electric furnace. A schematic diagram of the continuous flow reactor system is shown in Figure 6.1. The feed-a homogeneous solution of reactants (acetone and glycerol) and

solvent (ethanol) at a selected molar ratio was pumped into the reactor using a HPLC pump (Eldex) at a specific flow rate. The temperature and pressure of the reactor were controlled by a temperature controller and a back-pressure controller, respectively. In a typical run, 116.00 g of acetone, 92.00 g of glycerol and 46.00 g of ethanol (corresponding to 2:1:1 molar ratio of acetone: glycerol: ethanol) were mixed, and the homogeneity of the solution was confirmed by GC-MS analysis. Ethanol was used as solvent mainly to improve the solubility of glycerol in acetone. In each run, a pre-determined amount of catalyst was preloaded into the catalytic bed, in which the catalyst particles were supported on a porous Inconel metal disc (pore size: 100 μm) and some quartz wool. The amount of catalyst in each run was determined by the selected weight hourly space velocity (WHSV, reciprocal of reaction time) defined as follows:

$$WHSV(h^{-1}) = \frac{\text{Mass flow of glycerol}(g/h)}{\text{Mass of catalyst used}(g)} \quad (1)$$

Depending on the feeding rate, compositions of the feed and the amount of the catalyst used in each run, WHSV, varied from 2-8 h^{-1} .

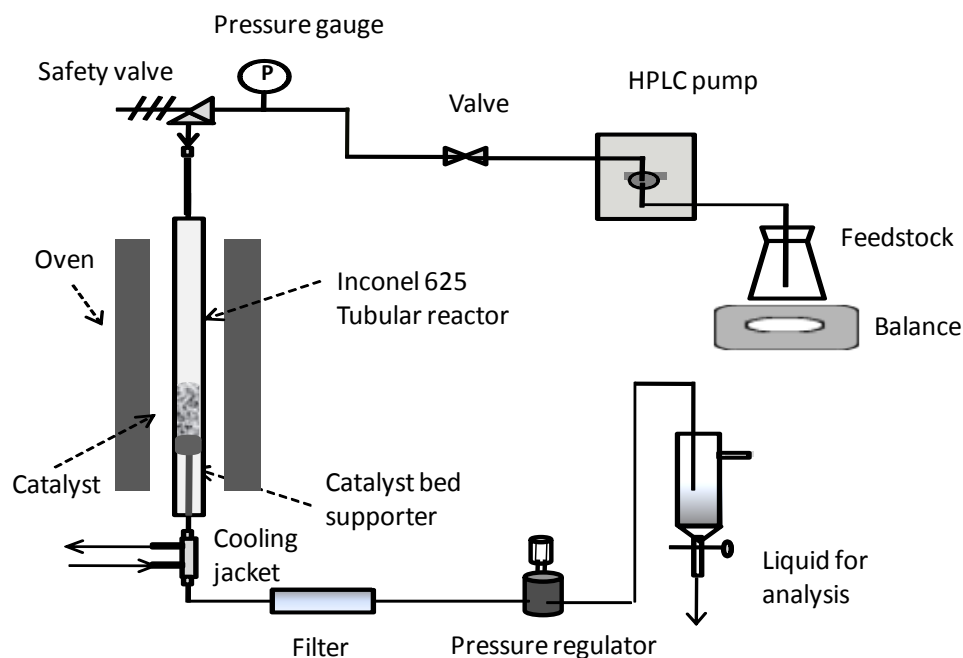


Figure 6.1 Schematic diagram of the continuous-flow reactor used for ketalization of glycerol

6.2.4 Product analysis

All the components in the reaction mixture were first identified by GC-MS on a Varian 1200 Quadrupole MS (EI) and Varian CP-3800 GC with VF-5 MS column (5% phenyl/95% dimethyl-polysiloxane, 30 m × 0.25 mm × 0.25 μm)], using helium as the carrier gas at a flow rate of 0.5 mL/s. The oven temperature was maintained at 120 °C for 2 min and then increased to 280 °C at 40 °C/min. Injector and detector temperature were 300 °C. Components in the reaction mixture were identified by NIST 98 MS library. Composition of the products and un-reacted reactants were quantitatively analyzed with a GC-FID (Shimadzu -2010) using similar separation conditions as mentioned above for the GC-MS, after careful calibration with glycerol and solketal of varying concentrations and dimethyl sulfoxide (DMSO) as an internal standard at a fixed concentration. Appendix C provides a typical GC-MS spectrum and the calibration tables and curves for GC-FID.

Solketal was separated and purified from un-reacted reactants and the reaction solvent by distillation. The purified product was identified by Fourier Transform Infrared Spectroscopy (FTIR) and GC-FID. In all the experiments, the selectivity to solketal was found to be more than 97% with an insignificant amount of undesired products like diethoxy ethane and 2,2-diethoxy propane etc. The reported yield and conversion are values after 4 h on-stream unless otherwise specified. Herewith, the solketal product yield, glycerol conversion and product selectivity are defined as follows:

$$\text{Yield (\%)} = \frac{\text{Moles of solketal formed}}{\text{Initial moles of glycerol}} \times 100 \quad (2)$$

$$\text{Conversion (\%)} = \frac{\text{Initial moles of glycerol} - \text{Final moles of glycerol}}{\text{Initial moles of glycerol}} \times 100 \quad (3)$$

$$\text{Selectivity(\%)} = \frac{\text{Moles of solketal formed}}{\text{Initial moles of glycerol} - \text{Final moles of glycerol}} \times 100 \quad (4)$$

6.3 Results and discussion

6.3.1 Fresh catalyst characterization

The fresh catalysts were characterized comprehensively for their textural properties (i.e., specific surface area, pore volume, pore diameter), and chemical properties such as hydrophobicity and acid strength, and thermal stability, as these properties are believed to be critical for determining the catalytic activities and choosing appropriate reaction conditions.

Table 6.1 Textural properties (measured by N₂ isothermal adsorption) and acidity for the fresh catalysts used in this study

Catalyst	BET surface ^a (m ² /g)	Pore volume ^a (cc/g)	Pore size ^a (nm)	Acidity ^b (eq/kg)	Mean particle size (μm) ^c
H-beta zeolite	480	0.25	2	5.7	45
Montmorillonite	264	0.36	5.5	4.6	13
Amberlyst dry	35	0.28	16.8	5.4	482
Amberlyst wet	33	0.2	24	5.6	490

^a Determined by N₂ isothermal adsorption (77 K); ^b Determined by ammonia TPD (378 K); ^c From the supplier

The results of the textural properties (measured by N₂ isothermal adsorption) and acidity for the fresh catalysts used in this study (measured by ammonia TPD) are presented in Table 6.1. It can be seen that H-beta zeolite has the maximum surface area (480 m²/g) with

minimum pore size (2 nm), and amberlyst wet has the least surface area (33 m²/g) with maximum pore size (24 nm). The acidity of all the catalysts (H-beta zeolite, Montmorillonite, Amberlyst dry and Amberlyst wet) are similar in the relatively narrow range of 4.6-5.7 eq/kg, while the other two catalysts (Polymax and Zirconium sulfate) were not analyzable. The textural properties and the acidity of the catalysts will be correlated with the activities of these catalysts for glycerol conversion for solketal synthesis, as reported in the later sections of this chapter.

The thermal stability of the catalysts was examined using thermogravimetric analysis (TGA). Figure 6.2 illustrates the percentage weight loss results for various catalysts vs. temperature. As shown from the TGA profiles, catalysts such as H-beta zeolite, montmorillonite, polymax and zirconium sulfate are very stable at elevated temperatures. Amberlyst dry and Amberlyst wet are however temperature sensitive. Temperatures above 100 °C cause thermal degradation of these catalysts. With these results, all our glycerol ketalization experiments were carried out below 100 °C. Characterizations of these two catalysts were also performed below 100 °C for the measurement of their surface area and acidity.

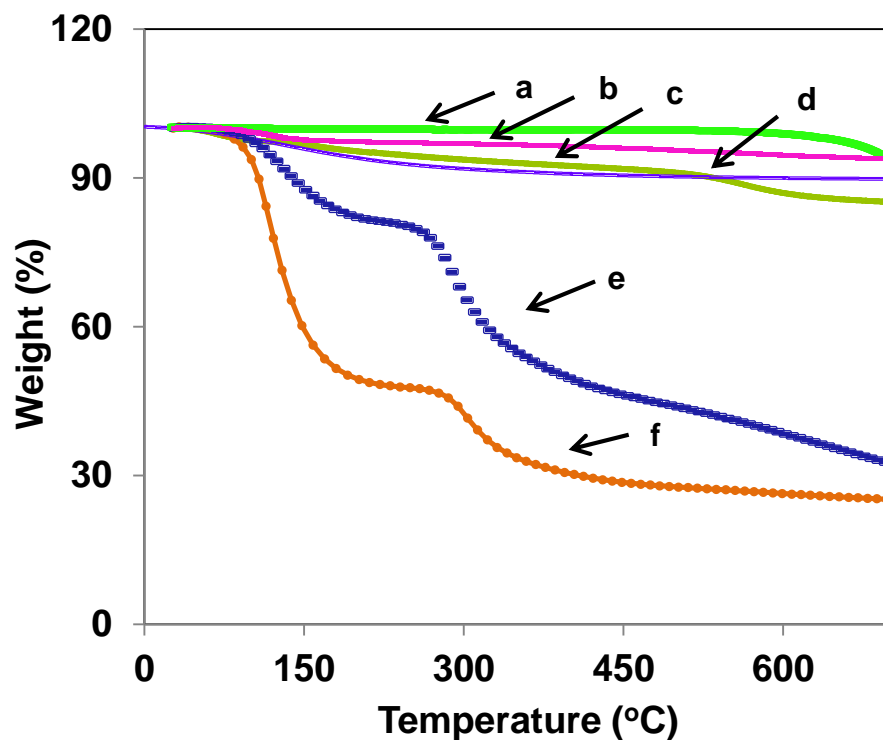


Figure 6.2 TGA profiles of fresh catalysts of Zirconium sulfate (a), Montmorillonite (b), Polymax (c), H-beta zeolite (d), Amberlyst dry (e) and Amberlyst wet (f)

6.3.2 Product characterization

FTIR spectroscopy was employed to confirm the presence of solketal in the purified solketal products. The FTIR spectrum of a typical solketal product is shown in Figure 6.3. A strong IR band at around 3400 cm^{-1} to 3600 cm^{-1} was observed which ascribes to the O-H stretching band resulted in the intermolecular and intramolecular hydrogen bonds present in the solketal. The IR absorption peaks at around 1000 cm^{-1} - 1100 cm^{-1} can be attributed to the symmetrical stretching of C-O band in solketal molecular structure,²⁵ confirming the production of solketal in the experiments. In this work, GC-MS and FT-IR were conducted for qualitative analysis of the products. The molecular weight of 132 of solketal is confirmed by MS, and the strong m/z signal at 43 can be assigned to the ionization of dioxolane group ($\text{CH}_3\text{-C-CH}_3$) formed by the opening of protecting group of solketal.²⁶

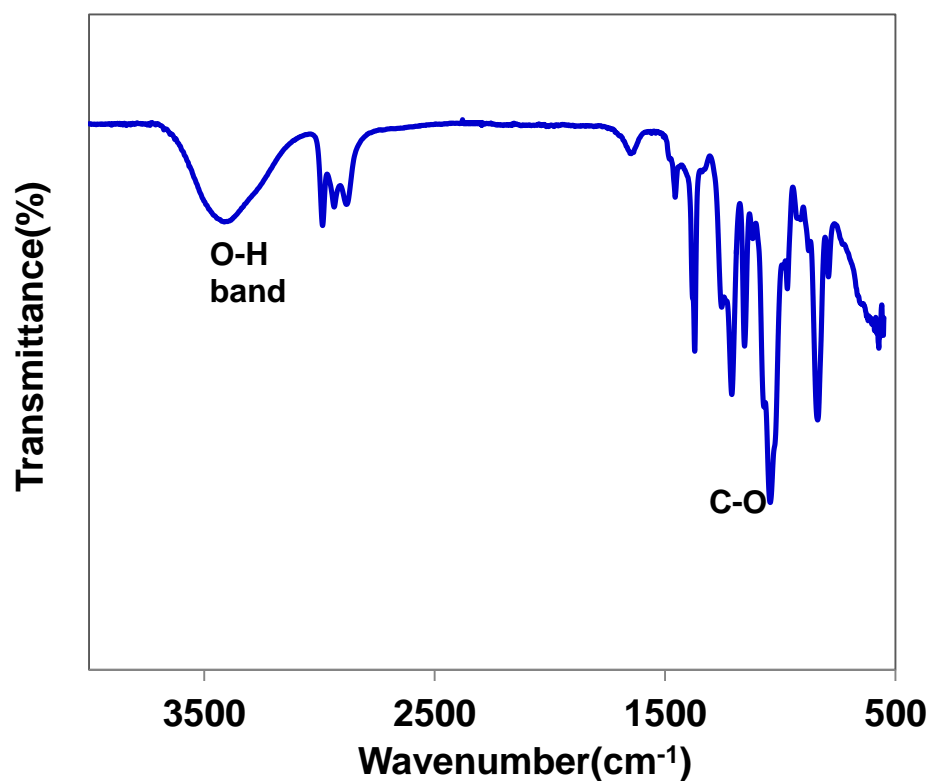


Figure 6.3 FTIR spectrum of a typical solketal product

6.3.3 Catalyst activities

In a first set of experiments, the influence of the acetone/glycerol molar ratio on the yield of solketal was investigated. Table 6.2 summarizes the glycerol conversion and the solketal yield from the experiments conducted at 40 °C, 600 psi and WHSV of 4 h⁻¹ with different acetone/glycerol molar ratios (acetone equivalent ratio) of 2.0 and 6.0. Clearly, increasing of the acetone equivalent ratio resulted in an increase of the solketal yield irrespective of the catalysts used. These results are actually expected as an excess in acetone could drive the reaction in its forward direction thermodynamically to increase the glycerol conversion. A higher concentration of reactants also promotes the reaction rate, leading to a higher product yield. Similar observations in a batch reactor were reported by Agirre *et al.*³ In

addition, the use of excess acetone could also help enhance the catalyst life time by removing the water formed on the catalyst surface (please be noted that adsorption of water on the catalyst surface would block the catalyst active sites and thus deactivate the catalyst).

Table 6.2 Effect of acetone/glycerol molar ratio at fixed temperature (40 °C), pressure (600 psi) and WHSV (4 h⁻¹)

Catalyst	Acetone equivalent ratio			
	2.0		6.0	
	Yield (%)	Conversion (%)	Yield (%)	Conversion (%)
H-beta zeolite	72± 2	73± 3	84± 2	85± 2
Montmorillonite	60 ± 1	60± 4	68± 1	69± 1
Amberlyst dry	70± 1	71± 2	86± 3	88± 3
Polymax	50± 1	51± 3	60± 2	61± 2
Zirconium sulfate	65± 3	66± 1	77± 2	79± 2
Amberlyst wet	71± 3	71± 3	88± 4	89± 3

Among all the solid acid catalysts tested, the maximum solketal yield was observed with Amberlyst wet (being 73% and 88% at the acetone/glycerol molar ratio of 2.0 and 6.0, respectively). Based on the solketal yield and glycerol conversion results from Table 6.2, the activity of all catalysts tested follows the following order of sequence: Amberlyst wet \approx H-beta zeolite \approx Amberlyst dry > Zirconium sulfate > Montmorillonite > Polymax.

As is well known, ketalization reaction proceeds via acidic catalytic mechanism. As such, catalysts with higher number of acidic sites would lead to higher activities. To examine the dependency of catalyst activity on its acidity, Figure 6.4 illustrates the relationship between the product yield and the catalyst acidity using the data from Table 6.1 and Table 6.2. An approximately linear relationship was observed in Figure 6.4, suggesting that catalysts of

higher acid strength, such as H-beta zeolite (5.7 eq/kg), Amberlyst dry (5.4 eq/kg) and Amberlyst wet (5.6 eq/kg), resulted in a high yield of solketal.

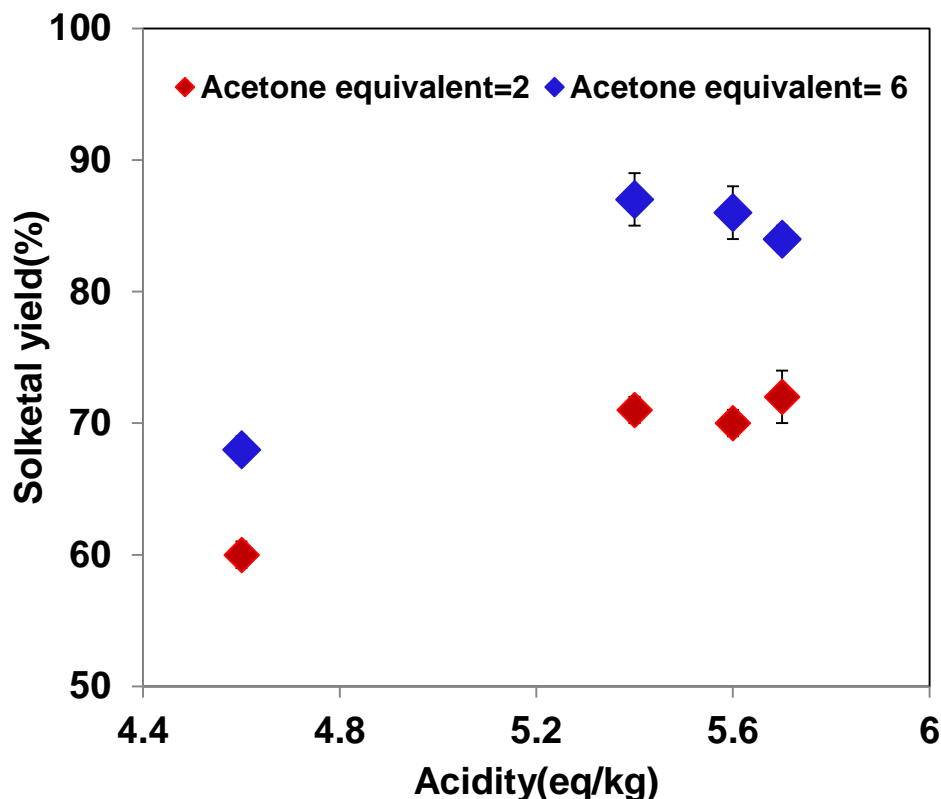


Figure 6.4 Solketal yield vs. acidity (relative abundance of acidic sites) for catalysts of H-beta zeolite (6.2 eq/kg), Montmorillonite (4.6 eq/kg), Amberlyst dry (5.5 eq/kg) and Amberlyst wet (5.4 eq/kg). Experimental conditions: 40 °C, 600 psi and WHSV of 4 h⁻¹ with different acetone equivalent ratios of 2.0 and 6.0.

Another set of experiments was conducted to study the effect of WHSV on the solketal yield and glycerol conversion at the reaction conditions of 40 °C, 600 psi and acetone equivalent of 2.0 under different WHSV (4.0 and 8.0 h⁻¹). The results are given in Table 6.3. It is evident that increasing the WHSV from 4 to 8 h⁻¹, both the product yield and glycerol conversion decrease irrespective of the catalysts used, simply because if the

reaction is not at equilibrium. Therefore, a shorter residence time (or larger WHSV) by necessity results in a lower conversion.²⁷

Table 6.3 Effect of weight hourly space velocity (WHSV, h⁻¹) on solketal yield and glycerol conversion (Other reaction conditions: 40 °C, 600 psi and acetone equivalent of 2.0)

Catalyst	WHSV (h ⁻¹)			
	4.0		8.0	
	Yield (%)	Conversion (%)	Yield (%)	Conversion (%)
H-beta zeolite	72± 3	73± 2	65± 2	66± 1
Montmorillonite	60± 1	61± 2	51± 1	52± 2
Amberlyst dry	70± 2	72± 4	66± 2	67± 3
Amberlyst wet	71± 2	72± 3	65± 3	66± 2
Polymax	50± 1	50± 2	35± 1	36± 2
Zirconium sulfate	65± 2	66± 3	58± 2	59± 1

The effect of temperature on the glycerol conversion to solketal in the continuous-flow reactor was also investigated. The experiments were conducted at three different temperatures (40, 70, and 100 °C) while keeping other reaction parameters constant (i.e., acetone/glycerol molar ratio of 2.0, WHSV of 8.0 h⁻¹, pressure of 600 psi, 4 h time-on-stream). The results are presented in Figure 6.5. For catalysts such as H-beta zeolite beta and Amberlyst (both 35 dry and 36 wet), the reaction seemed to be mainly thermodynamically controlled: a higher reaction temperature led to a lower yield and lower conversion (exothermic reaction, $\Delta H^{\circ}_{298} = -30058.40 \text{ J mol}^{-1}$). In contrast, for catalysts such as montmorillonite, polymax and zirconium sulfate, the reaction was kinetically controlled: An increase in reaction temperature led to a higher glycerol conversion and larger solketal yield. One can however note from the Figure that the yield obtained at 100 °C with the zirconium sulfate is actually higher than that with H-beta zeolite or Amberlyst catalyst at the same temperature. It thus implies that what caused the reduced product yield

with increasing temperature for H-beta zeolite or Amberlyst catalyst is not due to the thermodynamic equilibrium, as discussed above, but due to other reasons such as deactivation of these highly active catalysts at an elevated temperature and aqueous condition.

The effect of pressure on the reaction was tested by varying it from 14.7-800 psi (or 1-54 atm) under the experimental conditions of 25 °C, acetone: glycerol: ethanol molar ratio of 2:1:1, WHSV of 4 h⁻¹ with Amberlyst-36 wet catalyst, for 4h time-on-stream). It was found that the reaction pressure has a negligible effect on the product yield, as expected for liquid phase reactions. In this study, experiments as reported here were all conducted under elevated pressure (600 psi) to maintain liquid phase of the reaction mixture during reaction. At 600 psi and the maximum operating temperature and the maximum acetone concentration in the feed used in this work, the maximum amount of molecules in gas phase was calculated to be very small (<1%).

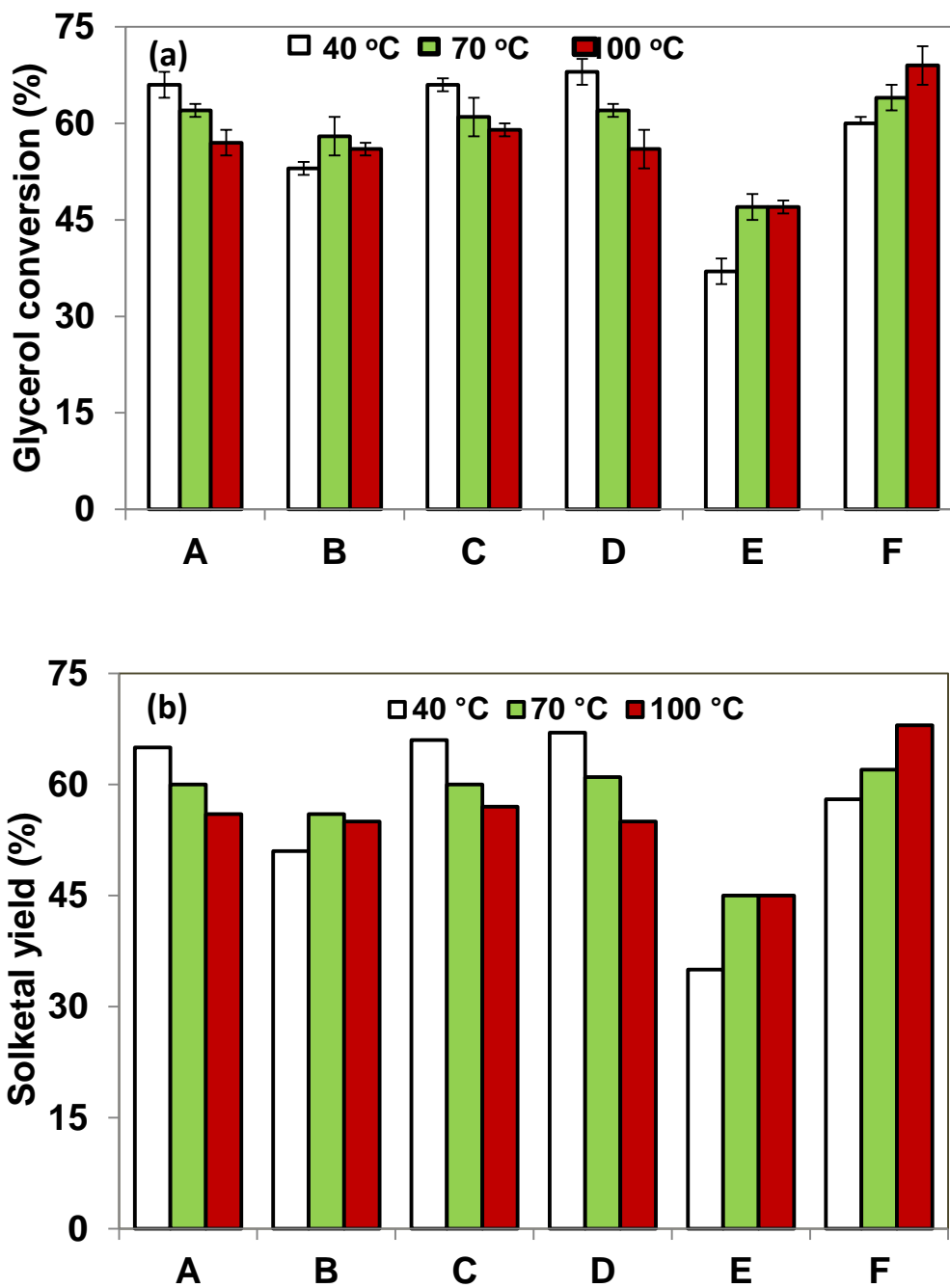


Figure 6.5 Variation of glycerol conversion (a) and solketal yield (b) with temperature for various catalysts (A: H-beta zeolite; B: Montmorillonite; C: Amberlyst dry; D: Amberlyst wet; E: Polymax; F: Zirconium sulfate). Other conditions were: $P = 600$ psi, molar ratio of acetone: glycerol: ethanol = 2:1:1, $WHSV = 4 \text{ h}^{-1}$)

The catalyst stability for various catalysts over a longer time-on-stream (up to 24 h) was investigated under the following experimental conditions: 25 °C, 600 psi, 2:1:1 molar ratio for acetone: glycerol: ethanol, and WHSV of 2 h⁻¹. The results are displayed in Figure 6.6. The poorest performance was observed with polymax, leading to a drastic declining of activity after 4 h on-stream. The fast deactivation of polymax could be due to the loss of acidity from the catalyst surface by the water produced during the reaction. In contrast, the catalyst of Amberlyst wet, H-beta zeolite, or Amberlyst dry exhibited superb stability over a long time-on-stream, producing solketal at a high yield > 70% during the whole course of the experiments for up to 24 h on-stream, although it is clear that these catalysts, except polymax, exhibited only a slight decrease in activity with increasing time on-stream. To understand the superb stability of the Amberlyst wet catalyst, the textural properties and acidity for its spent catalyst after 24 h time-on-stream were measured, and the results are presented comparatively against those of its fresh catalyst in Table 6.4. In addition, FTIR measurements of the fresh and spent catalyst of Amberlyst Wet after 24 h time-on-stream were measured and the spectra are displayed in Figure 6.7. As shown in Table 6.4 and Figure 6.7, it is apparent that the Amberlyst wet catalyst did not deteriorate significantly in its textural properties (specific surface area and pore structure) during the experiments for 24 h on-stream, which explains its superb stability for the reaction. However, from Table 6.4, the acidity (the abundance of active acid sites) of the Amberlyst wet catalyst did decrease slightly from 5.6 eq/kg for the fresh catalyst to 5.2 eq/kg for the spent catalyst, which might account for the slight deactivation of the catalyst during the experiments for 24 h on-stream.

Table 6.4 Textural properties and acidity for the fresh and spent catalyst (after 24 h time-on-stream) of Amberlyst wet

Catalyst	BET surface ^a (m ² /g)	Pore volume ^a (cc/g)	Pore size ^a (nm)	Acid strength ^b (eq/kg)
Amberlyst wet (Fresh)	33	0.2	24	5.6
Amberlyst wet (Spent)	32	0.2	25	5.2

^a: Determined by N₂ isothermal adsorption (77 K); ^b: Determined by ammonia TPD (378 K)

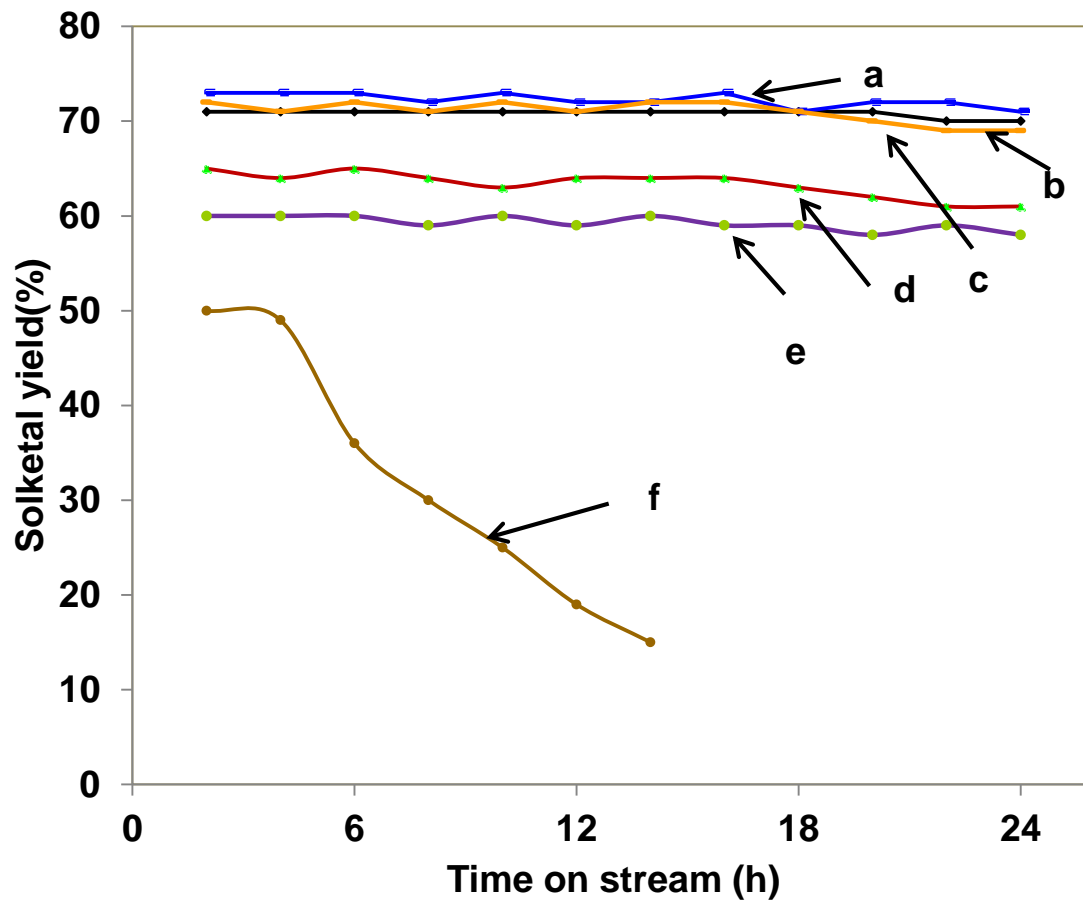


Figure 6.6 Solketal yield vs. time-on-stream with catalysts of Amberlyst wet (a), H-beta zeolite (b), Amberlyst dry (c), Zirconium sulfate (d), Montmorillonite (e) and Polymax(f)

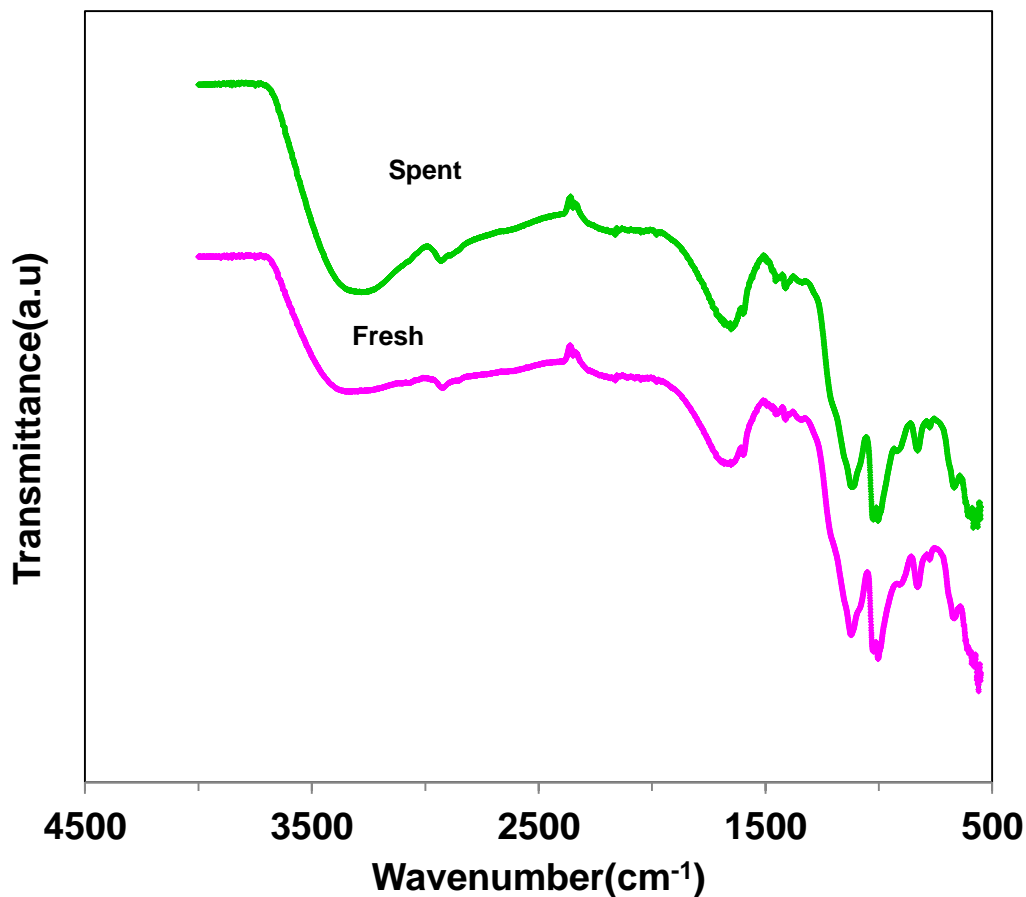


Figure 6.7 FTIR spectra of the fresh and spent Amberlyst wet (Experimental conditions: 40 °C, 600 psi and WHSV of 4 h⁻¹ with acetone equivalent of 2)

Reactor clogging is one of the major challenges in operating of a continuous-flow reactor process, particularly with heterogeneous catalysts. During the course of the current investigations, the clogging of the flow reactor was observed for some catalysts including beta zeolite, montmorillonite and polymax. An increase in flow rate and/or increase in the catalyst loading in the reactor would cause agglomeration of the particles which clogged the reactor resulting in a sharp increase in the reactor pressure. This suggests that these catalysts may not be suitable for being used for the present glycerol ketalization process using the flow reactor. Admittedly, the reactor clogging phenomenon could be efficiently avoided by diluting the catalyst with inert materials such as glass beads or by minimizing

the catalyst bed height. On the basis of the product yield and experimental conditions, the overall results of this study (88% yield for Amberlyst wet at 40 °C, 600 psi and WHSV of 4 h⁻¹) are better than what reported in literature.^{12,13}

6.4 Conclusions

A new continuous-flow process employing heterogeneous catalysts has been developed for the first time for efficiently converting glycerol into solketal. A total of 6 different catalysts were investigated with respect to their catalytic activity and stability at different reaction conditions (e.g., acetone/glycerol molar ratio, WHSV, temperature, pressure, etc.). The increase in the acetone/glycerol molar ratio resulted in an increase of the solketal yield irrespective of the catalysts used. Among all the solid acid catalysts tested, the use of Amberlyst wet produced the maximum solketal yield from experiments at 40 °C, 600 psi and WHSV of 4 h⁻¹ (being 73% and 88% at the acetone/glycerol molar ratio of 2.0 and 6.0, respectively). It appeared that catalysts with higher abundance of active acid sites exhibited higher activities: Amberlyst wet \approx H-beta zeolite \approx Amberlyst dry > Zirconium sulfate > Montmorillonite > Polymax. Both the solketal yield and glycerol conversion decreased, irrespective of the catalysts used, upon increasing the WHSV. The activities of all the catalysts, except polymax, showed only a slight decrease in its activity for up to 24 h on-stream likely due to the loss of its acidity during a long time on-stream.

References

1. Organization for Economic Co-operation and Development (OECD) and the Food and Agriculture Organization (FAO) of the United Nations, 2011-2020. Available at: <http://www.agri-outlook.org/48202074.pdf>. Accessed April 9, 2015
2. Deutsch J, Martin a, Lieske H. Investigations on heterogeneously catalysed condensations of glycerol to cyclic acetals. *Journal of Catalysis* 2007;245(2):428-435. doi:10.1016/j.jcat.2006.11.006.
3. Agirre I, García I, Requies J, *et al.* Glycerol acetals, kinetic study of the reaction between glycerol and formaldehyde. *Biomass and Bioenergy* 2011;35(8):3636-3642. doi:10.1016/j.biombioe.2011.05.008.
4. Silva PHR, Gonçalves VLC, Mota CJ a. Glycerol acetals as anti-freezing additives for biodiesel. *Bioresource Technology* 2010;101(15):6225-9. doi:10.1016/j.biortech.2010.02.101.
5. Maksimov a. L, Nekhaev a. I, Ramazanov DN, Arinicheva Y a., Dzyubenko a. a., Khadzhiev SN. Preparation of high-octane oxygenate fuel components from plant-derived polyols. *Petroleum Chemistry* 2011;51(1):61-69. doi:10.1134/S0965544111010117.
6. Len C, Luque R. Continuous flow transformations of glycerol to valuable products: an overview. *Sustainable Chemical Processes* 2014;2(1):1. doi:10.1186/2043-7129-2-1.
7. E. Garcı, M. Laca, E. Pe, A. Garrido, New class of acetal derived from glycerin as a biodiesel fuel component, *Energy & Fuels*. (2008) 4274–4280.
8. Frusteri F, Spadaro L, Beatrice C, Guido C. Oxygenated additives production for diesel engine emission improvement. *Chemical Engineering Journal* 2007;134(1-3):239-245. doi:10.1016/j.cej.2007.03.042.
9. Capeletti MR, Balzano L, de la Puente G, Laborde M, Sedran U. Synthesis of acetal (1,1-diethoxyethane) from ethanol and acetaldehyde over acidic catalysts. *Applied Catalysis A: General* 2000;198(1-2):L1-L4. doi:10.1016/S0926-860X(99)00502-5.
10. Chopade SP. Ion-exchange resin-catalysed ketalization of acetone with 1,4- and 1,2-diols: use of molecular sieve in reactive distillation. *Reactive and Functional Polymers* 1999;42(3):201-212. doi:10.1016/S1381-5148(98)00072-8.
11. Roldan L, Mallada R, Fraile JM, Mayoral JA, Menendez M. Glycerol upgrading by ketalization in a zeolite membrane. *Asia-Pacific Journal of Chemical Engineering* 2009; 4:279–284.

12. Vicente G, Melero J a., Morales G, Paniagua M, Martín E. Acetalisation of bio-glycerol with acetone to produce solketal over sulfonic mesostructured silicas. *Green Chemistry* 2010;12(5):899. doi:10.1039/b923681c.
13. Ferreira P, Fonseca IM, Ramos a. M, Vital J, Castanheiro JE. Valorisation of glycerol by condensation with acetone over silica-included heteropolyacids. *Applied Catalysis B: Environmental* 2010;98(1-2):94-99. doi:10.1016/j.apcatb.2010.05.018.
14. Nanda MR, Yuan Z, Qin W, Ghaziaskar HS, Poirier M-A, Xu CC. Thermodynamic and kinetic studies of a catalytic process to convert glycerol into solketal as an oxygenated fuel additive. *Fuel* 2014;117:470-477. doi:10.1016/j.fuel.2013.09.066.
15. Green D, Perry R. *Perry's Chemical Engineers' Handbook, Eighth Edition*. McGraw Hill Professional; 2007:2400.
16. Clarkson JS, Walker AJ, Wood MA. Continuous reactor technology for ketal formation : An improved synthesis of solketal. *Organic Process Research & Development* 2001;5(6):630-635. doi:10.1021/op000135p.
17. Monbaliu J-CM, Winter M, Chevalier B, *et al.* Effective production of the biodiesel additive STBE by a continuous flow process. *Bioresource Technology* 2011;102(19):9304-7. doi:10.1016/j.biortech.2011.07.007.
18. Noël T, Buchwald SL. Cross-coupling in flow. *Chemical Society reviews* 2011;40(10):5010-29. doi:10.1039/c1cs15075h.
19. Hartman RL, McMullen JP, Jensen KF. Deciding whether to go with the flow: evaluating the merits of flow reactors for synthesis. *Angewandte Chemie (International ed. in English)* 2011;50(33):7502-19. doi:10.1002/anie.201004637.
20. Jähnisch K, Hessel V, Löwe H, Baerns M. *Chemistry in Microstructured Reactors.*; 2004:406-46. doi:10.1002/anie.200300577.
21. Hessel V, Vural Gürsel I, Wang Q, Noël T, Lang J. Potential analysis of smart flow processing and micro process technology for fastening process development: use of chemistry and process design as intensification fields. *Chemical Engineering & Technology* 2012;35(7):1184-1204. doi:10.1002/ceat.201200038.
22. Razzaq T, Kappe CO. Continuous flow organic synthesis under high-temperature/pressure conditions. *Chemistry, an Asian journal* 2010;5(6):1274-89. doi:10.1002/asia.201000010.
23. Illg T, Löb P, Hessel V. Flow chemistry using milli- and microstructured reactors- from conventional to novel process windows. *Bioorganic & medicinal chemistry* 2010;18(11):3707-19. doi:10.1016/j.bmc.2010.03.073.

24. Sohn JR, Seo DH. Preparation of new solid superacid catalyst, zirconium sulfate supported on γ -alumina and activity for acid catalysis. *Catalysis Today* 2003;87(1-4):219-226. doi:10.1016/j.cattod.2003.09.010.
25. ChemSpider | Data Source Details | SDBS Spectral Database for Organic Compounds. Available at: <http://www.chemspider.com/DatasourceDetails.aspx?id=308>. Accessed December 9, 2014.
26. Suriyaprapadilok N, Kitiyanan B. Synthesis of Solketal from Glycerol and Its Reaction with Benzyl Alcohol. *Energy Procedia* 2011;9(0):63-69. doi:10.1016/j.egypro.2011.09.008.
27. Shang M, Noël T, Wang Q, Hessel V. Packed-Bed Microreactor for Continuous-Flow Adipic Acid Synthesis from Cyclohexene and Hydrogen Peroxide. *Chemical Engineering & Technology* 2013;36(6):1001-1009. doi:10.1002/ceat.201200703.

Chapter 7

7 Catalytic conversion of glycerol to oxygenated fuel additive in a continuous flow reactor: process optimization

Abstract

A continuous-flow process using ethanol solvent and heterogeneous catalyst amberlyst-36 was developed for conversion of glycerol to solketal, an oxygenated fuel additive, and the process was optimized in this study using response surface methodology. A model was proposed based on Box-Behnken design. At optimum conditions (temperature of 25 °C, acetone-to-glycerol molar ratio of 4 and weight hour space velocity of 2 h⁻¹) the maximum yield of 94±2% was obtained. The presence of impurities such as water and salt in glycerol significantly reduced the yield at the optimum conditions. The catalyst could be regenerated and reused for 24 h with an insignificant extent of deactivation. The use of methanol as solvent at the optimal conditions proved to have potential for making the system more economical. The economic analysis for the process revealed the potential of converting glycerol into solketal; an alternative to methyl tert-butyl ether as fuel additive.

Keywords: Continuous-flow reactor; Catalyst; Glycerol; Ketalization; Solketal

7.1 Introduction

The world biodiesel production has been boosted in recent years owing to an increasing demand of renewable and sustainable energy. Glycerol is produced as a by-product in the process of biodiesel production. The amount of glycerol generated is approximately 10 wt% of the biodiesel produced in a conventional biodiesel process.^{1,2} Hence a large amount of glycerol is expected on the market in near future. Due to the saturation of the glycerol market, the extra glycerol is now being considered as a waste by many biodiesel producers and going to affect the sustainability of the biodiesel industry.³ In this context, it is important to find some value added applications of glycerol. Upgrading glycerol into different valuable chemicals has been reported.^{4,5,6,7} Acetalization of glycerol is one of the methods considered to be promising and economically viable for the utilization of glycerol.⁸ In this process, glycerol reacts with an aldehyde or a ketone to form an acetal or a ketal, respectively, in the presence of an acid catalyst.⁹

Solketal (2, 2-dimethyl 1,3-dioxalane-4-methanol) is a ketal formed by the acid catalyzed reaction between glycerol and acetone.¹⁰ Roldan *et al.* reported the synthesis of solketal from glycerol using a zeolite membrane batch reactor, where a high amount of acetone was used (an equivalent ratio of 20) with 82% yield of solketal.¹¹ In another work, Vicente *et al.* reported 89.5% yield of solketal in a two-step batch process with an acetone equivalent ratio of 6.⁵ Important applications of solketal include being used as an additive to improve transportation fuel properties, as a plasticizer in polymer industry and a solvent in pharmaceutical industry.^{4,12,13}

Response surface methodology (RSM) is a technique generally used for modeling and optimization of the experimental observations in physical and chemical processes. The key aim of using RSM is to optimize the surface response and to determine the relationship between the input variables and the response data.¹⁴

The operational conditions for an optimum yield of solketal have been investigated in batch reactors;^{5,7,13} however hardly any attempt has been made for the process optimization in a continuous-flow reactor.

From our preliminary experiments for the catalytic conversion of glycerol to oxygenated fuel additive in a continuous-flow reactor, amberlyst-36 was found to be the best catalyst among others based on the yield and the catalyst's stability on stream.^{15,16} Process parameters including temperature (in the range 25- 65 °C), acetone-to-glycerol equivalent ratio (in the range of 2-6 mol/mol) and weight hourly space velocity (WHSV) (range of 2-4 h⁻¹) are considered to have significant effect on the product yield.

The present study mainly dealt with the optimization of the catalytic conversion of glycerol to solketal as an oxygenated fuel additive in a continuous flow reaction process. In this study, the optimization method was used to obtain a maximum yield in the shortest reaction time and at the lowest cost. The RSM technique was applied in the process optimization study and a quadratic model was proposed based on Box-Behnken design (BBD) including the interactions of the process variables.

7.2 Experimental

7.2.1 Materials

Glycerol, methanol, and acetone (both >99 wt% purity) were procured from Sigma Aldrich and used as received, and commercial grade ethanol was supplied from Commercial Alcohols Inc. Solketal [(S-) (+) – 1, 2- Isopropylidenglycerol, 99 wt%] was also obtained from Sigma Aldrich as a calibration standard for GC analysis. The solid acid catalyst: Amberlyst-36 (wet) was obtained from Rohm and Hass Co. (USA) and its key characteristics are listed in Table 7.1. Hereafter the catalyst will be simply referred to as Amberlyst.

Table 7.1 Catalyst characterization

Catalyst	BET surface ¹ (m ² /g)	Pore volume ^a (cc/g)	Pore size ^a (nm)	Relative conc. of acidic sites ^b (eq/kg)
Amberlyst (Fresh)	35 (32)	0.28 (0.32)	16.8 (18.2)	5.5 (4.6)
Regenerated catalyst ^c	33(37)	0.29 (0.33)	17.3 (18.5)	5.4(4.4)

^a Determined by N₂ isothermal adsorption; ^bDetermined by NH₃-TPD; ^c Regenerated by 0.5 M dilute H₂SO₄ acid washing; Values in parenthesis are measured from the catalyst after 24 h on-stream of reaction.

7.2.2 Experimental procedure

The experiments were carried out in a continuous-flow reactor system whose details were given in our recently published work.¹⁶ The ketalization reaction was carried out in a 316-stainless steel tubular reactor (ID: 7.7 mm, OD=9.5mm and length: 60 cm) placed in a tube furnace (model# 21135, Thermolyne). The reactor was loaded with a given amount of catalyst (typically 2 g) with pyrex wool as bed supporter. The feed was a mixture of acetone (A), glycerol (G) and ethanol (E) solvent at a specific molar ratio of A:G:E = X:1:1 where X is the acetone-to-glycerol equivalent ratio (varying from 2 to 6 mol/mol in this study). In a typical run, the feed containing a calculated amount of acetone and glycerol with ethanol as solvent were well mixed and pumped into the reactor with a HPLC pump (Lab Alliance series II) at a predetermined flow rate, depending on the target weight hourly space velocity (WHSV). The WHSV is defined as:

$$WHSV (h^{-1}) = \frac{\text{Flow of glycerol per hour}(g/h)}{\text{Weight of catalyst}(g)} \quad (1)$$

The pressure of the reactor was controlled by a back pressure regulator and was kept constant throughout the experiment (500 psi). The product stream from the reactor was

collected every 20 min and subjected to further analysis for determination of glycerol conversion and solketal yield.

7.2.3 Product analysis

The main components in the product mixture were first identified on a gas chromatograph, equipped with a mass selective detector [Varian 1200 Quadrupole GC/MS (EI), Varian CP-3800 GC equipped with VF-5 MS column (5% phenyl/95% dimethyl-polysiloxane, 30 m × 0.25 mm × 0.25 μm)], using helium as the carrier gas at a flow rate of 5×10^{-7} m³/s. The oven temperature was maintained at 120 °C for 2 min and then increased to 280 °C at a ramp rate of 40 °C/min. Injector and detector block temperature were maintained at 300 °C. The components were identified using the NIST 98 MS library with the 2002 update. The concentrations of the components in the product mixture (mainly glycerol and solketal) were then quantified using a GC-FID (Shimadzu -2010) operating at similar conditions as used in the above GC-MS measurement, after careful calibration with glycerol and solketal of varying concentrations and dimethyl sulfoxide (DMSO) as an internal standard at a fixed concentration. Appendix C provides a typical GC-MS spectrum and the calibration tables and curves for GC-FID.

The solketal yield and glycerol conversion were calculated using the following equations:

$$Yield (mol\%) = \frac{Mole\ of\ solketal\ formed}{Initial\ moles\ of\ glycerol\ fed\ into\ the\ reactor} \times 100\% \quad (2)$$

$$Conversion(\%) = \frac{Reduction\ in\ moles\ of\ glycerol\ in\ the\ reaction}{Initial\ moles\ of\ glycerol\ fed\ into\ the\ reactor} \times 100\% \quad (3)$$

7.2.4 Experimental design

Box-Behnken design (BBD) was applied in the optimization of the process. BBD is a class of rotatable second order design based on three level incomplete factorial designs.¹⁷ The

required number of experimental runs (N) for the development of BBD can be calculated from the following correlation:¹⁸

$$N = 2x(x - 1) + C_0 \quad (4)$$

where x is the number of factors and C_0 is the number of central points in the design. In this study, temperature (25- 65 °C), acetone equivalent ratio (2-6) and WHSV (2-4 h⁻¹) were three factors chosen for optimization and the yield of solketal is the only response in the ketalization study. Thus, from Eq. 4, a set of 17 runs (including 5 central points) were carried out. The different coded levels, -1 (low), 0 (central) and +1 (high) of the factors are given in Table 7.2. For statistical calculations, the relation between the coded values and real values were described as follows:¹⁹

$$X_i = \frac{x_i - \frac{(x_h + x_l)}{2}}{\frac{x_h - x_l}{2}} \quad (5)$$

where X_i is the dimensionless coded value (-1,0,+1) of the i^{th} independent variable, x_i is the un-coded (real) value of variable, x_h and x_l are the real value of x_i at its high and low level, respectively. The independent variables studied are temperature, acetone equivalent ratio and WHSV for X_1 , X_2 , and X_3 respectively. The relationship and interrelationships of the variables were determined by fitting the second order polynomial equation to data obtained and is given as

$$Y = b_0 + b_1X_1 + b_2X_2 + b_3X_3 + b_{11}X_1^2 + b_{22}X_2^2 + b_{33}X_3^2 + b_{12}X_1X_2 + b_{13}X_1X_3 + b_{23}X_2X_3 + e \quad (6)$$

where Y is the predicted value, b_0 is the constant term, b_1 , b_2 and b_3 are linear coefficients, b_{11} , b_{22} and b_{33} are the quadratic coefficients, b_{12} , b_{13} and b_{23} are the cross product coefficients and e is the experimental error term. The BBD matrix is given in Table 7.3. Minitab software package was used for determining the regression coefficients of the

model. Analysis of the variance (ANOVA) with Fisher's F -test was used to determine the statistical significance of the model coefficients. The fitted polynomial was expressed in three dimensional surface plot and contour plots to explain the relationship between the response and the levels of each parameter used in this study.

Table 7.2 Actual and corresponding coded values of each parameter

Variables	Symbol	Levels		
		-1	0	1
Temperature ($^{\circ}\text{C}$)	x_1	25	45	65
Acetone equivalent ratio	x_2	2	4	6
WHSV (h^{-1})	x_3	2	3	4

7.3 Result and discussion

7.3.1 Model fitting and statistical analysis

The measured response data for different coded combinations are given below in Table 7.3.

Table 7.3 Experimental design matrix and measured response values

Run order	X ₁	X ₂	X ₃	Response (yield %)
1	-1	0	1	78
2	0	0	0	83
3	-1	-1	0	75
4	0	0	0	85
5	-1	1	0	95
6	-1	0	-1	94
7	1	-1	0	65
8	0	0	0	82
9	0	1	-1	89
10	1	0	-1	83
11	0	-1	-1	74
12	1	0	1	67
13	0	0	0	83
14	1	1	0	82
15	0	1	1	80
16	0	0	0	84
17	0	-1	1	62

The obtained results are the average values of three separate measurements which are rounded up to the nearest whole number with a relative standard deviation of 3.6% at 95% confidence level. A modified second order polynomial model, by eliminating the

insignificant model terms, was used to fit the experimental data to obtain a regression equation using the coded factors as shown below:

$$Y = 83.42 - 5.63 X_1 + 8.75 X_2 - 6.63 X_3 - 4.20 X_2^2 - 2.95 X_3^2 \quad (7)$$

The adequacy of the proposed model was verified by using the ANOVA technique. The ANOVA results are presented in Table 7.4. The p -value was used to check the significance of each coefficient. The smaller is the p -value, the higher the significance of the corresponding coefficient.^{20,21} In this work, the p -value for all coefficients employed in the regression model is $\ll 0.05$, which suggested that the corresponding coefficient is significant and the model is suitable to be used in this experiment.

Table 7.4 ANOVA analysis for the reduced quadratic model of yield

Source	Sum of squares	Degree of freedom	Mean squares	F value	p -value
Model	1333.98	5	266.796	108.854	0.000000
X_1	253.13	1	253.125	103.276	0.000001
X_2	612.50	1	612.500	249.902	0.000000
X_3	351.12	1	351.125	143.260	0.000000
X_2^2	74.39	1	74.387	30.350	0.000184
X_3^2	36.68	1	36.678	14.965	0.002615
Residual	26.96	11	2.451		
Lack of fit	21.76	7	3.109	2.391	0.208731
Pure error	5.20	4	1.300		
Total	1360.94	16			

The lack-of fit measured the failure of the model to represent the data points which are not included in the regression. The F -value of 2.391 and p -value of 0.208731 represent that the lack-of-fit, is insignificant relative to the pure error.²²

Adequate precision compares the predicted values at the design points to the average prediction error. In this study, the adequate precision was calculated and found to be greater than 4. This high adequate precision value indicates that the model is competent to navigate through the design space and is able to predict the response accurately.

The regression coefficients and the corresponding p -values for all the model terms are given in Table 7.4. From p -values of each model term, it may be concluded that all the independent variables (X_1 , X_2 , and X_3) and the quadratic terms (X_2^2 and X_3^2) significantly affect the yield of solketal.

The coefficient of determination, R^2 , indicates the overall predictability of the model. It often shows how the model approximates the experimental data and can be defined as:²³

$$R^2 = \frac{SS_{Model}}{SS_{Total}} = 1 - \frac{SS_{Error}}{SS_{Total}} \quad (8)$$

Where SS_{Model} , SS_{Error} , and SS_{Total} are sum square model, sum square error, and sum square total, respectively. The R^2 value for the model was found to be 0.9802. It may be assumed that 98.02% of the total variations in the response could be explained by the model.^{24,25} However, this large value of R^2 does not necessarily indicate that the model is a suitable one. The adjusted R^2 is defined to correct the R^2 value. In this experiment, the obtained adjusted R^2 value was found to be 0.9712. The very close value of adjusted R^2 to R^2 suggests a high significance of the model. The variation of the model can also be explained by calculating the coefficient of variation (CV). In this model, the calculated low value of coefficient of variation was 1.43%, suggesting a very high degree of accuracy and confidence of tests.¹⁵

The relationship between the experimental and model predicted values of solketal yield is given in Figure 7.1. The points around the diagonal line imply that the deviation between the experimental and the predicted values is less. Hence, it can be concluded that the values

calculated from the model equation are very close to those obtained from the experiments, again suggesting the high accuracy of the proposed model. Moreover, the deviations can be explained by calculating the average absolute deviation (AAD) given by the following equation:¹⁸

$$\text{Average Absolute Deviation (AAD)} = \left[\frac{\sum_{i=1}^n \left(\frac{|y_{i \text{ exp}} - y_{i \text{ pre}}|}{y_{i \text{ exp}}} \right)}{n} \times 100 \right] \quad (9)$$

where $y_{i,pre}$ and $y_{i,exp}$ are the predicted and the experimental results, respectively with n as the experimental runs. The value of AAD was found to be 1.16%. The values of both R^2 and AAD confirmed that the given model defines the true behavior of the system.

The distribution of the data was determined by the probability plot displayed in Figure 7.2, which indicates a well normal distribution and the independence of the residuals.²⁰

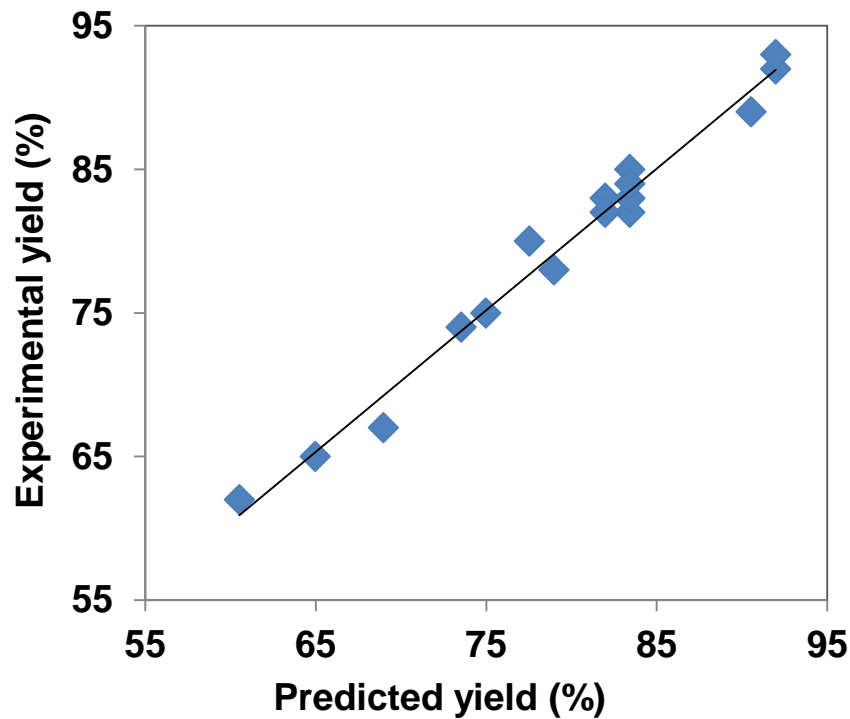


Figure 7.1 The experimental results versus the model predicted results

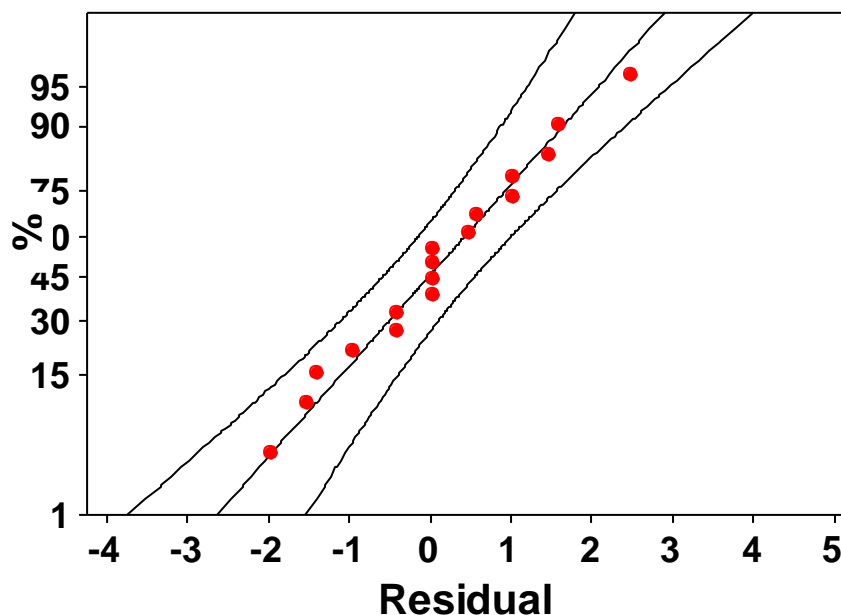


Figure 7.2 The normal probability plot of the residuals

7.3.2 Response surface analysis

The single effect of each parameter on the yield of solketal is shown in Figure 7.3, which is generally termed as the matrix plot. It was plotted by considering the mean value of the yield at each coded point. From the plot, it is clear that the solketal yield was increased by the decrease in temperature (X_1) and weight hour space velocity (X_3) and increased by the acetone equivalent ratio (X_2). This was expected as the reaction is exothermic, and a higher WHSV means a shorter contact time of glycerol with the catalyst, which reduced the glycerol conversion. The increase in the solketal yield with acetone equivalent is attributed to the presence of large amount of acetone. This excess reactant shifts the reaction equilibrium towards the products. Furthermore, the excess acetone acts as an entrainer and removes water from the reaction media which helps to drive the equilibrium towards the production of solketal.⁵ These results are supported by the data presented in previous Table 7.4, which indicates that the acetone equivalent ratio and the WHSV are the most effective

individual factors on the yield of solketal (acetone equivalent ratio: F -value - 249.902 and p -value - 0.000000, WHSV: F -value - 143.260 and p -value - 0.000000).

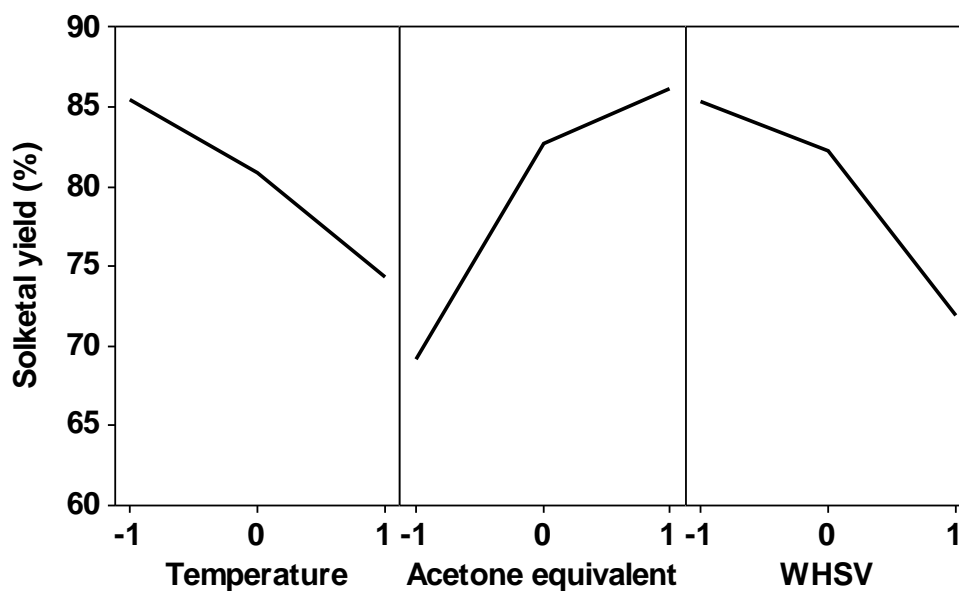


Figure 7.3 Matrix plot of X_1 (temperature), X_2 (acetone equivalent ratio) and X_3 (WHSV)

The response surface and contour plots of the model are given in Figure 7.4 (a-c) and Figure 7.5 (a-c). Three dimensional response surface plots and two-dimensional contour plots are very useful to analyze the interaction effects of different factors on the response. The response surface plot mainly explains the sensitiveness of the response towards the change of variables, whereas the contour plot describes the significant coefficient between the variables.^{26,27} These plots explain the effect of two factors on the response at a time, keeping the third factor constant at level zero.

The dependence of the solketal yield on the mutual interaction between temperature and acetone equivalent ratio can be best interpreted from the response surface and the contour plot given in Figure 7.4 a and Figure 7.5 a, which indicated that the solketal yield is inversely related to the temperature and directly related to the acetone equivalent ratio. As explained earlier, a high acetone equivalent ratio drives the reaction towards the product side to result in a higher yield. In the contour plot, no interaction effect between the

temperature and acetone equivalent was observed. The maximum yield was obtained at a temperature around -1 (coded value) and the acetone equivalent ratio of around 1 (coded value).

Figure 7.4 b and Figure 7.5 b represented the effects of temperature and WHSV on the yield of solketal. It can be seen that both temperature and WHSV have similar effects on the yield, i.e., inversely proportional to the yield. The reaction temperature has a little effect on the yield of solketal when the WHSV is kept in between 0 and 1 (coded values). However a remarkable enhancement in the solketal yield (from 85 – 95%) was observed at a lower temp (coded value: 0 to -1) and at a lower WHSV (coded value 0 to -1). This indicates that a lower temperature and lower WHSV are the favorable conditions to achieve a higher yield (close to 100%) of solketal.

The effects of acetone equivalent ratio and WHSV on the solketal yield could be seen in Figure 7.4 c and Figure 7.5 c. A maximum yield (~ 95%) was observed at a lower WHSV (coded value -1) and a higher acetone equivalent ratio (coded value between 0-1).

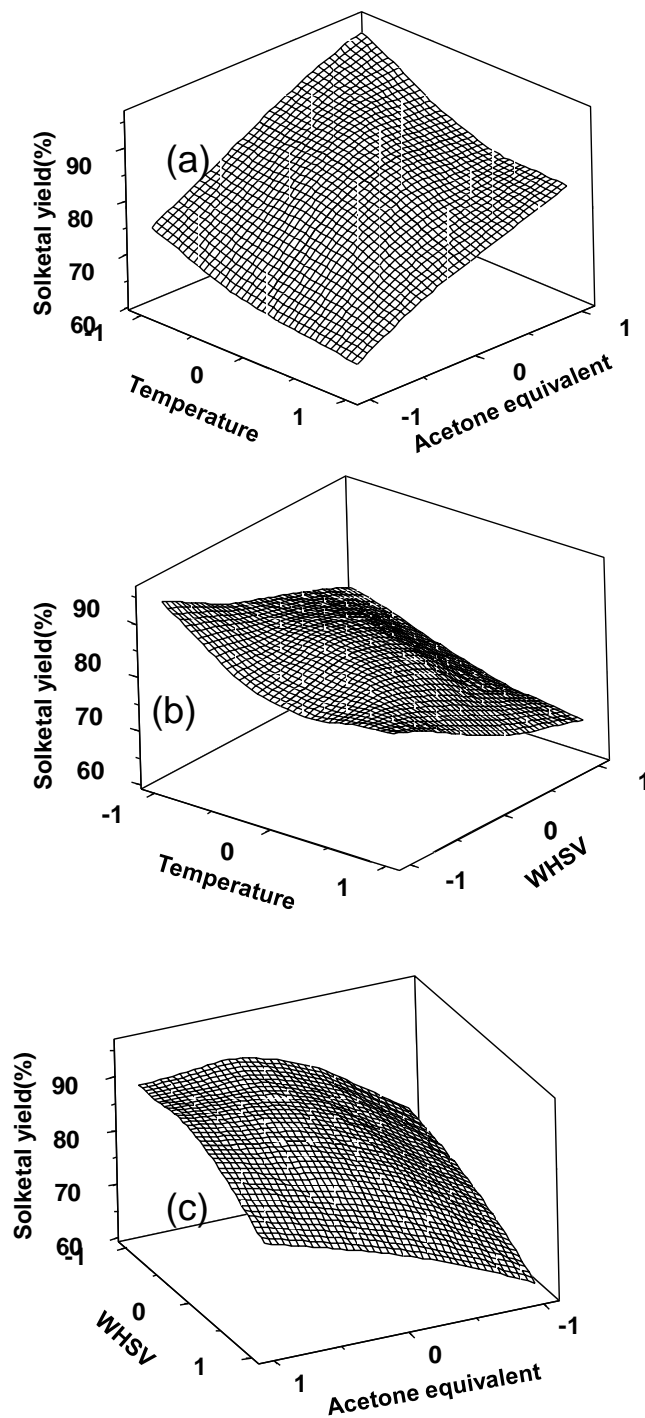


Figure 7.4 Surface plots for effects of temperature and acetone equivalent ratio on solketal yield (a), effect of temperature and WHSV on solketal yield (b) and effect of acetone equivalent ratio and WHSV on solketal yield (c).

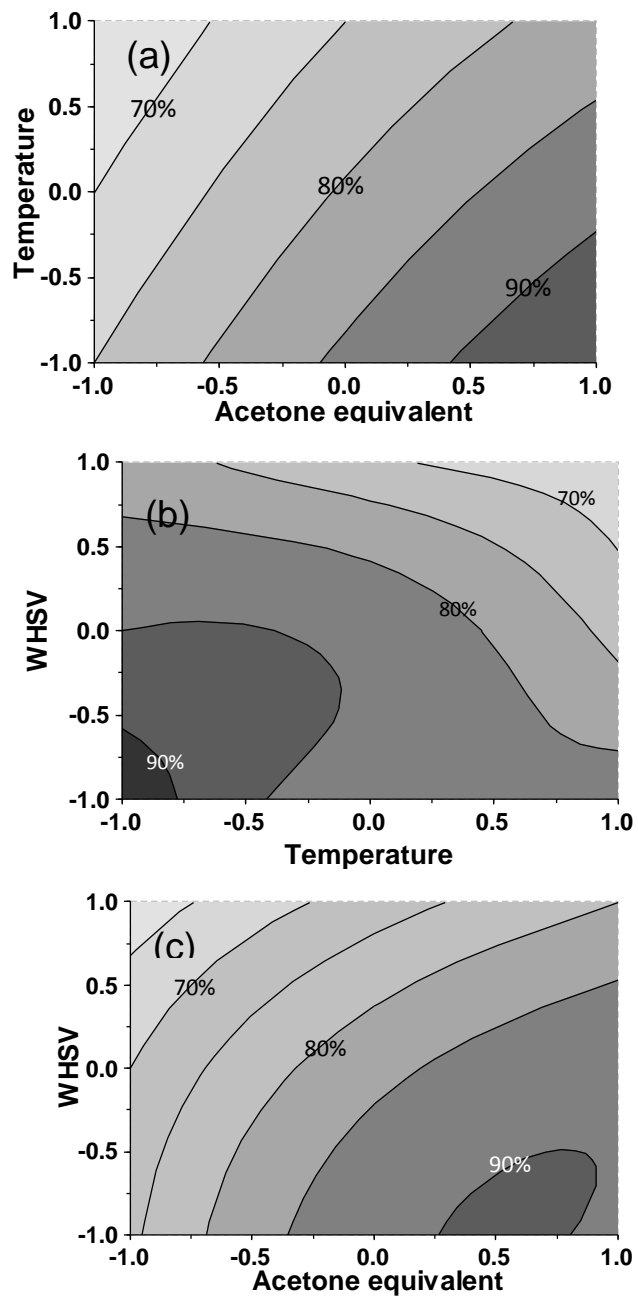


Figure 7.5 Contour plots for effects of temperature and acetone equivalent ratio on solketal yield (a), effect of temperature and WHSV on solketal yield (b) and effect of acetone equivalent ratio and WHSV on solketal yield (c).

7.3.3 Optimization of reaction parameters

In this study, the main objective was to find the conditions where maximum solketal yield can be obtained. The optimal values of the selected parameters obtained from the regression model and by analyzing the response surface and contour plots are given as: temperature of 25 °C, acetone equivalent ratio of 4, and WHSV of 2 h⁻¹. Both the predicted and observed yields at the optimum conditions are verified as shown in Table 7.5. Although from the regression model and by analyzing the response surface and contour plots, a temperature lower than 25 °C, a WHSV lower than 2 h⁻¹ and an acetone equivalent ratio larger than 4 would lead to even better solketal yield. However, from practical point of view, a too low temperature reduces the reaction rate, and a too small WHSV and a higher acetone equivalent ratio 4 would cause the process less economically viable (e.g., it would decrease the productivity and increase the load of distillation for solvent recovery). Moreover, the product yield at the optimum conditions was already as high as 93-94%.

Table 7.5 Predicted and experimental values of the response at the optimal conditions

Optimum conditions			Yield (%)	
Temperature (°C)	Acetone equivalent	Weight hour space velocity (h ⁻¹)	Experimental	Predicted
25	4	2	94.0	92.7

7.3.4 Effect of impurities on the solketal yield

Assuming the presence of salt and water as impurities in the glycerol obtained from biodiesel industry, an attempt was made to check their effects on the solketal yield at the optimum conditions. Figure 7.6 shows the effects of impurities on the product yield. It can be seen that the presence of water and/ or salt (sodium chloride) has adverse effects on the solketal yield. These effects can be explainable as the presence of water in the medium imposes a thermodynamic barrier, which limits the reaction in forward direction, and the presence of cations (Na⁺) could deactivate the catalyst by cationic exchange of the protons

of the acid resin catalyst, causing a decrease in the acidity (relative number of acidic sites per unit mass) of the catalyst. Similar observations have been reported for batch reactors.^{5,28}

From the results presented in Figure 7.6, insignificant reduction in the yield was observed when replacing the ethanol solvent by methanol in the reaction, which would make the system more economical.

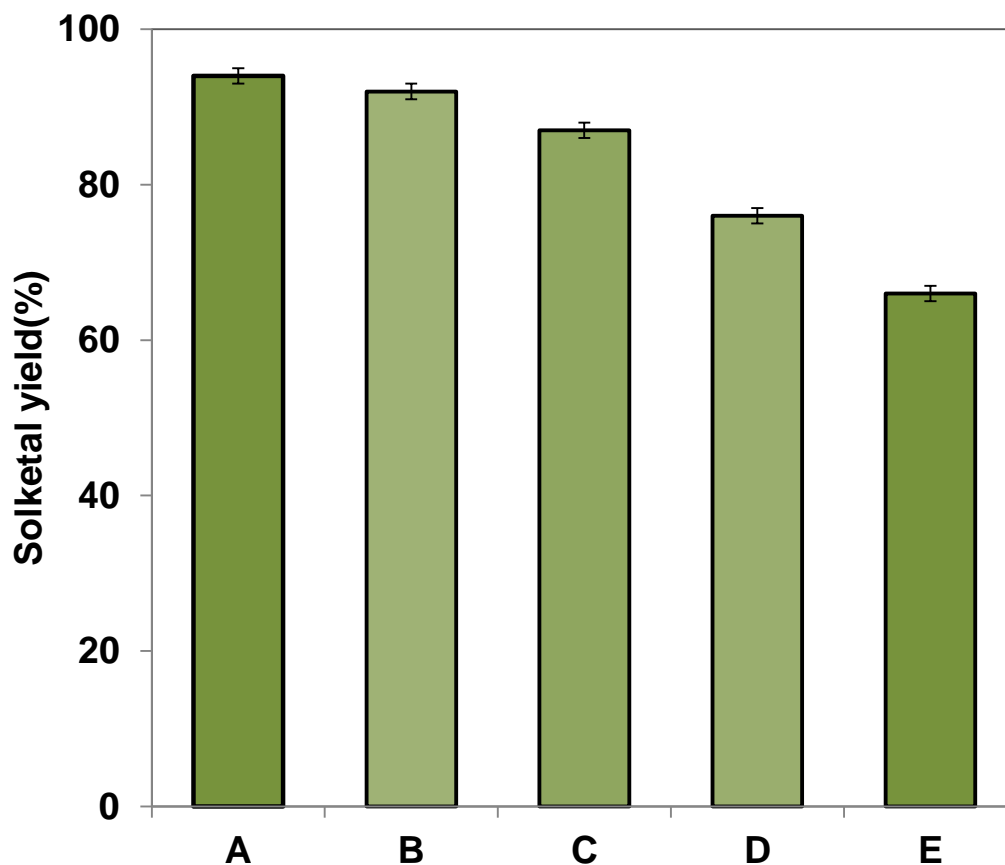


Figure 7.6 Effects of impurities on the yield of solketal. (A: Ethanol as solvent; B: Methanol as solvent; C: 1 wt% NaCl in ethanol as impurity; D: 2 wt% water in ethanol as impurity; E: 1 wt% NaCl+ 2 wt% water in methanol as solvent)

7.3.5 Catalyst life-time tests

The stability of the catalyst was investigated by studying the life time of the catalyst for a longer time on stream in continuous operation. The solketal yield and glycerol conversion vs. time on stream up to 24 h from the operation under the optimum conditions (i.e., 25 °C, acetone equivalent ratio of 4, and WHSV of 2 h⁻¹) with fresh and regenerated Amberlyst-36 catalyst is shown in Figure 7.7. From the figure, a decrease in the solketal yield from 94 to 89% was observed with the fresh catalyst after 24 h on stream. To recover the activity of the catalyst, it was regenerated by passing 0.5 M H₂SO₄ through the catalytic column followed by washing with methanol –water solution and drying it at 85 °C for 4 h.²⁹ The regenerated catalyst demonstrated almost equal initial activity as the fresh catalyst. However, the regenerated catalyst has a comparatively rapid deactivation process over the fresh catalyst: the solketal yield dropped from 95% to 85% after 24 h on stream. The catalyst deactivation was likely due to the reduction in the number of catalyst's acidic sites (as evidenced by the results shown previously in Table 7.1), which might be caused by the presence of some impurities (such as water and salts) in the glycerol feed.^{5,28}

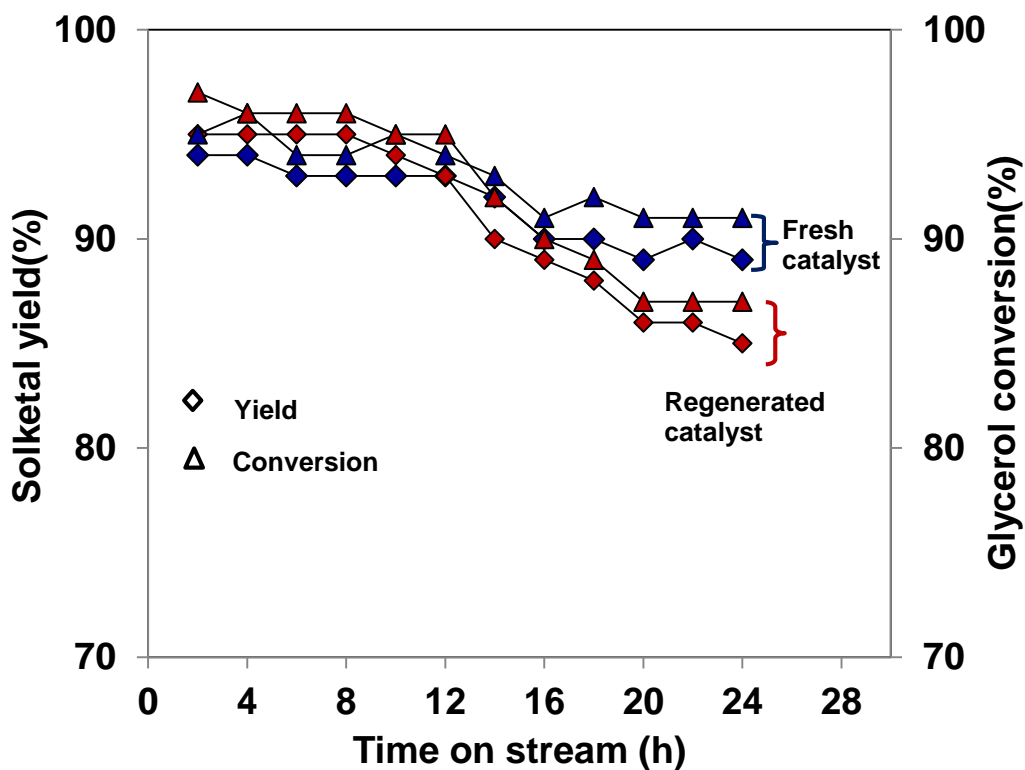


Figure 7.7 Solketal yield and glycerol conversion vs. time on stream up to 24 h from the operation under the optimum conditions with fresh and regenerated Amberlyst-36 catalyst

7.3.6 Economic (marginal benefit) analysis

Economic analysis is considered to be one of the key factors for the industrial production of solketal. Table 7.6 shows the market price for different chemicals required for the production of 1 kg of solketal. The operational cost was not considered during the cost estimation, but it is expected to be low as the mild operating conditions of our continuous flow reaction process (25 °C). Methanol and amberlyst catalyst can be recycled and reused after regeneration; hence a loss of 5 wt% and 10 wt%, respectively, is considered per operation cycle. From the Table, it is clear that the production cost of solketal is approx. \$1.05/kg. The cost of solketal could be an oxygenated fuel additive or diesel combustion promoter, potential alternative to methyl tert- butyl ether (MTBE) currently used on the fuel additive market at a market price of ~\$1.15/kg. The marginal benefit is about \$0.1/kg

or \$100/ton of the solketal product. The renewable source and lower environmental impact of solketal over MTBE are added advantages for solketal to replace the later as a fuel additive. Moreover, the flow reactor can be scaled up to a large scale commercial production easily, making the production of solketal more economical.

Table 7.6 Economical analysis (marginal benefit) for production of 1 kg solketal

Chemicals	Assay (%)	UnitPrice (\$/kg) ^a	Amount required (kg)	Cost (\$)	Marginal benefit(\$/kg)
Acetone	98	1	0.439	0.439	
Glycerol	98	0.50	0.697	0.348	
Amberlyst	99	118	0.020	0.236	
Methanol	98	0.5	0.050	0.025	
Sulfuric acid	98	0.4	0.050	0.0002	
Total	---	---	---	1.05	0.10

^a www.alibaba.com

7.4 Conclusions

The process for the continuous catalytic conversion of glycerol to oxygenated fuel additive, solketal was optimized. The solid acid catalyst amberlyst-36 wet demonstrated an excellent catalytic performance (active, stable, and regenerable) in the flow process. A maximum solketal yield of 94±2% was observed at the optimum condition (temperature: 25 °C, acetone equivalent: 4, WHSV: 2 h⁻¹). The presence of impurities like salt and water in glycerol (such as crude glycerol) reduced the yield significantly. The economic analysis demonstrated the possibility of solketal to substitute for MTBE as an oxygenated fuel additive or diesel combustion promoter.

References

1. Johnson DT, Taconi KA. The glycerin glut : options for the value-added conversion of crude glycerol resulting from biodiesel production. *Environmental Progress* 2009;26(4). doi:10.1002/ep.
2. Sun F, Chen H. Organosolv pretreatment by crude glycerol from oleochemicals industry for enzymatic hydrolysis of wheat straw. *Bioresource Technology* 2008;99(13):5474-9. doi:10.1016/j.biortech.2007.11.001.
3. Liu X, Jensen PR, Workman M. Bioconversion of crude glycerol feedstocks into ethanol by *Pachysolen tannophilus*. *Bioresource Technology* 2012;104:579-86. doi:10.1016/j.biortech.2011.10.065.
4. Clarkson JS, Walker AJ, Wood MA. Continuous Reactor Technology for Ketal Formation: An Improved Synthesis of Solketal. *Organic Process Research & Development* 2001;5(6):630-635. doi:10.1021/op000135p.
5. Vicente G, Melero J a., Morales G, Paniagua M, Martín E. Acetalisation of bio-glycerol with acetone to produce solketal over sulfonic mesostructured silicas. *Green Chemistry* 2010;12(5):899. doi:10.1039/b923681c.
6. Li L, Korányi TI, Sels BF, Pescarmona PP. Highly-efficient conversion of glycerol to solketal over heterogeneous Lewis acid catalysts. *Green Chemistry* 2012;14(6):1611. doi:10.1039/c2gc16619d.
7. Zhou CH, Zhao H, Tong DS, Wu LM, Yu WH. Recent Advances in Catalytic Conversion of Glycerol. *Catalysis Reviews* 2013;55(4):369-453. doi:10.1080/01614940.2013.816610.
8. Mota CJ a., da Silva CX a., Rosenbach, N, Costa J, da Silva F. Glycerin Derivatives as Fuel Additives: The Addition of Glycerol/Acetone Ketal (Solketal) in Gasolines. *Energy & Fuels* 2010;24(4):2733-2736. doi:10.1021/ef9015735.
9. Crotti C, Farnetti E, Guidolin N. Alternative intermediates for glycerol valorization: iridium-catalyzed formation of acetals and ketals. *Green Chemistry* 2010;12(12):2225. doi:10.1039/c0gc00096e.
10. Garcı E, Laca M, Pe E, Garrido A. New class of acetal derived from glycerin as a biodiesel fuel component. *Energy & Fuels* 2008;(15):4274-4280.
11. Roldan L, Mallada R, Fraile JM, Mayoral JA, Menendez M. Glycerol upgrading by ketalization in a zeolite membrane. *Asia-Pacific Journal of Chemical Engineering* 2009; 4:279-284.
12. Maksimov a. L, Nekhaev a. I, Ramazanov DN, Arinicheva Y a., Dzyubenko a. a., Khadzhiev SN. Preparation of high-octane oxygenate fuel components from plant-

- derived polyols. *Petroleum Chemistry* 2011;51(1):61-69. doi:10.1134/S0965544111010117.
13. Ferreira P, Fonseca IM, Ramos a. M, Vital J, Castanheiro JE. Valorisation of glycerol by condensation with acetone over silica-included heteropolyacids. *Applied Catalysis B: Environmental* 2010;98(1-2):94-99. doi:10.1016/j.apcatb.2010.05.018.
 14. Yetilmezsoy K, Demirel S, Vanderbei RJ. Response surface modeling of Pb(II) removal from aqueous solution by Pistacia vera L.: Box-Behnken experimental design. *Journal of hazardous materials* 2009;171(1-3):551-62. doi:10.1016/j.jhazmat.2009.06.035.
 15. Nanda MR, Yuan Z, Qin W, Ghaziaskar HS, Poirier M-A, Xu CC. Thermodynamic and kinetic studies of a catalytic process to convert glycerol into solketal as an oxygenated fuel additive. *Fuel* 2014;117:470-477. doi:10.1016/j.fuel.2013.09.066.
 16. Nanda MR, Yuan Z, Qin W, Ghaziaskar HS, Poirier M-A, Xu C (Charles). A new continuous-flow process for catalytic conversion of glycerol to oxygenated fuel additive: Catalyst screening. *Applied Energy* 2014;123:75-81. doi:10.1016/j.apenergy.2014.02.055.
 17. Xie X, Huang F, Wei X, Hu W, Ren Q, Yuan X. Modeling and optimization of pulsed green laser dicing of sapphire using response surface methodology. *Optics & Laser Technology* 2013;45:125-131. doi:10.1016/j.optlastec.2012.07.015.
 18. Moradi M, Daryan JT, Mohamadalizadeh A. Response surface modeling of H₂S conversion by catalytic oxidation reaction over catalysts based on SiC nanoparticles using Box–Behnken experimental design. *Fuel Processing Technology* 2013;109:163-171. doi:10.1016/j.fuproc.2012.10.013.
 19. Liu C, Sun Z-T, Du J-H, Wang J. Response surface optimization of fermentation conditions for producing xylanase by *Aspergillus niger* SL-05. *Journal of Industrial Microbiology & Biotechnology* 2008;35(7):703-11. doi:10.1007/s10295-008-0330-0.
 20. Statistics for Experimenters: Design, Innovation, and Discovery, 2nd Edition . Available at: <http://ca.wiley.com/WileyCDA/WileyTitle/productCd-0471718130.html>. Accessed December 9, 2014.
 21. Sheng Z, Li J, Li Y. Optimization of ultrasonic-assisted extraction of phillyrin from *Forsythia suspensa* using response surface methodology. *Journal of Medicinal Plants Research* 2012;6(9):1633-1644. doi:10.5897/JMPR11.1374.
 22. Pinzi S, Lopez-Gimenez FJ, Ruiz JJ, Dorado MP. Response surface modeling to predict biodiesel yield in a multi-feedstock biodiesel production plant. *Bioresource Technology* 2010;101(24):9587-93. doi:10.1016/j.biortech.2010.07.076.

23. Design and Analysis of Experiments, 6th Edition, Wiely. Available at: <http://bcs.wiley.com/he-bcs/Books?action=index&itemId=047148735X&itemTypeId=BKS&bcsId=2172>. Accessed December 9, 2014.
24. Yilmaz Y, Toledo RT. Oxygen radical absorbance capacities of grape/wine industry byproducts and effect of solvent type on extraction of grape seed polyphenols. *Journal of Food Composition and Analysis* 2006;19(1):41-48. doi:10.1016/j.jfca.2004.10.009.
25. Sinha K, Saha P Das, Datta S. Response surface optimization and artificial neural network modeling of microwave assisted natural dye extraction from pomegranate rind. *Industrial Crops and Products* 2012;37(1):408-414. doi:10.1016/j.indcrop.2011.12.032.
26. Yin G, Dang Y. Optimization of extraction technology of the *Lycium barbarum* polysaccharides by Box–Behnken statistical design. *Carbohydrate Polymers* 2008;74(3):603-610. doi:10.1016/j.carbpol.2008.04.025.
27. Sun Y-X, Liu J-C, Kennedy JF. Extraction optimization of antioxidant polysaccharides from the fruiting bodies of *Chroogomphis rutilus* (Schaeff.: Fr.) O.K. Miller by Box-Behnken statistical design. *Carbohydrate Polymers* 2010;82(1):209-214. doi:10.1016/j.carbpol.2010.04.076.
28. Da Silva CX a., Mota CJ a. The influence of impurities on the acid-catalyzed reaction of glycerol with acetone. *Biomass and Bioenergy* 2011;35(8):3547-3551. doi:10.1016/j.biombioe.2011.05.004.
29. Izci A, Hoşgün HL. Kinetics of synthesis of isobutyl propionate over amberlyst-15. In: *Turkish Journal of Chemistry*. Vol 31.; 2007:493-499.

Chapter 8

8 Purification of crude glycerol using acidification: effects of acid types and product characterization

Abstract:

Purification of crude glycerol is essential for its applications for high-value products. In this study, crude glycerol was purified by acidification using sulfuric, hydrochloric or phosphoric acid, and the results were compared. Phosphoric acid was found to be the best purifying agent among others. Acidification of a biodiesel plant waste crude glycerol (containing approximately 13 wt% glycerol and 6 wt% ash) for a total processing time of 1 h, produced a purified product containing approximately 96 wt% glycerol, and 0.7 wt% ash. Effects of pH values on the purification efficiency were investigated. The crude glycerol and the purified products were extensively characterized.

Keywords: Crude glycerol; Purification; Sulfuric acid; Hydrochloric acid; Phosphoric acid.

8.1 Introduction

With the increased concern over the depletion of fossil fuels worldwide, the search for alternative energy/chemical sources has been becoming urgent more than ever before. Biodiesel produced from renewable animal or plant oil has been one of two most commonly explored bio-fuels (the other is bio-ethanol) that could effectively reduce the global dependence on the fossil fuels and the greenhouse gas emission.

Biodiesel is mainly produced by the transesterification of animal fats or vegetable oils (triglyceride) with methanol in presence of an alkali or acid catalyst.^{1,2} During the transesterification process in a biodiesel plant, crude glycerol is the primary byproduct, accounting for about 10 wt% of the biodiesel product.^{3,4}

With the rapid growth of biodiesel industry all over the world, a large surplus of glycerol has been created,⁵ leading to the closure of several traditional glycerol production plant.⁶ This large amount of glycerol, once enters into the market would significantly affect the glycerol price. The current market value is US\$ 0.27- 0.41 per pound for pure glycerol,⁷ and US\$ 0.04 – 0.09 per pound for crude glycerol (80% purity).⁸ The world scenario of glycerol production is given in Figure 8.1. It was predicted that by 2020 the global production of glycerol will reach 41.9 billion liters.⁹ Thus, crude glycerol disposal and utilization has become a serious issue and a financial and environmental liability for the biodiesel industry. Economic utilizations of glycerol for value-added products are critically important for the sustainability of the biodiesel industry.

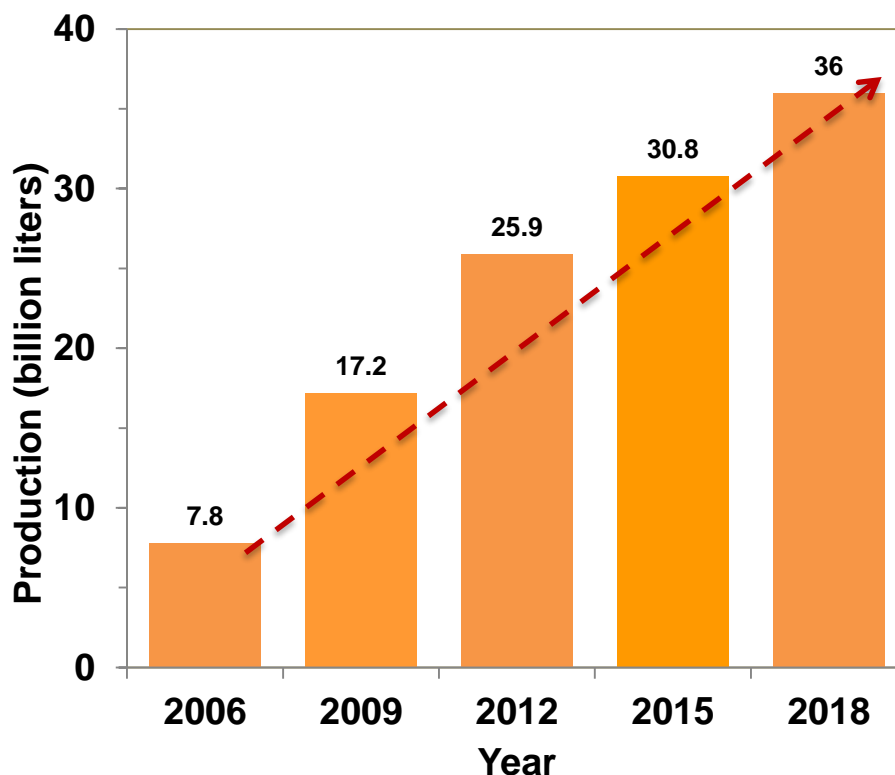


Figure 8.1 World's scenario of crude glycerol

Research has been conducted for the conversion of glycerol to different value added chemicals such as; propane-1, 3-diol,¹⁰ propane-1,2-diol,¹¹ acrolein,¹² hydrogen,^{13,14} acetal or ketal,^{15,16} biooil,^{17,18} polyhydroxyalkanoates,¹⁹ polyols and polyurethane foams,²⁰ glycerol carbonate,^{21,22} etc.

Crude glycerol however has purity of 15-80% and it contains a large amount of contaminants such as water, methanol, soap/free fatty acids (FFAs), salts, and unused reactants. The common practice of using alkaline catalysts during the transesterification process results a high pH (above 10) of this byproduct. The presence of contaminants in this renewable carbon source creates certain challenges for the conversion processes as it e.g., could plug the reactor, deactivate the catalysts, and inhibit bacterial activities (for bioconversion). Another major challenge for the utilization of crude glycerol is the

inconsistency in its composition since it varies with the feedstock and production procedures. As such, it is of great significance and interest to purify crude glycerol for the aforementioned value-added applications of glycerol. High purity glycerol is also an important feedstock for various industrial applications in food, cosmetic and pharmaceutical industries.

Different purification processes have been developed and reported in the literature, among which the most common processes are the use of ion exchange resin,²³ nano-cavitation technology,²⁴ membrane separation technology (MST), simple distillation under reduced pressure,²⁵ and acidification, followed by neutralization and solvent extraction,^{26,27} etc. Nevertheless, the purification processes using ion exchange resin and simple distillation are limited because of these processes generally produce a very low yield of pure glycerol (<15 wt%). The use of nano-cavitation technology for the purification of crude glycerol has been demonstrated, but its large-scale operation is very challenging.²⁴ MST could yield ultra-high purity glycerol provided that the crude glycerol undergoes prior purification that reduces salts and matter organic non glycerol (MONG, such as methyl ester).²⁸ Compared with other processes, the processes using acidification demonstrated to be more promising due to higher yields and their relatively lower costs.²⁶

Kongjao *et al.* (2010) reported the purification of crude glycerol (~30 wt% glycerol content) from a waste used-oil methyl ester plant using 1.19 M H₂SO₄ followed by neutralization and solvent extraction to get purified glycerol of ~93 wt% purity.²⁶ In a similar work, Ooi *et al.* (2001) demonstrated that crude glycerol was upgraded from purity of 34 wt% to 52 wt% by using sulfuric acid.²⁹ However, the main issue in these processes is the use of sulfuric acid, its corrosive nature and the non-biodegradability of the produced sulfate salts.³⁰

In this work, purification of crude glycerol obtained from a multi-feed biodiesel plant was carried out using different acids (sulfuric acid, hydrochloric acid, phosphoric acid) in order to investigate the effects of acid types and pH value on crude glycerol purification.

8.2 Materials and methods

8.2.1 Materials

Crude glycerol was obtained from a biodiesel plant of Methes Energies Canada Inc. (Mississauga, Ontario). All chemicals were purchased from Sigma Aldrich, including phenolphthalein, reagent grade HNO_3 , concentrated H_2SO_4 , concentrated HCl , concentrated H_3PO_4 , KOH , methyl orange, methanol and dimethyl sulfoxide.

8.2.2 Purification process

As the crude glycerol received is solid at room temperature, approximately 200 g of the crude glycerol was melted at 55 °C in a 500 mL beaker placed on a magnetic hot plate. The molten crude glycerol under gentle stirring was acidified with different acids (sulfuric acid, hydrochloric acid, and phosphoric acid) to the desired pH level and kept for a sufficiently long time to allow the formation of three separate layers. The top layer is fatty acid phase, the middle one is glycerol rich phase and the bottom one is inorganic salt phase. The bottom phase was separated by simple decantation. The fatty acid-rich top phase was separated from the glycerol-rich phase by using a separatory funnel. The extracted glycerol was neutralized using 12 M KOH solution followed by evaporation of water at 110 °C for 2 h and filtration to remove the precipitated salt.

The obtained glycerol was further purified by solvent extraction process using methanol as solvent to promote the precipitation of dissolved salts. The precipitated salts were separated by filtration and the filtrate was passed through a column of activated charcoal to de-color the glycerol product and remove odor and metal ions in the products.

8.2.3 Characterization of crude and purified glycerol

The crude and purified glycerol samples were characterized for the density, alkalinity, moisture content, glycerol content, ash content, metal content and the color intensity.

8.2.3.1 Density

The density was determined according to ASTM D 891-95 (2004). First, the weight of the dried pycnometer was recorded. Water was added into the pycnometer at room temperature

(22 ± 1 °C) and its mass and hence the volume of the pycnometer was recorded. Again, crude or purified glycerol was filled in the dried pycnometer at same temperature and the mass of the crude glycerol was reported. The density of the crude glycerol was obtained by taking the ratio between the mass of the sample and the volume of the pycnometer.

8.2.3.2 Alkalinity

The alkalinity of crude or purified glycerol was calculated according to IUPAC-ACD 1980(6th edition) method using the following formula

$$\text{Alkalinity} = \frac{100 \times V \times N}{W} \quad (1)$$

where V is the volume (mL) of the HCl solution consumed in the titration, N is the normality of HCl solution and W is the weight (g) of crude glycerol used for titration.

8.2.3.3 pH

Approximately 1.00 g of crude or purified glycerol was dissolved in 50.0 mL of deionized (DI) water. The pH of the solution was measured by a pH meter (SymphonyTM 89231-608, VWR) at room temperature (22 ± 1 °C) after calibration of the apparatus with buffer solutions of pH 7 and 10.

8.2.3.4 Water content

The water content of crude or purified glycerol was measured following the standard method ISO 2098-1972 by using the Karl-Fisher titrator V20.

8.2.3.5 Ash content

Ash content was analyzed according to standard method ISO 2098-1972 by burning 1 g of glycerol in muffle furnace at 750 °C for 3 h.

8.2.3.6 Glycerol content

Crude and purified glycerol samples were identified by gas chromatograph, equipped with a mass selective detector [Varian 1200 Quadrupole GC/MS (EI), Varian CP-3800 GC equipped with VF-5 MS column (5% phenyl/95% dimethyl-polysiloxane, 30 m × 0.25 mm

$\times 0.25 \mu\text{m})]$, using helium as the carrier gas at a flow rate of $5 \times 10^{-7} \text{ m}^3/\text{s}$. The oven temperature was maintained at $120 \text{ }^\circ\text{C}$ for 2 min and then increased to $280 \text{ }^\circ\text{C}$ at a ramp rate of $40 \text{ }^\circ\text{C}/\text{min}$. Injector and detector block temperature were maintained at $300 \text{ }^\circ\text{C}$. The component was identified using the NIST 98 MS library with the 2002 update. The concentration of the glycerol in the samples was analyzed quantitatively on a GC-FID (Shimadzu -2010) under the similar conditions as used for the GC-MS measurement.

8.2.3.7 Infrared spectroscopy

Fourier transform infrared spectra (FT-IR) were obtained using the KBr method on a Nicolet Magna-IR 560 spectrometer operating at 1 cm^{-1} resolution in the $400\text{-}4000 \text{ cm}^{-1}$ region.

8.2.3.8 Metal composition

Inductively coupled plasma- atomic emission spectrometry (ICP-AES) was conducted to quantify the metal content present in the samples, when standard calibration for each metal was made in the concentration range of 0 -400 ppm.

8.2.3.9 UV-Visible spectroscopy

For the crude and purified glycerol samples, their absorbance of light was examined by using Varian Cary 300 Bio UV Visible spectrophotometer (Lab Commerce, Inc. USA). The wavelength of incident light was chosen between 800-200 nm, out of which 800-400 nm accounts for visible light and 400-200 nm accounts for the UV region of light.

In addition, the heating value and viscosity of the glycerol samples were also measured to confirm the purity of the glycerol in the crude and purified glycerol samples.

8.2.3.10 NMR spectroscopy

^{13}C and ^1H NMR (nuclear magnetic resonance) spectra of resin dissolved in d_6 -DMSO were acquired at $25 \text{ }^\circ\text{C}$ on a Varian Inova 600 NMR spectrometer equipped with a Varian 5 mm triple-resonance indirect-detection HCX probe.

8.3 Results and discussion

8.3.1 Crude glycerol analysis

The crude glycerol obtained from the biodiesel plant was dark brown solid (Figure 8.2A) with a high pH (10.43) and low density (1.05 g/mL) as compared to the commercially available pure glycerol (Figure 8.2 B, pH: 6.97, density: 1.26 g/mL). The glycerol content was found to be very low in the range of 12-15 wt%, but it has high matter organic non glycerol (MONG ~ 70 wt%), high ash (~ 6 wt%) and water (~ 10 wt%) contents (Table 8.1). The high MONG content in crude glycerol is due to the presence of soap, methanol and methyl esters generated during the biodiesel production process, and the high ash content is mainly originated from the KOH catalyst during the transesterification process.

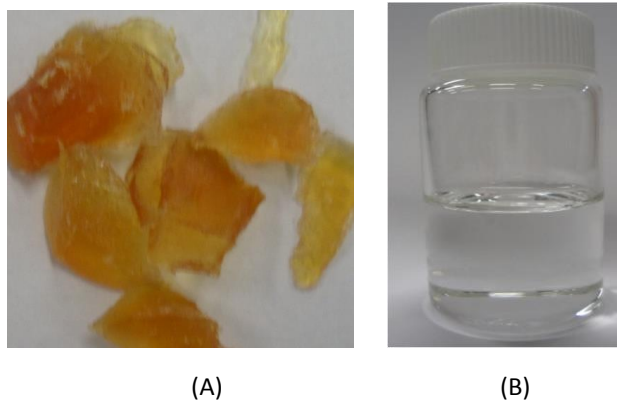


Figure 8.2 Pictures of crude glycerol (A) and pure glycerol (B)

Table 8.1 Composition and physical properties of various glycerol samples

Properties	Commercial glycerol ^a	Crude glycerol
Density (at 20 °C, g/mL)	1.27 ± 0.01	1.05 ± 0.26
pH	6.97 ± 0.03	10.30 ± 0.26
Water (wt%)	0.01 ± 0.00	9.20 ± 1.04
Ash (wt%)	0.0 ± 0.00	5.6 ± 0.51
Glycerol (wt%)	99.9 ± 0.00	12.0 ± 2.38
MONG (%)	0.0 ± 0.00	70.2 ± 4.37
Alkalinity	---	56.0 ± 1.02
K (ppm)	870 ± 40	45762 ± 3240
Na (ppm)	28 ± 10	140.5 ± 23.7
Viscosity (in cP at 50 °C, 250 rpm)	142 ± 1	---

^a Supplier's data

The main compounds detected by GC-MS analysis are listed in Table 8.2. In crude glycerol, propan-1-ol, hexanoic acid, glycerol, octanoic acid, dodecanoic acid, methyl tetradecanoate, 7-hexadecanoic acid, methyl ester, octadecanoic acids are the main components. In purified glycerol the main component was found to be dominantly glycerol (> 96%).

Table 8.2 Main compounds in crude glycerol detected by GC-MS analysis

Retention Time (min)	Compounds	Molecular weight (MW)
15.375	Glycerol (propane-1,2,3-triol)	92
29.333	propaneoctanoic acid, 2-hexyl-, methyl ester	282
29.592	methyl tetradecanoate	242
31.108	heptacosanoic acid, methyl ester	424
31.275	tetradecanoic acid, 12-methyl-, methyl ester	256
31.883	methyl stearate	298
33.158	eicosanoic acid, methyl ester	326
33.358	9-octadecenoic acid, methyl ester	296
33.425	9- hexadecenoic acid, methyl ester	268
33.9	hexadecanoic acid, methyl ester	270
35.208	heneicosanoic acid, methyl ester	340
35.208	triacontanoic acid, methyl ester	466
35.925	heptadecanoic acid, methyl ester	284
37.192	9,12- octadecadienoic acid, methyl ester	294

8.3.2 Effects of acid type and pH value

The performance of different mineral acids such as hydrochloric acid, sulfuric acid and phosphoric acid in the purification process was evaluated and compared. In this study, a given amount of crude glycerol was acidified individually as mentioned earlier using different acids to a fixed pH (pH=1) and the reactions are given in the following equations:

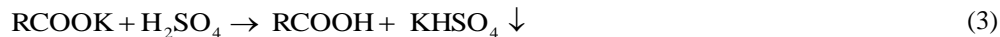
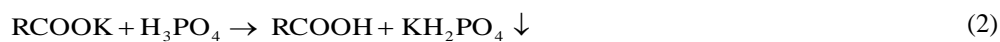




Table 8.3 compares the performance of different acids in purification of crude glycerol, with respect to the glycerol products purity, phase separation time, precipitation time and ash content of the purified glycerol products.

Table 8.3 Performance of different acids in purification of crude glycerol

Acids	Glycerol content (wt%)	Phase separation time (min)	Precipitation time (min)	Amount of Ash contents (%)
H ₃ PO ₄	96 ±1	30-45	10-15	1.4 ± 0.31
HCl	93 ±2	180-240	120-180	1.6 ± 0.53
H ₂ SO ₄	94 ±1	600-720	120-180	1.7 ± 0.25

From the above results, all acids resulted in a purified glycerol product are of very similar properties such as the glycerol content (96-93 wt%) and ash content (1.4-1.7 wt%). However, the time required for separation of the three distinct phases (glycerol, fatty acids and solid phases) was the shortest with phosphoric acid (30-45 min), medium (180-240 min) with HCl acid and the longest (600-720 min) with H₂SO₄ acid. Also, the precipitation time was shortest (10-15 min) with H₃PO₄ acid. Unlike the precipitates using sulfuric and hydrochloric acids (shown in equations 3 and 4, respectively), the precipitates with H₃PO₄ acid (equation 2) were found to be easily separated by filtration. This may be attributed to the poorly soluble phosphate salts in the glycerol phase.

Due to its superior performances in the process, phosphoric acid was chosen as acidifying agent for all further works. Moreover, the biogenic nature of phosphorus is an added advantage to the process. Being even better, the obtained phosphates could be directly used

as a fertilizer and as buffer solution. The roles of the phosphoric acid in the crude glycerol acidification process may be described in more details as follows. In the first step of purification, crude glycerol was acidified by H_3PO_4 , when the acid reacts with the soap molecules to form free fatty acids and less soluble sodium/potassium salts according to the reaction: $\text{RCOOK} + \text{H}_3\text{PO}_4 \rightarrow \text{RCOOH} + \text{KH}_2\text{PO}_4$. The acidification formed three distinct phases as pictured in Figure 8.3A. The middle glycerol-rich phase was obtained by decantation of solid residues, followed by separation of fatty acid layer from the glycerol rich phase (Figure 8.3B).

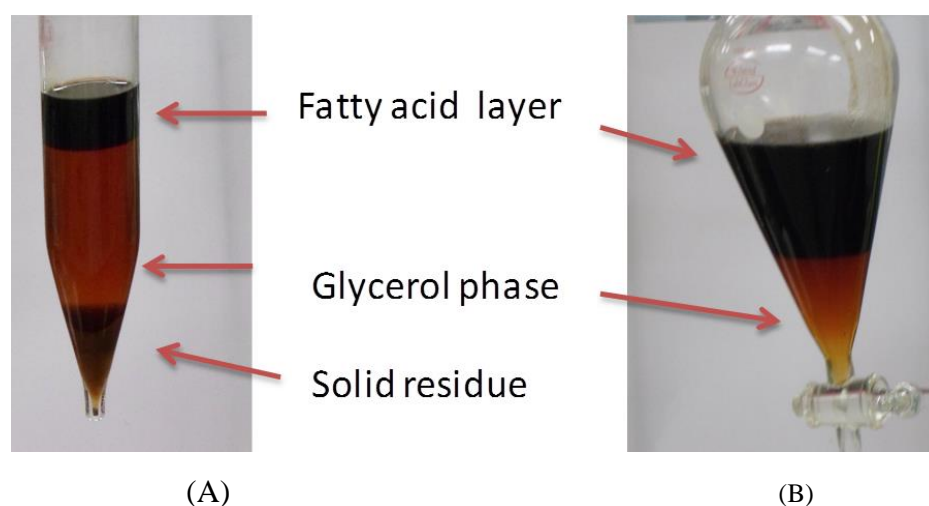


Figure 8.3 Photos showing the formation of three phases (A) and separation of purified glycerol phase from fatty acid layer (B)

The effects of pH levels on the weight percentages of various phases during acidification of crude glycerol using H_3PO_4 acid are given in Figure 8.4. From the figure, it can be seen that decreasing the pH from 6 to 1, in the acidification step led to a decrease in the weight fraction of the glycerol-rich phase from 70 wt% to 33 wt%, accompanied by an increase in the weight fraction of fatty acid (from 25 wt% to 45 wt%) and solid residues (from 5 wt% to 23 wt%). This was likely attributed to the fact that under strong acidic conditions, the acid neutralizes almost all the alkali species present in the crude glycerol to precipitate out

as solid residue (salt) at the bottom and reacts with the soap to form free fatty acids as the top phase.

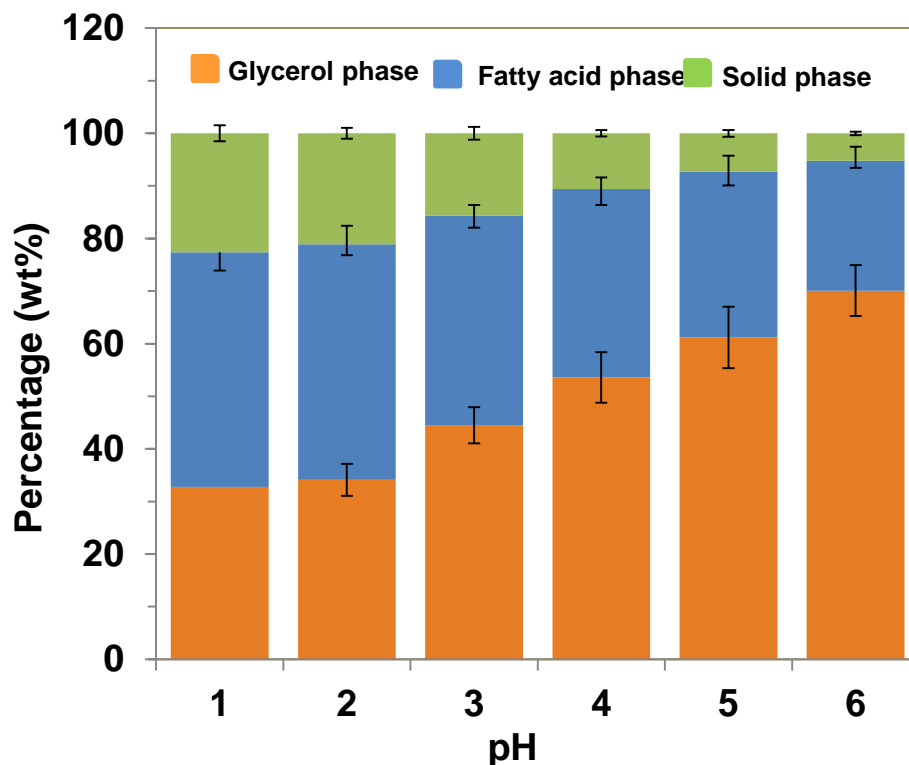


Figure 8.4 Effects of pH levels on the weight percentages of various phases during acidification of crude glycerol using H_3PO_4 acid

The effects of pH on the composition of purified glycerol products are shown in Figure 8.5. The ash contents of the purified glycerol at any pH values are lower than that of the original crude glycerol (5.6 wt%), as expected. As clearly shown in the Figure, there is a decreasing trend of both ash and MONG contents with decreasing pH (from 6 to 1). More solid phase can be produced while lowering the pH level of the crude glycerol during the acidification step. On the other hand, all purified glycerol products (at all pH values) have a much lower content of MONG (0-30 wt%), compared with approximately 70 wt% MONG for the crude glycerol. Thus, a decrease in the pH in the process resulted in a lower

content of organic impurities in the purified glycerol products. It should be noted that some short chain and medium chain fatty acids are soluble in the glycerol phase; hence complete elimination of MONG from the purified glycerol products is very difficult. The metal contents (mainly Na and K) of crude glycerol, commercially available glycerol and purified glycerol are given in the Table 8.1 and Table 8.3. The very high concentration of K in the crude glycerol is owing to the use of alkali catalysts in the biodiesel process.

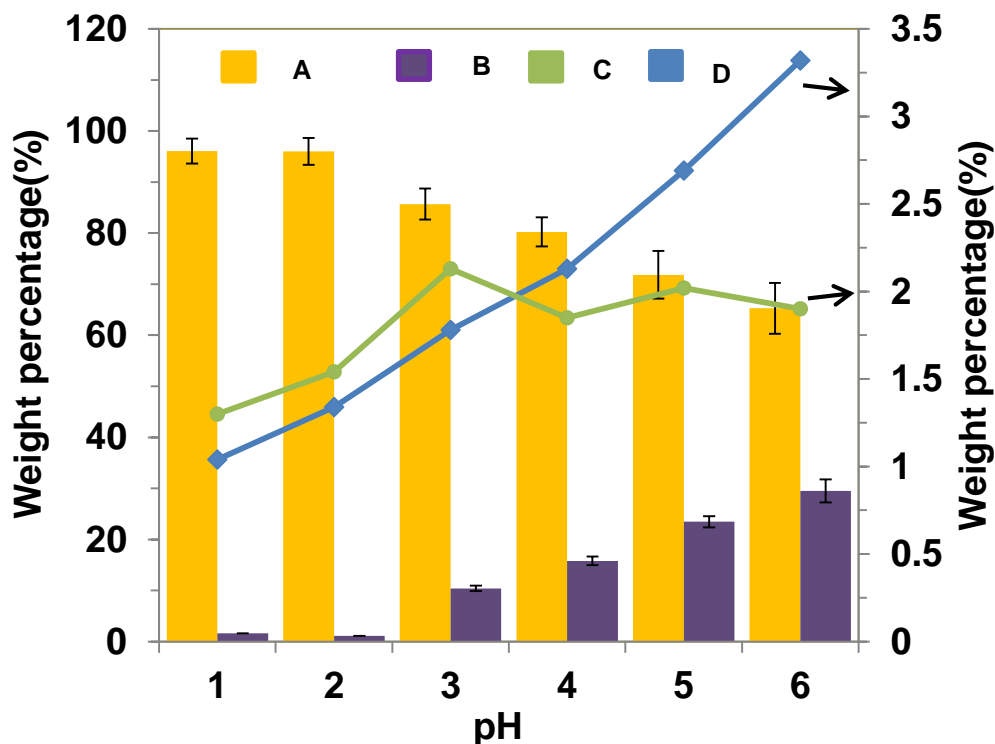


Figure 8.5 Composition of purified glycerol vs. pH (A: Glycerol B; MONG C: Water D: Ash)

8.3.3 Analysis of purified glycerol product

8.3.3.1 Physical properties

Composition and physical properties of purified glycerol (obtained with H_3PO_4 acid at pH = 1.0) and commercial glycerol are comparatively shown in Table 8.4. All properties including density, pH, water/ash/glycerol/MONG contents, K and Na concentration and viscosity are very similar, suggesting the success of the purification process using acidification.

Table 8.4 Composition and physical properties of purified glycerol and commercial glycerol

Properties	Commercial glycerol ^a	Purified glycerol
Density (at 20 °C, g/mL)	1.27 ±0.01	1.26 ± 0.02
pH	6.97 ± 0.03	6.98± 0.06
Water (wt%)	0.01± 0.00	1.30 ± 0.03
Ash (wt%)	0.0 ±0.00	1.04 ± 0.31
Glycerol (wt%)	99.9 ± 0.00	96.0 ±1.02
MONG (%)	0.0 ± 0.00	1.09 ± 0.02
Alkalinity	---	0
K (ppm)	870 ± 40	1165± 110
Na (ppm)	28± 10	82±22.0
Viscosity (in cp at 50 °C, 250 rpm)	142 ± 1	140 ±2

^a Supplier's data

8.3.3.2 FTIR analysis

The presence of different functional groups in the crude glycerol and purified glycerol was analyzed by FTIR and compared to those of a pure glycerol available commercially (Figure 8.6). In the crude glycerol, some additional peaks at 1580 cm⁻¹, 1740 cm⁻¹ and 3050 cm⁻¹ were observed. The absorbance peak at 1580 cm⁻¹ clearly indicates the presence of impurities containing carboxylate ions (COO⁻) (likely originated from soap) in the crude glycerol and the peak at 1740 cm⁻¹ indicates the presence of carbonyl group (C=O) of an ester or carboxylic acids.

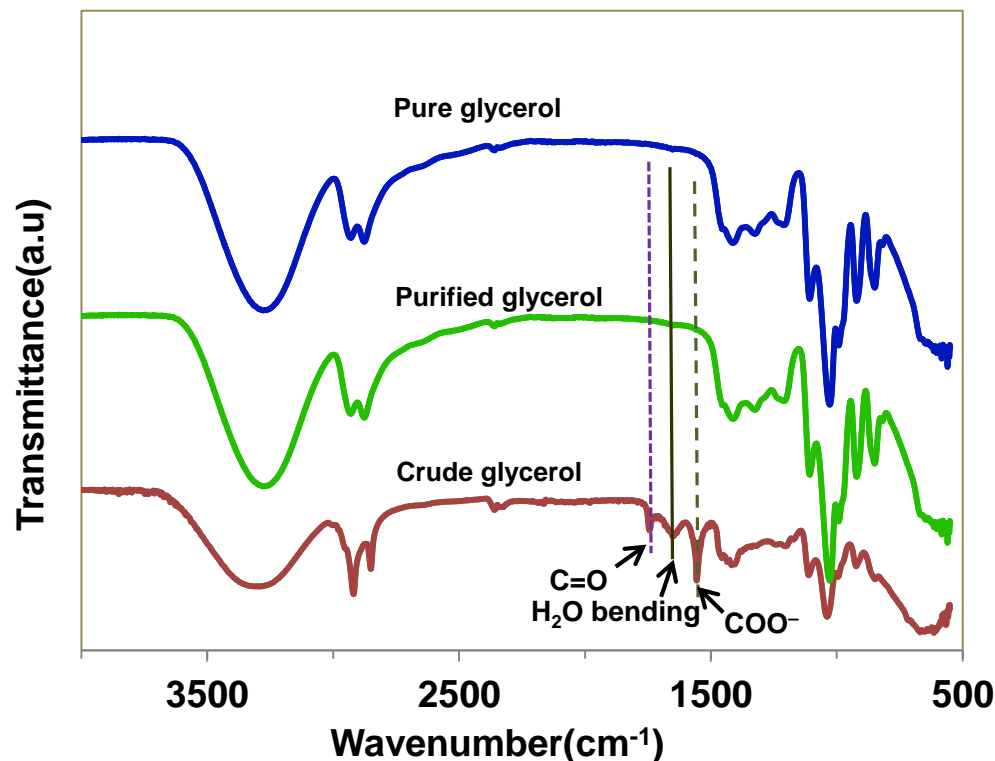


Figure 8.6 FTIR spectra of pure, purified and crude glycerol

The FTIR spectrum of the purified glycerol at pH = 1 clearly shows the absence of peaks at 1580, 1740, and 3050 cm^{-1} , indicating the complete removal of impurities like free fatty acid and methyl esters compounds, owing to the fact that the mineral acid could convert the soap molecules to fatty acids to be separated out via phase separation.

8.3.3.3 UV-VIS spectral analysis

UV –VIS spectroscopy gives information about the color and transparency of the liquid products. The greater the absorbance of radiation, the lesser is the transmittance and therefore the lesser the transparency. The spectroscopic results for crude glycerol, pure glycerol and the purified glycerol (after decoloration with activated charcoal) are illustrated in Figure 8.7. Since pure glycerol is very transparent it has negligible absorbance. On the contrary, due to the presence of contaminants like fatty acids, salts, soap and other impurities, crude glycerol is almost opaque and therefore has a very high absorbance.

During purification process of crude glycerol most of the contaminants were removed from the crude glycerol and after activated charcoal decoloration treatment most of the impurities were adsorbed. Hence the purified glycerol has an absorbance closer to pure glycerol in visible light region (400-800 nm). The UV-VIS spectra are in agreement with the naked eye observation. Photographs of the purified glycerol before and after activated charcoal decoloration treatment are displayed in Figure 8.8.

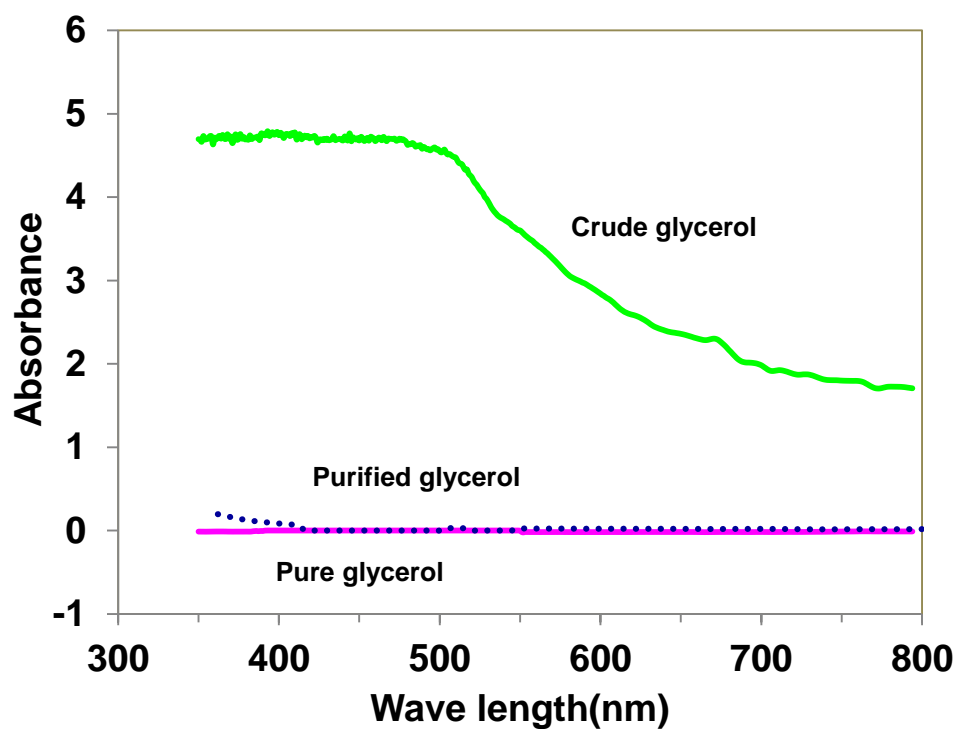


Figure 8.7 UV-Vis spectra of pure, purified and crude glycerol

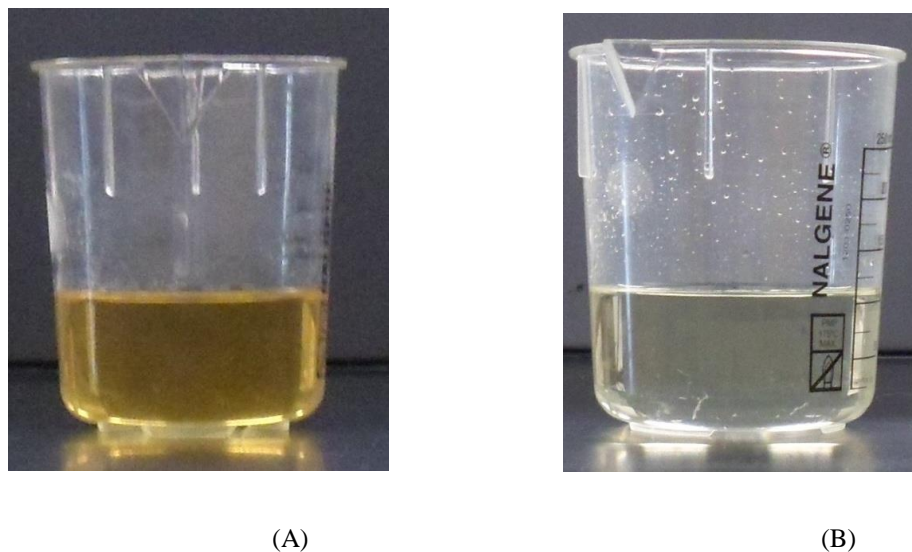


Figure 8.8 Purified glycerol before (A) and after (B) charcoal treatment

8.3.3.4 NMR spectral analysis

The purity of the purified glycerol was analyzed using ^{13}C and ^1H -NMR spectra and the results were compared with that of the pure glycerol available on-line.³¹ The ^{13}C -NMR of purified glycerol demonstrated two signals at 63.4 and 72.8 ppm for the presence of primary and secondary aliphatic carbon atoms, respectively (Figure 8.9). The ^1H -NMR spectra showed the presence four types of different signals at 4.5, 3.45, 3.4 and 3.3 ppm for the hydrogen from hydroxyl groups, secondary carbon atom, and two types of primary carbon atoms respectively. These results reflect that the physicochemical purification demonstrated in this work is efficient enough to enhance the glycerol level in the purified glycerol close to that of the commercial one.

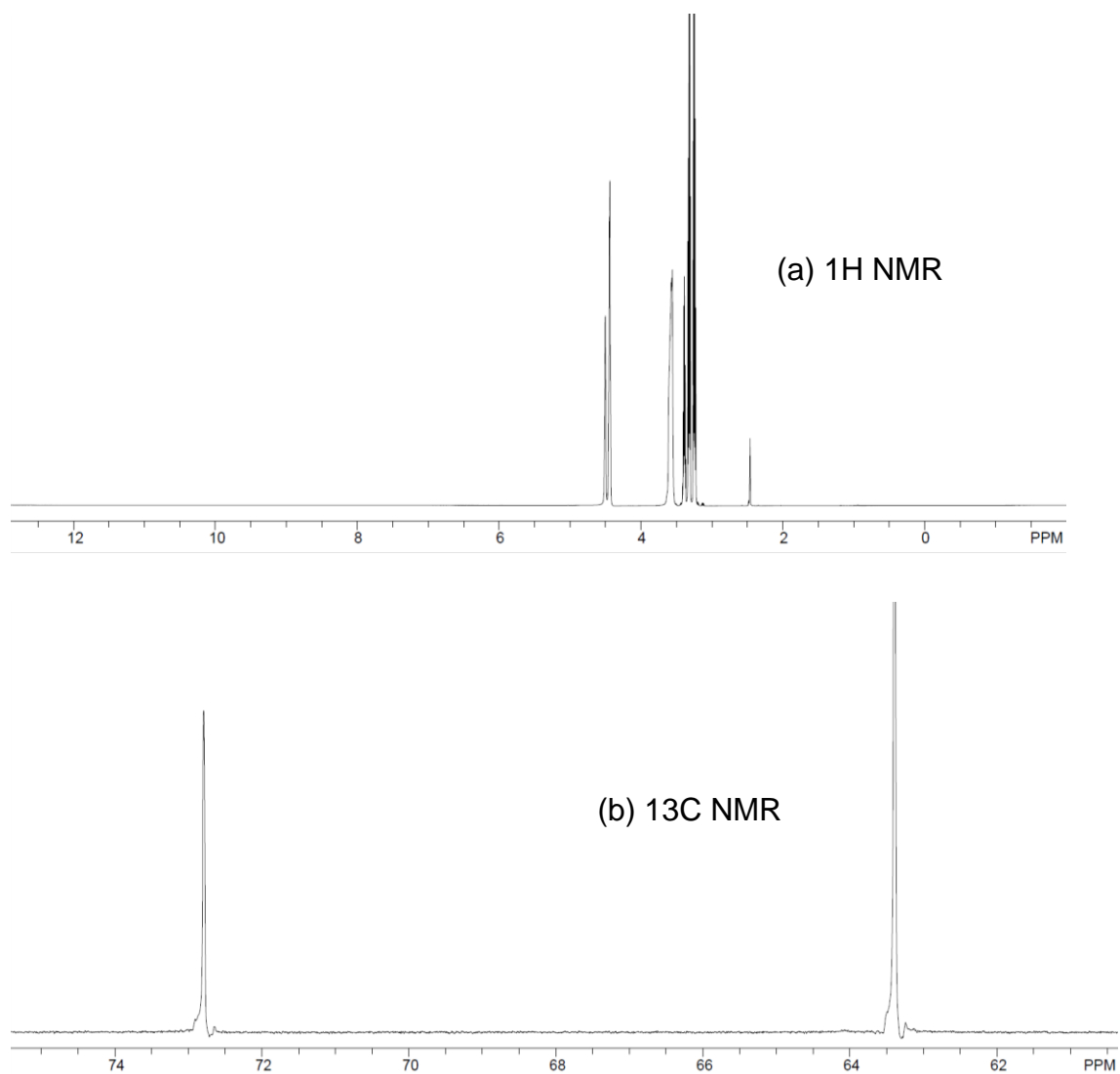


Figure 8.9 Spectra of ^1H NMR (a) and ^{13}C NMR for the purified glycerol

8.4 Conclusions

Phosphoric acid was found to be the best acidifying agent among the other mineral acids tested for crude glycerol acidification for purification. Glycerol content was increased from approximately 13 wt% in the crude glycerol to > 96 wt% in the purified glycerol products. The density, viscosity, pH and metal contents of the purified glycerol products were analyzed and found to be very close to that of the commercially available pure glycerol. The purity of the purified products was confirmed by FTIR and GC-MS/FID

measurements. UV-VIS spectroscopy demonstrated a nearly equal absorbance of the purified glycerol to that of pure glycerol. The biogenic nature of phosphorous, the high value applications of the phosphates with easy scalability of the process could make it very promising for commercialization.

References

1. Behr A, Eilting J, Irawadi K, Leschinski J, Lindner F. Improved utilisation of renewable resources: New important derivatives of glycerol. *Green Chemistry* 2008;10(1):13. doi:10.1039/b710561d.
2. Lin L, Cunshan Z, Vittayapadung S, Xiangqian S, Mingdong D. Opportunities and challenges for biodiesel fuel. *Applied Energy* 2011;88(4):1020-1031. doi:10.1016/j.apenergy.2010.09.029.
3. Zhou C-HC, Beltramini JN, Fan Y-X, Lu GQM. Chemoselective catalytic conversion of glycerol as a biorenewable source to valuable commodity chemicals. *Chemical Society reviews* 2008;37(3):527-49. doi:10.1039/b707343g.
4. Johnson DT, Taconi KA. The glycerin glut: Options for the value-added conversion of crude glycerol resulting from biodiesel production. *Environmental Progress* 2007;26(4):338-348. doi:10.1002/ep.10225
5. Organization for Economic Co-operation and Development (OECD) and the Food and Agriculture Organization (FAO) of the United Nations, 2011-2020. Available at: <http://www.agri-outlook.org/48202074.pdf>. Accessed April 9, 2015..
6. Glycerin Surplus | February 6, 2006 Issue - Vol. 84 Issue 6 | Chemical & Engineering News. Available at: <http://cen.acs.org/articles/84/i6/Glycerin-Surplus.html>. Accessed January 27, 2015.
7. Yang F, Hanna M a, Sun R. Value-added uses for crude glycerol-a byproduct of biodiesel production. *Biotechnology for Biofuels* 2012;5:13. doi:10.1186/1754-6834-5-13.
8. B. Sims, "Clearing the Way for Byproduct Quality," 2011. <http://www.biodieselmagazine.com/articles/8137/clearing-the-way-forbyproduct-quality>|Reference|Scientific Research Publish. Available at: <http://www.ljemail.org/reference/ReferencesPapers.aspx?ReferenceID=820106>. Accessed December 3, 2014.
9. Nanda MR, Yuan Z, Qin W, Ghaziaskar HS, Poirier M-A, Xu CC. Thermodynamic and kinetic studies of a catalytic process to convert glycerol into solketal as an oxygenated fuel additive. *Fuel* 2014;117:470-477. doi:10.1016/j.fuel.2013.09.066.
10. Kraus G a. Synthetic Methods for the Preparation of 1,3-Propanediol. *CLEAN - Soil, Air, Water* 2008;36(8):648-651. doi:10.1002/clen.200800084.
11. Kurosaka T, Maruyama H, Naribayashi I, Sasaki Y. Production of 1,3-propanediol by hydrogenolysis of glycerol catalyzed by Pt/WO₃/ZrO₂. *Catalysis Communications* 2008;9(6):1360-1363. doi:10.1016/j.catcom.2007.11.034.

12. Cheng L, Liu L, Ye XP. Acrolein Production from Crude Glycerol in Sub- and Super-Critical Water. *Journal of the American Oil Chemists' Society* 2012;90(4):601-610. doi:10.1007/s11746-012-2189-5.
13. Ito T, Nakashimada Y, Senba K, Matsui T, Nishio N. Hydrogen and ethanol production from glycerol-containing wastes discharged after biodiesel manufacturing process. *Journal of bioscience and bioengineering* 2005;100(3):260-5. doi:10.1263/jbb.100.260.
14. Sabourin-Provost G, Hallenbeck PC. High yield conversion of a crude glycerol fraction from biodiesel production to hydrogen by photofermentation. *Bioresource Technology* 2009;100(14):3513-7. doi:10.1016/j.biortech.2009.03.027.
15. Nanda MR, Yuan Z, Qin W, Ghaziaskar HS, Poirier M-A, Xu C (Charles). A new continuous-flow process for catalytic conversion of glycerol to oxygenated fuel additive: Catalyst screening. *Applied Energy* 2014;123:75-81. doi:10.1016/j.apenergy.2014.02.055.
16. Nanda MR, Yuan Z, Qin W, Ghaziaskar HS, Poirier M-A, Xu C (Charles). Catalytic conversion of glycerol to oxygenated fuel additive in a continuous flow reactor: Process optimization. *Fuel* 2014;128:113-119. doi:10.1016/j.fuel.2014.02.068.
17. Cheng D, Wang L, Shahbazi A, Xiu S, Zhang B. Catalytic cracking of crude bio-oil from glycerol-assisted liquefaction of swine manure. *Energy Conversion and Management* 2014;87:378-384. doi:10.1016/j.enconman.2014.06.084.
18. Xiu S, Shahbazi A, Shirley VB, Wang L. Swine manure/crude glycerol co-liquefaction: physical properties and chemical analysis of bio-oil product. *Bioresource Technology* 2011;102(2):1928-32. doi:10.1016/j.biortech.2010.08.026.
19. Mothes G, Schnorpfeil C, Ackermann J-U. Production of PHB from Crude Glycerol. *Engineering in Life Sciences* 2007;7(5):475-479. doi:10.1002/elsc.200620210.
20. Hu S, Wan C, Li Y. Production and characterization of biopolyols and polyurethane foams from crude glycerol based liquefaction of soybean straw. *Bioresource Technology* 2012;103(1):227-33. doi:10.1016/j.biortech.2011.09.125.
21. Nguyen NT. A Novel Biodiesel and Glycerol Carbonate Production Plant. 9(1). Available at: http://resolver.scholarsportal.info/resolve/15426580/v09i0001/nfp_anbagcpp.xml. Accessed January 27, 2015.
22. Hammond C, Lopez-Sanchez JA, Ab Rahim MH, *et al.* Synthesis of glycerol carbonate from glycerol and urea with gold-based catalysts. *Dalton transactions (Cambridge, England : 2003)* 2011;40(15):3927-37. doi:10.1039/c0dt01389g.

23. Ferreira MO, Sousa E, Pereira CG. Purification of Crude Glycerine Obtained from Transesterification of Cottonseed Oil. *International Journal of Chemical Reactor Engineering* 2013;11(1):1-8. doi:10.1515/ijcre-2012-0071.
24. Nano cavitation: a proven new concept. Available at: <http://www.ctinanotech.com/media/9b55db3c-fb67-46ae-8d4a-17e36e2a977a/Nano-Cavitation-a-Proven-New-Concept.pdf>. Accessed December 9, 2014.
25. Saleh J, Tremblay AY, Dubé MA. Glycerol removal from biodiesel using membrane separation technology. *Fuel* 2010;89(9):2260-2266. doi:10.1016/j.fuel.2010.04.025.
26. Kongjao S, Damronglerd S, Hunsom M. Purification of crude glycerol derived from waste used-oil methyl ester plant. *Korean Journal of Chemical Engineering* 2010;27(3):944-949. doi:10.1007/s11814-010-0148-0.
27. Aziati AANN, Sakinah AMM. Review: Glycerol Residue and Pitch Recovered From Oleo Chemical. *2nd International Conference on Chemical, Biological & Environmental Sciences (ICCEBS)* 2012:1-6.
28. Manosak R, Limpattayanate S, Hunsom M. Sequential-refining of crude glycerol derived from waste used-oil methyl ester plant via a combined process of chemical and adsorption. *Fuel Processing Technology* 2011;92(1):92-99. doi:10.1016/j.fuproc.2010.09.002.
29. Crude glycerine recovery from glycerol residue waste from a palm kernel oil methyl ester plant. Available at: <http://jopr.mpob.gov.my/wp-content/uploads/2013/09/jopr12dec2001-ooi1.pdf>. Accessed December 9, 2014.
30. Human and environmental risk assessment on ingredients of household cleaning products-Sodium sulfate. Available at: http://www.heraproject.com/files/39-F-06_Sodium_Sulfate_Human_and_Environmental_Risk_Assessment_V2.pdf. Accessed December 9, 2014.
31. ChemSpider | Data Source Details | SDBS Spectral Database for Organic Compounds. Available at: <http://www.chemspider.com/DatasourceDetails.aspx?id=308>. Accessed December 9, 2014.
32. Javani A, Hasheminejad M, Tahvildari K, Tabatabaei M. High quality potassium phosphate production through step-by-step glycerol purification: a strategy to economize biodiesel production. *Bioresource Technology* 2012;104:788-90. doi:10.1016/j.biortech.2011.09.134.

Chapter 9

9 Catalytic conversion of purified crude glycerol in a continuous-flow process for the synthesis of oxygenated fuel additive

Abstract

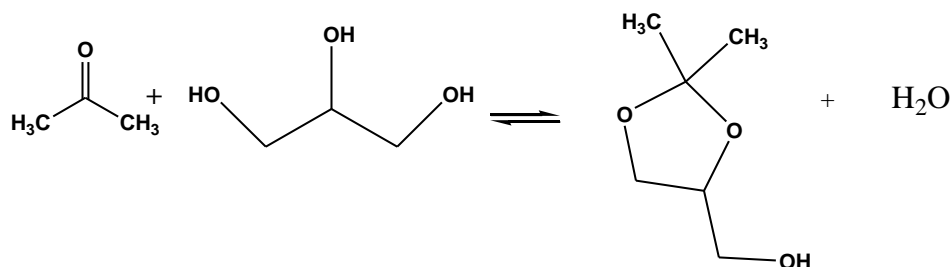
A continuous-flow reactor consisting of 2 parallel guard reactors and a main reactor was designed and used for the conversion of crude glycerol to solketal – an oxygenated fuel additive. In this process, ketalization of in-house purified crude glycerol was carried out over Amberlyst-36 wet catalyst under conditions of 25 °C, 200 psi, acetone-to-glycerol molar ratio of 4, achieving a very high yield and conversion, i.e., $92 \pm 2\%$ and $93 \pm 3\%$, respectively after 24 h on stream at WHSV of 0.38 h^{-1} . The catalyst was deactivated gradually during the reaction process mainly due to loss of active acid sites caused by the cationic exchange of the protons present in the catalyst. The continuous-flow process developed can be used for carrying out ketalization reaction and spent-catalyst regeneration simultaneously. The catalyst was effectively regenerated and remained active for four successive runs (96 h) without significant loss of activity.

Keywords: Ketalization; Crude glycerol; Purified crude glycerol; Continuous process; Guard bed reactor

9.1 Introduction

Glycerol is considered as an evolving green platform for different chemicals. Crude glycerol is usually obtained as a by-product of the biodiesel industry. The booming of biodiesel production has increased the concern regarding an oversupply of crude glycerol to the market. Therefore, the development of new valorization routes for conversion of crude glycerol into value-added fuel products or chemicals is critical for the sustainability of the biodiesel industry.¹

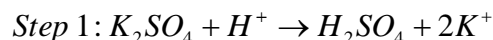
Direct addition of glycerol to fuel is not possible, because of its immiscibility, inflammability, decomposition and polymerization, leading to engine breakdown at high temperatures. Hence, chemical modification of glycerol is essential for its application as fuel products (diesel, gasoline or biodiesel) or fuel additives e.g., acetals and ethers.² Solketal [(2, 2-dimethyl-1, 3-dioxolan-4-yl) methanol], a ketal formed by the reaction of glycerol with acetone in the presence of an acid catalyst (Scheme 9.1), can be used as a fuel additive to reduce particulate emission and improve cold flow properties of gasoline fuel with enhancement in the octane number.³ When added to gasoline, it could also reduce gum formation and improve the oxidation stability.⁴ Other applications of solketal include a versatile solvent and a plasticizer in the polymer industry, and a solubilizing and suspending agent in pharmaceutical manufacture.^{5,6}



Scheme 9.1 Reaction scheme of ketalization of glycerol with acetone.

Conventionally, solketal is produced in a batch reactor using either a homogeneous acid such as hydrochloric acid, sulfuric acid, p-toluene sulfonic acid or a heterogeneous acid catalyst including Amberlysts, zeolites, montmorillonite, iridium, molybdenum catalysts, etc.^{7,8,9,10,11,12} Nevertheless, it is obvious that production of solketal in a continuous-flow process using heterogeneous catalysts is more advantageous over a batch process. However, hardly any work for the continuous synthesis of solketal from crude glycerol has been published, except the recent publications by the authors' group on synthesis of solketal from pure glycerol on a continuous process over heterogeneous acid catalysts such as Amberlyst resins.^{13,14,15}

Crude glycerol obtained from the biodiesel industry contains a large amount of contaminants such as water, methanol, soap/free fatty acids (FFAs), and salts.^{16,17} The presence of contaminants in this renewable carbon source creates certain challenges such as plugging of reactor and deactivation of catalysts for the catalytic conversion processes.^{18,19} Hence, the crude glycerol must be purified before it can be effectively used in different applications.²⁰ Purification of glycerol using such processes as acidification, neutralization followed by separation, ion exchange resin or their combination has been extensively studied, where impurities in the form of soluble salts/ or ash such as $\text{Na}_2\text{SO}_4/\text{KHSO}_4/\text{K}_2\text{SO}_4/\text{Na}_2\text{HPO}_4/\text{K}_2\text{HPO}_4$ were observed in the purified crude glycerol.^{21,22,23,24} It has been reported that these impurities could significantly influence the yield of solketal in the acid-catalyzed reaction between glycerol and acetone.²⁴ To address this challenge, we designed and developed a continuous-flow reactor system that contains a guard reactor (GR) packed with a cation exchange resin to remove these impurities from the purified glycerol while being fed to the catalytic reactor system (Figure 9.1). The purpose of the guard reactor is to remove the cationic contaminants present in the crude glycerol or purified crude glycerol, the known catalyst poisons in the ketalization process. The cation exchange resin in the guard reactor exchanges the cations present in the reaction feed by H^+ ion (Step 1) and prevents its deposition on the catalyst in the ketalization reactor downstream, so that deactivation of the catalyst could be retarded or prevented. The saturated cation exchange resin in the GR could be regenerated by flowing through a mineral acid (e.g., H_2SO_4) to restore its original activity (Step 2) as follows:



Previously, we have demonstrated the high efficiency of a continuous-flow reactor for the synthesis of solketal using commercial glycerol as feedstock.¹⁴ As the continuation of our previous work, purified crude glycerol and crude glycerol were used as feedstock in this work for the production of solketal. Amberlyst-36 wet was applied in both the guard reactor and the ketalization reactor for its high activity and ability to perform in aqueous condition, as demonstrated in the authors' previous studies.^{13,14,15} The objectives of the present study were to (1) design and construct a continuous-flow reactor system consisting of two parallel guard reactors and a main ketalization reactor, and (2) conduct ketalization of crude glycerol or purified crude glycerol, with simultaneous regeneration of the spent catalyst in one of the two guard reactors. Successful operation of the above continuous-flow reactor system would demonstrate promise of large-scale production of solketal- a high value oxygenated fuel additive, from crude glycerol (an abundant and inexpensive waste stream from the bio-diesel industry).

9.2 Materials and methods

9.2.1 Materials

Crude glycerol was obtained from a local biodiesel plant of Methes Energies Canada Inc, and was purified using the methods described in our previous work.²³ The composition of purified glycerol is given in Table 9.1. ACS reagent grade methanol and acetone (both >99 wt% purity) were purchased from Sigma Aldrich and used as received, and commercial grade ethanol was obtained from Commercial Alcohols Inc. Analytical reagent grade Solketal [(S-) (+) – 1, 2- Isopropylidene glycerol] was obtained from Sigma Aldrich as a calibration standard for GC analysis. The solid acid catalyst; Amberlyst-36 wet was obtained from Rohm and Hass Co. USA and its characteristics are given in Table 9.2. Hereafter the catalyst will be simply referred to as Amberlyst. Other chemicals such as concentrated H₃PO₄ and dimethyl sulfoxide were all purchased from Sigma Aldrich.

Table 9.1 Composition of purified glycerol

	Glycerol ^a (wt%)	Ash (wt%)	Water (wt%)	MONG ^b (wt%)	pH
Crude glycerol	12.01 ± 2.38	4.6 ± 0.51	9.12 ± 1.04	70.2 ± 4.37	10.3 ± 0.26
Purified	96.03 ± 1.01	3.81 ± 0.05	0.03 ± 0.00	0.13 ± 0.00	7.0 ± 0.08

^a Determined by GC-FID; ^b Matter organic non-glycerol (MONG)

9.2.2 Analytical methods

The BET surface area, total pore volume and average pore diameter of the fresh and spent Amberlyst catalyst were determined by nitrogen isothermal (at -196 °C) adsorption on a Micromeritics ASAP 2010 apparatus. The catalyst was dried at 90 °C overnight under nitrogen atmosphere prior to the measurements. The acidity (abundance of acidic sites. i.e., number of acidic sites per unit mass) of the catalysts was characterized by ammonia temperature programmed desorption (NH₃-TPD) using Micromeritics AutoChem II analyzer. Inductively coupled plasma-atomic emission spectrometry (ICP-AES) was employed to quantify the metal content present in the samples. The water content in the feed and products was measured following the standard method ISO 2098-1972 on a Karl-Fisher titrator V20. The pH of the feed was measured with a pH meter (Symphony™ 89231-608, VWR) at room temperature (22±1°C). Matter Organic Non Glycerol (MONG) was determined according to following equation:

$$MONG (wt\%) = 100\% - [glycerol (wt\%) + water (wt\%) + ash (wt\%)] \quad (1)$$

where ash content of the crude glycerol or the purified crude glycerol was measured according to the standard method (ISO 2098-1972) by ashing 1 g glycerol at 750 °C in air for 3 h. The particle size of the catalyst was determined by a particle size analyzer (HELOS VARIO/KR).

9.2.3 Continuous reactor for the synthesis of solketal from purified crude glycerol

The schematic diagram for the continuous-flow reactor system designed and constructed in this study for synthesis of solketal from crude glycerol or purified crude glycerol is given

in Figure 9.1. It is a bench scale continuous down-flow tubular reactor (Inconel 625 tubing, 9.55 mm OD, 6.34 mm ID and 600 mm length) connected in series to two parallel guard reactors of larger dimensions (SS 316L tubing, 12.64 mm OD, 9.67 mm ID and 520 mm length). The feed (a homogeneous solution of acetone, crude glycerol or purified crude glycerol and ethanol at a pre-selected molar ratio) is pumped into the reactor system through the guard reactor using a HPLC pump (Eldex) at a specific flow rate. In a typical run, a mixture of 116 g of acetone, 46 g of purified glycerol and 46 g of ethanol (4:1:2 molar ratio of acetone: glycerol: ethanol) fed to the reactor system by a HPLC pump at 0.23 mL/min. Ethanol was used as solvent to improve the solubility of glycerol in acetone and hence help the feeding. In a typical run, a total of 8 g catalyst was loaded into the reactor (6 g in the guard reactor; and 2 g in the main reactor), in which the catalyst particles were supported on a porous Inconel metal disc (pore size: 100 μm) and some quartz wool. All experiments in this work were performed at optimum conditions (25 $^{\circ}\text{C}$, 200 psi, acetone-to-glycerol ratio of 4/1 (mol/mol)), as determined by previous studies of the authors.^{13,14,15} Depending on the feeding rate, molar weight compositions of the feed and the total amount of catalyst packed in both reactors (i.e., 8 g), the weight hour space velocity, WHSV (h^{-1}) was calculated as:

$$\text{WHSV} (\text{h}^{-1}) = \frac{\text{Mass flow of glycerol} / \text{h}}{\text{Mass of catalyst used}} \quad (2)$$

In some tests with purified crude glycerol and the guard reactor (PCG-GR), after reaction for 24 h on-stream the Amberlyst catalyst in the guard bed reactor was regenerated by flowing 0.5 M sulfuric acid through the guard column. The regenerated catalyst was washed with distilled water and methanol, sequentially followed by drying with a nitrogen flow for 5 h, and reused on stream for another 24h followed by regeneration again.²⁵

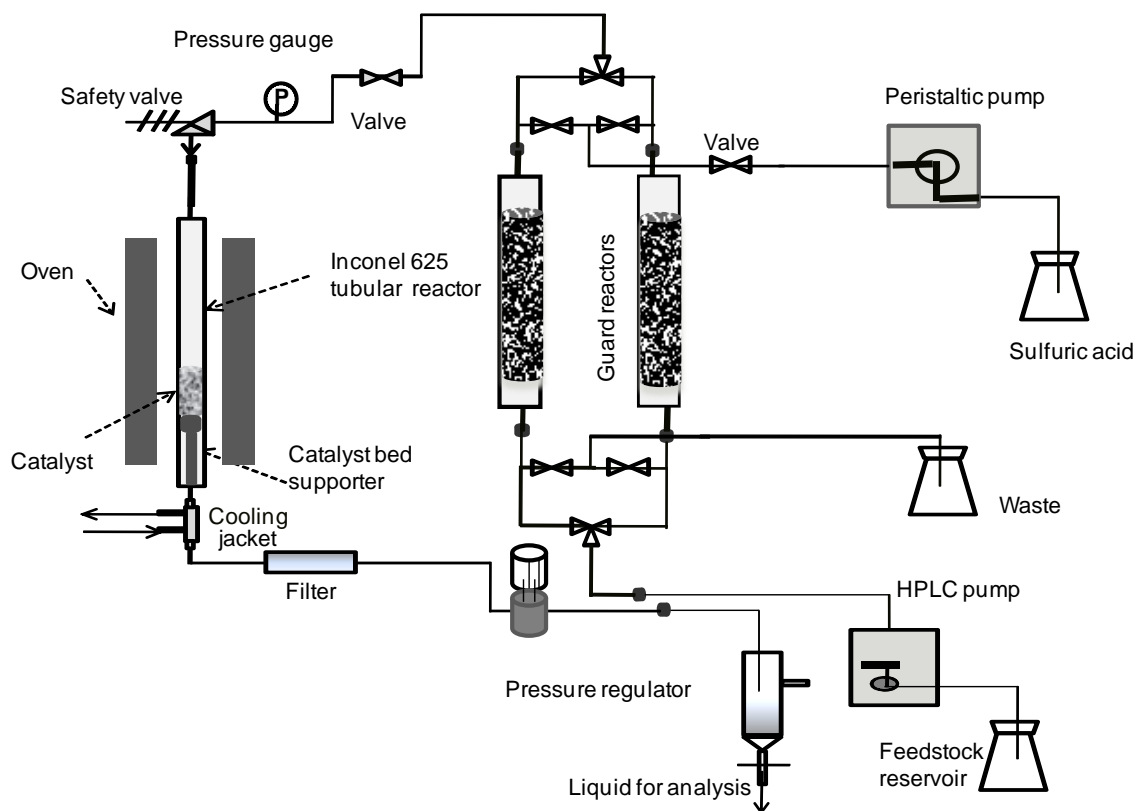


Figure 9.1 Schematic diagram of the continuous flow reactor.

9.2.4 Product analysis

Components of the reaction mixtures were first identified with a gas chromatograph, equipped with a mass selective detector [Varian 1200 Quadrupole GC/MS (EI), Varian CP-3800 GC equipped with VF-5 MS column (5% phenyl/95% dimethyl-polysiloxane, 30 m × 0.25 mm × 0.25 μm)], using helium as the carrier gas. The oven temperature was maintained at 120 °C for 2 min and then ramped to 280 °C at 40 °C/min. The Injector and detector block temperatures were maintained at 300 °C. Chemical components of the reaction mixtures were identified by means of the NIST 98 MS library with the 2002 update.

The concentrations of the components in the product mixture (mainly glycerol and solketal) were then quantified using a GC-FID (Shimadzu -2010) operating at similar conditions as used in the above GC-MS measurement, after careful calibration with glycerol and solketal of varying concentrations and dimethyl sulfoxide (DMSO) as an internal standard at a fixed concentration. Appendix C provides a typical GC-MS spectrum and the calibration tables and curves for GC-FID.

The yield of solketal, glycerol conversion and selectivity are defined below:

$$\text{Yield (\%)} = \frac{\text{Moles of solketal formed}}{\text{Initial mole of glycerol}} \times 100\% \quad (3)$$

$$\text{Conversion (\%)} = \frac{\text{Initial mole of glycerol} - \text{Final mole of glycerol}}{\text{Initial mole of glycerol}} \times 100\% \quad (4)$$

$$\text{Selectivity (\%)} = \frac{\text{Moles of solketal formed}}{\text{Initial mole of glycerol} - \text{Final mole of glycerol}} \times 100\% \quad (5)$$

9.3 Results and discussion

The results of continuous ketalization of crude glycerol (CG) or purified crude glycerol (PCG) with or without the guard reactor (GR) at 25 °C, 200 psi, acetone-to-glycerol ratio of 4/1 (mol/mol), and WHSV of 0.38 h⁻¹ are presented in Figure 9.2. The figure illustrates plots of solketal yield (%) vs. time-on-stream (h) in various operations: crude glycerol without guard reactor (CG-NGR), crude glycerol with the guard reactor (CG-GR), purified crude glycerol without guard reactor (PCG-NGR), and purified crude glycerol with the guard reactor after regeneration of the catalyst inside the guard reactor for 0 time (PCG-GR0), 1 time (PCG-GR1), 2 times (PCG-GR2) and 3 times (PCG-GR3). It is clearly shown that when crude glycerol was used as the feedstock without guard reactor the maximum solketal yield obtained in the very first hour was 56 % but decreased rapidly to <5% within 4 h on-stream, which was expected since the crude glycerol was rich in impurities such as ash (4.6%), water (9%) and matter organic non-glycerol (MONG) (70%) (Table 9.1), which would quickly deactivate the solid acid catalyst. When purified crude glycerol

without guard reactor was used, a higher solketal yield (>60%) was maintained for up to 8 h on-stream, likely attributed to the significantly reduced contaminants in the purified crude glycerol as compared to those of the crude glycerol (ash: 3.8% vs 4.6%; water: 0.03% vs 9% and MONG: 0.13% vs 70%). Similar observations were obtained by the authors in another study where addition of salt (NaCl) to pure glycerol greatly reduced the activity of the Amberlyst catalysts.¹⁵

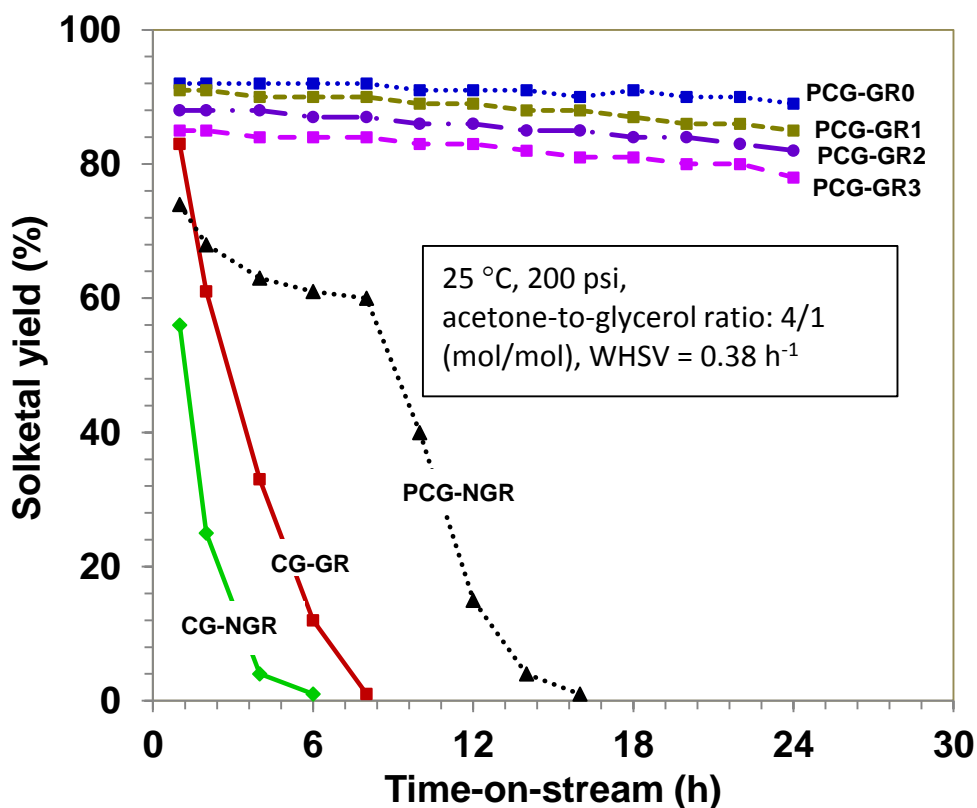


Figure 9.2 Solketal yield (%) vs. time-on-stream (h) in various operations: crude glycerol without guard reactor (CG-NGR), crude glycerol with the guard reactor (CG-GR), purified crude glycerol without guard reactor (PCG-NGR), and purified crude glycerol with the guard reactor after regeneration of the catalyst inside the guard reactor for 0 time (PCG-GR0), 1 time (PCG-GR1), 2 times (PCG-GR2) and 3 times (PCG-GR3)

In contrast, a very high yield of solketal (92%) with a conversion of 93% was obtained in the experiment where purified crude glycerol and the guard reactor were used. This might be attributed to the removal of the cationic impurities present in the purified crude glycerol by the guard bed reactor through ion exchange. This however would transform the solid acid resin catalyst from its active acidic form to the corresponding cationic form (Na^+/K^+) and hence slowly deactivate. In order to validate this hypothesis, the catalyst in the guard reactor after each 24 h on-stream was regenerated by flowing H_2SO_4 solution and reused for another 24 h on-stream. Although the regeneration could not completely restore the catalytic activity, while after each regeneration step the solketal yield could be improved initially, and it decreased with increasing time-on-stream. This could be due to the combined effect of water of reaction and initial low activity of the catalyst (due to incomplete restoration of catalytic activity during regeneration). After 3 times regeneration or 96 h on-stream the solketal yield was still as high as >80%, suggesting that the coupling of two guard reactors with a main reactor enables simultaneous operation of ketalization reaction and spent catalyst regeneration, leading to continuous operation of the reactor for a longer time while maintaining a high product yield.

To investigate the catalyst deactivation mechanism, the concentration of acidic sites and the cation content of spent catalyst after 24h on-stream operation were analyzed by NH_3 -TPD and ICP-AES analysis, respectively, and the results are displayed in Table 9.2. From NH_3 -TPD, 24 h on-stream operation markedly reduced the number of active acidic sites from 5 eq/kg (fresh catalyst) to 2.4 eq/kg (spent catalyst). The ICP-AES result showed that the spent catalyst contains around 1100 ppm of K^+/Na^+ ions (Table 9.2), which confirms that the deactivation of the Amberlyst catalyst was mainly due to the cationic exchange reaction between K^+/Na^+ and H^+ on the catalyst's surface.

Table 9.2 Characteristics of the fresh and spent catalysts

Catalyst	Particle size (μm)	BET specific surface area (m^2/g)	Total pore volume (mL/g)	Average pore diameter (nm)	Number of acid sites (eq/kg)	K^+/Na^+ content (ppm)
Fresh	490	50	0.35	30	5	0
Spent ^a	442	35	0.21	34	2.4	1100

^a After ketalization reaction at 25 °C, 200 psi, acetone-to-glycerol molar ratio of 4:1 for 96 h on-stream at WHSV of 0.38 h⁻¹

Clogging of reactors is one of the major challenges in operating a continuous-flow reactor process, particularly with heterogeneous catalysts. During the course of the experiment, no clogging of the main reactor was observed, however clogging was often found in the guard bed reactor. This could be attributed to the disintegration of the catalyst particles during the repeated regeneration process causing the destruction of resin structure.²⁶ The smaller fragments clogged the reactor resulting in a sharp increase in the guard bed pressure. The regenerated catalyst particles (after the experiment for 96 h on-stream) were sampled and photographed as illustrated in Figure 9.3, and the average particle size of the spent and fresh catalysts were measured by particle size analyzer (PSA) and the particle size distribution plot is presented in Figure 9.4. From Figure 9.3, it can be clearly seen that the spent catalysts from the guard bed reactor contain a substantial fraction of fine particles which were absent in fresh catalysts. Figure 9.4 (A and B) demonstrated a comparatively narrow particle size distribution for the fresh catalysts over the spent catalysts. The particle size of fresh catalysts is in the range of 435-875 μm with the Sauter-mean diameter (SMD) of 625 μm , however that of the spent catalysts is in the range of 4-875 μm with the SMD of 448 μm , which is in good agreement with the photographs illustrated in Figure 9.3.

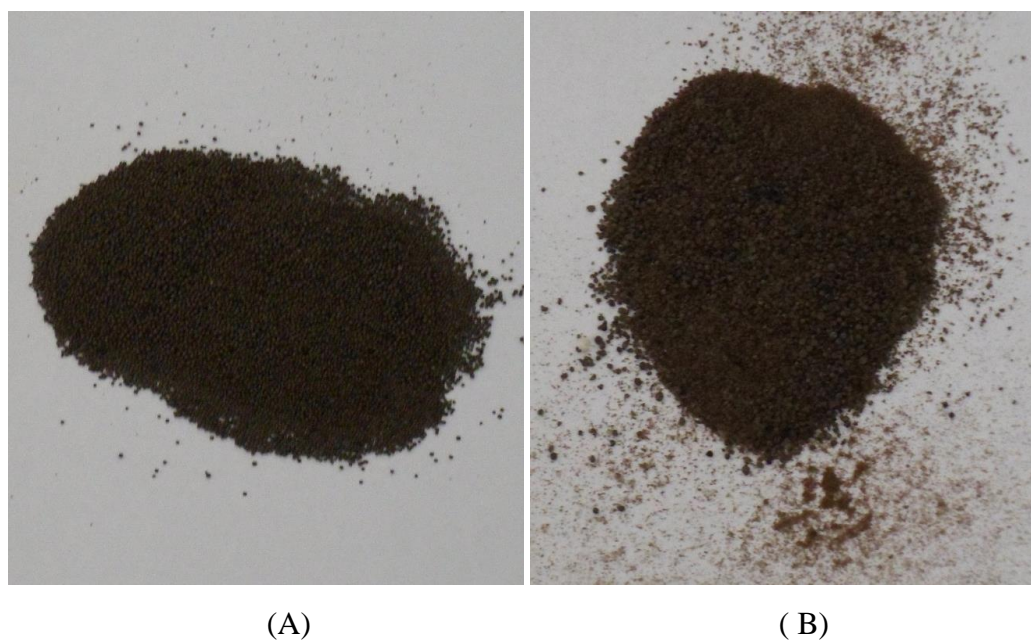


Figure 9.3 Fresh (A) and spent (B) catalysts

The textural properties derived from the N_2 adsorption-desorption isotherms of the fresh and the spent catalyst are listed in Table 9.2. It can be observed that the BET surface area and the total pore volume were reduced from $50 \text{ m}^2/\text{g}$ and 0.35 ml/g , respectively for the fresh catalyst to $35 \text{ m}^2/\text{g}$ and 0.21 ml/g , respectively for the spent catalyst. Interestingly, the average pore diameter increased from 30 nm (in fresh catalyst) to 35 nm (in spent catalyst) during the reaction, which might result from the blockage of the fine pores by the cation exchange with the acid sites of the catalysts.

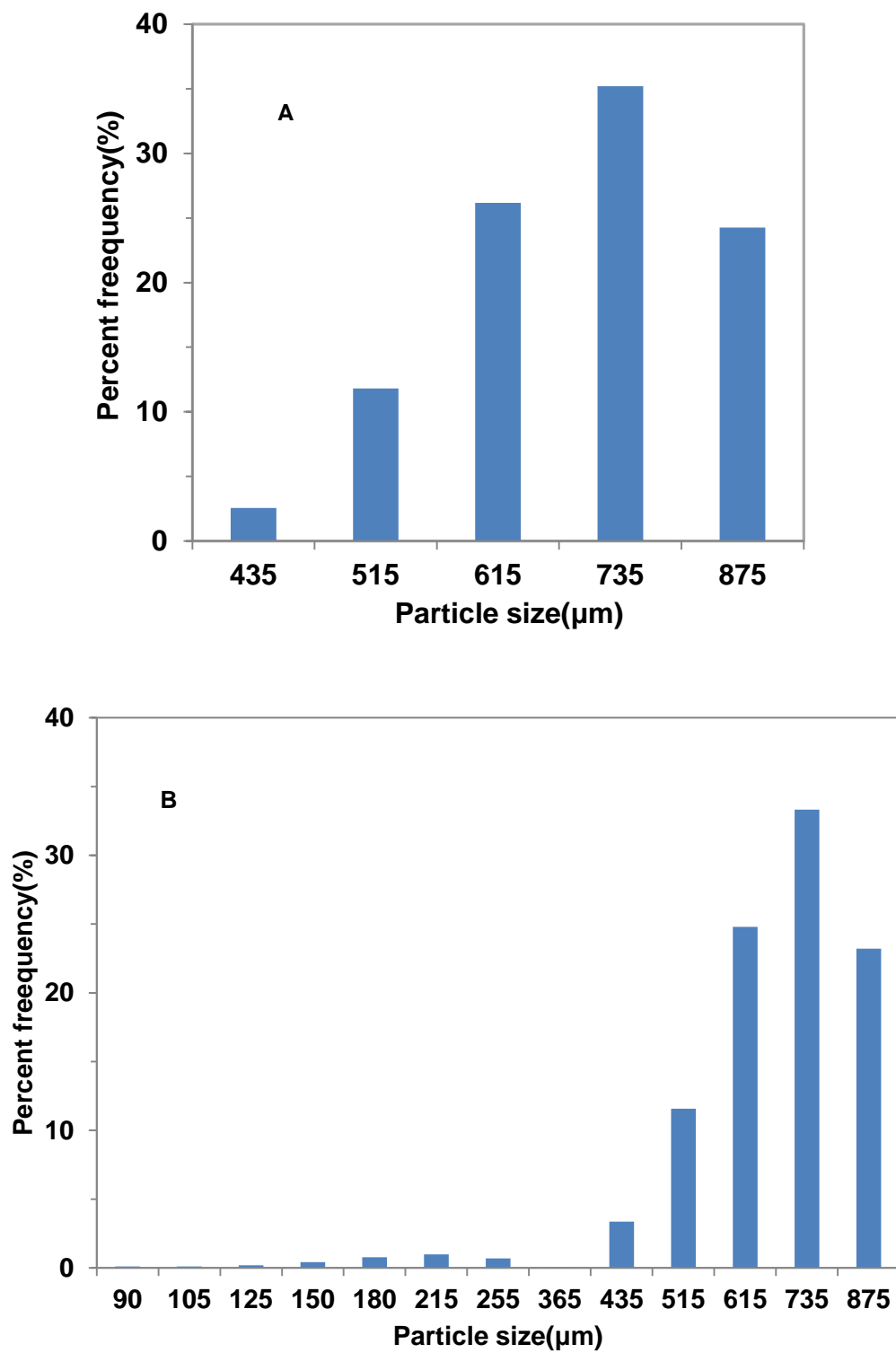


Figure 9.4 Particle size distributions of the fresh (A) and spent (B) catalysts

9.4 Conclusions

A novel continuous-flow reactor consisting of 2 parallel guard reactors and a main reactor was developed for continuous conversion of crude glycerol and purified crude glycerol to solketal by ketalization reaction with acetone. The reaction, carried out over Amberlyst-36 wet catalyst under conditions of 25 °C, 200 psi, and acetone-to-glycerol molar ratio of 4, achieved a 92 ± 2 % solketal yield after 24h on stream at WHSV of 0.38 h^{-1} . The continuous-flow reactor developed enables simultaneous glycerol ketalization and spent catalyst regeneration, leading to continuous operation of the reactor for a longer time while maintaining a high product yield.

References

1. Vicente G, Melero J a., Morales G, Paniagua M, Martín E. Acetalisation of bio-glycerol with acetone to produce solketal over sulfonic mesostructured silicas. *Green Chemistry* 2010;12(5):899. doi:10.1039/b923681c.
2. Royon D, Locatelli S, Gonzo EE. Ketalization of glycerol to solketal in supercritical acetone. *The Journal of Supercritical Fluids* 2011;58(1):88-92. doi:10.1016/j.supflu.2011.04.012.
3. Pariente S, Tanchoux N, Fajula F. Etherification of glycerol with ethanol over solid acid catalysts. *Green Chemistry* 2009;11(8):1256. doi:10.1039/b905405g.
4. Mota CJ a., da Silva CX a., Rosenbach, N, Costa J, da Silva F. Glycerin derivatives as fuel additives: The addition of glycerol/Acetone Ketal (solketal) in gasolines. *Energy & Fuels* 2010;24(4):2733-2736. doi:10.1021/ef9015735.
5. Maksimov AL, Nekhaev AI, Ramazanov DN, Arinicheva YA, Dzyubenko AA, Khadzhiev SN. Preparation of high-octane oxygenate fuel components from plant-derived polyols. *Petroleum Chemistry* 2011;51(1):61-69. doi:10.1134/S0965544111010117.
6. Clarkson JS, Walker AJ, Wood MA. Continuous reactor technology for ketal formation: an improved synthesis of solketal. *Organic Process Research & Development* 2001;5(6):630-635. doi:10.1021/op000135p.
7. Process for preparing acetaldehyde diethyl acetal. 1996. Available at: <http://www.google.com/patents/US5527969>. Accessed April 28, 2015.
8. Frusteri F, Spadaro L, Beatrice C, Guido C. Oxygenated additives production for diesel engine emission improvement. *Chemical Engineering Journal* 2007;134(1-3):239-245. doi:10.1016/j.cej.2007.03.042.
9. Deutsch J, Martin a, Lieske H. Investigations on heterogeneously catalysed condensations of glycerol to cyclic acetals. *Journal of Catalysis* 2007;245(2):428-435. doi:10.1016/j.jcat.2006.11.006.
10. Roldan L, Mallada R, Fraile JM, Mayoral JA, Menendez M. Glycerol upgrading by ketalization in a zeolite membrane. *Asia-Pacific Journal of Chemical Engineering* 2009; 4:279-284
11. Crotti C, Farnetti E, Guidolin N. Alternative intermediates for glycerol valorization: iridium-catalyzed formation of acetals and ketals. *Green Chemistry* 2010;12(12):2225. doi:10.1039/c0gc00096e.
12. Umbarkar SB, Kotbagi T V., Biradar A V., et al. Acetalization of glycerol using mesoporous MoO₃/SiO₂ solid acid catalyst. *Journal of Molecular Catalysis A: Chemical* 2009;310(1-2):150-158. doi:10.1016/j.molcata.2009.06.010.

13. Nanda MR, Yuan Z, Qin W, Ghaziaskar HS, Poirier M-A, Xu CC. Thermodynamic and kinetic studies of a catalytic process to convert glycerol into solketal as an oxygenated fuel additive. *Fuel* 2014;117:470-477. doi:10.1016/j.fuel.2013.09.066.
14. Nanda MR, Yuan Z, Qin W, Ghaziaskar HS, Poirier M-A, Xu C (Charles). A new continuous-flow process for catalytic conversion of glycerol to oxygenated fuel additive: Catalyst screening. *Applied Energy* 2014;123:75-81. doi:10.1016/j.apenergy.2014.02.055.
15. Nanda MR, Yuan Z, Qin W, Ghaziaskar HS, Poirier M-A, Xu C (Charles). Catalytic conversion of glycerol to oxygenated fuel additive in a continuous flow reactor: Process optimization. *Fuel* 2014;128:113-119. doi:10.1016/j.fuel.2014.02.068.
16. Singh SP, Singh D. Biodiesel production through the use of different sources and characterization of oils and their esters as the substitute of diesel: A review. *Renewable and Sustainable Energy Reviews* 2010;14(1):200-216. doi:10.1016/j.rser.2009.07.017.
17. Balat M, Balat H. Progress in biodiesel processing. *Applied Energy* 2010;87(6):1815-1835. doi:10.1016/j.apenergy.2010.01.012.
18. Kongjao S, Damronglerd S, Hunsom M. Purification of crude glycerol derived from waste used-oil methyl ester plant. *Korean Journal of Chemical Engineering* 2010;27(3):944-949. doi:10.1007/s11814-010-0148-0.
19. Isahak WNRW, Ismail M, Yarmo MA, Jahim JM, Salimon J. Purification of Crude Glycerol from Transesterification RBD Palm Oil over Homogeneous and Heterogeneous Catalysts for the Biolubricant Preparation. *Journal of Applied Sciences* 2010;10(21):2590-2595. doi:10.3923/jas.2010.2590.2595.
20. Carmona M, Lech A, de Lucas A, Pérez A, Rodríguez JF. Purification of glycerol/water solutions from biodiesel synthesis by ion exchange: Sodium and chloride removal. Part II. *Journal of Chemical Technology and Biotechnology* 2009;84(8):1130-1135. doi:10.1002/jctb.2144.
21. Carmona M, Valverde JL, Pérez A, Warchol J, Rodríguez JF. Purification of glycerol/water solutions from biodiesel synthesis by ion exchange: sodium removal Part I. *Journal of Chemical Technology & Biotechnology* 2009;84(5):738-744. doi:10.1002/jctb.2106.
22. Ferreira MO, M.B.D. Sousa E, Pereira CG. Purification of Crude Glycerine Obtained from Transesterification of Cottonseed Oil. *International Journal of Chemical Reactor Engineering* 2013;11(1):1-8. doi:10.1515/ijcre-2012-0071.

23. Nanda, M; Yuan Z, Qin W, M.A, Poirier; Xu C. Purification of crude glycerol using acidification : effects of acid types and product characterization. *Austin Journal of Chemical Engineering* 2015;1(1):1-7.
24. Da Silva CX a., Mota CJ a. The influence of impurities on the acid-catalyzed reaction of glycerol with acetone. *Biomass and Bioenergy* 2011;35(8):3547-3551. doi:10.1016/j.biombioe.2011.05.004.
25. He B, Ren Y, Cheng Y, Li J. Deactivation and in Situ Regeneration of Anion Exchange Resin in the Continuous Transesterification for Biodiesel Production. *Energy & Fuels* 2012;26(6):3897-3902. doi:10.1021/ef300524w.
26. Chakrabarti A, Sharma MM. Cationic ion exchange resins as catalyst. *Reactive Polymers* 1993;20(1-2):1-45. doi:10.1016/0923-1137(93)90064-M.

Chapter 10

10 B₂O₃ promoted Cu/Al₂O₃ catalysts for selective hydrogenolysis of glycerol and crude glycerol to 1,2-propanediol

Abstract

The performance of boron oxide (B₂O₃) promoted Cu/Al₂O₃ catalyst in the selective hydrogenolysis of glycerol for the production of 1,2-propane diols (1,2-PDO) was investigated. The catalysts were characterized using N₂-adsorption-desorption isotherm, ICP-AES, XRD, NH₃-TPD, TGA, TPR and TEM. Incorporation of B₂O₃ to Cu/Al₂O₃ was found to enhance the catalytic activity. At the optimum conditions (250 °C temperature, 6 MPa H₂ pressure, 0.1 h⁻¹ WHSV and 5Cu-B/Al₂O₃ catalyst), 10 wt% aqueous solution of glycerol was converted into 1,2-PDO at 98±2% glycerol conversion and 98±2% selectivity. The effect of temperature, pressure, glycerol concentration, boron addition amount, and liquid hourly space velocity were studied. Different grades of glycerol (pharmaceutical, technical or crude glycerol) were used in the process in order to investigate the stability and resistance to deactivation for the selected 5Cu-B/Al₂O₃ catalyst.

Keywords: Boron oxide; Cu/Al₂O₃; Glycerol; Hydrogenolysis reaction; 1,2-Propanediol

10.1 Introduction

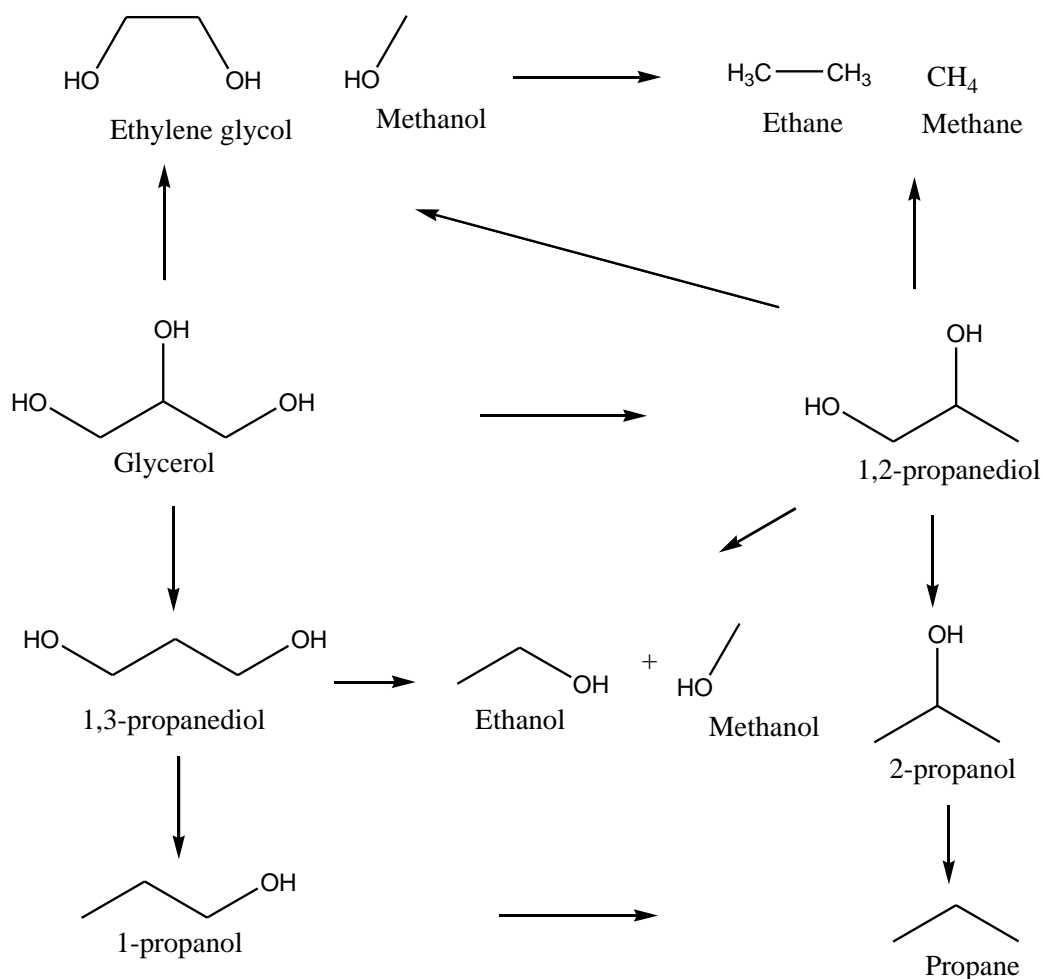
It has been predicted that the booming biodiesel industry will lead to generation of a large amount of glycerol as a by-product or waste stream from the bio-diesel production processes, which will saturate the current global market of glycerol, due to its limited applications developed at present.¹ Therefore, finding new applications for glycerol is an urgently need for the biodiesel industry for better economics and sustainability.

Chemical valorization is one of the pathways in which glycerol could be converted to different high-value chemicals for various applications. Catalytic conversion of glycerol to different value-added chemicals such as acrolein,² solketal,^{3,4} glyceric acids,^{5,6} and propanediols^{7,8} are of great industrial importance. Recently, much attention has been given to valorize glycerol to 1,2-propanediol (1,2-PDO) via catalytic hydrogenolysis.^{9,10,11,12,13,14} 1,2-PDO, a three- carbon diol with a stereogenic centre at the central carbon atom, is one of the most valuable chemicals that can be derived from glycerol. It is mainly used for manufacturing polyester resins, liquid detergents, cosmetics, tobacco humectants, flavors and fragrances, personal care, paints, animal feed, antifreeze, and pharmaceuticals.^{15,16} Conventionally, it is produced by hydration of propylene oxide derived from petroleum-based propylene either by chlorohydrin or by hydroperoxide processes.¹⁷ Therefore the development of an alternative renewable process for the production of 1,2-PDO is highly desirable from the environmental point of view.

Hydrogenolysis of glycerol to 1,2-PDO over metal-based catalysts such as Pt, Ru, Ir, Rh, Pd, Ni and Cu has been extensively reported in literature.^{18,19,20,21,22,23} Noble-metal and Ni-based catalysts have demonstrated excellent catalytic activity,²⁴ nevertheless, these catalysts often promote excessive C-C cleavage, resulting in the formation of degraded lower carbon compounds, such as ethylene glycol, ethanol, methanol and methane.²⁵ Hydrogenolysis of glycerol to different chemical compounds is given in Scheme 10.1. The conversion of glycerol to 1,2-PDO involves the selective cleavage of a C-O bond at one of the primary carbon atoms without breaking the C-C bonds of glycerol. Cu-based catalysts, due to their intrinsic properties have been reported to very effective for selectively cleaving the C-O bond in preference over the C-C bonds in glycerol.²⁶ The catalytic activity of Cu-based catalyst over different supports such as SiO₂,²⁷ ZnO,^{28,29} Al₂O₃,^{30,31} Cr₂O₃,¹²

Zeolites,³² MgO,² etc. have been investigated. Most of these studies were carried out in a batch reactor, while continuous-flow processes would be more desirable due to the ease of the process scale-up and the potential for commercialization of the process.

Promoters are usually incorporated in a catalyst to enhance its activity and stability. A suitable promoter increases the catalyst surface area and dispersion of the catalyst particles by preventing the agglomeration and sintering of the metals and improves the mechanical strength of the catalyst. Rh, Pd, and silicotungstic acid ($\text{H}_4\text{SiW}_{12}\text{O}_{40}$) can be effective promoters for Cu-based catalysts for hydrogenolysis of glycerol to 1,2-PDO, however, the use of these expensive promoters in this process would limit its commercialization potential.^{15,30,33} The use of inexpensive promoters such as boric acid has been reported in Ni/SiO₂,³⁴ and Cu/SiO₂ catalyst systems with excellent interaction with the Ni/Cu metal atoms, resulting in better metal dispersion, suitable acidity and greatly improved catalytic activity.²⁴



Scheme 10.1 Hydrogenolysis of glycerol to different chemicals

The selective hydrogenolysis of glycerol to 1,2-PDO has been investigated either in the presence or absence of a solvent.^{35,36} For instance, Gandaris *et al.* demonstrated a novel catalytic conversion process by employing formic acid as both a solvent and a source of hydrogen.^{19,37} Chaminand *et al.* examined the influence of solvent (aqueous and organic) on the hydrogenolysis of glycerol over Rh/C catalyst in a batch reactor at 180 °C, 80 bar H₂ and for 168 h and reported a higher glycerol conversion in an organic solvent (sulfolane) (32%) than in water (21%).²² As an inexpensive green solvent, water is certainly more desirable than any organic solvents; however it is challenging to carry out the glycerol selective hydrogenolysis reaction in aqueous medium since water is formed as a by-product

during the reaction that could create thermodynamic barrier to shift the reaction in the forward direction. However, considering the environmental impact of organic solvents and the green/low-cost nature of water, water has been commonly used as a solvent for the selective hydrogenolysis of glycerol to 1,2-PDO.^{24,38,39}

The use of crude glycerol as a feedstock for the synthesis of propylene glycol is an important concept for the economical production of propylene glycol and sustainability of the biodiesel industry. However, as mentioned earlier, crude glycerol contains various impurities derived from the biodiesel production processes, including water, sodium or potassium hydroxides, esters, fatty acids, and alcohols. When crude glycerol is used as a feedstock for the conversion reaction, the impurities would cause operating problems by either deactivating the catalyst or plugging the reactors.⁸ There is not much research carried so far on hydrogenolysis of real crude glycerol in a flow reactor, so more work is needed in this regard.

As such, the present work aimed to develop highly active and inexpensive catalysts (boric acid incorporated Cu/Al₂O₃ catalysts) and a continuous-flow process for conversion of glycerol and crude glycerol into 1, 2-PDO in aqueous medium. The scope of the present work is to study the performance of highly dispersed B₂O₃ loaded Cu-based catalysts for the glycerol hydrogenolysis reaction. The effects of various process parameters (Cu loading, B addition amount, temperature, H₂ pressure, weight hourly space velocity, purity of the glycerol feedstock, etc.) on the reaction were also investigated. Moreover, the stability of the selected B₂O₃ loaded Cu-based catalyst was studied.

10.2 Experimental

10.2.1 Materials

Glycerol (99.9%) and methanol (99%) were purchased from Sigma Aldrich and used as received. Reagent grade anhydrous ethanol was supplied from Commercial Alcohols Inc.. 1, 2-PDO (99.9%), 1, 3- PDO (99.9%), ethylene glycol (99.9%), acetol (99.8%), and DMSO (99.9%) as standards for GC calibration were also obtained from Sigma Aldrich. Copper (II) nitrate hydrate [Cu(NO₃)₂.3H₂O], γ - alumina, and boric acid (H₃BO₃) were

purchased from Sigma Aldrich. High purity gases, hydrogen and nitrogen (>99.999%) were supplied by Praxair, Canada.

10.2.2 Catalyst preparation

Firstly, Cu/Al₂O₃ catalyst was prepared by the wet impregnation method using a calculated amount of water-soluble metal salt of copper (II) nitrate hydrate [Cu(NO₃)₂·3H₂O] dissolved in water and γ -Al₂O₃ support material.³⁰ The water was removed by rotary evaporation and the catalyst was then dried at 90 °C for 12 h to form Cu/Al₂O₃ precursor. The B₂O₃ modified Cu/Al₂O₃ catalysts were prepared by incipient wetness impregnation of Cu/Al₂O₃ precursor with aqueous solutions containing the desired amount of H₃BO₃. After impregnation, these samples were dried overnight at 90 °C and then calcined at 400 °C for 5 h under a N₂ flow of 20 mL/min at a heating rate of 2 °C/min. The obtained catalysts are designated as xCu-yB/ Al₂O₃, where x and y represents the mass loading (wt%) of copper and boron, respectively.

10.2.3 Catalyst characterization

The surface area, total pore volume and average pore size of the selected catalysts were measured by nitrogen isothermal (at -196 °C) adsorption with a ASAP 2010 BET apparatus after degassing the samples at 300 °C for 8 h in vacuum.

The acidity of the catalysts was measured by ammonia temperature programmed desorption (NH₃-TPD) using Micromeritics AutoChem II analyzer. Around 0.35 g of the catalyst was pretreated in He at 400 °C to remove moisture and other adsorbed gases on the surface for 1 h. After cooling to 100 °C, the catalyst was saturated with pure NH₃ for 30 min, and then purged with He to remove the physisorbed NH₃ for 30 min. The sample was heated to 500 °C at a ramp rate of 5 °C /min and the NH₃ desorbed was detected by a mass spectrometer.

The crystalline structure of selected catalysts was examined by powder X-ray diffraction (XRD) on a PANalytical X'Pert Pro diffractometer with Cu K α as the radiation source. Step-scans were taken over the range of 2 θ from 6 to 95°.

Temperature programmed reduction (TPR) profiles of the catalysts were collected using a Micromeritics Autochem 2920 equipped with a thermal conductivity detector (TCD). These catalysts were first heated from ambient temperature to 550 °C at 10 °C/min under a 5 vol% O₂/He mixture flow at 50 mL/min for pre-treatment and then exposed to a flowing gas of 10 vol% H₂/Ar at 50 mL/min and were heated from room temperature to 500 °C at a heating rate of 10 °C/min.

The morphologies of the fresh/spent catalysts were observed using a JEOL 2100F transmission electron microscope (TEM) equipped with an energy-dispersive X-ray spectroscopy (EDS-INCA system from oxford instrument).

The thermogravimetric analysis (TGA) of the fresh/spent catalysts was conducted on a thermogravimetric analysis (TGA, Perkin Elmer Pyris 1 TGA unit). The TGA measurements were performed at 10 °C/min over a temperature range of 50 °C to 800 °C under a constant flow of air of 20 ml/min.

10.2.4 Catalytic tests

Hydrogenolysis of glycerol experiments were carried out in a bench-scale continuous down-flow tubular reactor (Inconel 316 tubing, 9.55 mm OD, 6.34 mm ID and 600 mm length) heated with an electric furnace. In a typical run, around 2.0 g of the catalyst was loaded in the constant temperature section of the reactor and supported on a porous Inconel metal disc (pore size: 100 μm) and some quartz wool. Prior to each run, the catalyst was reduced in situ in flowing H₂ (100 cm³/min) at 300 °C for 3 h under atmospheric pressure. The feed - a 10 wt% aqueous solution of glycerol (unless otherwise specified), was pumped using a HPLC pump (Eldex) at a predetermined flow rate into the reactor. This translates to a corresponding weight hourly space velocity (WHSV), defined by the mass of the glycerol per mass of catalyst per hour (h⁻¹). All the experiments were performed at a specified temperature and hydrogen pressure (controlled by a temperature controller and a back-pressure controller, respectively) along with co-feeding of H₂ gas (100 mL/min). The liquid and gas products were cooled and collected in a gas-liquid separator immersed in an ice-water trap.

10.2.5 Product analysis

The components in the reaction mixture were firstly qualitatively analyzed by GC-MS on a Varian 1200 Quadrupole MS (EI) and Varian CP-3800 GC with a VF-5 MS column (5% phenyl/95% dimethyl-polysiloxane, 30 m × 0.25 mm × 0.25 μm)], using helium as the carrier gas at a flow rate of 0.5 mL/s. The oven temperature was maintained at 70 °C for 1 min and then increased to 290 °C at 40 °C/min. Injector and detector temperature were 300 °C. The components were identified by NIST 98 MS library. Quantification of the chemical composition was performed on a GC-FID (Shimadzu -2010) calibrated with 1,2-PDO (99.9%), ethylene glycol (99.9%), and acetol (99.8%). DMSO was used as internal standard. The GC-FID analysis was carried out using the similar separation conditions as mentioned above for the GC-MS analysis. Appendix D provides a typical GC-MS spectrum and the calibration tables and curves for GC-FID. The gas samples were analyzed by a GC-TCD (Agilent 3000 Micro-GC).

The product yields, glycerol conversion and selectivity to 1,2-PDO are defined as follows. In this study, the reported values in most of the Figures and Tables are results obtained after 4h on-stream unless otherwise specified.

$$\text{Yield (\%)} = \frac{\text{Moles of the product formed}}{\text{Initial mole of glycerol}} \times 100 \quad (1)$$

$$\text{Conversion (\%)} = \frac{\text{Initial mole of glycerol} - \text{Final mole of glycerol}}{\text{Initial mole of glycerol}} \times 100 \quad (2)$$

$$\text{Selectivity(\%)} = \frac{\text{Moles of one product formed}}{\text{Initial mole of glycerol} - \text{Final mole of glycerol}} \times 100 \quad (3)$$

10.3 Results and discussion

10.3.1 Catalyst characterization

The textural properties of the fresh/spent Cu/Al₂O₃ catalysts loaded with various amounts of B₂O₃ determined by N₂ adsorption-desorption are presented in Table 10.1. As shown in the Table, an initial improvement in the total pore volume and the BET surface area of the catalyst can be observed by the addition of B₂O₃ (0.25 wt% of Al₂O₃) to 5Cu/Al₂O₃ catalyst, implying that incorporation of a small amount of B₂O₃ might promote the dispersion of the 5Cu/Al₂O₃ catalyst. However, the excess of B₂O₃ loading reduced the surface area and the total pore volume, which could be due to the coverage of the sample surface and blocking of some pores by B₂O₃, as evidenced by the reduction in average pore diameter.

Table 10.1 Textural properties of the fresh/spent Cu/Al₂O₃ catalysts loaded with various amounts of B₂O₃ determined by N₂ adsorption-desorption

Catalyst	BET surface area (m ² /g)	Total pore volume (cc/g)	Pore diameter (Å)	Amount of Cu (wt%) ^a
Al ₂ O ₃	211	0.54	103	
5 Cu/Al ₂ O ₃	182	0.47	100	
5 Cu-0.25B/Al ₂ O ₃	197	0.49	96	
5 Cu-1B/Al ₂ O ₃	184	0.47	99	4.8
5 Cu-3B/Al ₂ O ₃	169	0.38	87	
5 Cu-1B/Al ₂ O ₃ (Spent)	167	0.35	94	4.5

^a measured by ICP-AES

The XRD patterns of the reduced catalysts are displayed in Figure 10.1. In this Figure, all the catalysts have similar XRD patterns and the XRD peaks at $2\theta = 36.3, 45.5, 60.6$ and 66.5 are ascribed to the X-ray diffraction of γ -Al₂O₃ in these catalysts. No X-ray diffraction

lines of either Cu or B species were detected due to the small loading of these elements (below the detection limit of XRD, ~ 5 wt%), which may also suggest high dispersion of the corresponding Cu and B particles in these catalysts.

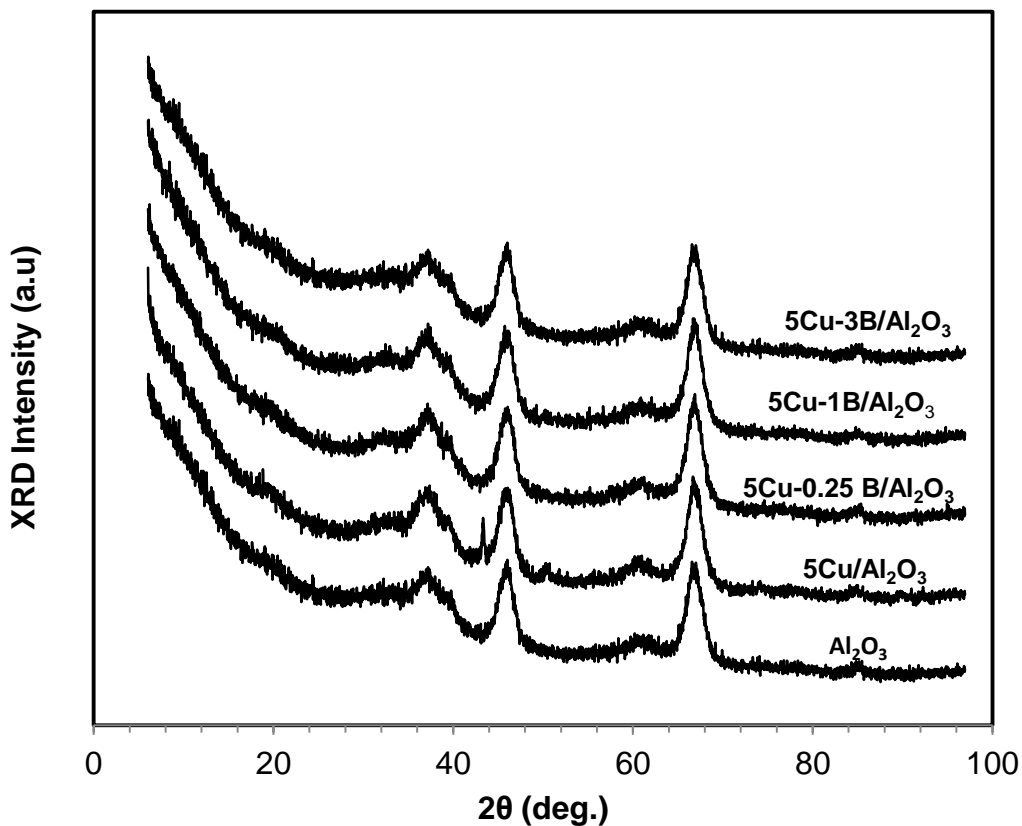


Figure 10.1 XRD patterns of the fresh Cu/Al₂O₃ catalysts loaded with various amounts of B₂O₃

The reducibility of the catalysts was investigated using temperature programmed reduction (TPR). Figure 10.2 illustrates the hydrogen TPR profiles of all the catalysts used in this study. Except 5Cu-0.25B/Al₂O₃, all catalyst samples show a well-resolved single peak in the temperature range of 160-280 °C. The symmetric profile of the reduction peak indicates

the homogeneous nature of the reduced samples and the formation of small monodispersed metallic Cu particles.³⁰ In case of 5Cu-0.25B/Al₂O₃, there exists a main reduction peak (200 °C) and a weak-shoulder peak (220 °C) which might suggest the presence of two different Cu valence states (Cu⁺¹ and Cu⁰).⁴⁰ From the TPR profiles, generally it can be observed that the reduction peak temperature shifts towards a higher temperature with increasing in B content, which might be due to the stronger interaction between CuO and B₂O₃.²⁵

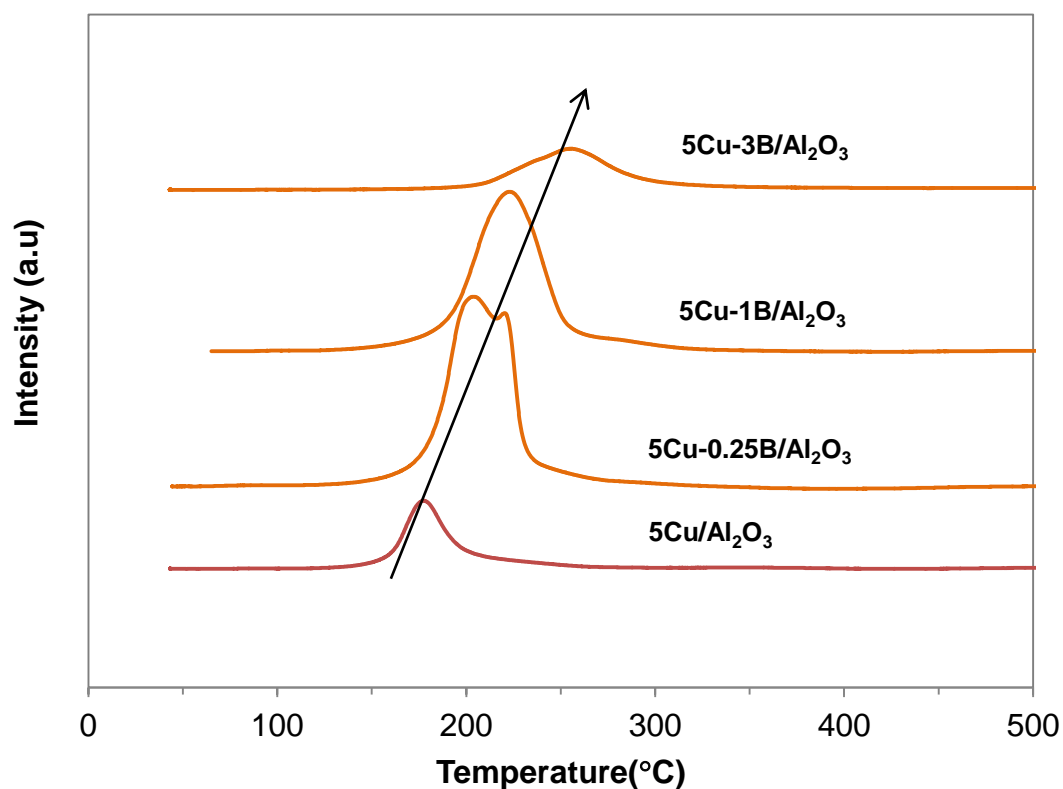


Figure 10.2 H₂-TPR profiles of the fresh Cu/Al₂O₃ catalysts loaded with various amounts of B₂O₃

The catalyst acidity has an important role in the bifunctional mechanism (dehydration and hydrogenation) of selective hydrogenolysis of glycerol to 1,2-PDO.¹⁹ Thus, NH₃-TPD was used to investigate the strength of surface acid sites, and the NH₃-TPD profiles of the fresh Cu/Al₂O₃ catalysts loaded with various amounts of B₂O₃ are presented in Figure 10.3

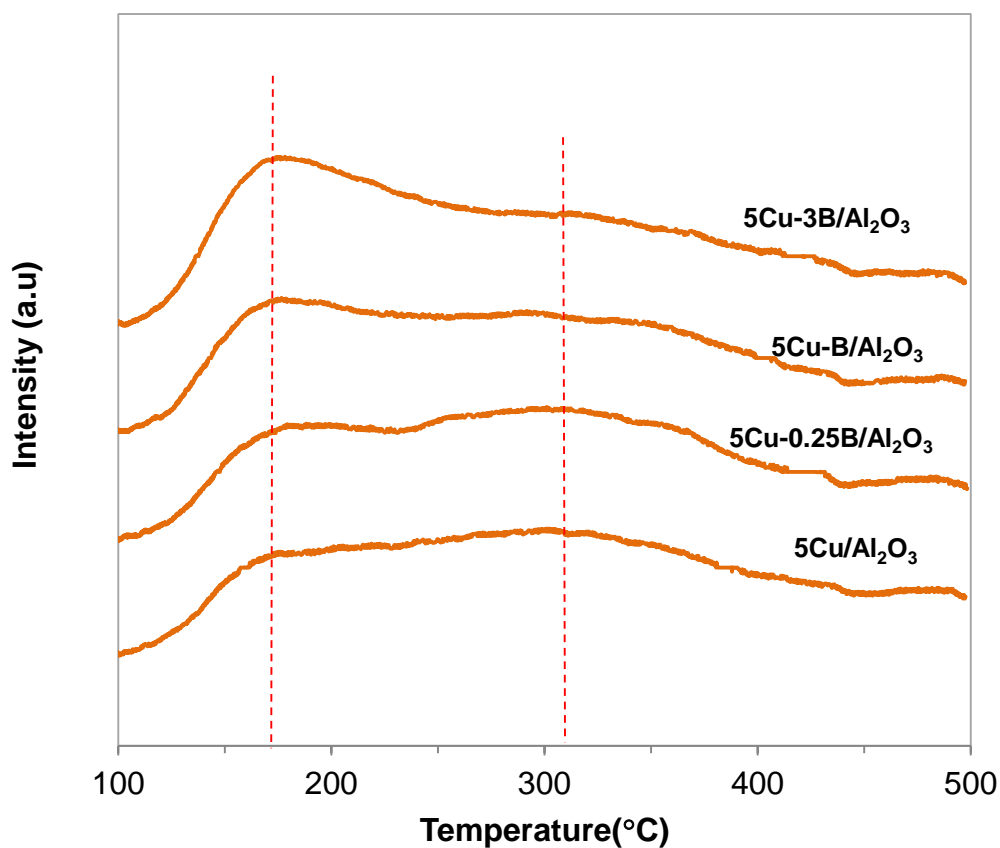


Figure 10.3 NH₃-TPD profiles of the fresh Cu/Al₂O₃ catalysts loaded with various amounts of B₂O₃

The higher ammonia desorption amount/temperature, the more is the strength of the acid sites. As shown in this Figure, two broad ammonia desorption peaks, one at ~170°C, and the other at ~310 °C were observed in all the catalysts, indicating that relatively weak-

intermediate acid sites are present on the catalyst surface.⁴¹ The peak intensity and area of ammonia desorption peaks increase with increasing the B amount, suggesting that the addition of B enhances the acidity of the Cu/Al₂O₃ catalyst, as also reported by Zheng *et al.* in loading boron on Ni-based catalysts for hydrogenation of thiophene-containing ethylbenzene.³⁵

10.3.2 Influence of process parameters

10.3.2.1 Effects of copper loading

The effects of Cu loading on activity of Cu/Al₂O₃ catalysts for glycerol hydrogenolysis were investigated at 230 °C, 5 MPa H₂ and 0.2 h⁻¹ WHSV and the results are summarized in Table 10.2. It can be seen that, with the increase of Cu loading the glycerol conversion first increased and reached a maximum of 71% at a Cu loading of 5wt%. This is attributed to the presence of extra active sites produced by the incorporation of Cu which accelerated the reaction process. A further increase in Cu loading from 5 wt% to 15 wt%, resulted a slight reduction of glycerol conversion to 68%. This reduced activity likely due to the agglomeration of excess Cu, which reduced the dispersion of Cu and blocked the reactive sites on the surface of the catalyst. However, the selectivity towards 1, 2-PDO remains almost unaffected by Cu loading and remained in the range of 85-87%. Since 5 wt% loading of Cu metal over alumina demonstrated the best catalytic performance, it was selected for all further experiments. From the Table, the main byproducts from Cu/Al₂O₃-catalyzed glycerol hydrogenolysis are acetol, ethylene glycol (EG) plus relatively much smaller amounts of compounds denoted as “others” in Table 10.2.

Table 10.2 Effects of Cu loading on activity of Cu/Al₂O₃ catalysts for glycerol hydrogenolysis

Catalyst	Conversion (%)	Selectivity (%)			
		1,2-PDO	EG	Acetol	Others
Al ₂ O ₃	Not detected				
1Cu/Al ₂ O ₃	26 ± 2.3	85± 3.0	2±0.2	11±0.1	2±0.2
3Cu/Al ₂ O ₃	45 ± 2.0	88± 2.0	1±0.1	7 ±0.6	4±0.6
5Cu/Al ₂ O ₃	71 ±3.0	87±1.0	3±0.2	6±0.2	2±0.1
10Cu/Al ₂ O ₃	70 ±2.0	87± 2.0	1±0.1	4±0.5	3±0.3
15Cu/Al ₂ O ₃	68 ±1.0	86± 3.0	2±0.2	6±0.4	3±0.4

10.3.2.2 Effects of B loading

The effects of B loading on 5Cu/Al₂O₃ were studied at the reaction conditions of 230 °C, 6MPa H₂, 0.2 h⁻¹(WHSV), and the results are presented in Figure 10.4. The glycerol conversion and 1,2-PDO selectivity for the catalyst 5Cu/Al₂O₃ without B addition was 73% and 87% , respectively. As clearly shown in this Figure, introducing boron (B) to 5Cu/Al₂O₃ catalyst significantly improved both glycerol conversion and 1, 2-PDO selectivity. At these experimental conditions, 5Cu-1B/Al₂O₃ demonstrated the best performance among catalysts with other B addition amounts, achieving 80% glycerol conversion and 98% selectivity towards 1,2-PDO. Similar results have been reported by Zhu *et al.* for B₂O₃ loaded Cu/SiO₂ catalysts for the synthesis of propylene glycol.²⁴ The enhancement in the catalytic activity by B addition might be attributed to the synergistic effect caused by Cu-B surface interaction which accelerates the surface dispersion and hence activity of Cu metal.²⁴ The improvement in the selectivity towards 1,2-PDO was accompanied by the impairment in the selectivity towards ethylene glycol and acetol, suggesting that the C-C cleavage was suppressed and the conversion of the surplus acetol to 1,2-PDO was promoted over the B loaded catalyst surface. A further increase in boron

content reduced the glycerol conversion and 1, 2-PDO selectivity, which might be due to the masking effect of boron over the Cu catalyst surface and the pores, as evidenced by the substantial decreases in both BET surface area and total pore volume (Table 10.1).

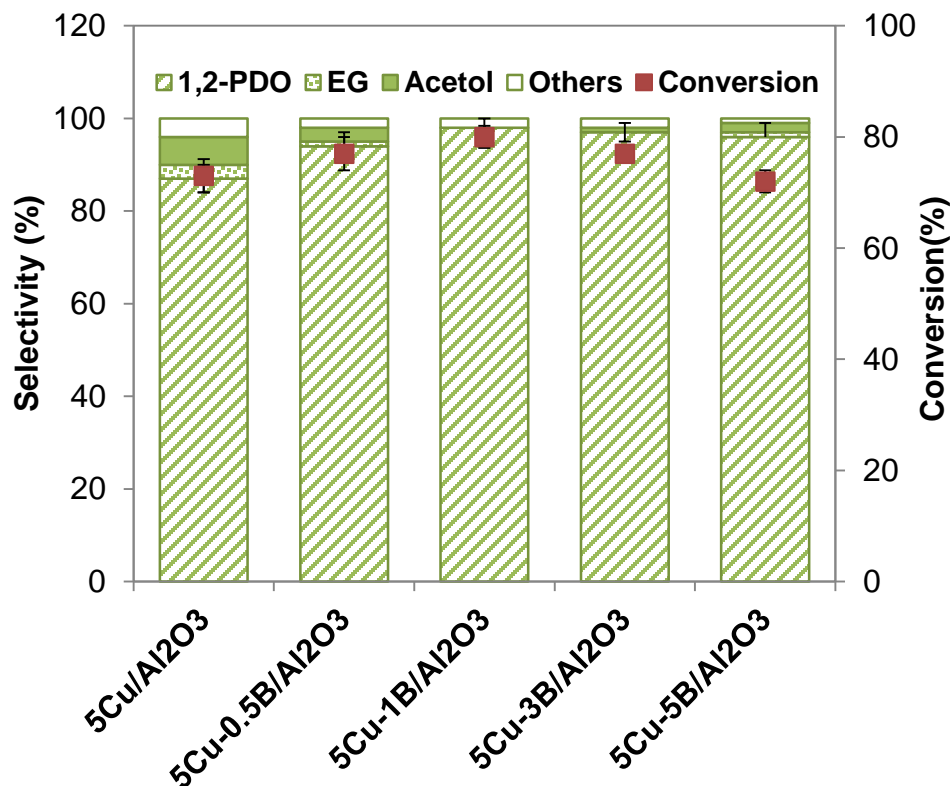


Figure 10.4 Effects of B loading (0-5 wt%) on 5Cu/Al₂O₃ on activity of Cu/Al₂O₃ catalysts for glycerol hydrogenolysis (Experimental conditions: 230 °C, 6 MPa H₂, 10 wt% aq. glycerol, WHSV 0.2 h⁻¹)

10.3.2.3 Effects of temperature

With the best performing 5Cu-1B/Al₂O₃ catalyst, glycerol hydrogenolysis was carried out at various temperatures (170 - 270 °C), 5 MPa H₂, 10 wt% aqueous glycerol and WHSV 0.2 h⁻¹. The effects of temperature on the activity of 5Cu-1B/Al₂O₃ catalyst for glycerol hydrogenolysis are illustrated in Figure 10.5. As expected, the glycerol conversion climbed dramatically from 15% (170 °C) to 99% (270 °C) with negligible variation in the 1, 2-PDO

selectivity of 96-98% at 170-250 °C. 1, 2-PDO selectivity for 5Cu-1B/Al₂O₃ catalyst notably decreased to 85% with further increasing the reaction temperature to 270 °C. The lower selectivity towards 1,2-PDO at higher temperatures is likely related to the formation of large amounts of undesired by-products, such as the over-hydrogenolysis products: 1-propanol, 2-propanol, and the C-C cleavage products, e.g., methanol, ethanol, and ethylene glycol, as described previously.⁴²

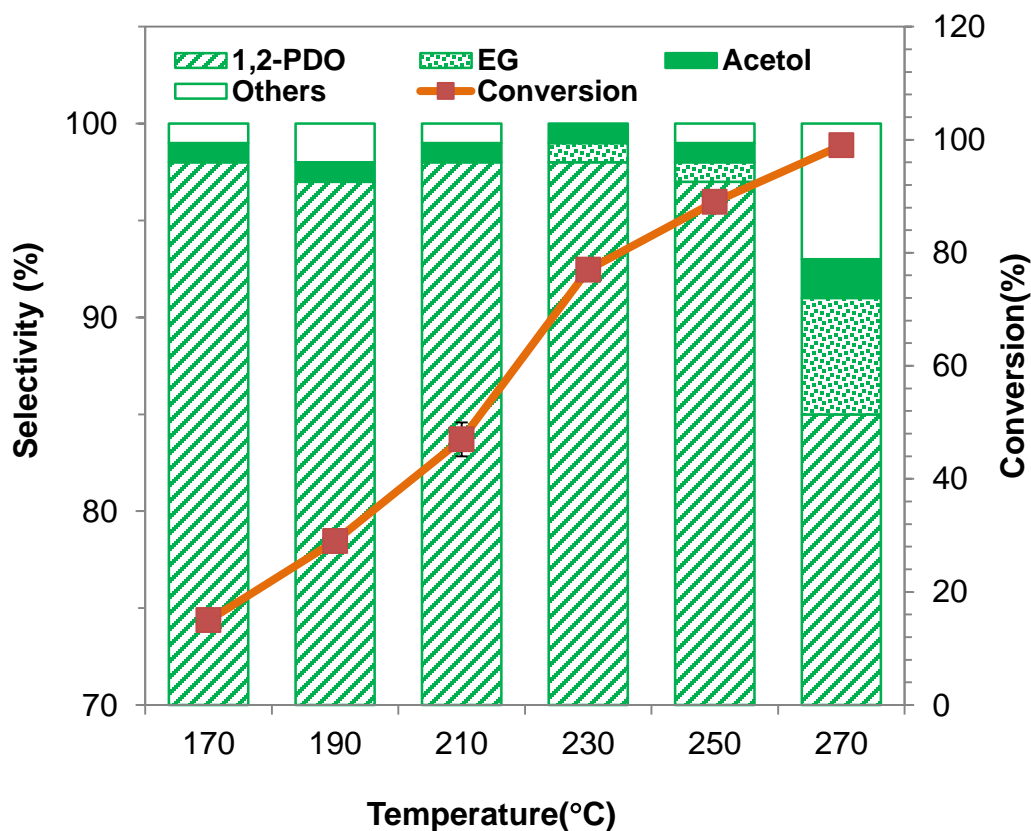


Figure 10.5 Effects of temperature on the activity of 5Cu-1B/Al₂O₃ catalyst for glycerol hydrogenolysis (5 MPa H₂, 10 wt% aq. glycerol and WHSV 0.2 h⁻¹)

10.3.2.4 Effects of hydrogen pressure

Figure 10.6 shows effects of hydrogen pressure (2-8 MPa) on the performance of 5Cu-1B/Al₂O₃ catalyst for glycerol hydrogenolysis (240 °C, 10 wt% aq. glycerol and WHSV 0.4 h⁻¹). Generally both the glycerol conversion and 1,2-PDO selectivity increased by

increasing the hydrogen pressure from 2 MPa H₂ to 6 MPa, as expected. A further increase in hydrogen pressure did not result in any additional increase in the glycerol conversion and 1,2-PDO selectivity. At 6 MPa H₂, the glycerol conversion and 1, 2-PDO selectivity attained 98% and 95%, respectively. The low hydrogen pressure (2 MPa) condition favored the formation of the dehydration product in the reaction, i.e., acetol.

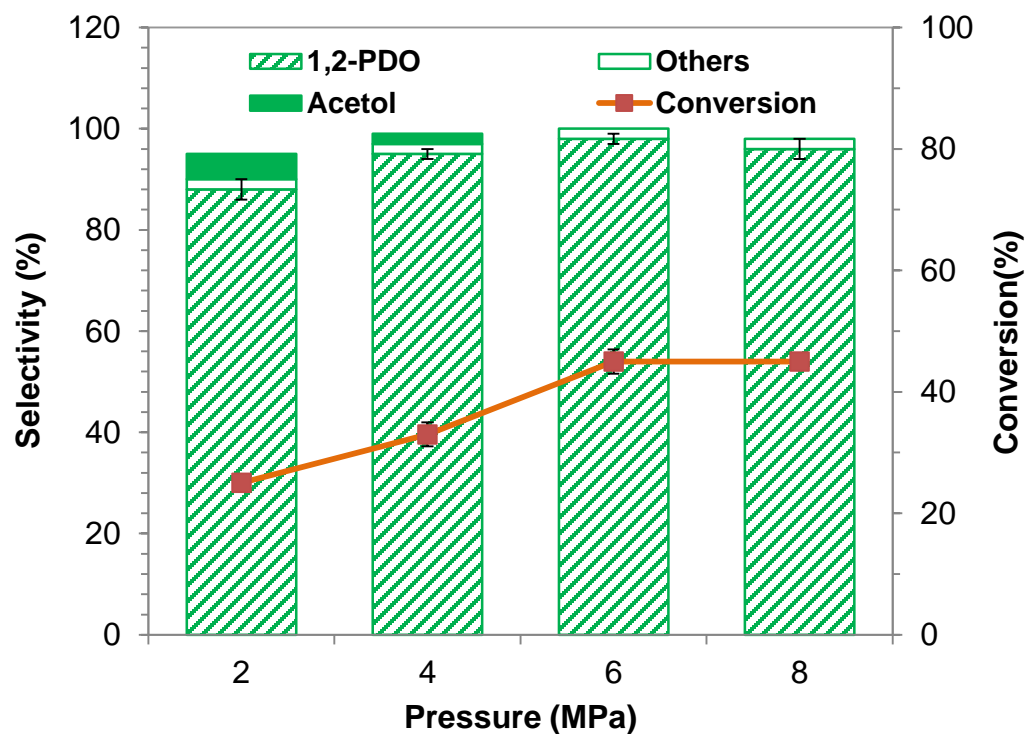


Figure 10.6. Effects of hydrogen pressure (2-8 MPa) on the performance of 5Cu-1B/Al₂O₃ catalyst for glycerol hydrogenolysis (240 °C, 10 wt% aq. glycerol and WHSV 0.4 h⁻¹)

10.3.2.5 Effects of weight hourly space velocity

Effects of WHSV (0.05-0.8 h⁻¹) on the performance of 5Cu-1B/Al₂O₃ catalyst for glycerol hydrogenolysis (250 °C, 6 MPa H₂, 10 wt% aq. glycerol) were studied and the results are shown in Figure 10.7. It is evident that the glycerol conversion drops continuously with

increasing WHSV because of the shortened residence time. However, the selectivity of 1,2-PDO remains almost unchanged (96-98%) when the WHSV varies between 0.1- 0.8 h⁻¹, but it was as low as 78% when the WHSV was reduced to 0.05 h⁻¹, which is likely caused by the excessive hydrogenolysis reaction converting 1,2-PDO to ethylene glycol and other lower alcohols like ethanol and methanol at a too long residence time.⁴⁰ Hence to get a good conversion of glycerol with high selectivity to 1, 2-PDO, the optimal WHSV is likely 0.1 h⁻¹.

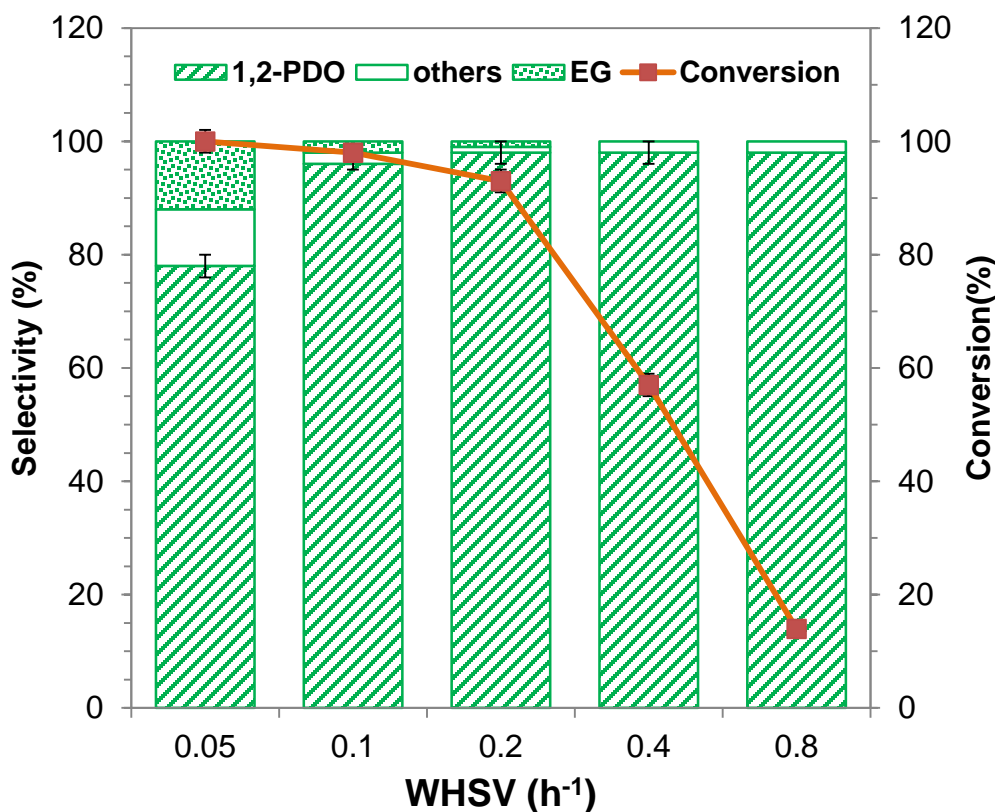


Figure 10.7 Effects of WHSV (0.05-0.8 h⁻¹) on the performance of 5Cu-1B/Al₂O₃ catalyst for glycerol hydrogenolysis (250 °C, 6 MPa H₂, 10 wt% aq. glycerol)

10.3.3 Effects of glycerol feedstock purity

One of the objectives of the present work was to evaluate the possibility of using low-grade glycerol for hydrogenolysis to 1, 2-PDO. Specifically, crude glycerol (54.7% purity) and

technical grade glycerol (91.6 % purity) were tested, in comparison to pharmaceutical grade glycerol (99.9 % purity). The mass composition of different grades of glycerol used in this work is given in Table 10.3. The presence of impurities would adversely affect the performance of the catalyst, as discussed previously. For instance, the presence of water imposes a thermodynamic barrier, limiting the reaction. The salt impurities could deactivate the catalyst surface and other organic impurities present in crude glycerol could compete with the glycerol in the adsorption on the catalyst surface, hence retard its reaction.

Table 10.3 Composition of different grades of glycerol

Glycerol grade	Purity (%)	Water (%)	Ash (%)	MONG (%)
Pharmaceutical	99.9	0.1	<0.001	N.D
Technical	91.6	4.3	1.4	2.7
Crude	54.7	12.8	7.3	25.2

MONG: matter organic non-glycerol; n.d.: not detected

Figure 10.8 shows the glycerol conversions and selectivity of different products achieved with different grades of glycerol with 5Cu-1B/Al₂O₃ catalyst at the reaction conditions of 250 °C, 10 wt% aq. solution, 6 MPa, WHSV 0.1 h⁻¹. As expected, reactions performed with technical grade and crude glycerol resulted in substantially reduced glycerol conversion and 1,2-PDO selectivity, which clearly indicates the negative impact of the impurities in the glycerol feedstock on the hydrogenolysis of glycerol due to the deactivation of the catalyst.⁸

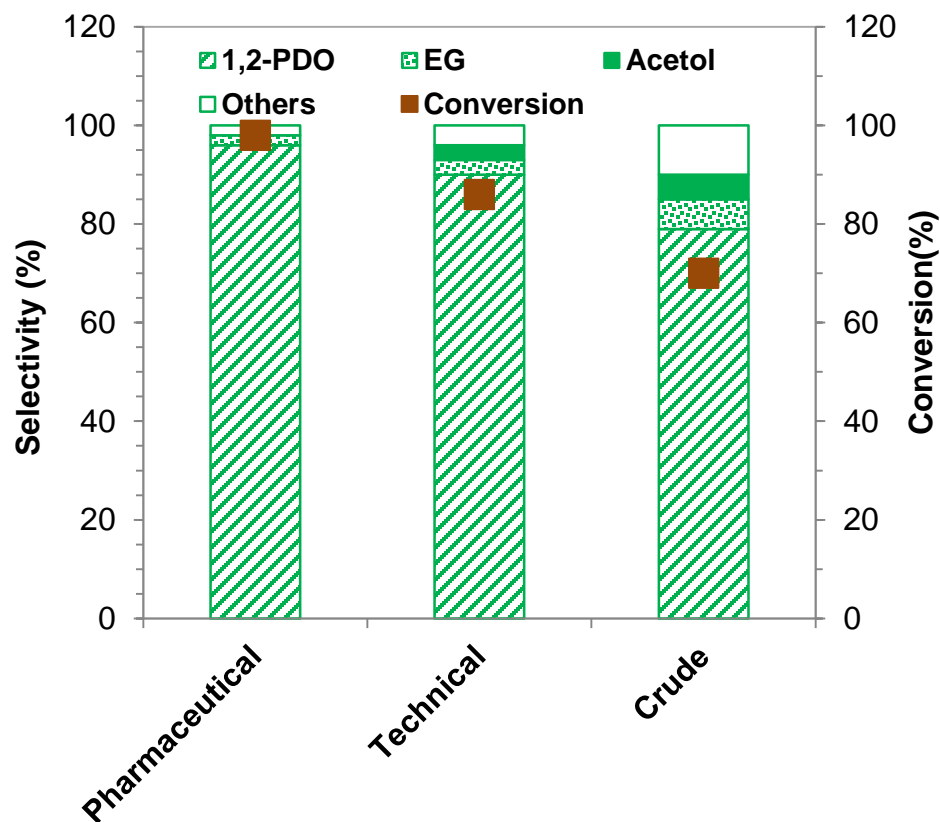


Figure 10.8. Influence of different grades of glycerol on glycerol conversion and product selectivities with 5Cu-1B/Al₂O₃ catalyst (Reaction conditions: 250 °C, 10 wt% aq. glycerol feedstock, 6 MPa, WHSV 0.1 h⁻¹).

10.3.4 Long term stability and catalyst deactivation

The long term performance of glycerol hydrogenolysis over 5Cu-1B/Al₂O₃ catalyst was tested at 250 °C, 6 MPa H₂ flow, and 0.1 h⁻¹, and the results are given in Figure 10.9. No sign of any decline in the catalyst activity (>95% glycerol conversion and >97% 1,2-PDO selectivity) was observed up to 60 h, despite the harsh reaction conditions, which suggest promise of the 5Cu-1B/Al₂O₃ catalyst for industrial application. After this time, the glycerol conversion gradually decreased. Meanwhile, the product distribution did not show any appreciable change during this period. These results are in good-agreement with those reported in the literature.³⁰

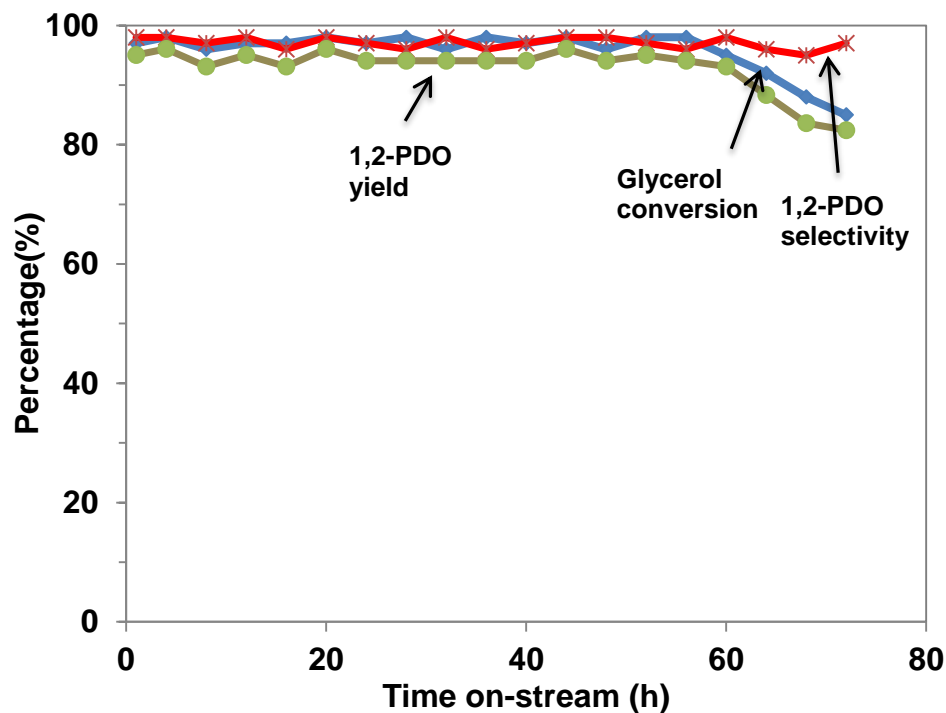


Figure 10.9 Long term stability of 5Cu-1B/Al₂O₃ catalyst in glycerol hydrogenolysis conducted at 250 °C, 6 MPa H₂ flow and 0.1 h⁻¹.

Deactivation of the catalyst was observed after 60 h on stream, as shown in Fig. 10.9. Usually, in a heterogeneous system, the catalyst deactivation occurs due to destruction of support structure, sintering, coking, fouling or leaching of catalyst.⁴³ Comparison of the surface area and the pore volume of the fresh and spent catalyst (Table 10.1), it is revealed that both the BET surface area and total pore volume for the spent catalyst were reduced, suggesting sintering of the Cu metal or deposition of fouling materials inside the pores of the 5Cu-1B/Al₂O₃ catalyst might occur during the long term stability test. To prove this hypothesis, TEM and TGA measurements were performed on the fresh and spent (after 70h on stream) catalysts of 5Cu-1B/Al₂O₃. TEM micrographs of fresh and spent catalyst are illustrated in Figure 10.10 a/b, where the presence of Cu particles was confirmed by EDX. Limited by the magnification of the TEM instrument, however, only clusters of the Cu particles were observable in the fresh and spent catalysts.

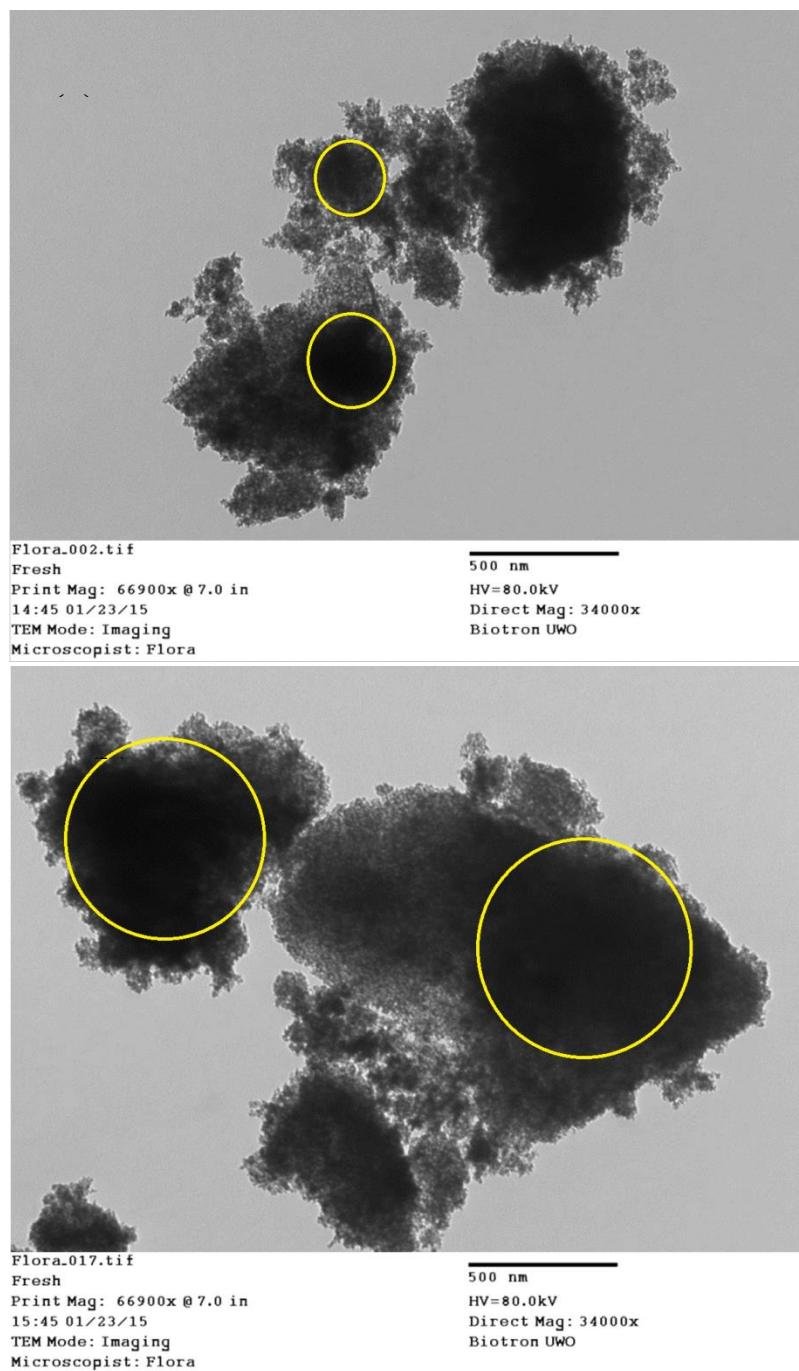


Figure 10.10 TEM micrographs of fresh (a) spent catalyst (b) of 5Cu-1B/Al₂O₃ after 70 h on stream

Figure 10.11 shows the TG thermogram of fresh and spent catalysts of 5Cu-1B/Al₂O₃ after 70 h on stream. The TGA measurements were performed at 10 °C/min over a temperature range of 50 °C to 800 °C under a constant flow of air of 20 ml/min. From the TG thermograms of the fresh and spent catalysts, a total of 30 wt% weight loss was observed over the range of 50 °C to 800 °C for the spent catalyst, compared with only <8 wt% weight loss for the fresh catalyst. This result may evidence the deposition of fouling materials due to polymerization of glycerol on the spent catalyst, which could contribute to the deactivation of the catalyst by blocking the catalyst active sites.

Moreover, the concentration of Cu metal in the fresh and the spent catalyst was measured by ICP-AES and given in Table 10.1. A negligible change in the concentration of Cu between the fresh and spent catalyst was observed (4.79% to 4.46%) indicating a trivial role of leaching on the catalyst deactivation.

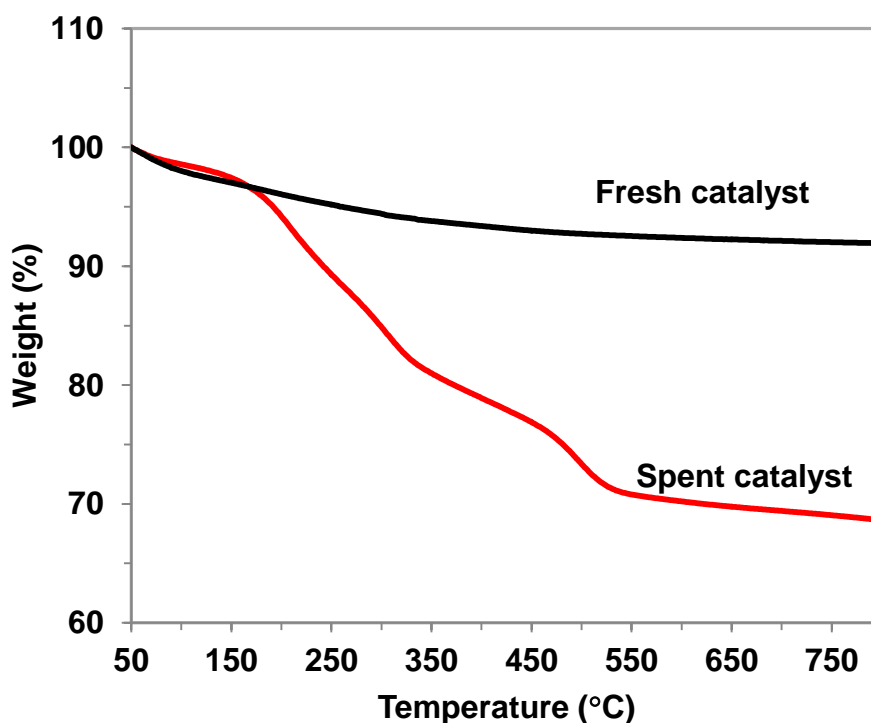


Figure 10.11 Thermogravimetric analysis of fresh and spent catalyst of 5Cu-1B/Al₂O₃ after 70 h on stream

10.4 Conclusions

The addition of B_2O_3 into Cu/Al_2O_3 catalysts enhanced the catalytic activity for the glycerol hydrogenolysis reaction. Among all catalysts prepared and tested, 5Cu-1B/ Al_2O_3 demonstrated the best catalytic performance with $98 \pm 2\%$ glycerol conversion and $98 \pm 2\%$ 1, 2-PDO selectivity in hydrogenolysis of 10 wt% aqueous solution of glycerol at the optimum conditions (250 °C temperature, 6 MPa H_2 pressure, and $0.1 h^{-1}$ WHSV). Process parameters such as temperature, hydrogen pressure, and liquid hourly space velocity significantly influenced the catalytic activity for the glycerol hydrogenolysis reaction. The use of different grades of glycerol, including the pharmaceutical grade glycerol, technical grade glycerol and crude glycerol (glycerol purity varying from 54.7% to 99.9 %), in the process showed that the presence of impurities could reduce the glycerol conversion and 1,2-PDO selectivity. The long term stability test demonstrated that the 5Cu-1B/ Al_2O_3 catalyst could be used up to 60 h without any appreciable change in activity. Destruction of the support structure, sintering of Cu metal, and coke deposition on the catalyst were found to be the main factors that deactivated the catalyst after 60 h on stream.

References

1. Maris E, Ketchie W, Murayama M, Davis R. Glycerol hydrogenolysis on carbon-supported PtRu and AuRu bimetallic catalysts. *Journal of Catalysis* 2007;251(2):281-294. doi:10.1016/j.jcat.2007.08.007.

2. Yuan Z, Wang J, Wang L, *et al.* Biodiesel derived glycerol hydrogenolysis to 1,2-propanediol on Cu/MgO catalysts. *Bioresource Technology* 2010;101(18):7099-103. doi:10.1016/j.biortech.2010.04.016.
3. Nanda MR, Yuan Z, Qin W, Ghaziaskar HS, Poirier M-A, Xu C (Charles). A new continuous-flow process for catalytic conversion of glycerol to oxygenated fuel additive: Catalyst screening. *Applied Energy* 2014;123:75-81. doi:10.1016/j.apenergy.2014.02.055.
4. Nanda MR, Yuan Z, Qin W, Ghaziaskar HS, Poirier M-A, Xu CC. Thermodynamic and kinetic studies of a catalytic process to convert glycerol into solketal as an oxygenated fuel additive. *Fuel* 2014;117:470-477. doi:10.1016/j.fuel.2013.09.066.
5. Behr A, Eilting J, Irawadi K, Leschinski J, Lindner F. Improved utilisation of renewable resources: New important derivatives of glycerol. *Green Chemistry* 2008;10(1):13. doi:10.1039/b710561d.
6. Ma L, He D, Li Z. Promoting effect of rhenium on catalytic performance of Ru catalysts in hydrogenolysis of glycerol to propanediol. *Catalysis Communications* 2008;9(15):2489-2495. doi:10.1016/j.catcom.2008.07.009.
7. Feng J, Fu H, Wang J, Li R, Chen H, Li X. Hydrogenolysis of glycerol to glycols over ruthenium catalysts: Effect of support and catalyst reduction temperature. *Catalysis Communications* 2008;9(6):1458-1464. doi:10.1016/j.catcom.2007.12.011.
8. Atia H, Armbruster U, Martin a. Dehydration of glycerol in gas phase using heteropolyacid catalysts as active compounds. *Journal of Catalysis* 2008;258(1):71-82. doi:10.1016/j.jcat.2008.05.027.
9. Auttanat T, Jongpatiwut S, Rirksomboon T. Dehydroxylation of glycerol to propylene glycol over Cu-ZnO / Al₂O₃ Catalyst : Effect of feed purity. *World Academy of Science, Engineering and Technology*, 2012, 6. 2012;6(4):400-403..
10. Barbelli ML, Santori GF, Nichio NN. Aqueous phase hydrogenolysis of glycerol to bio-propylene glycol over Pt-Sn catalysts. *Bioresource Technology* 2012;111:500-3. doi:10.1016/j.biortech.2012.02.053.
11. Dasari M a., Kiatsimkul P-P, Sutterlin WR, Suppes GJ. Low-pressure hydrogenolysis of glycerol to propylene glycol. *Applied Catalysis A: General* 2005;281(1-2):225-231. doi:10.1016/j.apcata.2004.11.033.
12. Deng C, Duan X, Zhou J, Chen D, Zhou X, Yuan W. Size effects of Pt-Re bimetallic catalysts for glycerol hydrogenolysis. *Catalysis Today* 2014;234:208-214. doi:10.1016/j.cattod.2014.02.023.

13. D'Hondt E, Van de Vyver S, Sels BF, Jacobs P a. Catalytic glycerol conversion into 1,2-propanediol in absence of added hydrogen. *Chemical communications (Cambridge, England)* 2008;(45):6011-2. doi:10.1039/b812886c.
14. Kim ND, Park JR, Park DS, Kwak BK, Yi J. Promoter effect of Pd in CuCr₂O₄ catalysts on the hydrogenolysis of glycerol to 1,2-propanediol. *Green Chemistry* 2012;14(9):2638. doi:10.1039/c2gc00009a.
15. Balaraju M, Rekha V, Prasad PSS, Devi BLAP, Prasad RBN, Lingaiah N. Influence of solid acids as co-catalysts on glycerol hydrogenolysis to propylene glycol over Ru/C catalysts. *Applied Catalysis A: General* 2009;354(1-2):82-87. doi:10.1016/j.apcata.2008.11.010.
16. Zhou C-HC, Beltramini JN, Fan Y-X, Lu GQM. Chemoselective catalytic conversion of glycerol as a biorenewable source to valuable commodity chemicals. *Chemical Society reviews* 2008;37(3):527-49. doi:10.1039/b707343g.
17. Vasiliadou ES, Eggenhuisen TM, Munnik P, de Jongh PE, de Jong KP, Lemonidou a. a. Synthesis and performance of highly dispersed Cu/SiO₂ catalysts for the hydrogenolysis of glycerol. *Applied Catalysis B: Environmental* 2014;145:108-119. doi:10.1016/j.apcatb.2012.12.044.
18. Gandarias I, Arias PL, Requies J, El Doukkali M, Güemez MB. Liquid-phase glycerol hydrogenolysis to 1,2-propanediol under nitrogen pressure using 2-propanol as hydrogen source. *Journal of Catalysis* 2011;282(1):237-247. doi:10.1016/j.jcat.2011.06.020.
19. Xiao Z, Wang X, Xiu J, Wang Y, Williams CT, Liang C. Synergetic effect between Cu⁰ and Cu⁺ in the Cu-Cr catalysts for hydrogenolysis of glycerol. *Catalysis Today* 2014;234:200-207. doi:10.1016/j.cattod.2014.02.025.
20. Panyad S, Jongpatiwut S, Sreethawong T, Rirkomboon T, Osuwan S. Catalytic dehydroxylation of glycerol to propylene glycol over Cu-ZnO/Al₂O₃ catalysts: Effects of catalyst preparation and deactivation. *Catalysis Today* 2011;174(1):59-64. doi:10.1016/j.cattod.2011.03.029.
21. Chaminand J, Djakovitch L auren., Gallezot P, Marion P, Pinel C, Rosier C. Glycerol hydrogenolysis on heterogeneous catalysts. *Green Chemistry* 2004;6(8):359. doi:10.1039/b407378a.
22. Miyazawa T, Kusunoki Y, Kunimori K, Tomishige K. Glycerol conversion in the aqueous solution under hydrogen over Ru/C + an ion-exchange resin and its reaction mechanism. *Journal of Catalysis* 2006;240(2):213-221. doi:10.1016/j.jcat.2006.03.023.
23. Zhu S, Gao X, Zhu Y, Zhu Y, Zheng H, Li Y. Promoting effect of boron oxide on Cu/SiO₂ catalyst for glycerol hydrogenolysis to 1,2-propanediol. *Journal of Catalysis* 2013;303:70-79. doi:10.1016/j.jcat.2013.03.018.

24. Furikado I, Miyazawa T, Koso S, Shima A, Kunimori K, Tomishige K. Catalytic performance of Rh/SiO₂ in glycerol reaction under hydrogen. *Green Chemistry* 2007;9(6):582. doi:10.1039/b614253b.
25. Huang Z, Liu H, Cui F, Zuo J, Chen J, Xia C. Effects of the precipitation agents and rare earth additives on the structure and catalytic performance in glycerol hydrogenolysis of Cu/SiO₂ catalysts prepared by precipitation-gel method. *Catalysis Today* 2014;234:223-232. doi:10.1016/j.cattod.2014.02.037.
26. Huang Z, Cui F, Xue J, Zuo J, Chen J, Xia C. Cu/SiO₂ catalysts prepared by hom- and heterogeneous deposition-precipitation methods: Texture, structure, and catalytic performance in the hydrogenolysis of glycerol to 1,2-propanediol. *Catalysis Today* 2012;183(1):42-51. doi:10.1016/j.cattod.2011.08.038.
27. Wang S, Liu H. Selective hydrogenolysis of glycerol to propylene glycol on Cu-ZnO catalysts. *Catalysis Letters* 2007;117(1-2):62-67. doi:10.1007/s10562-007-9106-9.
28. Bienholz A, Schwab F, Claus P. Hydrogenolysis of glycerol over a highly active CuO/ZnO catalyst prepared by an oxalate gel method: influence of solvent and reaction temperature on catalyst deactivation. *Green Chemistry* 2010;12(2):290. doi:10.1039/b914523k.
29. Hao S-L, Peng W-C, Zhao N, Xiao F-K, Wei W, Sun Y-H. Hydrogenolysis of glycerol to 1,2-propanediol catalyzed by Cu-H₄SiW₁₂O₄₀/Al₂O₃ in liquid phase. *Journal of Chemical Technology & Biotechnology* 2010;(May):n/a-n/a. doi:10.1002/jctb.2456.
30. Vila F, López Granados M, Ojeda M, Fierro JLG, Mariscal R. Glycerol hydrogenolysis to 1,2-propanediol with Cu/ γ -Al₂O₃: Effect of the activation process. *Catalysis Today* 2012;187(1):122-128. doi:10.1016/j.cattod.2011.10.037.
31. Niu L, Wei R, Yang H, Li X, Jiang F, Xiao G. Hydrogenolysis of glycerol to propanediols over Cu-MgO/USY catalyst. *Chinese Journal of Catalysis* 2013;34(12):2230-2235. doi:10.1016/S1872-2067(12)60695-0.
32. Xia S, Yuan Z, Wang L, Chen P, Hou Z. Catalytic production of 1,2-propanediol from glycerol in bio-ethanol solvent. *Bioresource Technology* 2012;104:814-7. doi:10.1016/j.biortech.2011.11.031.
33. Zheng J, Xia Z, Li J, *et al.* Promoting effect of boron with high loading on Ni-based catalyst for hydrogenation of thiophene-containing ethylbenzene. *Catalysis Communications* 2012;21:18-21. doi:10.1016/j.catcom.2012.01.025.
34. Ma L, He D. Influence of catalyst pretreatment on catalytic properties and performances of Ru-Re/SiO₂ in glycerol hydrogenolysis to propanediols. *Catalysis Today* 2010;149(1-2):148-156. doi:10.1016/j.cattod.2009.03.015.

35. Perosa A, Tundo P. Selective Hydrogenolysis of Glycerol with Raney Nickel †. *Industrial & Engineering Chemistry Research* 2005;44(23):8535-8537. doi:10.1021/ie0489251.
36. Gandarias I, Fernández SG, El Doukkali M, Requies J, Arias PL. Physicochemical Study of Glycerol Hydrogenolysis Over a Ni–Cu/Al₂O₃ Catalyst Using Formic Acid as the Hydrogen Source. *Topics in Catalysis* 2013;56(11):995-1007. doi:10.1007/s11244-013-0063-9.
37. Guerreiro ED, Gorriz OF, Rivarola JB, Arrúa LA. Characterization of Cu/SiO₂ catalysts prepared by ion exchange for methanol dehydrogenation. *Applied Catalysis A: General* 1997;165(1-2):259-271. doi:10.1016/S0926-860X(97)00207-X.
38. Lewandowski M, Sarbak Z. The effect of boron addition on hydrodesulfurization and hydrodenitrogenation activity of NiMo/Al₂O₃ catalysts. *Fuel* 2000;79(5):487-495. doi:10.1016/S0016-2361(99)00151-9.
39. Zhou J, Guo L, Guo X, Mao J, Zhang S. Selective hydrogenolysis of glycerol to propanediols on supported Cu-containing bimetallic catalysts. *Green Chemistry* 2010;12(10):1835. doi:10.1039/c0gc00058b.
40. Xiao Z, Li C, Xiu J, Wang X, Williams CT, Liang C. Insights into the reaction pathways of glycerol hydrogenolysis over Cu–Cr catalysts. *Journal of Molecular Catalysis A: Chemical* 2012;365:24-31. doi:10.1016/j.molcata.2012.08.004.
41. Telkar MM, Rode CV, Rane VH, Jaganathan R, Chaudhari RV. Selective hydrogenation of 2-butyne-1,4-diol to 2-butene-1,4-diol: roles of ammonia, catalyst pretreatment and kinetic studies. *Applied Catalysis A: General* 2001;216(1-2):13-22. doi:10.1016/S0926-860X(01)00547-6.
42. Zhou J, Zhang J, Guo X, Mao J, Zhang S. Ag/Al₂O₃ for glycerol hydrogenolysis to 1,2-propanediol: activity, selectivity and deactivation. *Green Chemistry* 2012;14(1):156. doi:10.1039/c1gc15918f.

Chapter 11

11 Techno-economic analysis for production of an oxygenated fuel additive from crude glycerol in Canada

Abstract

The present study aims to conceptually design an integrated plant for the production of solketal - an oxygenated fuel additive with a capacity of 16,000 L/day using crude glycerol as the feedstock. The operating costs of the process were evaluated. The process incorporated pretreatment of the crude glycerol by acidification and production of solketal by ketalization of the purified crude glycerol with acetone. The following costs were considered in the present analysis: feedstock and raw materials, labor, electricity, plant overhead and maintenance, capital depreciation, etc. The pretreatment and production costs were estimated to be \$0.144/L and \$0.86/L, respectively. Using crude glycerol as the feedstock over the commercially available pure glycerol, an annual cost saving of \$565,724 can be predicted from the plant with a capacity of 16,000 L solketal per day.

Keywords: Solketal; Crude glycerol; Cost analysis; Pretreatment; Ketalization

11.1 Introduction

The awareness of the fast depletion of fossil fuels and their environmental impact in recent decades has resulted in an increasing interest in alternative energy resources for energy and chemical production. Biodiesel has demonstrated its potential as a green substitute to the petroleum-based diesel fuel. Biodiesel has many advantages, of which the prominent ones are: (1) its compatibility with commercial diesel engines, and (2) its biodegradability and low toxicity and emission in relation to fossil fuels.^{1,2}

Recently, biodiesel is produced by transesterification of triglycerides with methanol in presence of acidic or basic catalysts.³ In addition, the process yields a main by-product - glycerol amounting approx. 10 wt% of the total biodiesel produced.⁴ The crude glycerol generated from a biodiesel plant contains a wide range of impurities such as methanol, water, salt, and free fatty acids.⁵ Typical composition of crude glycerol is shown in Table 11.1.^{6,7,8} The composition of crude glycerol depends on the nature of feedstock materials and the process used for biodiesel production.⁹ Valorization of the byproduct will greatly improve the overall economy of biodiesel industry. For instance, with more than 1500 applications, pure glycerol has a price as high as \$0.6-0.9/kg, contributing a credit to the biodiesel industry.¹⁰ However, the recent glycerol market has been saturated by thriving of biodiesel plants causing a decline in crude glycerol price. Crude glycerol can be available in the current market at a price as low as \$0.05/kg.^{9,11,12} This reduced price of glycerol will have a significant impact on the sustainability of the biodiesel industry. Therefore, high-value applications of glycerol, such as catalytic conversion of glycerol to solketal, should be developed.^{13,14,15}

Solketal is a versatile chemical that can be used as an oxygenated fuel additive to improve various fuel properties.^{16,17} It can also be utilized as a solvent in polymer industries, and a solubilizing and suspending agent in pharmaceutical industries.¹⁸ The presence of contaminants in crude glycerol creates certain challenges such as plugging of reactor and deactivation of catalyst in the conversion process to solketal in a flow reactor.^{19,20} Therefore, these contaminants need to be removed prior to the conversion.

Table 11.1 Crude glycerol composition

Component	Concentration (wt%)
Methanol	1-30
Glycerine	45-84
Water	6-35
Salt	1-12
Soap/Free fatty acid	1-25

Crude glycerol can be purified using different techniques including ion exchange resin (IER), nanocavitation, membrane separation technology, simple distillation and acidification followed by separation.^{21,22,23} Among the above mentioned techniques, crude glycerol purification by acidification demonstrated to be more efficient than others in terms of economy and product purity.²³ Therefore, pretreatment of crude glycerol using acidification process was considered in the present study.

In our previous studies, we have studied the purification of crude glycerol (chapter 8),¹⁹ and the ketalization of purified crude glycerol (chapter 9). In this work, we conceptually designed a large-scale solketal production process integrating the crude glycerol pretreatment by acidification and catalytic conversion of purified crude glycerol into solketal by ketalization with acetone at the optimum conditions determined from our previous studies (chapter 9). The economic assessment was carried out to evaluate the feasibility of this conceptually designed process in real world application.

11.2 Solketal production processes

11.2.1 Plant capacity

Currently, there is no plant for the production of solketal from crude glycerol. This study targets at techno-economic analysis of production of solketal from crude glycerol at large-scale with a capacity of 16,000 L/day (4000 ton/year). The conceptually designed pilot plant is an integration of two sequential units, namely pre-treatment (for purification of crude glycerol) and production (of solketal) units which is illustrated in Figure 1.

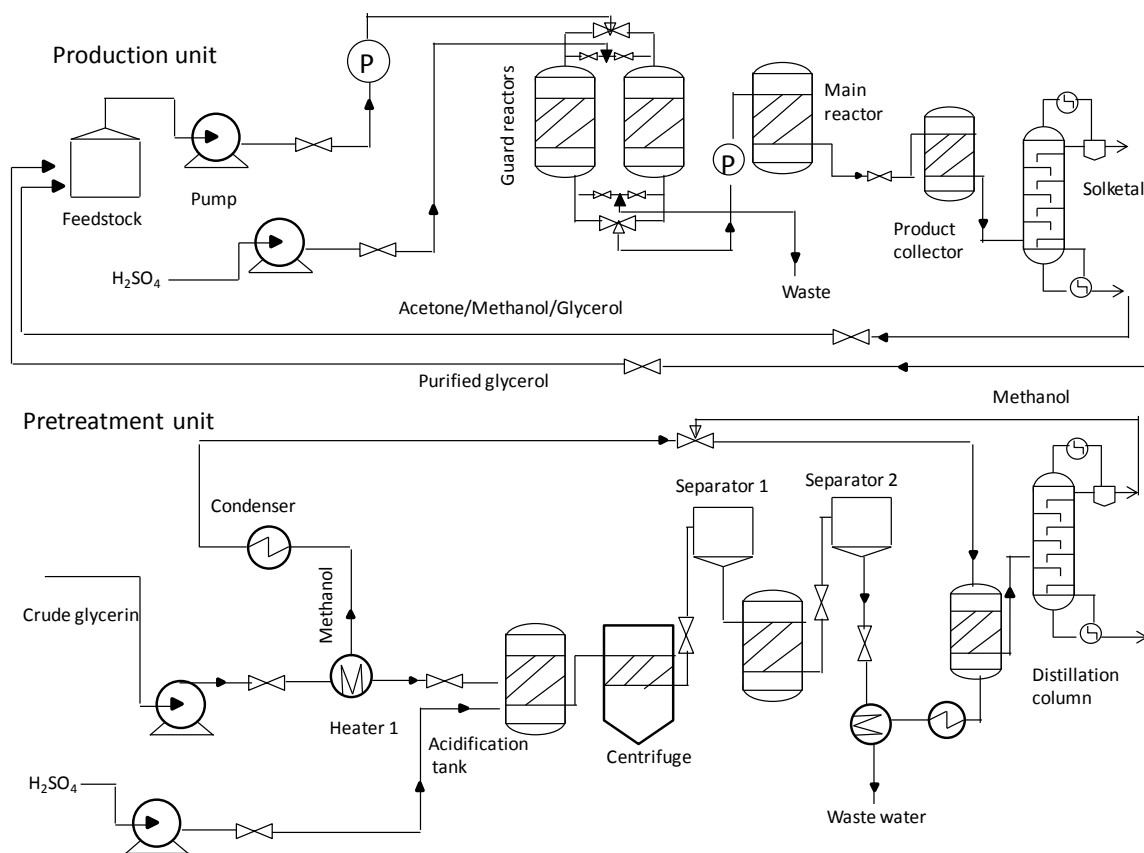


Figure 11.1 Process flow diagram for a large-scale solketal production process using crude glycerin

11.2.2 Feedstock and materials

Crude glycerol supplied from a local biodiesel plant will be used as the feedstock for the pretreatment unit. The feed stream composition for this unit consists of 64.7% glycerol, 8.6% water, 12.3% methanol, 4.8% salt, and 9.6% soap/free fatty acids by weight. The purified crude glycerol (PCG) from the pre-treatment unit along with acetone and methanol are the feed for the ketalization unit. During the ketalization process, Amberlyst-35 wet will be employed as catalyst due to its ability for high conversion of glycerol to solketal at room temperature and to perform well under aqueous condition, as demonstrated in our previous studies.^{13,16}

11.2.3 Pretreatment and production units

As mentioned earlier, crude glycerol contains impurities such as water, methanol, free fatty acids, and salts, hence needs to be purified prior to use as a raw material in other industries.²⁴ For the pre-treatment process, firstly the crude glycerol is evaporated (Heater 1) at a low temperature (around 70 °C), as shown in Figure 1, where more than 95% of the methanol is recovered and to be reused in the downstream production unit. The bottom stream from the evaporator is neutralized using sulfuric acid followed by centrifugation to produce three distinct layers; free fatty acids (top layer), glycerol (middle layer) and sulfate salts (bottom layer), which are subsequently separated. The recovered glycerol is washed with water using a weight ratio of 2.4 (water/ glycerol) followed by neutralization with alkali. The insoluble organic phase is separated out from the aqueous phase which mainly contains glycerol with dissolved salts and methanol although at a low concentration. The aqueous glycerol is passed through the evaporator to remove water and methanol. The glycerol is extracted by solvent extraction using methanol followed by distillation.

The production of solketal is shown in the production unit. The obtained glycerol from the pretreatment unit (> 95% purity) is cooled to room temperature and used as feed mixed with acetone and methanol. The feedstock is then passed through the guard bed reactor containing cationic exchange resin Amberlyst-35 wet catalyst to remove the cations present in the PCG. Then the feed is passed through the main reactor containing the same catalyst

at room temperature. The product contains water, methanol, acetone, glycerol and solketal, which are separated by fractional distillation. The ion-exchange resins employed in the guard bed reactor was regenerated using a 0.5 M sulfuric acid after deactivation (usually after 24 h).

11.2.4 Byproducts

In the pretreatment process, various impurities such as methanol, free fatty acids and sulfate salts are generated. Some impurities will be recovered and recycled/ or reused in some other steps of the process or sold as value-added by-products, which can improve the profitability of the process. For example the recovered methanol can be used as solvent in the solvent extraction step in the pretreatment unit, and the sulfate salts can be used as fertilizers. Similarly, the downstream product of the production unit contains methanol, acetone, and un-reacted glycerol which could be recycled to the feedstock tank in the same process.

11.3 Results and discussion

11.3.1 Selection of operating conditions

Several authors have evaluated effects of the operating parameters such as acid types, pH and precipitation time on the crude glycerol purification process.^{19,23,25,26} The authors demonstrated that crude glycerin treated with sulfuric acid or phosphoric acid at a low pH (usually 2) and at a moderate precipitation time (10-15 min) has the maximum glycerol content of $96 \pm 2\%$, as reported in previous chapter 8.

The synthesis of solketal has been extensively studied in both batch and flow processes and the glycerol conversion and solketal yield have been reported.^{14,15,16} Effects of reaction temperature, amount of catalyst, acidity of catalyst, acetone to glycerol molar ratio on the conversion of glycerol to solketal were also analyzed. It was reported that the reaction is exothermic, therefore a low temperature favoring the formation of solketal.²⁰ Nanda *et al.* reported the kinetics of the ketalization reaction and optimized the process to get a maximum solketal yield of $94 \pm 2\%$ and glycerol conversion of $96 \pm 2\%$ at the following

optimal conditions: 25 °C, acetone to glycerol molar ratio (A/G) of 4, and weight hourly space velocity (WHSV) of 2 h⁻¹ using purified crude glycerol (>95%).²⁷

11.3.2 Quality parameters

Laboratory analyses were performed to determine purities of PCG and solketal, in accordance to various ASTM and AOCS (American Oil Chemists' Society) protocols. The results are given in Table 11.2. Most of the properties such as the viscosity, density, pH of PCG and viscosity, density, flash point and boiling point of solketal are comparable to those of the commercially available products. Improvement is still needed in some characteristics such as water content, ash content and K content in the PCG product.

Table 11.2 Quality analyses of the PCG and solketal product

Test	Method	Laboratory product	Commercial product ^{i,ii}
Purified crude glycerol (PCG)			
Ash content	IUPAC III A4	1.4± 0.31	0.0002 ± 0.00
Density	ASTM D4052	1.258 ±0.02	1.267 ± 0.00
Moisture by KF	ASTM D6304	1.6 ±0.03	0.01 ± 0.00
Glycerine	GA-SOP 419	96 ± 1.02	99.98 ± 0.00
Free fatty acid	AOCS 5a -40	0.00 ± 0.00	0
pH		6.98 ±0.06	6.97 ± 0.03
MONG		0.12 ± 0.00	0
Viscosity (at 50 °C)		140 ± 2	142 ± 1
K (PPM)		1165 ± 110	870 ± 40
Solketal			
Density		1.05 ± 0.03	1.06
Boiling point (°C)		189 ± 0.05	190
Viscosity (cp @ 20 °C)		11 ± 0.05	11
Flash point (°C)		79 ± 1	80

ⁱ: <http://gorgeanalytical.com/testing-services/glycerin-testing>; ⁱⁱ: <http://www.hommel-pharma.com/dateien/SOLKETAL-e.PDF>, MONG: Matter organic non glycerol

11.3.3 Economic assessment

Economic assessment results for the pre-treatment process of crude glycerol are shown in Table 11.3. In the Table, the costs are broken down to different charges such as feedstock (crude glycerol/PCG/or acetone), raw materials (sulfuric acid, sodium hydroxide, and methanol), labor, electricity, quality analysis, plant overhead and general administrative, co-product sale and capital depreciation. The pre-treatment cost per liter is given in column

2 and the share of each item is given in column 3. Column 4 presents the pre-treatment cost for 5000 ton of crude glycerol which is the annual production capacity of the biodiesel plant at Sombra, Sarnia. Generally, for most of the industrial processes, the cost of feedstock stands in between 55- 75% of the total production cost.²⁸ However, in the present study, the feedstock (crude glycerol) represents only 32% of the total pre-treatment cost because of its extremely low price in the market. Transportation cost was not considered in this study since the plant was assumed to be close to the biodiesel production sites at Sombra, Sarnia. The raw materials (H_2SO_4 , NaOH, and methanol) and the capital costs have a major share (27% and 20%, respectively) in the pre-treatment process. The raw material cost mainly depends on the quality of the final product, i.e., the higher purity in the PCG the higher the raw material consumption (costs).²⁹ Theoretically the methanol used in the process can be recycled, but a consumption of 10% methanol in each step was estimated considering the loss in separation. Overall, the approximate pre-treatment cost was calculated to be about \$0.14/L, slightly higher than the purification cost reported in literature (\$0.1124/L).¹² This might be due to the addition of solvent extraction step in the process. The pre-treatment cost of crude glycerol is much less than the sale prices of commercially available 98% pure glycerol (\$600- 800/ton), hence it is expected that the production cost of solketal using PCG would be much lower than that using pure glycerol as feedstock.

Table 11.3 Pretreatment cost of crude glycerol

Chemicals	\$/Liter	Share (%)	\$/gal	Thousand \$/year
Crude glycerol	0.058	31.72	0.219	290600
H ₂ SO ₄	0.009	4.91	0.034	45000
NaOH	0.012	6.55	0.045	60000
Methanol	0.027	14.99	0.102	137347
Labour	0.005	2.66	0.019	24400
Electricity	0.003	2.4	0.011	22050
Quality analysis	0.003	1.52	0.011	13900
Plant overhead, and administrative cost	0.017	9.38	0.064	85950
Maintenance and operating charges	0.011	6.11	0.042	56000
Capital depreciation	0.036	19.75	0.136	180890
Co-product sale credit	-0.039		-0.148	-195500
Total pre-treatment cost	0.144	100	0.545	720637

The economic analysis was also carried out for the solketal production process with the purified crude glycerol (PCG) as the feedstock. The production cost was compared with that of the process using pure glycerol as feedstock, as shown in Table 11.4. The obtained GPC from crude glycerol (\$0.86/L) is lower than the solketal production cost from pure glycerol (\$1.00), hence could represent a saving of 16% in the process. A profit of \$565724 /y will be realized in the process using PCG as the feedstock over the process using pure glycerol

Moreover, the production of solketal from crude glycerol could attain a profit of more than 28% over other fuel additives used for similar purposes (such as MTBE: \$1.15/L, ETBE: 1.10\$/L).³⁰

Table 11.4 Conversion cost of glycerol to solketal

Chemicals	Production Cost of 1 L solketal with PCG (\$)	Share (%)	Production Cost of 1 L of solketal with PG ^b (\$)	Share (%)
Acetone	0.31	39.49	0.31	30.62
Glycerol ^a	0.08	9.72	0.42	42.7
A-35 wet	0.016	2.02	0.004	0.39
Methanol	0.003	0.44	0.002	0.17
Sulfuric acid	0.013	1.61	0.003	0.29
Electricity	0.02	2.57	0.02	1.99
Labour	0.02	2.57	0.02	1.99
Quality analysis	0.01	1.28	0.01	0.99
Maintenance and operating charges	0.08	10.48	0.052	5.14
Plant overhead, and administrative	0.11	13.54	0.07	6.52
Capital depreciation	0.20	26.01	0.10	10.20
Solketal production cost (\$/L)	0.8620	100	1.00	100
Solketal production cost (000,\$/year) ^c	3448116		4013840	

^a: For production of 1 L solketal requires 0.734 g (0.582 L) 95% PCG; ^b: PG-Pure (commercial) glycerol; ^c: For 4000 ton

Although more rigorous analysis of solketal market and its production cost could be carried out, the obtained results in this work indicate that the production of solketal from crude glycerol using combined pretreatment and ketalization processes is more profitable than that using pure glycerol as the feedstock

11.4 Conclusions

A conceptually design of an integrated process was proposed and investigated for the production of 4000 ton solketal per year using crude glycerol as the feedstock. The process incorporated pretreatment of the crude glycerol by acidification and production of solketal by ketalization of the purified crude glycerol with acetone. The operating costs of the process were evaluated. The cost analysis demonstrated that the production cost of solketal using crude glycerol as the feedstock after pretreatment is much lower than that using the commercially available glycerol. A profit of 565724 \$/year could be realized in the process. This study demonstrated that the process is not only technically feasible but also economically viable for the production of solketal from crude glycerol at large scale.

References

1. Vicente G, Martínez M, Aracil J. Integrated biodiesel production: a comparison of different homogeneous catalysts systems. *Bioresource Technology* 2004;92(3):297-305. doi:10.1016/j.biortech.2003.08.014.
2. Crotti C, Farnetti E, Guidolin N. Alternative intermediates for glycerol valorization: iridium-catalyzed formation of acetals and ketals. *Green Chemistry* 2010;12(12):2225. doi:10.1039/c0gc00096e.
3. Carmona M, Valverde JL, Pérez A, Warchol J, Rodriguez JF. Purification of glycerol/water solutions from biodiesel synthesis by ion exchange: sodium removal Part I. *Journal of Chemical Technology & Biotechnology* 2009;84(5):738-744. doi:10.1002/jctb.2106.
4. Corma A, Iborra S, Velty A. Chemical routes for the transformation of biomass into chemicals. *Chemical Reviews* 2007;107(6):2411-502. doi:10.1021/cr050989d.
5. Rywińska A, Rymowicz W. High-yield production of citric acid by *Yarrowia lipolytica* on glycerol in repeated-batch bioreactors. *Journal of Industrial Microbiology & Biotechnology* 2010;37(5):431-5. doi:10.1007/s10295-009-0687-8.
6. Liu X, Jensen PR, Workman M. Bioconversion of crude glycerol feedstocks into ethanol by *Pachysolen tannophilus*. *Bioresource Technology* 2012;104:579-86. doi:10.1016/j.biortech.2011.10.065.
7. Liang Y, Cui Y, Trushenski J, Blackburn JW. Converting crude glycerol derived from yellow grease to lipids through yeast fermentation. *Bioresource Technology* 2010;101(19):7581-6. doi:10.1016/j.biortech.2010.04.061.
8. Saenge C, Cheirsilp B, Suksaroge TT, Bourtoom T. Potential use of oleaginous red yeast *Rhodotorula glutinis* for the bioconversion of crude glycerol from biodiesel plant to lipids and carotenoids. *Process Biochemistry* 2011;46(1):210-218. doi:10.1016/j.procbio.2010.08.009.
9. Ramadhas A, Jayaraj S, Muraleedharn C. Biodiesel production from high FFA rubber seed oil. *Fuel* 2005;84(4):335-340. doi:10.1016/j.fuel.2004.09.016.
10. Pagliaro M, Ciriminna R, Kimura H, Rossi M, Della Pina C. From glycerol to value-added products. *Angewandte Chemie (International ed. in English)* 2007;46(24):4434-40. doi:10.1002/anie.200604694.
11. Bournay L, Casanave D, Delfort B, Hillion G, Chodorge JA. New heterogeneous process for biodiesel production: A way to improve the quality and the value of the crude glycerin produced by biodiesel plants. *Catalysis Today* 2005;106(1-4):190-192. doi:10.1016/j.cattod.2005.07.181.

12. Posada JA, Cardona CA. Design and analysis of fuel ethanol production from raw glycerol. *Energy* 2010;35(12):5286-5293. doi:10.1016/j.energy.2010.07.036.
13. Nanda MR, Yuan Z, Qin W, Ghaziaskar HS, Poirier M-A, Xu CC. Thermodynamic and kinetic studies of a catalytic process to convert glycerol into solketal as an oxygenated fuel additive. *Fuel* 2014;117:470-477. doi:10.1016/j.fuel.2013.09.066.
14. Vicente G, Melero J a., Morales G, Paniagua M, Martín E. Acetalisation of bio-glycerol with acetone to produce solketal over sulfonic mesostructured silicas. *Green Chemistry* 2010;12(5):899. doi:10.1039/b923681c.
15. Deutsch J, Martin a, Lieske H. Investigations on heterogeneously catalysed condensations of glycerol to cyclic acetals. *Journal of Catalysis* 2007;245(2):428-435. doi:10.1016/j.jcat.2006.11.006.
16. Nanda MR, Yuan Z, Qin W, Ghaziaskar HS, Poirier M-A, Xu C (Charles). A new continuous-flow process for catalytic conversion of glycerol to oxygenated fuel additive: Catalyst screening. *Applied Energy* 2014;123:75-81. doi:10.1016/j.apenergy.2014.02.055.
17. Royon D, Locatelli S, Gonzo EE. Ketalization of glycerol to solketal in supercritical acetone. *The Journal of Supercritical Fluids* 2011;58(1):88-92. doi:10.1016/j.supflu.2011.04.012.
18. Maksimov AL, Nekhaev AI, Ramazanov DN, Arinicheva YA, Dzyubenko AA, Khadzhiev SN. Preparation of high-octane oxygenate fuel components from plant-derived polyols. *Petroleum Chemistry* 2011;51(1):61-69. doi:10.1134/S0965544111010117.
19. Nanda, M; Yuan Z, Qin W, M.A, Poirier; Xu C. Purification of crude glycerol using acidification : effects of acid types and product characterization. *Austin Journal of Chemical Engineering* 2015;1(1):1-7.
20. Mota CJ a., da Silva CX a., Rosenbach, N, Costa J, da Silva F. Glycerin derivatives as fuel additives: The addition of glycerol/Acetone Ketal (solketal) in gasolines. *Energy & Fuels* 2010;24(4):2733-2736. doi:10.1021/ef9015735.
21. Ferreira MO, M.B.D. Sousa E, Pereira CG. Purification of Crude Glycerine Obtained from Transesterification of Cottonseed Oil. *International Journal of Chemical Reactor Engineering* 2013;11(1):1-8. doi:10.1515/ijcre-2012-0071.
22. Cavitation Technologies, Inc. Available at: <http://www.ctinanotech.com/>. Accessed July 7, 2015.
23. Kongjao S, Damronglerd S, Hunsom M. Purification of crude glycerol derived from waste used-oil methyl ester plant. *Korean Journal of Chemical Engineering* 2010;27(3):944-949. doi:10.1007/s11814-010-0148-0.

24. Acevedo JC, Hernández JA, Valdés CF, Khanal SK. Analysis of operating costs for producing biodiesel from palm oil at pilot-scale in Colombia. *Bioresource Technology* 2015;188:117-123. doi:10.1016/j.biortech.2015.01.071.
25. Ooi TL, Yong KC, Dzulkefly K, Yunus WMZW, Hazimah AH. Crude glycerine recovery from glycerol residue waste from a palm kernel oil methyl ester plant. *Journal of Oil Palm Research* 2001;13(2):16-22. Available at: <http://www.mendeley.com/research/crude-glycerine-recovery-glycerol-residue-waste-palm-kernel-oil-methyl-ester-plant/>. Accessed July 2, 2015.
26. Isahak WNRW, Ismail M, Yarmo MA, Jahim JM, Salimon J. Purification of Crude Glycerol from Transesterification RBD Palm Oil over Homogeneous and Heterogeneous Catalysts for the Biolubricant Preparation. *Journal of Applied Sciences* 2010;10(21):2590-2595. doi:10.3923/jas.2010.2590.2595.
27. Nanda MR, Yuan Z, Qin W, Ghaziaskar HS, Poirier M-A, Xu C (Charles). Catalytic conversion of glycerol to oxygenated fuel additive in a continuous flow reactor: Process optimization. *Fuel* 2014;128:113-119. doi:10.1016/j.fuel.2014.02.068.
28. Posada JA, Naranjo JM, López JA, Higueta JC, Cardona CA. Design and analysis of poly-3-hydroxybutyrate production processes from crude glycerol. *Process Biochemistry* 2011;46(1):310-317. doi:10.1016/j.procbio.2010.09.003.
29. Posada J a., Higueta JC, Cardona C a. Optimization on the Use of Crude Glycerol from the Biodiesel Production to Obtain Poly-3-Hydroxybutyrate. 2011:327-334. doi:10.3384/ecp11057327.
30. Mtbe, Etbe Suppliers and Manufacturers at Alibaba.com. Available at: <http://www.alibaba.com/showroom/mtbe.html>. Accessed July 24, 2015.

Chapter 12

12 Conclusions and future work

12.1 Conclusions

The rapid growth of the biodiesel industry has generated a large amount of crude glycerol which is now considered as a waste by-product of the industry. Therefore, the identification of high-value applications for this waste-stream- glycerol is of some urgency to uphold the sustainability of the biodiesel industry. In this context the catalytic conversion of glycerol is a promising way in which this low-value glycerol can be valorized to different value-added chemicals. Fuel and polymer industries are among the fields where a large amount of glycerol could be utilized in form of its derivatives. Valorization of glycerol to oxygenated fuel additives such as solketal, and polymer components including 1, 2- and 1, 3-propanediols are among the most promising applications of glycerol with significant industrial importance.

In this research work, pure glycerol was converted to solketal and 1, 2-propanediol effectively in different processes in a continuous-flow reactor over inexpensive catalysts. The effects of process parameters were studied and the processes were optimized. The efficiency of the processes was also assessed by using crude glycerol (from biodiesel plant) and purified crude glycerol as feedstock. Necessary modifications were also made in the processes to avoid operating issues like reactor clogging and catalyst deactivation. The detailed conclusions of this thesis work are given below.

1. Thermodynamic and kinetic studies for the synthesis of solketal in liquid phase were carried out in a well-controlled batch reactor in the presence of an acid catalyst (Amberlyst-35). The thermodynamic equilibrium constant K_c at various temperatures ranging from 293 to 323 K was determined. The reaction is exothermic and the standard enthalpy, entropy and Gibbs free energies at 298 K were found to be $-30.1 \pm 1.6 \text{ kJ mol}^{-1}$, $-0.1 \pm 0.01 \text{ kJ mol}^{-1} \text{ K}^{-1}$ and $-2.1 \pm 0.1 \text{ kJ mol}^{-1}$, respectively. The kinetic studies of the same reaction demonstrated that the rate of the reaction increased with increasing temperature, the catalyst addition

amount and acetone-to-glycerol (A/G) molar ratio. In this batch study of the liquid phase reaction, pressure showed negligible influence on the reaction thermodynamics and kinetics as expected, and no effect of the agitation speed on the reaction rate was observable at >400 rpm. Langmuir- Hinshelwood model demonstrated to be useful for describing the kinetic mechanism of the ketalization reaction of glycerol with acetone. Based on the Langmuir- Hinshelwood model, the values of the activation energy (E_a) of the overall reaction was determined to be $55.6 \pm 3.1 \text{ kJ mol}^{-1}$.

2. A new continuous-flow process employing heterogeneous catalysts has been developed for the first time for efficiently converting glycerol into solketal. A total of 6 different catalysts were investigated with respect to their catalytic activity and stability at different reaction conditions (e.g., acetone/glycerol molar ratio, WHSV, temperature, pressure, etc.). The increase in the acetone/glycerol molar ratio resulted in an increase of the solketal yield irrespective of the catalysts used. Among all the solid acid catalysts tested, the use of Amberlyst wet produced the maximum solketal yield from experiments at 40 °C, 600 psi and WHSV of 4 h⁻¹ (being 73% and 88% at the acetone/glycerol molar ratio of 2.0 and 6.0, respectively). It appeared that catalysts with stronger acidity exhibited higher activities: Amberlyst wet \approx H-beta zeolite \approx Amberlyst dry > Zirconium sulfate > Montmorillonite > Polymax. Both the solketal yield and glycerol conversion decreased, irrespective of the catalysts used, upon increasing the WHSV. The activities of all the catalysts, except polymax, showed only a slight decrease in its activity for up to 24 h on-stream likely due to the loss of its acidity during a long time on-stream.
3. The process for the continuous catalytic conversion of glycerol to oxygenated fuel additive, solketal was optimized. The solid acid catalyst amberlyst-36 wet demonstrated an excellent catalytic performance (active, stable, and regenerable) in the flow process. A maximum solketal yield of $94 \pm 2\%$ was observed at the optimum condition (temperature: 25 °C, acetone equivalent: 4, and WHSV: 2 h⁻¹).

The presence of impurities like salt and water in glycerol (such as crude glycerol) reduced the yield significantly.

4. Phosphoric acid was found to be the best acidifying agent among the other mineral acids tested for crude glycerol acidification for purification. Glycerol content was increased from approximately 13 wt% in the crude glycerol to > 96 wt% in the purified crude glycerol products. The density, viscosity, pH and metal contents of the purified crude glycerol products were analyzed and found to be very close to that of the commercially available pure glycerol. The purity of the purified products was confirmed by FTIR and GC-MS/FID measurements. UV-VIS spectroscopy demonstrated a nearly equal absorbance of the purified glycerol to that of pure glycerol. The biogenic nature of phosphorous, the high value applications of the phosphates with easy scalability of the process make it very promising for commercialization.
5. A new continuous-flow reactor consisting of 2 parallel guard reactors and a main reactor was developed for continuous conversion of crude glycerol and purified crude glycerol to solketal by ketalization reaction with acetone. The reaction, carried out over Amberlyst-36 wet catalyst under conditions of 25 °C, 200 psi, and acetone-to-glycerol molar ratio of 4, achieved a 92 ± 2 % solketal yield after 24 h on stream at WHSV of 0.38 h^{-1} . The continuous-flow reactor developed enables simultaneous glycerol ketalization and spent catalyst regeneration, leading to continuous operation of the reactor for a longer time while maintaining a high product yield.
6. The addition of B_2O_3 into $\text{Cu}/\text{Al}_2\text{O}_3$ catalysts enhanced the catalytic activity for the glycerol hydrogenolysis reaction. Among all catalysts prepared and tested, $5\text{Cu}-1\text{B}/\text{Al}_2\text{O}_3$ demonstrated the best catalytic performance with 98% glycerol conversion and 98% 1,2-PDO selectivity in hydrogenolysis of 10 wt% aqueous solution of glycerol at the optimum conditions (250 °C temperature, 6 MPa H_2 pressure, 0.1 h^{-1} WHSV). Process parameters such as temperature, hydrogen pressure, and liquid hourly space velocity significantly influenced the catalytic

activity for the glycerol hydrogenolysis reaction. The use of different grades of glycerol, including the pharmaceutical grade glycerol, technical grade glycerol and crude glycerol (glycerol purity varying from 54.7% to 99.9 %) in the process showed that the presence of impurities could reduce the glycerol conversion and 1,2-PDO selectivity. The long term stability test demonstrated that the 5Cu-1B/Al₂O₃ catalyst could be used up to 60 h without any appreciable change in activity. Destruction of the support structure, sintering of Cu metal, and coke deposition on the catalyst were found to be the main factors that deactivated the catalyst after 60 h on stream.

7. A conceptual design for an integrated solketal production plant with a production capacity of 4000 ton solketal per year using crude glycerol as feedstock was investigated. The cost analysis demonstrated that the production cost of purified crude glycerol is much less than the commercially available glycerol with same purity level. Also, the economical assessment showed that a profit of \$565724 /year could be obtained from the solketal production process using purified crude glycerol. This study demonstrates technical feasibility and economic viability for the production of solketal from crude glycerol at large scale.

12.2 Future work

The future works for this thesis work are given below:

1. Ketalization of glycerol with acetone was successfully demonstrated in a flow reactor. Currently, the solketal available in market is obtained from batch reactor processes; hence it would be economical to commercialize the flow process for the production of solketal. Therefore a market analysis could be initiated to check the feasibility of the process for industrialization.
2. In the process of purification of crude glycerol via phosphoric acid, phosphate based salts were produced. These salts have the potential to be used in high value applications such as pH indicator, and fertilizers after careful separation. A

thorough investigation could show the economical purification of these compounds in the process.

3. The two different processes: purification of crude glycerol and ketalization of purified crude glycerol in the flow reactor could be integrated to a single system with different units so that both the processes would be carried out simultaneously. This on-line purification - ketalization is more economical than the previous processes.
4. Integration of upgrading the crude glycerol and hydrogenolysis of purified crude glycerol to the on-line purification- hydrogenolysis process could be realized. The marginal profit analysis of the technology can ensure the possible commercialization of the process.
5. In the hydrogenolysis process, liquid products such as 1,3-propanediol, ethylene glycol, propanol, ethanol, methanol, and gaseous products including methane, ethane, and propane are produced as byproducts. These chemicals have potential industrial values. Therefore, separate investigations could be started by using proper reaction conditions and suitable catalysts to enhance the selectivity towards these chemical compounds from glycerol, so that glycerol could be a novel bio-renewable resource for them.

Appendices

Appendix A: Thermodynamic relations

$$\Delta G = \Delta G^0 + RT \ln K_c$$

At equilibrium, $\Delta G = 0$,

$$\text{So } \Delta G^0 = -RT \ln K_c$$

$$\Delta G^0 = \Delta H^0 - T\Delta S^0$$

$$-RT \ln K_c = \Delta H^0 - T\Delta S^0$$

Appendix B: Kinetic model

The Kinetic model described in this work based on the concentration of the respective species and has following steps:

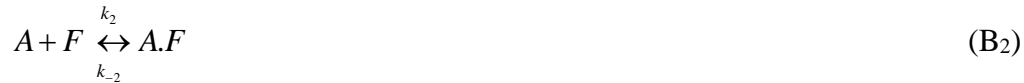
Step 1- Adsorption of glycerol:



where k_1 and k_{-1} are the forward and backward rate constants, respectively. The adsorption coefficient can be written as

$$K_{F,G} = \frac{k_1}{k_{-1}} = \frac{[GF]}{[G][F]}$$

Step 2: Adsorption of acetone



where k_2 and k_{-2} are the forward and backward rate constants, respectively. The adsorption coefficient can be written as

$$K_{F,A} = \frac{k_2}{k_{-2}} = \frac{[AF]}{[A][F]}$$

Step 3: Surface reaction between the adsorbed species of glycerol and acetone to give adsorbed hemiacetal



where k_3 and k_{-3} are the forward and backward rate constants, respectively. The adsorption coefficient can be written as

$$K_3 = \frac{k_3}{k_{-3}} = \frac{[I_1F][F]}{[AF][BF]}$$

Step 4: Surface reaction to obtain adsorbed water (WF) (rate determining step)



where k_4 and k_{-4} are the forward and backward rate constants, respectively. The adsorption coefficient can be written as

$$K_4 = \frac{k_4}{k_{-4}} = \frac{[I_2F][WF]}{[I_1F][F]}$$

Step 5: Surface reaction of formation of adsorbed solketal (SF)



where k_5 and k_{-5} are the forward and backward rate constants, respectively. The adsorption coefficient can be written as

$$K_5 = \frac{k_5}{k_{-5}} = \frac{[SF][F]}{[I_2F][GF]}$$

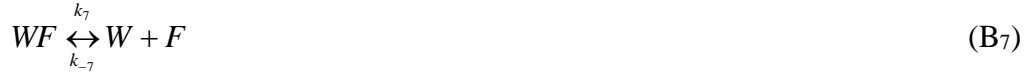
Step 6: Desorption of solketal



where k_6 and k_{-6} are the forward and backward rate constants, respectively. The adsorption coefficient can be written as

$$K_{F,S} = K_6 = \frac{k_{-6}}{k_6} = \frac{[SF]}{[S][F]}$$

Step 7: Desorption of water (WF)



where k_7 and k_{-7} are the forward and backward rate constants, respectively. The adsorption coefficient can be written as

$$K_{F,W} = \frac{k_{-7}}{k_7} = \frac{[WF]}{[W][F]}$$

Assuming the surface reaction in step 4 as the rate determining step, the rate expression for the Langmuir-Hinshelwood model is

$$\begin{aligned} R &= k_4 \theta_{I_1 \cdot F} \theta_F - k_{-4} \theta_{I_2 \cdot F} \theta_{W \cdot F} \\ &= k_4 \theta_{I_1 \cdot F} \theta_F - \frac{k_4}{K_4} \theta_{I_2 \cdot F} \theta_{W \cdot F} \\ &= k_4 \left[\theta_{I_1 \cdot F} \theta_F - \left(\frac{1}{K_4} \right) \theta_{I_2 \cdot F} \theta_{W \cdot F} \right] \end{aligned} \quad (\text{B8})$$

Where $\theta_{I_1 \cdot F}$, $\theta_{I_2 \cdot F}$ and $\theta_{W \cdot F}$ are the fractions of catalyst sites occupied by $I_1 \cdot F$, $I_2 \cdot F$ and $W \cdot F$, respectively. θ_F is the vacant sites and K_4 is the adsorption coefficient for step 4.

The total concentration composed of vacant and adsorbed species on the catalyst surface can be expressed as

$$\begin{aligned} C_0 &= C_F + C_{G \cdot F} + C_{A \cdot F} + C_{S \cdot F} + C_{W \cdot F} + C_{I_1 \cdot F} + C_{I_2 \cdot F} \\ &= C_F + K_{F,G} C_G C_F + K_{F,A} C_A C_F + K_{F,S} C_S C_F + K_{S,W} C_W C_F + K_{F,G} K_{F,A} K_3 C_G C_A C_F + \frac{K_{F,S} C_S C_F}{K_{F,G} K_F C_G} \\ &= C_F \left[1 + K_{F,G} C_G + K_{F,A} C_A + K_{F,S} C_S + K_{S,W} C_W + K_{F,G} K_{F,A} K_3 C_G C_A + \frac{K_{F,S} C_S}{K_{F,G} K_F C_G} \right] \end{aligned} \quad (\text{B9})$$

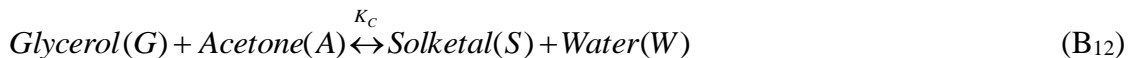
Taking θ_j as the fraction of catalyst sites occupied by a particular species, it can be expressed as

$$\theta_j = \frac{C_{j.F}}{C_0} \quad (\text{B10})$$

From equation (B8) using the corresponding values of θ_j , we have

$$\begin{aligned} R &= k_4 \left[\frac{C_{I_1.F} C_F}{C_0 \cdot C_0} - \left(\frac{1}{K_4} \right) \frac{C_{I_2.F}}{C_0} \frac{C_{WF}}{C_0} \right] \\ &= k_4 \left[\frac{K_3 C_{G.F} C_{A.F} C_F}{C_F \cdot C_0 \cdot C_0} - \left(\frac{1}{K_4} \right) \frac{C_{S.F} C_F}{K_5 C_0 C_{G.F}} \frac{C_{WF}}{C_0} \right] \\ &= k_4 \left[\frac{K_3 K_{F,G} K_{F,A} C_G \cdot C_A \cdot C_S^2}{C_F \cdot C_0 \cdot C_0} - \left(\frac{1}{K_4} \right) \frac{K_{F,S} K_{F,W} C_S C_W}{K_{F,G} K_5 C_G} \frac{C_F^2}{C_0^2} \right] \\ &= k_4 \left[\frac{K_{F,G} K_{F,A} K_3 C_G \cdot C_A}{C_0^2} - \left(\frac{1}{K_4} \right) \frac{K_{F,S} K_{F,W} C_S C_W}{K_{F,G} K_5 C_G} \right] \left(\frac{C_F}{C_0} \right)^2 \\ &= k_4 \frac{K_{F,G} K_{F,A} K_3 C_G C_A - \left(\frac{1}{K_4} \right) \frac{K_{F,S} K_{F,W} C_S C_W}{K_{F,G} K_5 C_G}}{\left[1 + K_{F,G} C_G + K_{F,A} C_A + K_{F,S} C_S + K_{F,W} C_W + K_{F,G} K_{F,A} K_3 C_G \cdot C_A + \frac{K_{F,S} C_S}{K_{F,G} K_5 C_G} \right]^2} \\ &= k_4 K_{F,G} K_{F,A} K_3 \frac{C_G C_A - \left(\frac{K_{F,S} K_{F,W}}{K_{F,G} K_{F,A}} \frac{1}{K_3 K_4 K_5} \right) \frac{C_S C_W}{C_G}}{\left[1 + K_{F,G} C_G + K_{F,A} C_A + K_{F,S} C_S + K_{F,W} C_W + K_{F,G} K_{F,A} K_3 C_G \cdot C_A + \frac{K_{F,S} C_S}{K_{F,G} K_5 C_G} \right]^2} \end{aligned} \quad (\text{B11})$$

The overall reaction can be expressed as



where K_c is the over all equilibrium constant and can be given as

$$KC = \frac{C_S C_W}{C_G C_A} = \frac{\frac{C_{SF}}{C_F K_{F,S}} \frac{C_{WF}}{C_F K_{F,W}}}{\frac{C_{GF}}{C_F K_{F,G}} \frac{C_{AF}}{C_F K_{F,A}}} = \frac{K_{F,G} K_{F,A} C_{SF} C_{WF}}{K_{F,S} K_{F,W} C_{GF} C_{AF}} = \frac{K_{F,G} K_{F,A}}{K_{F,S} K_{F,W}} K_3 K_4 K_5 \quad (\text{B13})$$

Adding Equations (B1)-(B3), we get

$$G + A + 2F \overset{K'_{I1}}{\leftrightarrow} I_1 F + GF \quad (\text{B14})$$

where

$$K'_{I1} = \frac{C_{I1F} C_{GF}}{C_G C_A C_F^2} = \left(\frac{C_{GF}}{C_G \cdot C_F} \right) \left(\frac{C_{AF}}{C_A \cdot C_F} \right) \left(\frac{C_{I1F} C_F}{C_{GF} \cdot C_{AF}} \right) = K_{F,G} K_{F,A} K_3$$

Taking

$$KI_1 = \frac{K'_{I1}}{K_{F,G}} = K_{F,G} K_{F,A} K_3 \quad (\text{B15})$$

Similarly, adding Equations (B1), (B5), and (B6), we get

$$I_2 F + G \overset{K'_{I2}}{\leftrightarrow} S + F$$

Where

$$K'_{I2} = \frac{C_S C_F}{C_{I_2 F} C_G} = \frac{K_5 K_{FG}}{K_{F,S}}$$

Taking

$$K_{I_2} = \frac{K_{F,G}}{K'_{I_2}} = \frac{K_{F,G}}{K_5 K_{FG}} K_{FS} = \frac{K_{FS}}{K_5}$$

Using the values of K_{I1} , K_{I2} , and K_c , Equation B12 can be written as

$$R = k \frac{C_G C_A - \frac{C_S C_W}{K_C C_G}}{\left[1 + K_{F,G} C_G + K_{F,A} C_A + K_{F,S} C_S + K_{F,W} C_W + K_{I_1} C_G C_A + K_{I_2} \frac{C_S}{C_G} \right]^2} \quad (\text{B}_{16})$$

Where

$$k = k_4 \cdot K_{F,G} K_{F,A} K_3$$

Appendix C: GC-MS/FID data for ketalization of glycerol to solketal

Calibration Table for standards

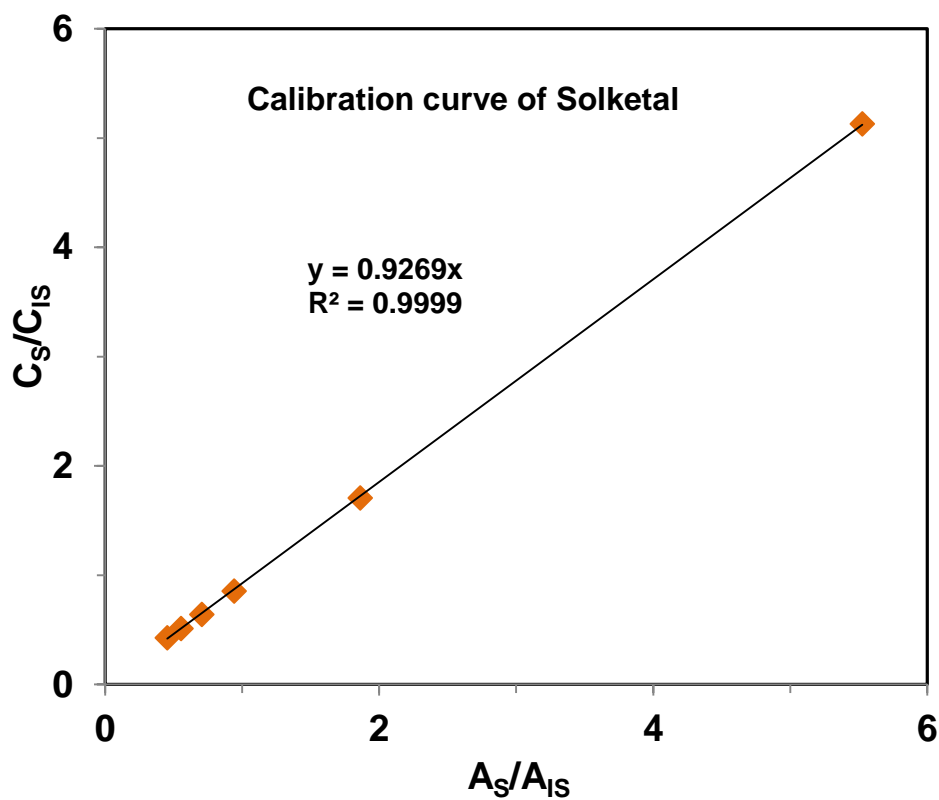
Standards	Conc. of Glycerol (ppm)	Conc. of Solketal (ppm)	Conc. of DMSO (IS) (ppm)	Area of Glycerol	Area of Solketal	Area of DMSO
Std 1	1389.00 (1389.43)	2052.00 (2052.20)	400	278513	400683	72518
Std 2	463.00 (462.39)	684.00 (682.96)	400	95788	147148	79092
Std 3	231.50 (231.68)	342.00 (342.20)	400	30704	52807	56113
Std 4	173.62 (174.18)	256.50 (257.26)	400	27460	46383	65725
Std 5	138.90 (139.24)	205.20 (205.67)	400	21764	33967	61413
Std 6	115.75 (115.69)	171.00 (170.88)	400	16381	27805	61413

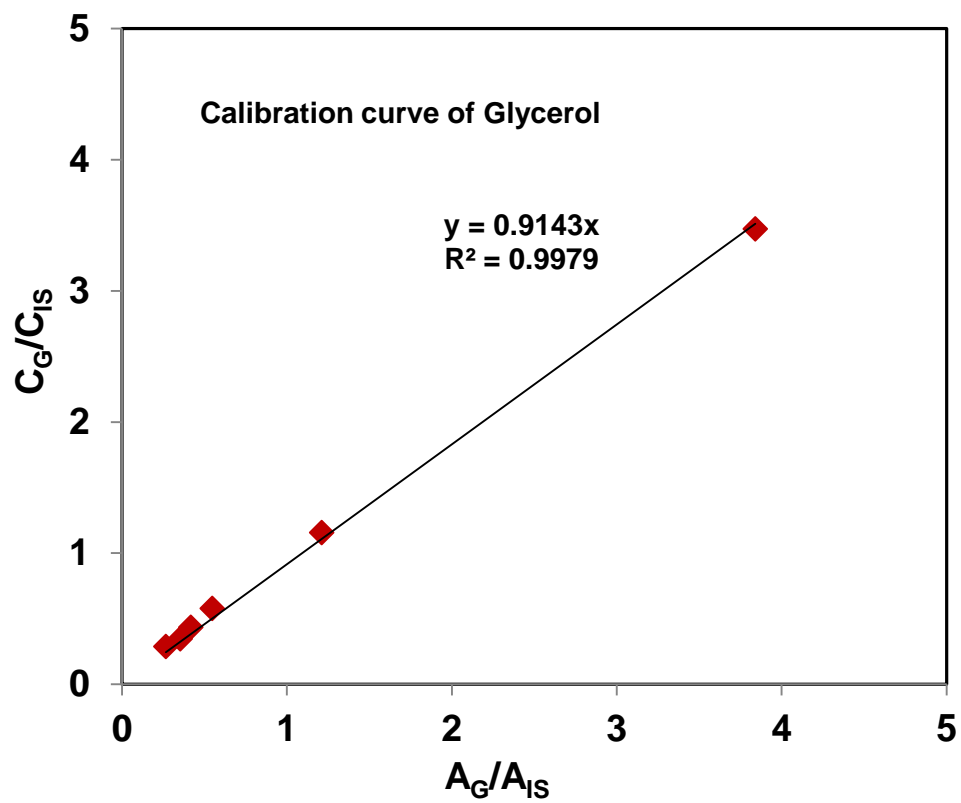
()Bracketted value is the actual concentration

Operating conditions:

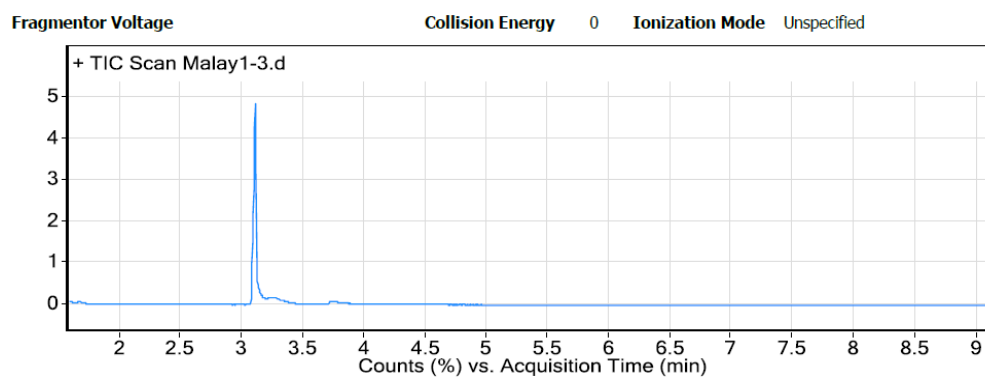
SPL 1: Temperature= 300.0°C, Mode= Split, Flow= Linear, Pressure= 94.4 kPa, Column flow= 0.84 mL/min, Linear velocity= 25.0 cm/sec, Purge flow= 3.0 mL/min, Split ratio= 20.0

Column: Temperature=120.0 °C, Equilibrium time= 2 min, Ramp=40.0 °C, Final Temperature= 280 °C for 4 min; FID: Temperature= 300.0 °C

Calibration curves



A typical GC-MS Spectrum of product



Retention time (min)	Compound	Molecular weight (MW)
3.1	Solketal	132
3.3	DMSO	78
3.7	Glycerol	92

Appendix D: GC-MS/FID data for hydrogenation of glycerol to 1,2-PDO

Calibration Table for standards

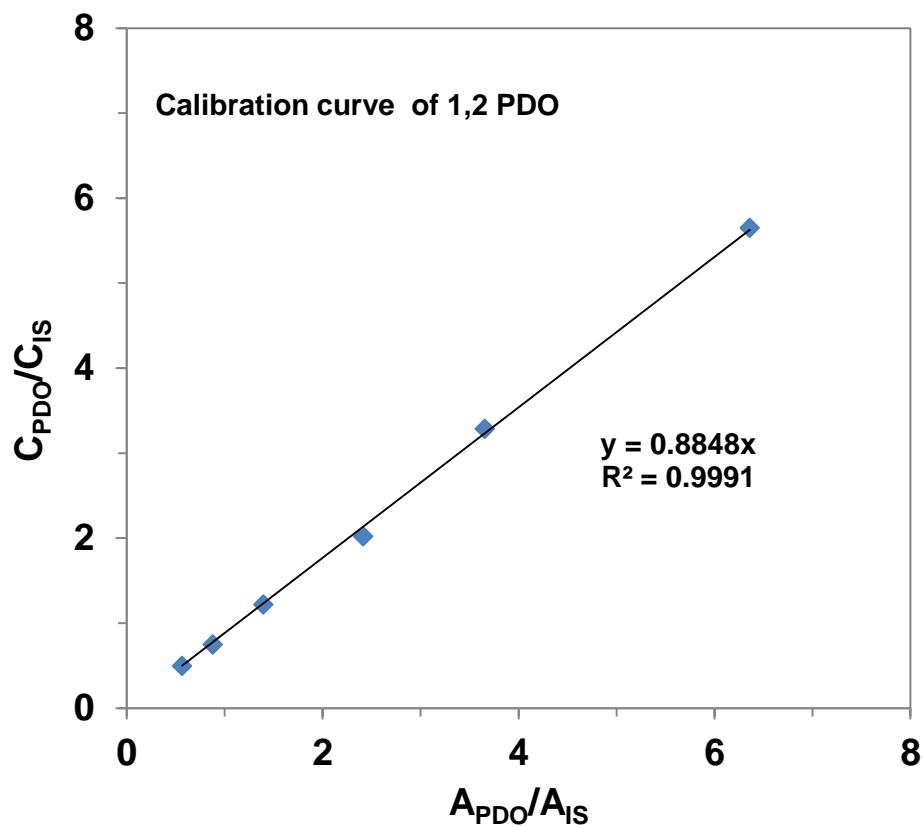
Standards	C _{PDO} (ppm)	C _G (ppm)	C _{EG} (ppm)	C _A (ppm)	C _{IS} (ppm)	A _{PDO}	A _G	A _{EG}	A _A	A _{IS}
Std 1	2260.00	2573.00	1321.00	1273.00	400	454279	449684	290248	262893	71429
Std 2	1313.95	1495.93	768.02	740.12	400	243471	272541	172055	140926	66621
Std 3	808.01	919.91	472.29	455.13	400	135108	135573	97563	74472	55972
Std 4	486.54	553.93	284.39	274.06	400	76444	82835	55825	41000	54827
Std 5	299.10	340.52	174.83	168.47	400	45456	40920	25143	23091	51682
Std 6	197.76	225.15	115.59	111.39	400	26649	22720	14618	12997	47169

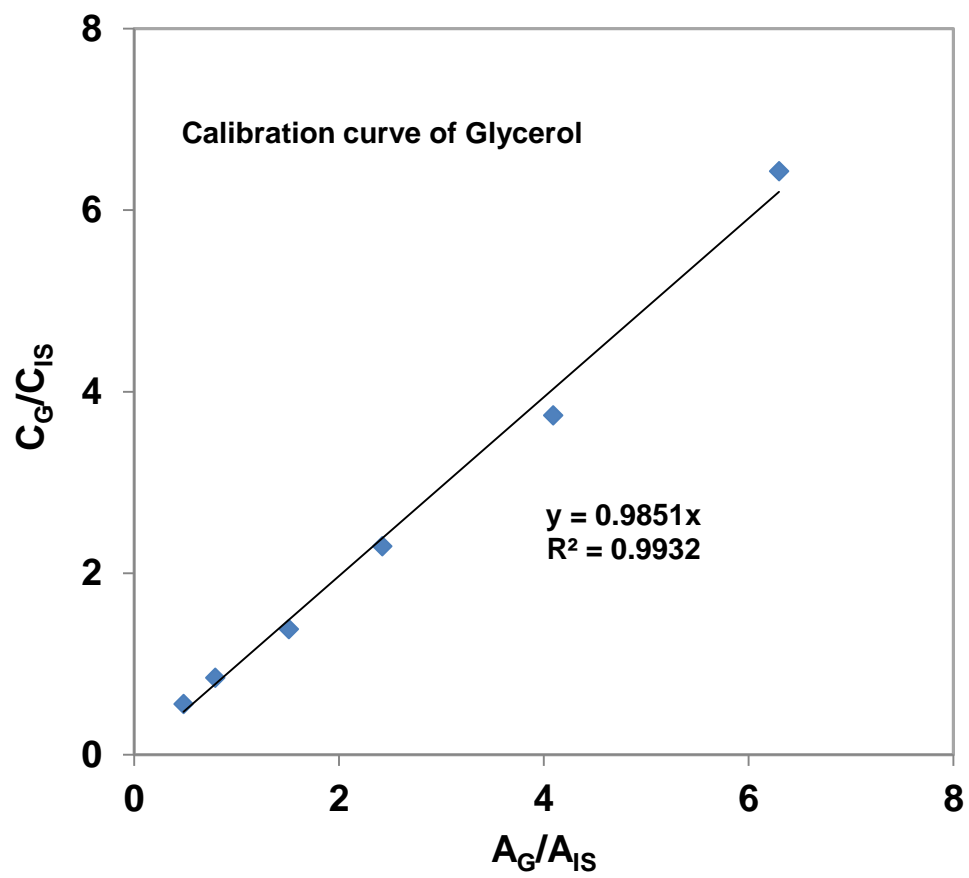
PDO: 1,2-propanediol; G: Glycerol; EG: Ethylene glycol; A: Acetol; IS: Internal Standard (DMSO);

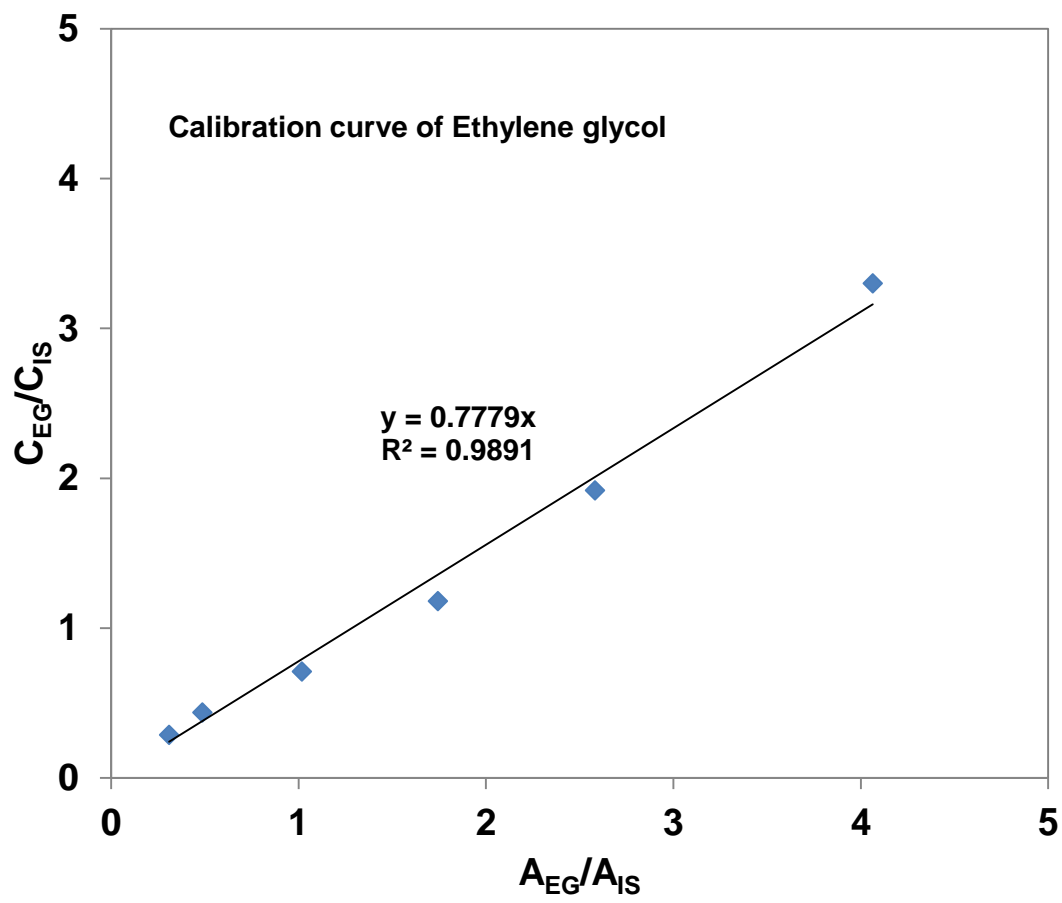
Operating conditions:

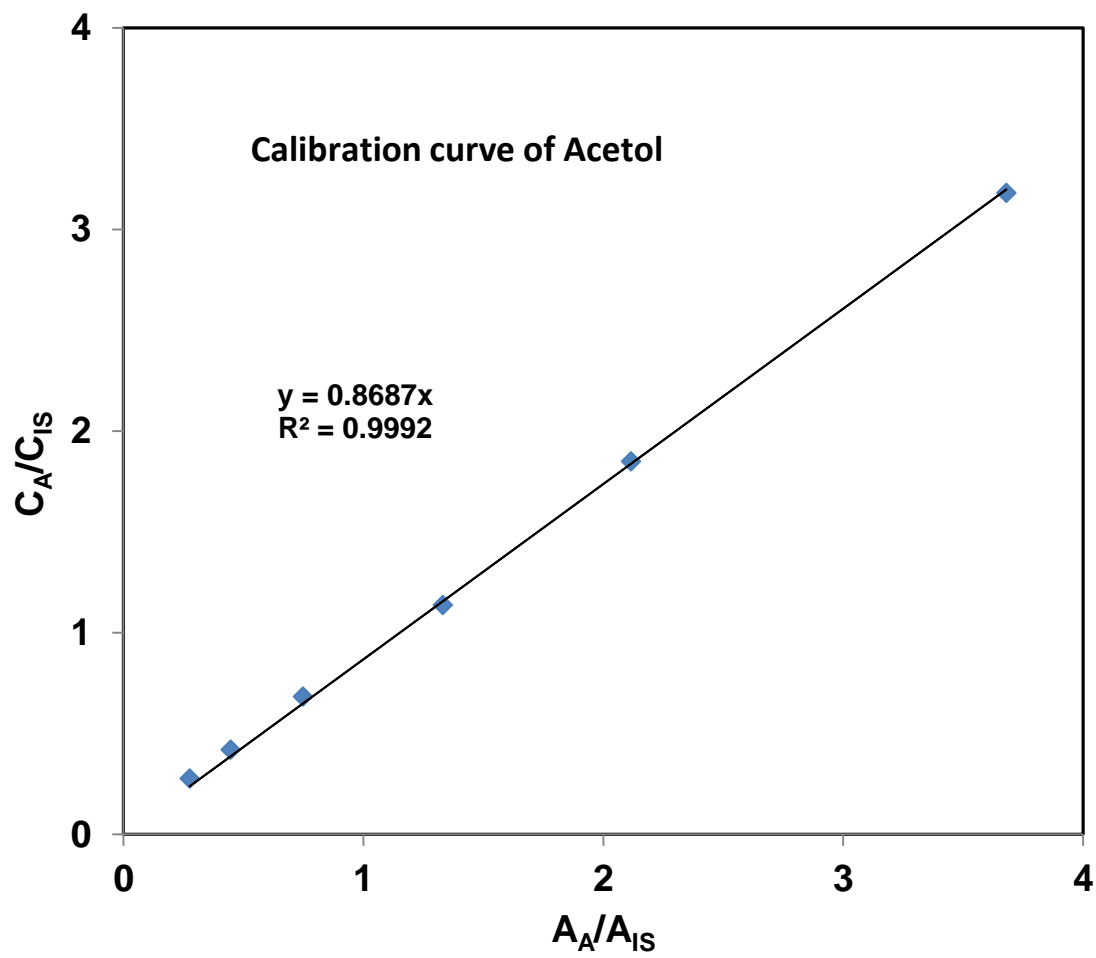
SPL 1: Temperature= 300.0 °C, Mode= Split, Flow= Linear, Pressure= 86.0 kPa, Column flow= 0.93 mL/min, Linear velocity= 25.0 cm/sec, Purge flow= 3.0 mL/min, Split ratio= 20.0

Column: Temperature=70.0 °C, Equilibrium time= 1 min, Ramp=40.0 °C, Final Temperature= 290 °C for 4 min; FID: Temperature= 300.0 °C

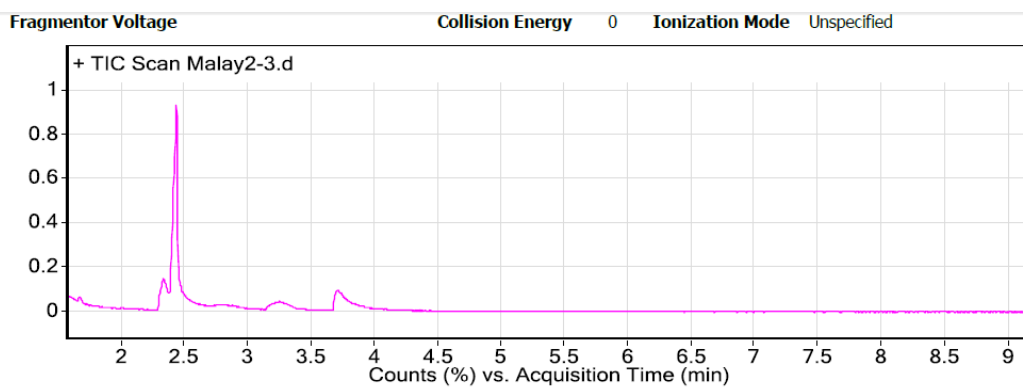
Calibration curves







A typical GC-MS Spectrum of product



Retention time (min)	Compound	Molecular weight (MW)
2.1	Acetol	74
2.3	Ethylene glycol	46
2.4	Propylene glycol	76
3.2	DMSO	78
3.7	Glycerol	92

Appendix E: Permission to Reuse Copyrighted Materials

Permission to Table 2.1 and Table 2.3

This is a License Agreement between Malaya Nanda ("You") and Royal Society of Chemistry. The license consists of your order details, the terms and conditions provided by Royal Society of Chemistry, and the payment terms and conditions.

[Get the printable license.](#)

License Number	3677790135522
License date	Jul 28, 2015
Licensed content publisher	Royal Society of Chemistry
Licensed content publication	Chemical Society Reviews
Licensed content title	Chemoselective catalytic conversion of glycerol as a biorenewable source to valuable commodity chemicals
Licensed content author	Chun-Hui (Clayton) Zhou, Jorge N. Beltramini, Yong-Xian Fan, G. Q. (Max) Lu
Licensed content date	Nov 22, 2007
Volume number	37
Issue number	3
Type of Use	Thesis/Dissertation
Requestor type	academic/educational
Portion	figures/tables/images
Number of figures/tables/images	2
Distribution quantity	7
Format	print and electronic
Will you be translating?	no
Order reference number	None
Title of the thesis/dissertation	Catalytic conversion of glycerol to value added chemical products
Expected completion date	Aug 2015
Estimated size	350
Total	0.00 CAD

Permission to Scheme 2.13

This is a License Agreement between Malaya Nanda ("You") and Elsevier ("Elsevier"). The license consists of your order details, the terms and conditions provided by Elsevier, and the payment terms and conditions.

Get the printable license.

License Number	3563211392845
License date	Feb 06, 2015
Licensed content publisher	Elsevier
Licensed content publication	Journal of Catalysis
Licensed content title	Investigations on heterogeneously catalysed condensations of glycerol to cyclic acetals
Licensed content author	J. Deutsch,A. Martin,H. Lieske
Licensed content date	25 January 2007
Licensed content volume number	245
Licensed content issue number	2
Number of pages	8
Type of Use	reuse in a thesis/dissertation
Portion	figures/tables/illustrations
Number of figures/tables/illustrations	1
Format	both print and electronic
Are you the author of this Elsevier article?	No
Will you be translating?	No
Original figure numbers	Scheme 2
Title of your thesis/dissertation	Catalytic conversion of glycerol to fuel additives and chemicals
Expected completion date	Apr 2015
Estimated size (number of pages)	220
Elsevier VAT number	GB 494 6272 12
Permissions price	0.00 CAD
VAT/Local Sales Tax	0.00 CAD / 0.00 GBP
Total	0.00 CAD

Permission to Figure 3.1

This Agreement between Malaya Nanda ("You") and John Wiley and Sons ("John Wiley and Sons") consists of your license details and the terms and conditions provided by John Wiley and Sons and Copyright Clearance Center.

License Number	3558840122901
License date	Jan 30, 2015
Licensed Content Publisher	John Wiley and Sons
Licensed Content Publication	Asia-Pacific Journal of Chemical Engineering
Licensed Content Title	Glycerol upgrading by ketalization in a zeolite membrane reactor
Licensed Content Author	Laura Roldán, Reyes Mallada, José M. Fraile, José A. Mayoral, Miguel Menéndez
Licensed Content Date	Mar 20, 2009
Licensed Content Pages	6
Type of use	Dissertation/Thesis
Requestor type	University/Academic
Format	Print and electronic
Portion	Figure/table
Number of figures/tables	1
Original Wiley figure/table number(s)	Figure 2
Will you be translating?	No
Title of your thesis / dissertation	Catalytic conversion of glycerol to fuel additives and chemicals
Expected completion date	Apr 2015
Expected size (number of pages)	220
Requestor Location	Malaya Nanda, 1280 Willa Drive
Billing Type	Invoice
Billing address	Malaya Nanda 1280 Willa Drive
Total	0.00 CAD

Permission to Figure 3.2

PERMISSION/LICENSE IS GRANTED FOR YOUR ORDER AT NO CHARGE

This type of permission/license, instead of the standard Terms & Conditions, is sent to you because no fee is being charged for your order. Please note the following:

- Permission is granted for your request in both print and electronic formats, and translations.
- If figures and/or tables were requested, they may be adapted or used in part.
- Please print this page for your records and send a copy of it to your publisher/graduate school.
- Appropriate credit for the requested material should be given as follows: "Reprinted (adapted) with permission from (COMPLETE REFERENCE CITATION). Copyright (YEAR) American Chemical Society." Insert appropriate information in place of the capitalized words.
- One-time permission is granted only for the use specified in your request. No additional uses are granted (such as derivative works or other editions). For any other uses, please submit a new request.

If credit is given to another source for the material you requested, permission must be obtained from that source.

Permission to Scheme 3.3

This Agreement between ("You") and Elsevier ("Elsevier") consists of your order details and the terms and conditions provided by Elsevier and Copyright Clearance Center.

License number	Reference confirmation email for license number
License date	Jan 30, 2015
Licensed content publisher	Elsevier
Licensed content publication	Bioresource Technology
Licensed content title	Effective production of the biodiesel additive STBE by a continuous flow process
Licensed content author	Jean-Christophe M. Monbaliu, Marc Winter, Bérengère Chevalier, Frank Schmidt, Yi Jiang, Ronald Hoogendoorn, Michiel A. Kousemaker, Christian V. Stevens
Licensed content date	October 2011
Licensed content volume number	102
Licensed content issue number	19
Number of pages	4
Type of Use	reuse in a thesis/dissertation
Portion	figures/tables/illustrations
Number of figures/tables/illustrations	1
Format	both print and electronic
Are you the author of this Elsevier article?	No
Will you be translating?	No
Original figure numbers	Figure 1
Title of your thesis/dissertation	Catalytic conversion of glycerol to fuel additives and chemicals
Expected completion date	Apr 2015
Elsevier VAT number	GB 494 6272 12
Billing Type	Invoice
Billing address	Malaya Nanda, 1280 Willa Drive,
Permissions price	0.00 CAD
VAT/Local Sales Tax	0.00 CAD / 0.00 GBP
Total	0.00 CAD

Permission to Figure 4.5

This is a License Agreement between Malaya Nanda ("You") and Elsevier ("Elsevier"). The license consists of your order details, the terms and conditions provided by Elsevier, and the payment terms and conditions.

License Number	3677810207149
License date	Jul 28, 2015
Licensed content publisher	Elsevier
Licensed content publication	Catalysis Today
Licensed content title	Aqueous phase hydrogenolysis of glycerol to 1,2-propanediol without external hydrogen addition
Licensed content author	Debdut Roy,Bala Subramaniam,Raghunath V. Chaudhari
Licensed content date	25 October 2010
Licensed content volume number	156
Licensed content issue number	1-2
Number of pages	7
Type of Use	reuse in a thesis/dissertation
Portion	figures/tables/illustrations
Number of figures/tables/illustrations	1
Format	both print and electronic
Are you the author of this Elsevier article?	No
Will you be translating?	No
Original figure numbers	Figure 2
Title of your thesis/dissertation	Catalytic Conversion of glycerol to value added chemical products
Expected completion date	Aug 2015
Estimated size (number of pages)	350
Elsevier VAT number	GB 494 6272 12
Permissions price	0.00 CAD
VAT/Local Sales Tax	0.00 CAD / 0.00 GBP
Total	0.00 CAD

Permission to Figure 4.6

Can I make an electronic copy for use in an e-reserve system?	Yes	<p>You may include material from this resource in e-reserves, which are electronic copies of articles stored on a secure network for use by students in connection with a specific class.</p> <p>More/Less Information</p>
Can I post a copy in a course management system?	Yes	<p>You may include material from this resource in course management systems like OWL (Sakai).</p> <p>More/Less Information</p>
Can I put it in a course pack?	Yes	<p>You may include material from this resource in course packs, which are compilations of articles for use by students in a class.</p> <p>More/Less Information</p>
Can I link to it?	Yes	<p>You can create a persistent electronic link to an individual article or ebook.</p> <p>More/Less Information</p>
Can I make print or electronic copies?	Yes	<p>You may make print and electronic copies for personal use.</p> <p>More/Less Information</p>

Permission to Figure 4.8

This is a License Agreement between Malaya Nanda ("You") and Royal Society of Chemistry. The license consists of your order details, the terms and conditions provided by Royal Society of Chemistry, and the payment terms and conditions.

Get the printable license.

License Number	3677810852086
License date	Jul 28, 2015
Licensed content publisher	Royal Society of Chemistry
Licensed content publication	Green Chemistry
Licensed content title	Ag/Al ₂ O ₃ for glycerol hydrogenolysis to 1,2-propanediol: activity, selectivity and deactivation
Licensed content author	Jinxia Zhou,Jing Zhang,Xinwen Guo,Jingbo Mao,Shuguang Zhang
Licensed content date	Nov 1, 2011
Volume number	14
Issue number	1
Type of Use	Thesis/Dissertation
Requestor type	academic/educational
Portion	figures/tables/images
Number of figures/tables/images	1
Distribution quantity	7
Format	print and electronic
Will you be translating?	no
Order reference number	None
Title of the thesis/dissertation	Catalytic Conversion of glycerol to value added chemical products
Expected completion date	Aug 2015
Estimated size	350
Total	0.00 CAD

Permission to Chapter 5

This is a License Agreement between Malaya Nanda ("You") and Elsevier ("Elsevier"). The license consists of your order details, the terms and conditions provided by Elsevier, and the payment terms and conditions.

License Number	3558860410982
License date	Jan 30, 2015
Licensed content publisher	Elsevier
Licensed content publication	Fuel
Licensed content title	Thermodynamic and kinetic studies of a catalytic process to convert glycerol into solketal as an oxygenated fuel additive
Licensed content author	None
Licensed content date	30 January 2014
Licensed content volume number	117
Licensed content issue number	n/a
Number of pages	8
Type of Use	reuse in a thesis/dissertation
Portion	full article
Format	both print and electronic
Are you the author of this Elsevier article?	Yes
Will you be translating?	No
Title of your thesis/dissertation	Catalytic conversion of glycerol to fuel additives and chemicals
Expected completion date	Apr 2015
Estimated size (number of pages)	220
Elsevier VAT number	GB 494 6272 12
Permissions price	0.00 CAD
VAT/Local Sales Tax	0.00 CAD / 0.00 GBP
Total	0.00 CAD

Permission to Chapter 6

This is a License Agreement between Malaya Nanda ("You") and Elsevier ("Elsevier"). The license consists of your order details, the terms and conditions provided by Elsevier, and the payment terms and conditions.

License Number	3558850648193
License date	Jan 30, 2015
Licensed content publisher	Elsevier
Licensed content publication	Applied Energy
Licensed content title	A new continuous-flow process for catalytic conversion of glycerol to oxygenated fuel additive: Catalyst screening
Licensed content author	None
Licensed content date	15 June 2014
Licensed content volume number	123
Licensed content issue number	n/a
Number of pages	7
Type of Use	reuse in a thesis/dissertation
Portion	full article
Format	both print and electronic
Are you the author of this Elsevier article?	Yes
Will you be translating?	No
Title of your thesis/dissertation	Catalytic conversion of glycerol to fuel additives and chemicals
Expected completion date	Apr 2015
Estimated size (number of pages)	220
Elsevier VAT number	GB 494 6272 12
Permissions price	0.00 CAD
VAT/Local Sales Tax	0.00 CAD / 0.00 GBP
Total	0.00 CAD

Permission to Chapter 7

This is a License Agreement between Malaya Nanda ("You") and Elsevier ("Elsevier"). The license consists of your order details, the terms and conditions provided by Elsevier, and the payment terms and conditions.

License Number	3558860059037
License date	Jan 30, 2015
Licensed content publisher	Elsevier
Licensed content publication	Fuel
Licensed content title	Catalytic conversion of glycerol to oxygenated fuel additive in a continuous flow reactor: Process optimization
Licensed content author	None
Licensed content date	15 July 2014
Licensed content volume number	128
Licensed content issue number	n/a
Number of pages	7
Type of Use	reuse in a thesis/dissertation
Portion	full article
Format	both print and electronic
Are you the author of this Elsevier article?	Yes
Will you be translating?	No
Title of your thesis/dissertation	Catalytic conversion of glycerol to fuel additives and chemicals
Expected completion date	Apr 2015
Estimated size (number of pages)	220
Elsevier VAT number	GB 494 6272 12
Permissions price	0.00 CAD
VAT/Local Sales Tax	0.00 CAD / 0.00 GBP
Total	0.00 CAD

Permission to Chapter 8

The author retains the copyright of the published article.

You can use the content published in the manuscript as a chapter in your thesis.

Curriculum Vitae

- Name:** Malaya Nanda
- Post-secondary Education and Degrees:** The University of Western Ontario
London, Ontario, Canada
2011-2015 PhD.
- The University of Guelph
Guelph, Ontario, Canada
2009-2010 M.A.Sc.
- Ravenshaw University
Cuttack, Orissa, India
2007-2008 MPhil.
- Honours and Awards:** Doctoral Fellowship, University of Western Ontario
2011-2015
- MITAC Scholarship
2014-2015
Ivan Mahek Scholarship
2012-2013
- Related Work Experience** Teaching Assistant
The University of Western Ontario
2011-2012
- Publications:**
- Patent**
1. Nanda, M., Yuan, Z., Poirier Marc-Andre, Xu C., Continuous room-temperature production of solketal from crude glycerol for gasoline fuel additive or diesel fuel combustion promoter- *U.S Patent* filed with Imperial Oil-2014
- Published article:**
1. Nanda, M., Yuan, Z., Qin, W., Ghaziaskar, H.S., Poirier Marc-Andre, Xu, C., A new continuous-flow process for catalytic conversion of glycerol to oxygenated fuel additive: catalyst screening, *Applied Energy*, 2014,123, 75-81

2. Nanda, M., Yuan, Z., Qin, W., Ghaziaskar, H.S., Poirier Marc-Andre, Xu, C., Catalytic conversion of glycerol to oxygenated fuel additive in a continuous flow reactor: process optimization, *Fuel*, 2014, 128, 113-119
3. Nanda, M., Yuan, Z., Ghaziaskar, H.S., Qin, W., Poirier Marc-Andre, Xu, C., Thermodynamics and kinetic studies of a catalytic process to convert glycerol into solketal as an oxygenated fuel additive, *Fuel*, 2014, 117, 470-477
4. Nanda, M., Yuan, Z., Qin, W., Poirier Marc-Andre, Xu, C. Purification of Crude Glycerol Using Acidification: Effects of Acid Types and Product Characterization: *Austin J Chem Eng*, 2014, 1, 1-7.

Publications in Progress:

1. Nanda, M., Yuan, Z., Qin, W., Poirier Marc-Andre, Xu, C. Catalytic conversion of purified crude glycerol in a continuous-flow process for the synthesis of oxygenated fuel additive- submitted to *Fuel Process Technology*, February 2015
2. Nanda, M., Yuan, Z., Qin, W., Poirier Marc-Andre, Xu, C. Recent advancement on innovative and potential technologies towards the sustainable production of solketal: A minireview – submitted to *Renewable & Sustainable Energy Reviews*, May 2015
3. Nanda, M., Yuan, Z., Qin, W., Poirier Marc-Andre, Xu, C. Selective hydrogenolysis of glycerol to 1,2-propanediol over B₂O₃ incorporated Cu/Al₂O₃ catalyst - to be submitted
4. Nanda, M., Yuan, Z., Qin, W., Poirier Marc-Andre, Xu, C. Catalytic valorization of glycerol to propylene glycol: Recent developments and future perspectives” – under preparation
5. Nanda, M., Yuan, Z., Qin, W., Poirier Marc-Andre, Xu, C. Crude glycerol: A liability or an evolving opportunity- Under preparation
6. Nanda, M., Yuan, Z., Qin, W., Xu, C. Techno-economic analysis of an oxygenated fuel additive from crude glycerol in Canada- Under preparation